"DEVELOPMENT OF MODEL FOR THE CROP-DROUGHT IMPACTS VULNERABILITY ASSESSMENT FOR KOLAR AND CHIKKABALLAPUR DISTRICTS IN KARNATAKA, INDIA"

Thesis submitted to Kuvempu University for the Degree of

DOCTOR OF PHILOSOPHY

By: -

HARISHNAIKA .N

Research Scholar
Dept. of Applied Geology
Kuvempu University, Shankaraghatta,
Shimoga-577451

Under the Guidance of: -

Prof. SYED ASHFAQ AHMED

Professor
Dept. of Applied Geology
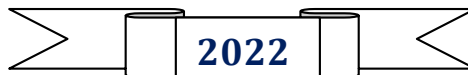Kuvempu University, Shankaraghatta,
Shimoga-577451

Dept, of P.G. Studies and Research in Applied Geology
Kuvempu University, Jnana Sahyadri.
Shankaraghatta -577451

2022

DECLARATION

*I hereby declare that the thesis entitled **"Development Of Model For The Crop-Drought Impacts Vulnerability Assessment For Kolar And Chikkaballapur Districts In Karnataka, India"** which is being submitted for the award of the degree of Doctor of Philosophy in Applied Geology is the original work carried out by me in the Department of Applied Geology, Kuvempu University, Jnanasahyadri, Shankaraghatta, Shimoga-577451 under the guidance of Prof. Syed Ashfaq Ahmed Professor, Department of Applied Geology, Kuvempu University.*

Date: 6-10-2022

Place: *Shankaraghatta*

(HARISHNAIKA N)

Kuvempu University

Prof. Syed Ashfaq Ahmed
Applied Geology
Cell: 9845142267
E-mail:ashfaqsa@hotmail.com
ashfaqs@kuvempu.ac.in

Dept. of P.G. Studies and Research in Applied Geology
Kuvempu University
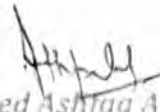*Jnanasahyadri , Shankaraghatt- 577451*
Shivamogga, Karnataka, INDIA

Certificate

This is to certify that the work on the thesis entitled *"Development Of Model For The Crop-Drought Impacts Vulnerability Assessment For Kolar And Chikkaballapur Districts In Karnataka, India"* submitted to the Kuvempu University by **HARISHNAIKA N** for the award of the degree of Doctor of Philosophy in Applied Geology is based on the result bonified research work carried out by him in the department of Applied Geology. Kuvempu University, under my supervision during the period 2019-2022 this thesis or part thereof has not been submitted for the award of any other degree or diploma from this university or elsewhere

Date: 6 . 10 . 2022

Place: Shankaraghatta

Prof. Syed Ashfaq Ahmed
Dept. of P.G. Studies and Research
In Applied Geology
Kuvempu University
CHAIRMAN
Dept. of P.G. Studies and
Research in Applied Geology
Kuvempu University
SHANKARAGHATTA-577 451

ACKNOWLEDGEMENTS

Document Information

Analyzed document	KU-TH-GEO-HARISHNAIKA-N-22.pdf (D143932454)
Submitted	2022-09-12 11:54:00
Submitted by	Walmiki R H
Submitter email	walmiki_rh@rediffmail.com
Similarity	6%
Analysis address	walmiki_rh.kuvempu@analysis.urkund.com

Sources included in the report

SA **Anand Agricultural University, Anand / BHUKYA SRINIVAS.pdf**
Document BHUKYA SRINIVAS.pdf (D134756174)
Submitted by: librarian@aau.in
Receiver: librarian.aaua@analysis.urkund.com
⊞ 6

SA **Sam Higginbottom Ins Of Agri, Tech & Sciences / PhD thesis Sunil Kumar ID 18PHAM202.pdf**
Document PhD thesis Sunil Kumar ID 18PHAM202.pdf (D117850898)
Submitted by: sunilkumaragromet@gmail.com
Receiver: shweta.gautam.shuats@analysis.urkund.com
⊞ 2

SA **Sardar Vallabhbhai National Institute Of Tech / Thesis 2022 Saranya C. Nair.pdf**
Document Thesis 2022 Saranya C. Nair.pdf (D140984048)
Submitted by: vlm@ced.svnit.ac.in
Receiver: vlm.svnit@analysis.urkund.com
⊞ 20

SA **University of Delhi, New Delhi / Analysing the Impact of Thermal Stress on Vegetation_OCR.pdf**
Document Analysing the Impact of Thermal Stress on Vegetation_OCR.pdf (D94126304)
Submitted by: head@geography.du.ac.in
Receiver: head.dept.of.geography.du@analysis.urkund.com
⊞ 1

SA **Central University of Karnataka, Gulbarga / new thesis.docx**
Document new thesis.docx (D20985456)
Submitted by: sruthiswathandran@gmail.com
Receiver: parashu.kattimani.cukar@analysis.urkund.com
⊞ 10

Entire Document

CHAPTER -1 INTRODUCTION

Dedicated to My

Beloved

Family, Friends, Teachers

&

**Who's directly and indirectly supported
to my Research Work.**

LIST OF TABLES

LIST OF FIGURES

CHAPTER-1

CHAPTER-2

CHAPTER-03

ABSTRACT

Drought is an insidious meteorological and hydrological natural phenomenon causing many adverse impacts on the environment, agriculture, and socio-economic condition, especially in semi-arid regions like Kolar and Chikkaballapura districts in the state of Karnataka. When the precipitation level is inadequate to meet the demands of human activities, it leads to drought extension over a season or longer period. The present article is investigating the application of the standard precipitation index (SPI) to detect drought incidents which are widely used to understand rainfall variability. Therefore, this study attempts to analyse drought during pre-monsoon, southwest monsoon, northeast monsoon, and annual period using SPI for the Kolar and Chikkaballapura districts of Karnataka state. The outcome of this analysis demonstrates that drought occurrences are frequent in particular years and seasons with negative values of SPI along with dry, wet, and normal events. To apply any management plan to the increasing nuisance, deep knowledge is essential about meteorological, agricultural, and hydrological drought. The rainfall data for the period 1951–2019 at the eleven grid points were acquired from the India Meteorological Department with $(0.25^0 \times 0.25^0)$ high spatial resolution. The result revealed that a moderate dry event was observed in the pre-monsoon period at Kolar in 1993 with − 0.67. Extreme drought condition was recorded during the southwest monsoon season in 1980 at Kolar with − 2.22 and for the northeast monsoon, − 1.67 was observed at Malur station in 1988. The seasonal crops of the southwest monsoon (June–September) are heavily dependent on this rainfall and it contributes to 58% of the annual precipitation. If there is a drop in the rainfall received during the southwest monsoon, the effect on the growing stage of crops leads to reduced crop yield.

This research examines the temporal sequence of trends for rainfall data, calculated for 11 grid stations. LOWESS curves showed the correlation between the predicted and observed time series. The temporal rainfall trend was evaluated using the non-parametric MK and Sen's slope method which was applied to notice the rainfall tendency and slope with a 5% significance level. In the study period, non-parametric tests reveal a significant positive trend at 7 meteorological grid stations for June, but the remaining 4 stations exhibit a non-significant positive trend in June and the significant negative trend was noticed in October only for the Sidlaghatta station and a non-

significant negative trend appeared in October and December with 6 and 4 stations, respectively. The output of the study indicates that yearly precipitation is rising showing the highest in Bangarapete with a change of 53.22%, and the lowest in Sidlaghatta with a value of −3.56%.

Climate change is dramatically warming, and as a result, drought scenarios occur frequently and at various times throughout the world. As a result, picking a suitable indicator for drought assessment is crucial. The most widely used instruments for monitoring droughts globally are the standardized precipitation evapotranspiration index (SPEI) standardized precipitation index (SPI) and Rainfall anomaly index (RAI). The SPEI considers both the temperature and the amount of precipitation in its calculation; however, the SPI just takes the amount of precipitation into account. In this study, the SPEI and SPI at 11 meteorological grid stations in Kolar and Chikkaballapura from 1979 to 2019 were calculated at 3-, 6-, and 12-month intervals. In the Gudibande station, the More extreme drought period primarily occurred for approximately 17, 18, and 10 months in SPI (3, 6, and 12-month scales, respectively), with a frequency of about 3.1. SPEI time scale statistics for Chikkaballapura indicated a more severe drought with a frequency value of 2.4. Srinivasapura and Gudibande experienced their driest years in May 1993 (-3.92) and August 2003 (-3.78), respectively. Overall consistent years of drought were reported in 1983, 1985, 2003, 2007, and 2019. The Planning for water use, agricultural activity, and economic activity, all of which depend on precipitation and temperature over the research period benefit from this research. The characterization of droughts in the area at various time scales will help develop short, medium, and long-term planning needed to negate such calamities events in the future.

The repercussions of drought, a natural hazard, are extensive and include economic damage, soil degradation, threats to human health, and a threat to our way of life. The present investigation used GIS and remote sensing techniques to evaluate the vegetation health index throughout the semi-arid districts of Karnataka state between 2015 and 2019. The VCI, TCI, and VHI indices were divided into 5 drought-related categories: no drought, mild, moderate, severe, and extreme drought. The findings show that Chinthamani taluk has the highest percentage of severe agricultural drought, which covers an area of around 740.20 sq. km (21%). Bagepalli is roughly 397.70 sq. km

(19%) and Sidhlaghatta taluk is about 26% of the total area in the S-W monsoon (338.55 sq. km). Malur (23%; 704.05 sq. km), Mulubhagilu (28%; 909.99 km^2), and Bangarapete (20%; 879.64 km^2) were all badly damaged by the North-East Monsoon's high drought from 2015 to 2019 in respect of the area's agriculture and vegetation. In the northeast of both the Kolar and Chikkaballapura districts, there was severe to moderate drought. In comparison to the other study years employing the CDI, 2016 and 2017 saw a lower percentage of drought environments. This investigation examines more profitably, overcomes drought conditions, and allows decision-makers to be monitored.

To investigate the potential for predicting annual rainfall, the LMR was analyzed. Afterward, various statistical assessment metrics, including RMSE, MSE, and MAPE, were utilized to assess the efficacy of these two methods. In general, the analysis's RMSEs show that the LMR model is more accurate than the ANN models at forecasting WA's long-term seasonal rainfall. During the prediction interval for the research area, the RMSE of the built LMR models is fairly low. The anticipated future precipitation at each location during the 1951–2050 study period. The Bagepalli, Bangarapete, and Malur stations provided a future prediction of rainfall that gradually increases using their historical mean rainfall data collection. The Chikkaballapura station has the lowest rainfall value, around R = 0.0032, while the Bangarapete station showed highly significant variations in the future forecast, R = 0.2279, compared to the other Grid stations (about 700-900mm).

CHAPTER -01 -INTRODUCTION

CHAPTER-04 – Long-term Rainfall Trend Analysis

CHAPTER-05 Combined Drought Indices by Remote sensing Technique

CHAPTER-06 Rainfall Future Prediction and Forecasting

CHAPTER-07 Conclusions and Recommendations

CHAPTER -1
INTRODUCTION

Chapter-1
Background

1.1 Rainfall

Precipitations are the amount of rainfall, in the form of rain (water from clouds), that falls onto the Earth's surface, whether it is on water bodies or land. It evolves when air masses move over wetland surfaces or warm water sources. Atmospheric convection and turbulence carry the water vapour or moisture, moves rising into air masses where they form into clouds. The clouds gradually release this water vapor, which is fallen as rainfall into the earth.

1.2 Scientific Foundations and Historical Background

Precipitation is the main important concept in the hydrological cycle in the earth, which is the continuous motion of above Earth's surface and water below. This hydrological cycle involves water stored in the sea and oceans, but also in lakes, ice caps, rivers, and glaciers, and also underground. Water moisture evaporates from these sources and it finally condensed into clouds through the atmospheric conditions, where it moves various distances in the atmosphere before falling (rainfall) back to the earth's surface as precipitation (and different forms of rainfall), falls in the Earth eventually detects its way to storage in water containers where it started the cycle again. It is key to know that all water resources on Earth have neither been created nor vanished over millions of years. The water present one million years ago, for example, is being used today for bathing, cooking, drinking, and other uses.

1.3 Impacts and Issues

Clouds have not been made without dust particles of inorganic and organic substances such as silica, pollen, and bacteria. These natural materials are suspended in the earth's atmosphere and serve as a conveyor for water vapour condensation, so this is called CCN (cloud condensation nuclei). However; the chance of precipitation can be increased by artificially building particles, Such as pollution from industrial factories, and automobile exhaust. When such particles as smoke, smog, and soot are produced, they take to the increased

making of clouds, which straight increases the chances of precipitation. Under atmospheric natural conditions, thousands of these cloud condensation nuclei particles may be within a mean cubic inch of the earth's atmosphere. However, in industrialized areas, these artificial particles gradually increase the concentration of CCN to over 40-50 million dust particles per cubic inch.

Artificially making CCN dust particles can move huge distances and rest in the atmosphere for longer periods. According to research performed by the U.S. NASA (National Aeronautics and Space Administration), huge and more severe storms are made when the earth's atmosphere over large cities is polluted by the activities of humans. This enhanced pollution in the atmosphere produces more precipitation not only for the big cities but also for rural areas downwind.

1.4 Hydrological Cycle:

The hydrological cycle is the continuous process of circulation of water into the atmosphere and earth through the cyclic process. It involves the process of the horizontal and vertical shift of vapour, evaporation, condensation, rainfall, and movement of water from land to the oceans floor; it is the main parameter in controlling the climate condition through its impact on the clouds, land vegetation, ice, and soil moisture and snow. 30 to 35% of the mid-latitude heat transfer from the equatorial to the Polar Regions is attributed to the hydrologic cycle.

1.5 Natural Changes in Arid lands

Desertification is sometimes created by natural parameter influences other than the absence of precipitation. This process has been progressing in some areas, in conjunction with long-term variation in climatic conditions, mainly decreased precipitation. Until the 20TH century, humans were able to directly move their agricultural practices away from land and provide unusable land by desertification. However, this idea has been provided less tenable by the huge population increase of human beings during the past several centuries, a variation that has increased the notice paid to the degradation of productive dry lands.

1.6 Drought

Generally, Drought is known as a creeping environmental hazard phenomenon (Karavitis et al. 2011) which can cause by moisture deficient within a region (Uddameri et al. 2019) that can bring severe causes to Environmental, Agricultural, and Socio-Economic consequences around the world (Piao et al. 2010; Jiang et al. 2020) and has Spatio-temporal features which are significantly dissimilar by one place to another region. The climate zones are found by longer periods of mean Precipitation, Temperature, and Extreme weather parameters. Precipitation in a semiarid and subhumid country like India is extremely valuable in terms of time and space; as a result, deviations in precipitation trends cause extreme natural hazards like floods and droughts that have an impact on all-natural habitats. (He et al. 2009) like animals, plants, and important human beings. Drought events may elucidate as a natural climatic and recurrent event due to the less than normal rainfall when compared to it with the long-term mean precipitation and expansion to the long-term period (Dai 2011; Tirivarombo et al. 2018). According to the American Meteorological Society, there are three different types of drought: agricultural, meteorological, and hydrological drought. (Sona et al. 2012; D. Udmale et al. 2014; Bhunia et al. 2020). The lack of precipitation has an impact on the surface and subsurface water supplies, and it has been shown that there is a lack of groundwater due to stream water flow. (Haroon et al. 2016), Meteorological drought is defined in termed the magnitude of a precipitation shortfall event as drought effects are noticed by step, first indicating the scarcity of water storage in the reservoir than as a decrease in streamflow which results in depletion of groundwater table then a shortage of soil moisture and at the end, it directly affects the human society and economy (Tsakiris 2017). Agricultural drought is completely the result of a deficiency in soil moisture. Only the southwest monsoon received nearly 80% share of the total rainfall over the country (Panda and Sahu 2019). Although considered the primary input for agriculture, precipitation plays an erratic role in terms of quantity and distribution, for better water management and crop planning. The course of rainfall is crucial. The impact of rainfall variability on an area's agricultural productivity and sustainability, both over time and space

Droughts are evident after a long period without rainfall, but it is difficult to control their extent, onset, and end. In these conditions, many drought indices have been developed scientifically, which assess the deviation of climate conditions in a year from the normal conditions. These drought indexes serve as operational indicators and monitoring tools for water resources management in the region. Palmer developed the PDSI (Palmer Drought Severity Index) in 1965, which takes into account evapotranspiration, precipitation, and soil water holding capacity. The use of PDSI is restricted due to the requirement of the significant, computational complexity of meteorological data and applicability on different period scales.

A drought is a serious event that may impact on Economic, Agricultural, Social, and other life activities of world society. It is an abnormally, prolonged dry spell period when there is very little shortage of water for normal requirements. It is a temporary natural disaster, which arises from less rainfall and conducts economic losses. It is a very slow process, on the earth, no one knows when it happens, it can last many months and days and its effect and severity cannot be said. The characteristic of non-structural drought effects has certainly obstructed the development of reliable, timely, and accurate estimates of ultimately and severity, the methodology of drought awareness plans by most state and central governments.

The impacts of dry periods and hazards can be shortened through preparedness and mitigation. Drought is an increase in the period where precipitation falls below the statistical essential requirements for an area. It is not only a purely physical event but rather an interaction between human demands and natural water availability. There are 2 major kinds of drought explanation: operational and conceptual. Operational drought definitions analyze the spatial extent, end, beginning, and severity effects of a drought in a region. They are based on scientific reasoning, which attends to the analysis of particular amounts of hydrological and meteorological information. Conceptually, it can be explained as "an extended period of deficient rainfall resulting in large scale damage to crops, finally, it resulting in loss of crop yield."(NDMC -National Drought Mitigation Centre, 2006). Conceptual drought may also be very

important in setting up the drought policy. They are helpful in drought policies developing, mitigation strategies, monitoring systems, and the making of plans. Characterizing drought is difficult; it founds on differences in needs, regions, and disciplinary views.

Drought regularly starts with less amount of rainfall, but it may (or may not, turn on how severe and long it is) affect streams, soil moisture, ecosystems, groundwater, and human beings. This guide to the recognition of various drought types (agricultural, hydrological, meteorological, ecological socio-economic,), reflects the concept of various sectors on water scarcity. Figure 1 regularly describes these perspectives.

1.6.1 Types of Droughts

Drought can be categorized into four major classes:

1.6.1.1 Meteorological Drought:

It defines precipitation deficiency, where the rainfall is reduced by greater than 30% from normal rainfall in any given region. These areas' specific deficiency of rainfall is highly different from area to area.

1.6.1.2 Hydrological Drought:

These are related to the lack of water on the earth's surface or subsurface of the earth due to a shortfall in rainfall. Even though all drought periods have derived from a rainfall deficiency, this hydrological drought is majorly concerned with how this lack of rainfall affects parameters of the hydrological cycle such as stream flow, soil moisture, reservoir levels, groundwater, etc.

1.6.1.3 Agricultural Drought:

This links different characteristics of hydrological drought or meteorological to agricultural effects, focusing on rainfall shortages, variation between actual potential evaporates transpiration, soil water deficits, soil, and reduced reservoir levels or groundwater. Plant water requirements depend on induced weather and climate conditions, biological features of the plant and its phase of growth, and biological and physical properties of the soil.

1.6.1.4 Socio-Economic Drought:

It is connected with the demand and supply of the feature of economic goods jointly with parameters of hydrological drought, meteorological and agricultural drought period. This drought mainly happens when there the requirement for an economic good exceeds their contribution due to climate and weather-related deficiency in the water supply.
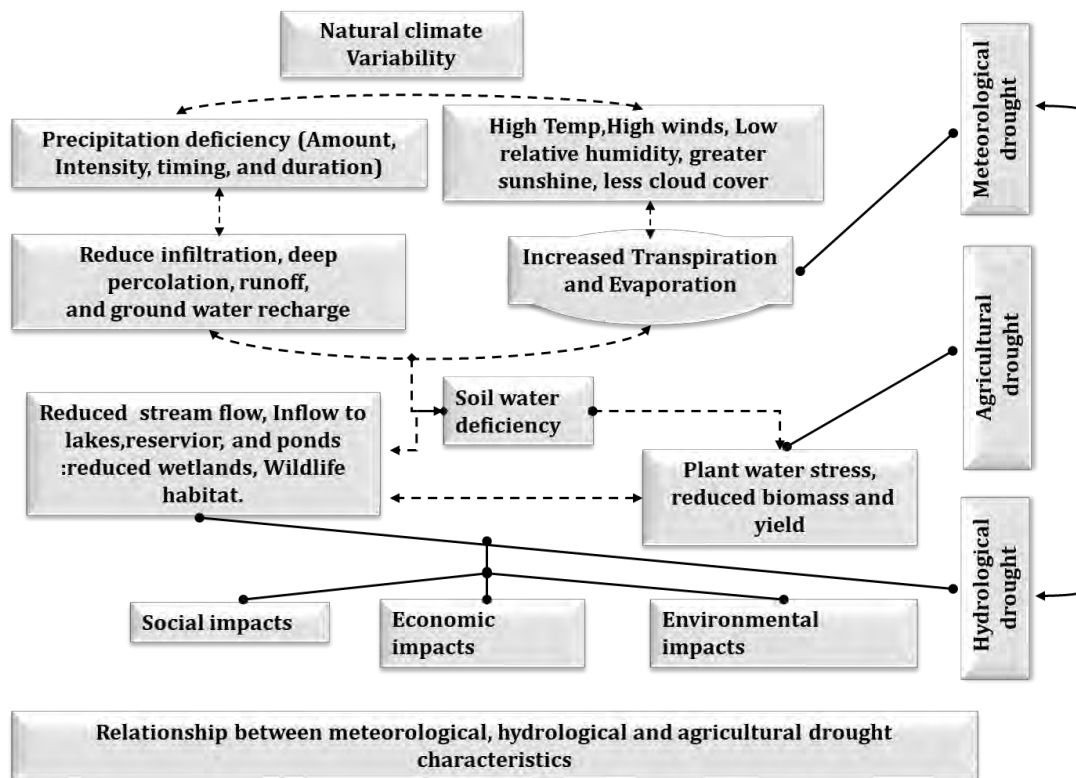
Figure.1 Relationship between Meteorological, Hydrological, and Agricultural Drought Characteristics

1.7 Drought in India

India is mainly an agricultural country as more than 65- 70% of its county population is dependent on agrarian. Rainfall is the major source of agriculture. It is deliberate in terms of the meteorological drought event. It is known that the provider of water through precipitation cannot be as even regular as it can be along irrigation. Nearly 20-30% of the total regions of the nation lie in the dry farming area, where yearly precipitation is between 50 and 110 cm without any irrigation practice support. Consequently, even after full utilization of irrigation perspective in the nation. It is evaluated that about 71 million hectares of the

cultivated area will fall under rain-fed agriculture practices, extension over parts of Rajasthan, Haryana, Gujarat, Madhya Pradesh Uttar Pradesh, Andhra Pradesh, Maharashtra, Karnataka, and Tamil Nadu. The Farmer experiences the very worst effects of drought years. Due to the shortage of precipitation. More than 60 % of the area in the nation is drought-prone regions, out of which 45 % is severe natural drought. The nation experiences a drought period every 2-3 years in one or other parts. The country experiences the worst drought in 1987 of the Century. The monsoon precipitation was normal condition only in 13 out of 35 meteorological subdivisions in India. The overall shortage in precipitation was 20 % as compared to 27% in 1918 and 26% in 1972 the worst years.

1.7.1 In Karnataka

The draught, a hydro-meteorological natural disaster, has affected Karnataka state throughout the years of research with varying degrees of intensity and magnitude. The initial reason for the emergence or continuation of the drought condition in the various districts of a state has been differences in the temporal and spatial distribution of precipitation during the monsoon and monthly seasons. The impact of drought on communities is directly correlated with the length, severity, and frequency of dry periods, which ultimately makes communities more vulnerable.

The infrastructure and resources that the agricultural community in Karnataka state depends on for survival have suffered severe damage as a result of the drought, which has been occurring repeatedly and with increasing severity. As a region that depends heavily on agriculture, 75% to 81% of the state's farmland is in rain-fed regions. During the Kharif and Rabi crop seasons, unpredictable seasonal precipitation seriously contributes to crop failure, placing farmers in a very difficult situation. Often, dry events have the latent effect of reducing agricultural crop production to such a large extent that the farmers' livelihoods are threatened. As a result, this has led to widespread migration of those affected in the community, an increase in malnutrition affecting women, the elderly, and children, as well as an uptick in school enrolment, and an increase in the incidence of farmer suicide. In addition to causing crops to tremble, it also leads to the loss of vegetation, livestock forage,

and water resources. Recurring and intermittent drought is also a factor in the decline of agriculture's contribution to the state of Karnataka's GDP and the state's overall financial future burden. Karnataka is located in a region of the nation that experiences frequent droughts. The enormous amount of rain-fed land is further complicated by recurring climatic variations, particularly drought and flooding.

Karnataka has the nation's composition of agro-climatic conditions. According to the Planning Commission for Agro-climatic Regional Planning, Karnataka is located in Area X (10) Hilly region and Southern Plateau and Area 11(XII) West Ghats region and Coast Plains. Based on humidity, Soil structure, Topography, Elevation, Rainfall, Vegetation, and Other agro-climatic parameters, the area has been divided into 10 (ten) Agro-climatic regions. Many of them are in the semi-dry zone, which has had more erratic precipitation in recent years and a mean annual precipitation range of 400 to 700 mm. District-wise Cultivated Area, Under Rainfed Cultivation and Irrigation on Table 1

The area of Karnataka, which is the eighth-largest state in the nation, is roughly 1.91 lakh square kilometers. The consists of climatological regions that are classified into 10 different agro-climate areas, including sub-humid, humid, arid, and semiarid regions. The state is divided into 31 districts, 176 taluks, 747 hoblis, 6000 Gram Panchayaths, and Villages (29,406). About 6.57 crore people call the entire state home, 67% of whom live in rural areas and depend on agriculture. Arid to semi-arid conditions apply to about 2/3 of the total geographic regions.

Table 1. District-wise Cultivated Area, Under Rainfed Cultivation and Irrigation

District Area in Hectors	Gross Cultivated area	Net Cultivated Area	Gross Irrigated Area	Net Irrigated Area	Gross Rainfed cultivated area	Net Rainfed cultivated area
Kolar	177060	166521	30262	19723	146798	146798
Chikkaballapura	213397	202704	59719	50170	153678	152534

Table 1.1. Continued**,** Number of Agricultural Land Holdings and Operated Area by District (Agricultural Census 2010-11)

Districts	Total Geographical Area	Cultivated Area Agri, Census 2010 - 11	% of Cultivated area to total Geographical Area
Kolar	374965	233923	63
Chikkaballapura	404512	226343	57

1.8 Geospatial Application on Drought Monitoring

The advantages of GIS and remote sensing systems, such as their spatial, spectral, and temporal capabilities, have a high potential for managing, accessing, and monitoring natural resources. In contrast, the diversity of convectional field-based methodologies is more time-consuming, costly to maintain, and challenging in remote locations. The primary defect of conventional methods was the relative unimportance of the surveys, which prevented them from keeping up with changes in the natural resources over longer periods and space. The goal of this research was to create a methodological approach that would make it easier to find a suitable location for the implementation of an innovative system aimed at improving rainfed agriculture in semi-arid areas of Karnataka.

1.9 Aim of the Research:

The goal of the current study is to identify some problems with long-term drought and land production efficiency. Applying widely-used statistical techniques to create a mapping methodology that focuses on drought management and sustainable use of water planning. The main objective of this study is to generate and utilize a spatial and temporal historical dataset to evaluate and assess the drought vulnerability in the districts of Kolar and Chikkaballapura.

1.9.1 Research Objectives:

1. Evaluate and compare the performance of drought indices concerning identifying the historical drought events and determinants and identify factors important for mitigating crop drought vulnerability.

2. Standardized Precipitation Index (SPI), Standardized Precipitation Evaporation Index (SPEI), Evapotranspiration Deficit Index (ETDI), Soil Moisture Deficit Index (SMDI),

3. Spatio-Temporal Rainfall Trend Assessment Over a long-term period, Using Non-Parametric Techniques.

4. Develop an impact-based Combined Drought Index (CDI) concerning the Remote sensing datasets to assess the vulnerabilities across the districts.

1.9.2 Methodological Framework

The following methodology is designed to achieve the research goal and objectives

➤ The spatial maps of LULC, Soil, slope, drainage, lithology, groundwater potential zone, and elevation maps are prepared for thematic layer evaluations.

➤ The temporal and spatial distribution of Rainfall temperature, PET, ET, LST, and Soil moisture are analyzed by using IMD and MODIS data sets computing by appropriate statistical methods.

➤ Evaluate and compare the effectiveness of drought indices in detecting past drought events and determinants and identify factors important for mitigating crop drought vulnerability using the advanced statistical approach (SPI, SPEI, RAI, rainfall deviation, ETDI, and SMDI).

➤ Assessment of the temporal and spatial precipitation and temperature trend by advanced non-parametric techniques like LOWESS curves, Pettit, Mann-Kendall, SNHT, Buishand range test

➤ Develop an impact-based agricultural CDI index like LST, NDVI, TCI, VCI, and VHI using advanced remote sensing techniques and GIS models.

1.9.3 Materials

Geospatial and statistical methods combined with multi-thematic spatial and non-spatial maps have been used to plan system innovations for the water crisis in the districts of Kolar and Chikkaballapura.

1.9.3.1 Satellite Images:

The Satellite data like Sentinel-2, Landsat-7, and Landsat-8 space-based series have made it possible to acquire a historical multispectral and thermal database with dates from 2010 to 2019 at both medium and high resolution with 8- and 16-day intervals. All station elevations are determined using a digital elevation model from ALOS-PALSAR (Radiometric Terrain Correction), which has a spatial resolution of approximately 12.5 meters obtained from ASF

The Moderate Resolution Imaging Spectroradiometer (MODIS) with our understanding of the dynamics processes taking place on land (continent), in the seas (water bodies), and in the earth's atmosphere will be enhanced by these data. The development of a validated, global, associated with earth arrangement model that can accurately predict planetary help and change policymakers to make advise decisions about the preservation of our environment is greatly aided by MODIS data. For simplicity of ability to handle in a GIS environment, all data are Geo-referenced and projected to CGS (Geographic coordinate system), WGS 1984 (World Geodic system), with UTM zone 43 north.

1.9.3.2 Software and Tools Used for Research:

Satellite images are improved and processed in ERDAS Imagine 2014 for visualization and to carry out digital image processing techniques. Using GIS software called Arc map 10.8, all spatial data in a GIS domain is handled. The software used in this study for the assessment of rainfall and drought periods includes Microsoft Excel, XLSTAT 2020, R studio, and Mat Lab.

1.10 The Outcome of the Research

Here is a more thorough explanation of how this study was conducted.

1) To look into the drought observation to clarify dry and wet years at the district level and then assess how the climatic conditions have changed over time.

2) From 1951 to 2019, examine the variations in the spatiotemporal pattern of meteorological drought at seasonal and annual time scales. Such a study has never been done in this area before.

3) Monitoring and predicting future droughts as well as understanding how drought characteristics change over time and space. Overall, the research findings will be advantageous for the design and implementation of water resource management strategies and drought control in the study area.

1.11 Structure of the Thesis

The work done in this study is divided into six distinct chapters that will form the basis for implementing and developing sustainable cropping pattern strategies, water, and land resource management planning, variation of rainfall trends and assessment of drought for water scares in Kolar and Chikkaballapura.

Chapter.1: General Introduction

It includes the objective, materials, and methodology used to achieve the research goals, as well as a brief introduction to the aspects of types of drought and historical drought events presented in this chapter. it mainly focuses on the different types of drought-like Meteorological, Hydrological and Agricultural drought is defined termed the magnitude of a precipitation shortfall event as drought effects are noticed by step, first indicating the scarcity of water storage in the reservoir than as a decrease in stream flow which results in depletion of groundwater table then a shortage of soil moisture and at the end, it directly affects the human society and economy

Chapter.2: Study Area

It provides general information on the study location, climate, soil, topography, and meteorological aspects in the districts of Kolar and Chikkaballapura. This chapter provided information on the research field and the

most significant basic statistics. The study area has a diversity of different Soils, Geomorphological Features, Lithological properties, Drainage channels, Slopes, Land use, and land cover types and is situated in the southernmost part of the Indian state of Karnataka. The study of precipitation, temperature, moisture and other weather parameters has a significant impact on the hydrological cycle, resulting in both too much and not enough rainfall. Due to the region's varying climate, the semi-arid zone always implies lower rainfall amounts.

Chapter 3: Evaluate and Compare the Performance of Drought Indices

This study's main objective is to compare the drought conditions that are currently present in both districts. In this context, crop management, irrigation management, the building of irrigation infrastructure, and the design of irrigation facilities all depend on the spatiotemporal classification of drought using various drought Indices like SPI, SPEI, RAI, NDVI, ET, PET, LST, rainfall deviation, ETDI, and SMDI. This assessment of dry occurrences is crucial in dry areas for the planning of agricultural activity, water use, and economic activity, all of which are heavily reliant on rainfall. Characterizing and evaluating the region's droughts at different time scales will aid in creating the short-, medium-, and long-term plans required to prevent similar catastrophes in the future. This study's main objective is to compare the drought conditions that are now present in both areas. In this context, crop management, irrigation methods, the building of irrigation infrastructure, and the design of irrigation facilities all depend on the spatiotemporal classification of drought using diverse approaches. Authorities, farmers, and researchers in that area can utilize this information to plan their crops, organize their schedules, and manage their irrigation systems. Additionally, thoughtful planning might boost food production while preserving the environment. Encouraging rural populations to engage in agriculture this study uses long-term rainfall data to describe the drought using the SPI, SPEI, and RAI methodologies.

Chapter 4: Spatial-Temporal Rainfall Trend Assessment by Non-parametric Techniques

This study examines the temporal progression of rainfall trends that were computed for 11 grid stations. The correlation between the predicted and actual time series was demonstrated by LOWESS curves. The non-parametric MK and Sen's slope method, which was used to observe the rainfall tendency and slope with a 5% significance level, was used to evaluate the temporal rainfall trend and used Pettit's, SNHT, and bushiand test for detecting homogeneity in the rainfall data. Applying the scientific methods, the pattern of precipitation patterns is shown along with a territorial description, statistical tables, and interpretive figures. Our understanding of rainfall trends in these districts appears to have improved as a result of the evaluation. In 69 years of the study period, this work uses eleven meteorological grid stations to discover whether there is a discernible monthly and annual trend.

Chapter 5: Vegetation Health and Drought Analysis by Combined Drought Indices

The current study used GIS and remote sensing techniques to monitor the vegetation health index throughout the semi-arid regions of Karnataka state between 2015 and 2019. The Vegetation Condition Index (VCI) and Temperature Condition Index were determined using Landsat-8 dataset images with a spatial resolution of 30 m and from various platforms (TCI). The NDVI (Normalized Difference Vegetation Index) datasets are necessary for the operation of the VCI. LST was used for the Temperature Condition Index (land surface temperature datasets). The Vegetation Health Index (VHI) was created as a result.

Chapter 6: Linear Multiple Regression Model for Long-Term Rainfall Forecasting

The major goal of this chapter was to employ machine learning techniques to identify the pertinent atmospheric variables that generate precipitation and predict the severity of daily precipitation. As a result, the research findings are listed below. The ability of monsoon rainfall to anticipate annual precipitation has been examined in this study. Utilizing both non-linear

and linear modeling techniques. This is because annual rainfall at various stations has the highest correlation with the 12-month average values of climate indices

Chapter 7: Conclusions and Recommendations

Overall, the research indicates in this chapter, the spatial multi-thematic layer is used to create a LULC, soil, slope, drainage, Geomorphology, Lithology, and Groundwater potential zone of the area by using GIS technology. The Research studied 69 years of seasonal and annual occurrence of drought frequency and duration in different identified stations in the study area from 1951 to 2019 using SPI and SPEI. Analyzing the spatiotemporal characteristics of various times drought indices such as ETDI, SMDI, CDI, and GIS, and remote sensing-based agricultural drought can be improved and monitored by the Vegetation Health Index composed of TCI and VCI agricultural drought indices. This Research showed the duration, severity, and spatial extent of agricultural drought areas using TCI, NDVI, VCI, and VHI at different grid stations in both districts during the Pre, Southwest, and Northeast monsoon seasons. In the dry semi-arid region of Kolar and Chikkaballapura in Karnataka, India, the characterization and assessment of droughts in the area at seasonal time scales will be useful for developing short, medium, and long-term planning needed to negate such calamities in the future.

Reference:

1. Uddameri, V., Singaraju, S., Hernandez, E.A., 2019. Is standardized precipitation index (SPI) a useful indicator to forecast groundwater droughts? — insights from a karst aquifer. J. Am. Water Resour. Assoc. 55, 70–88. https://doi.org/10.1111/1752-1688.12698.
2. Piao, S., Ciais, P., Huang, Y., Shen, Z., Peng, S., Li, J., Zhou, L., Liu, H., Ma, Y., Ding, Y., Friedlingstein, P., Liu, C., Tan, K., Yu, Y., Zhang, T., Fang, J., 2010. The impacts of climate change on water resources and agriculture in China. Nature 467, 43–51.
3. He, Y., Wetterhall, F., Cloke, H.L., Pappenberger, F., Wilson, M., Freer, J., 2009. Tracking the uncertainty in flood alerts driven by grand. Meteorol. Appl. 101, 91–101. https://doi.org/10.1002/met.
4. Tirivarombo, S., Osupile, D., Eliasson, P., 2018. Drought monitoring and analysis: standardised precipitation evapotranspiration index (SPEI) and standardised precipitation index (SPI). Phys. Chem. Earth 106, 1–10. https://doi.org/10.1016/j.pce.2018.07.001.
5. Sona, N.T., Chen, C.F., Chen, C.R., Chang, L.Y., Minh, V.Q., 2012. Monitoring agricultural drought in the lower mekong basin using MODIS NDVI and land surface temperature data. Int. J. Appl. Earth Obs. Geoinf. 18, 417–427. https://doi.org/10.1016/j.jag.2012.03.014.
6. Bhunia, P., Das, P., Maiti, R., 2019. Meteorological drought study through SPI in three drought prone districts of West Bengal, India. Earth Syst. Environ. 4 https://doi. org/10.1007/s41748-019-00137-6.
7. Haroon, M.A., Zhang, J., Yao, F., 2016. Drought monitoring and performance evaluation of MODIS-based drought severity index (DSI) over Pakistan. Nat. Hazards 84, 1349–1366. https://doi.org/10.1007/s11069-016-2490-y.
8. Panda, A., Sahu, N., 2019. Trend analysis of seasonal rainfall and temperature pattern in Kalahandi, Bolangir and Koraput districts of Odisha, India. Atmos. Sci. Lett. 20 https://doi.org/10.1002/asl.932. Pei, Z., Fang, S., Wang, L., Yang, W., 2020. Comparative analysis of drought indicated by the SPI and SPEI at various timescales in inner Mongolia. China Water 12. https://doi.org/10.3390/w12071925.
9. Strategies for agriculture and rural livelihood in the Maharashtra state of India. Open Agric. J. 8, 41–47. https://doi.org/10.2174/1874331501408010041.

CHAPTER -2
STUDY AREA

Chapter-2

Study Area

2. Details of the Geographical Location of the Study Area

This research has been studied in Kolar and Chikkaballapura districts situated between $12^0$45'N - $13^0$57'N lat and $77^0$24'E – $78^0$35'E long as shown in. These districts are stationed in the southeastern region, which is the dry semi-arid agro-climatic zone of Karnataka state, India. As per the Koppen-Geiger ¨ climate classification system, 30 sub-types and five main classes are defined to classify the global climate pattern. The seasonal variations in monthly rainfall and temperature are the critical parameters that define the classification system. The climate system for the study area is defined by Aw (Equatorial Winter Dry) covering the major portion and along the northern region, we find BSh (Arid Steppe Hot) Figure 2. It covers a spatial area that is extended up to 8241.02 km2 (Kolar-3992.02 km2 and Chikkaballapura - 4249 km2) with the terrain topographic elevation ranging from 507 m to 1389 m from the mean sea level. The slope is steep across the hilly ranges and gentle across the plains. The mean rainfall of the Kolar is 748 mm per year and Chikkaballapura records 756 mm per year. The annual mean temperature of the area ranges between 14.5 ∘C and 35.7 ∘C. There is no perennial river in the districts but two existing rivers namely Palar (south pennar), and Papakani (north penner) basins drain into this area. Both rivers are very small and their tributary area carries water only in the rainy season.

2.1 Approachability & Administrative Setup:

There are six taluks in the district. Specifically, the taluks of Gauribidanur, Chintamani, Chikkaballapura, Bagepalli, Sidhlaghatta, and Gudibande. The district's rail and highway connections are excellent. The western portions of the district are traversed by the south central (SCR) railway that runs between Bangalore and Hyderabad. In the Kolar district, there are five taluks. Specifically, the taluks of Bangarapete, Kolar, Mulubhagilu, Srinivaspura, and Malur. The administrative boundary of the district is indicated in Figure 2.
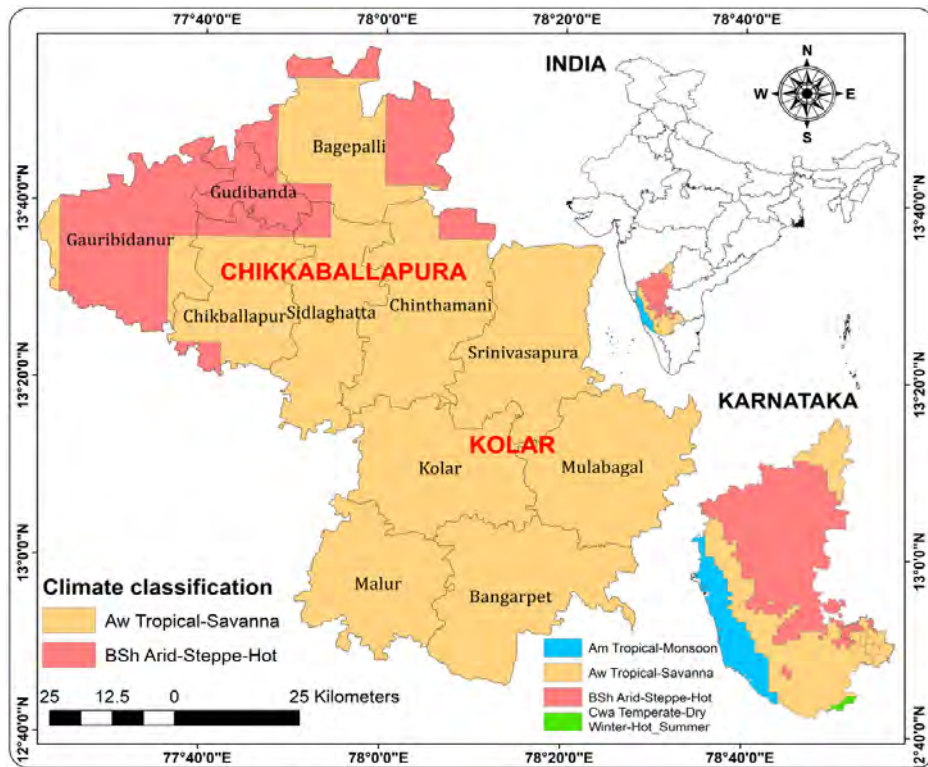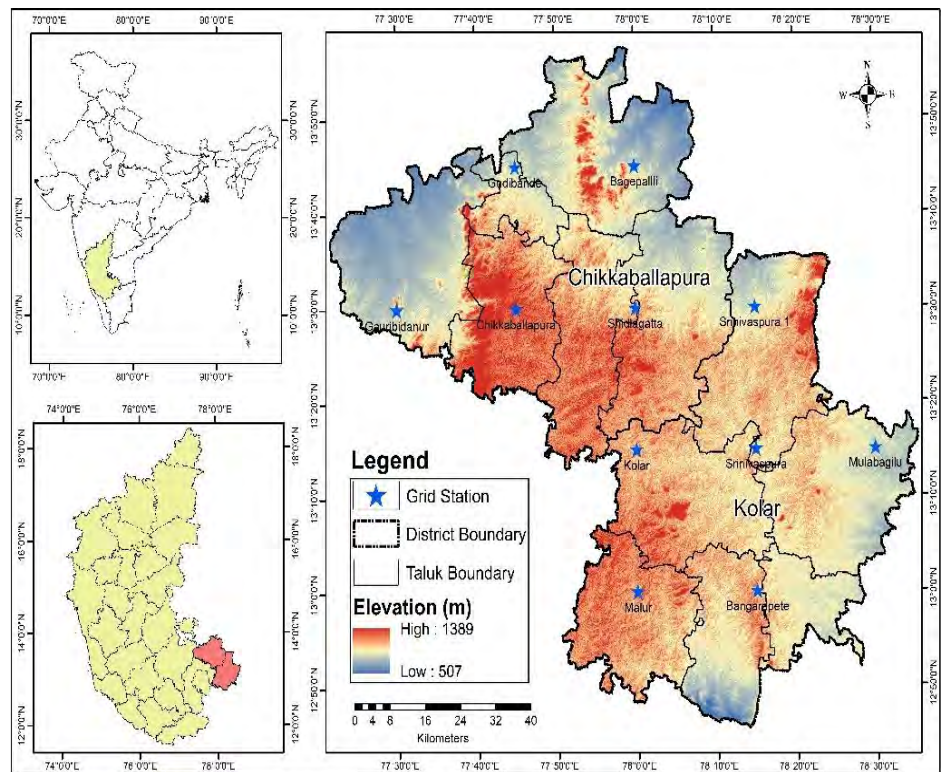
Figure.2 Geographic Location and Elevation of Kolar and Chikkaballapura

2.2 Demographic Features:

According to the 2011 census, approximately 12.55 lakh people are living in the Chikkaballapura district, with a population density of 297 people per square kilometer. In the district, there are 963 females per 1000 males (census 2001), with 2.22 lakhs living in urban areas and 9.26 lakhs in rural areas. According to the 2011 census, approximately 15.41 lakhs people are living in the Kolar district, with a population density of 384 people per square kilometer. In the district, there are 975 females per every 1000 males (census 2001), with 4.84 lakhs living in urban areas and 10.56 lakhs in rural areas.

2.3 Basins and Drainage System

In the Chikkaballapura district, there are no perennial rivers; instead, three river basins—the Ponnaiyar, Pennar, and Palar drain the region. All of these rivers and their small tributaries only carry water during the monsoon season. The Palar River rises in the Ambajidurga region of the Chintamani Taluk and flows in a northwest to southeast direction. In nature, river drainage takes the form of a highly dendritic type. The river Pennar rises in Bangalore's Doddapallapura district and flows northward through the taluks of Gauribidinur, Sidlaghatta Gudibande, and Bagepalli.

The river Papagni joins Sidlaghatta and travels through to the taluks of Chintamani, Bagepalli, and Sidlaghatta as it flows in a northerly direction. The drainage and basin map of Chikkaballapur is shown in Figure 2.1. North Papakani originates in the Nandhi Hills in Chikkaballapur, flows through the Gauribidinur Taluks for approximately 54 km, and then enters the state of Andhra Pradesh in the Ananthapura district.

In the Kolar district, which lacks perennial rivers, three river basins—Ponnaiar, North Pennar, and Palar—drain the region. Only during the monsoon season do all bodies of water and the small tributaries that flow into them transport water.

2.4 Lithology and Groundwater Scenario of Districts

Both districts are supported by Gneisses, Granites, Schists, Alluvium, and Laterites. The basic dykes are located at the aforementioned formations in

localized areas. Granites and Gneisses make up a sizable portion of the districts. The Schists rocks are mainly restricted to two areas: the N-W portion of Gauribidanur and the area surrounding KGF (Kolar Gold Fields). Smaller areas of the Srinivaspura, Sidlaghatta, and Kolar regions contain the Laterites rock. In both districts, the river courses contain alluvium rock. The rock lineaments or fractures are primarily found in structural valleys and have a NE-SW trend. Hard rock fissures, zones, and weathered fractures can be used to measure the movement and occurrence of ground water.
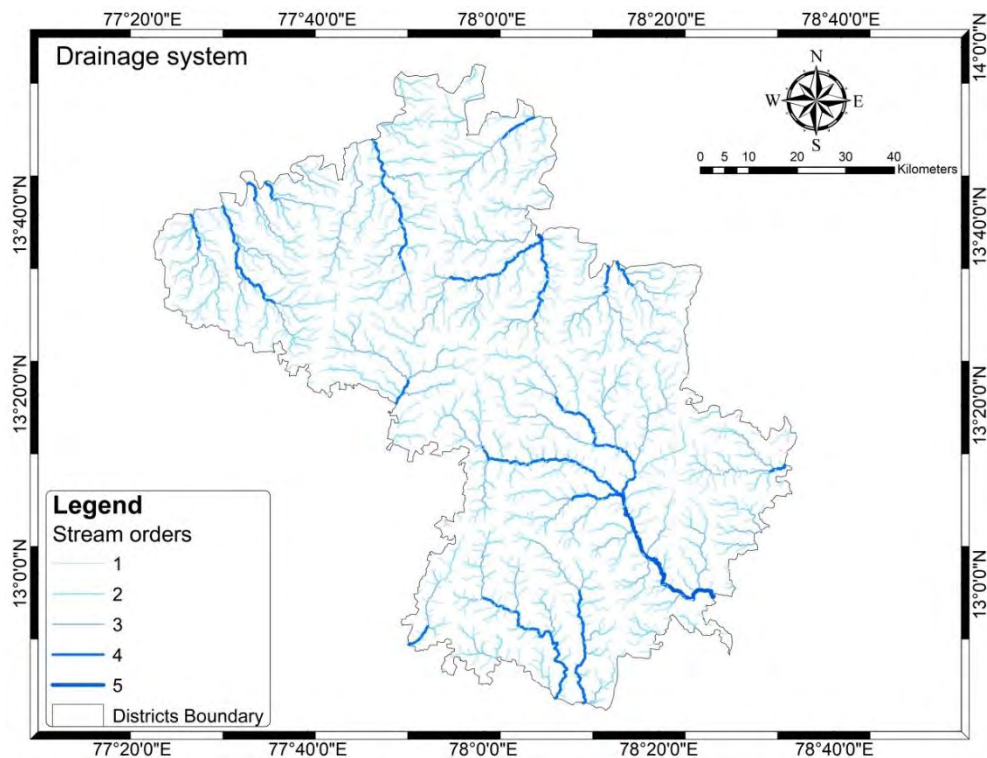
Figure.2.1 Drainage Map of Kolar and Chikkaballapura District

The groundwater appears to be in a phreatic phase and is partially contained. Additionally, when there is a high water table, it takes the form of alluvium. Except for the regions of Chikkaballapura and Sidlaghatta, the thickness of weathered rock in the area ranges from 50 to 70 meters and is between 7 and 19 meters. The actual range of the piezometer's water level is 13 to 51 mbgl. Groundwater levels must be managed by physiographic characteristics and regional rainfall patterns. The Peninsular Gneissic Complex, Granites, Gneisses, Horn Blende Schist, and Amphibolite Schist are the primary types of extremely old rock beds that make up the district. Figures 2.2 depict the scenario for lithology and groundwater.
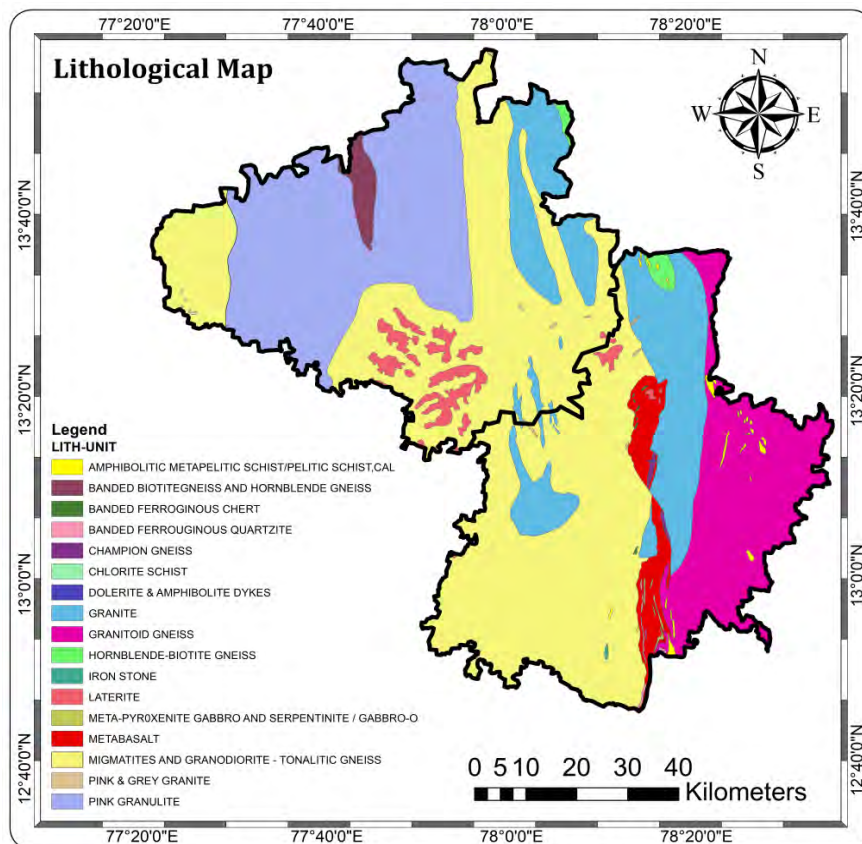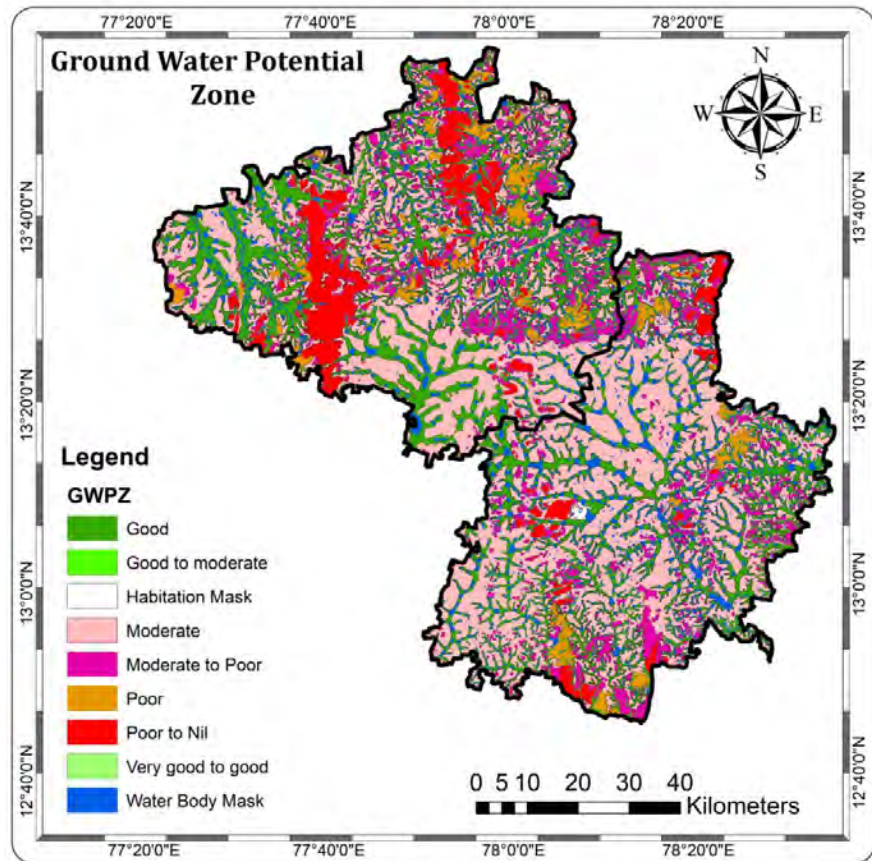
Figure.2.2 Lithology and Ground Water Map

2.5 Soils and Geomorphology:

The terrain in the districts of Kolar and Chikkaballapura ranges from flat to undulating. The district's eastern and northern portions, which make up the Palar River Basin valley, are well-cultivated land. The elevation ranges between 507 m and 1389 m above mean sea level. The district's various soil types are found on a variety of landforms, including ridges, hills, plains, valleys, and pediments. About 71% of the district's total area is suitable for horticulture and agriculture practices, while the remaining 4% is suitable for pasture and forestry. The scattered soil types range from red sandy soil to red loamy soil and lateritic soil, and the existing area is suitable for mining, quarrying, and as a habitat for wildlife. Figures 2.3 and 2.4 depicted the Geomorphology and Soil.
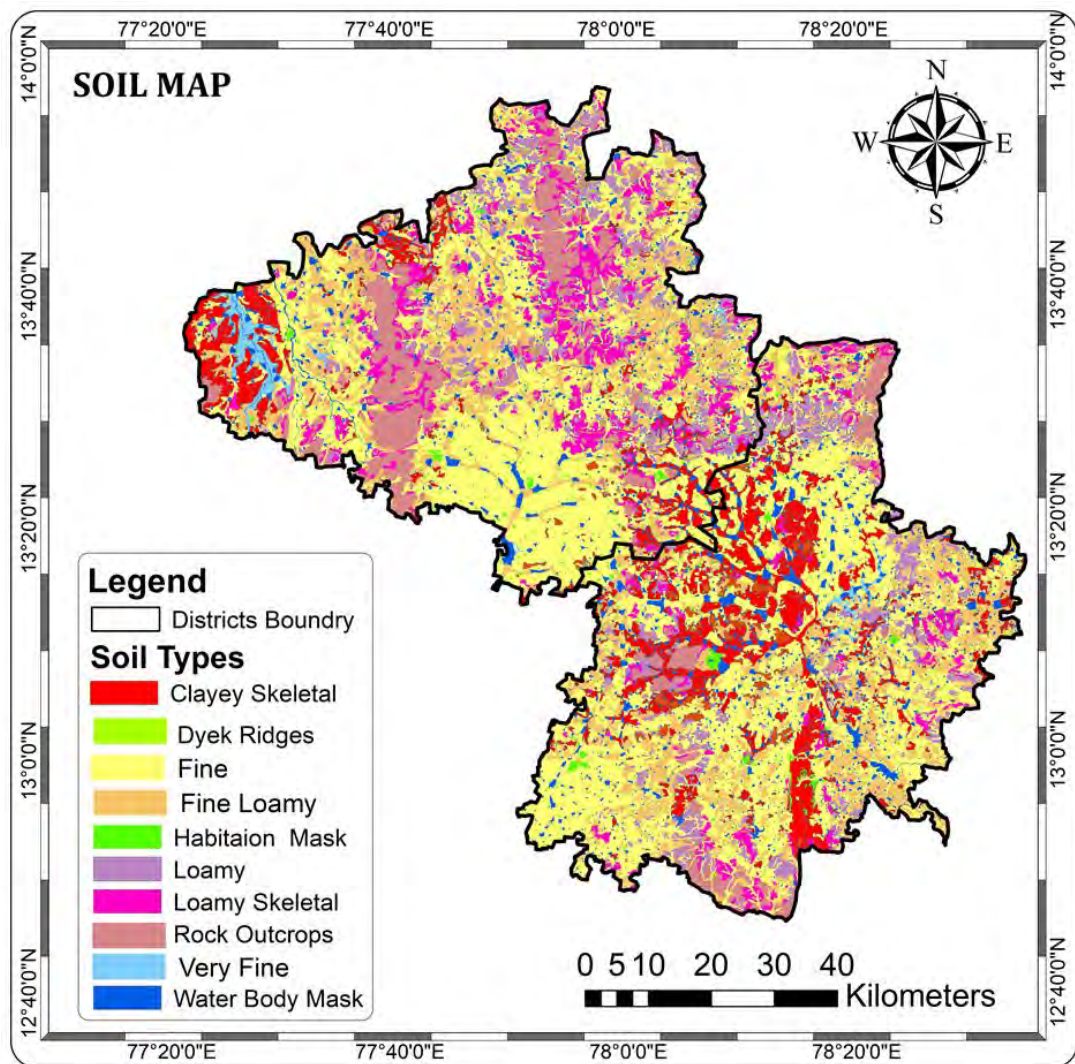
Figure.2.3 Soil Map
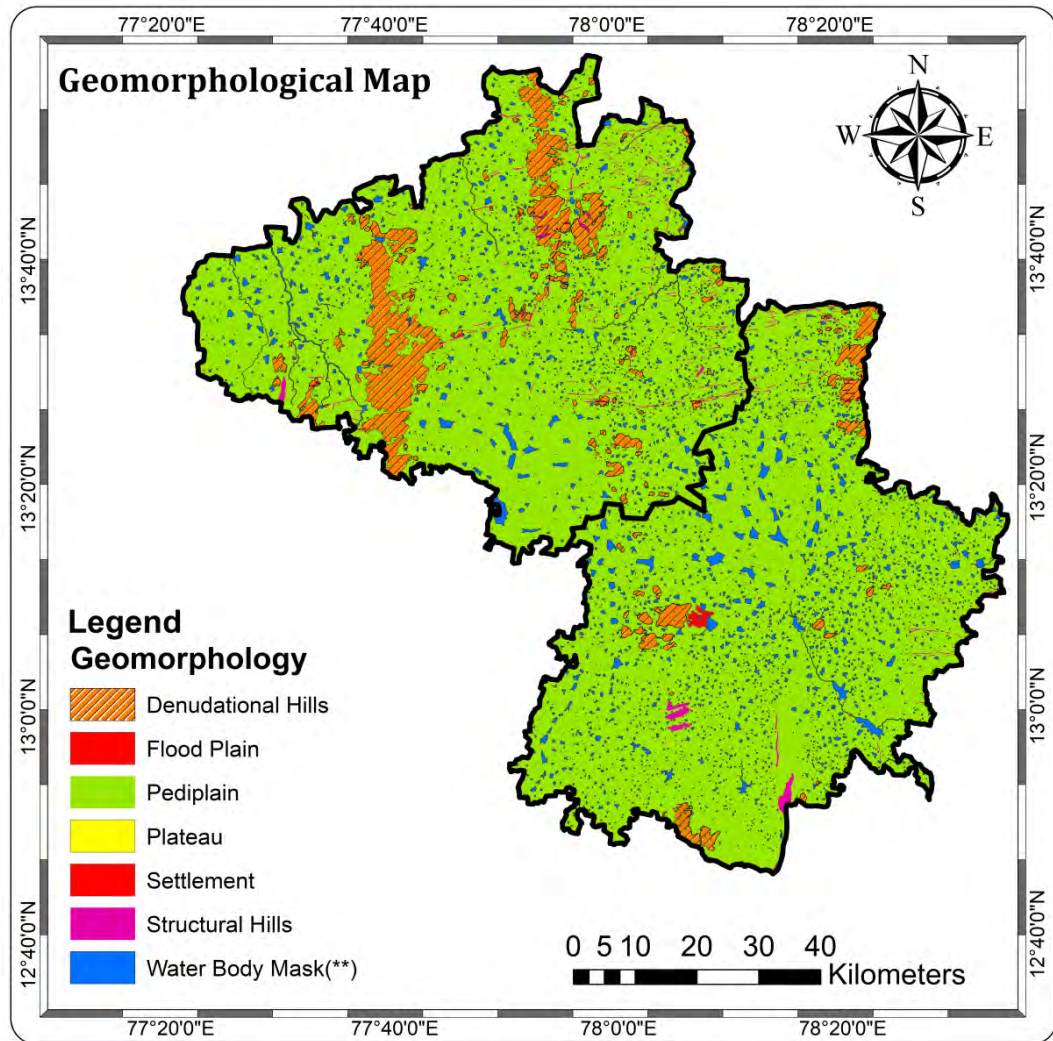
Figure.2.4 Geomorphology Map

2.6 Slope

The slope is a significant feature of the area because it explains the kinetic energy required for water resources to move in the direction of the watershed outlet. The slope varies greatly from place to place. If the area has a steep slope, the rainwater quickly descends towards the hill and collects more in the lowland valleys; however, if the area has a gentle slope, the water causes flooding at the top of the slope. In the districts of Kolar and Chikkaballapura, slopes were present in a variety of forms, ranging from steep to flat. At its northernmost point, the Chikkaballapura represented a very steep slope that was over 35%. The hilly topography of the eastern part of the Kolar district is evident; each area's sloping range is shown in Figure 2.5.
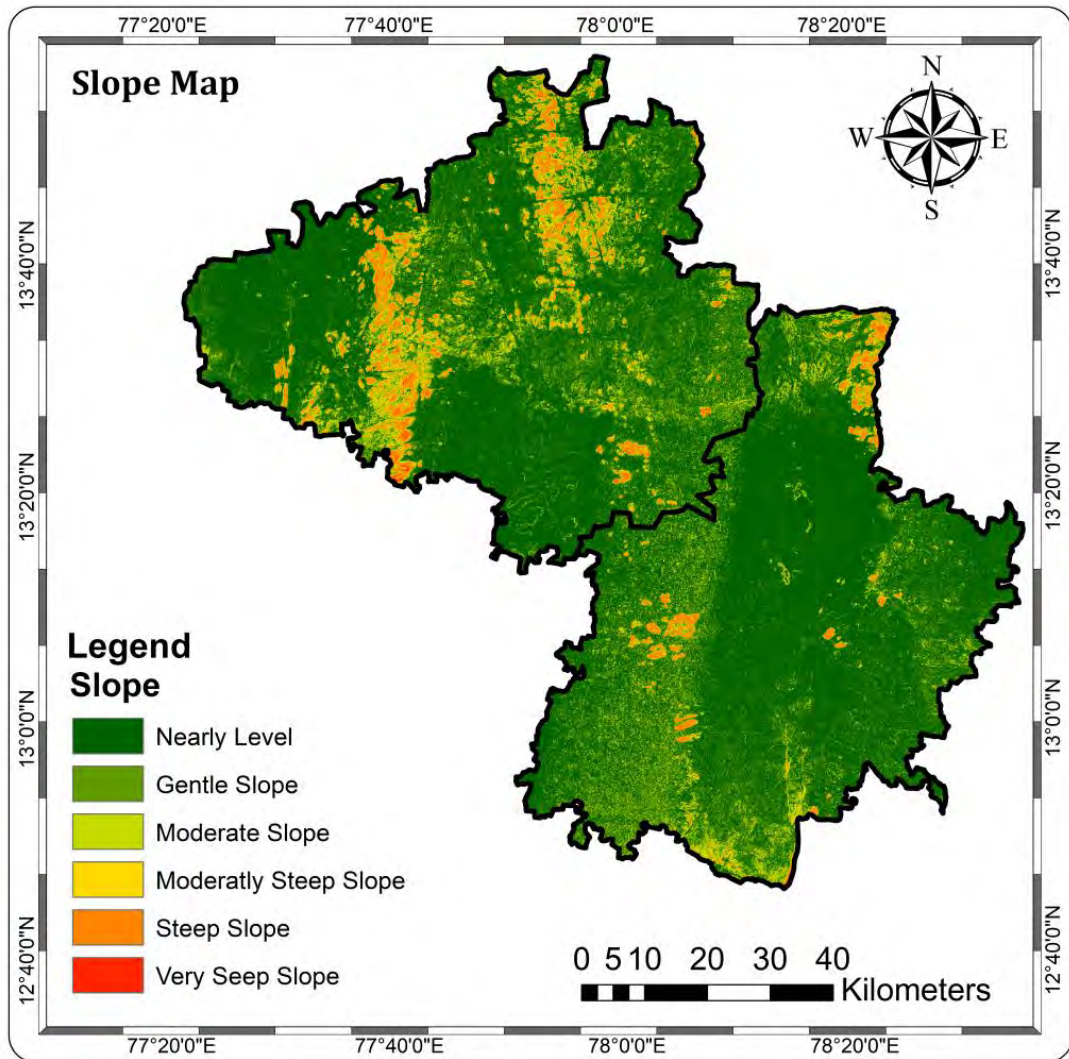
Figure 2.5 Slope Map

2.7 Land Use Land Cover

A forest area makes up 10% of the district's overall region, while cultivable land makes up 67%. The area is uncultivated in 18% of the area. The Area in the forms indicates that the total region of the districts is 35%. The three main crops grown in districts are finger millet, pulses, and groundnuts. Approximately 47% of the total area is used to grow finger millet. Mulberry, Paddy, Potato, Sugarcane, and Vegetables are the main irrigated crops. Grapes and Mangos are the two main commercial fruit crops. 97% of the total irrigated land is in the districts that primarily use dug wells for irrigation. Since 2000, the district's irrigation practices have relied heavily on boreholes.

Table 2 Land Use and Land Cover Statistics

Class	Square Kilometre
Forest Blank	32.78
Acacia Plantation	12.89
Agricultural Plantation	407.89
Barren Rocky/Stony Waste	209.21
Built-up	237.74
Crop Land	5210.24
Dry Deciduous 25-40%	11.92
Eucalyptus Plantation	423.90
Forest Plantation	20.68
Mining/Quarry Area	109.37
Mixed Plantation	321.65
River Island	1.06
Scrub Forest	731.62
Scrub Land	254.17
Water body	332.54
Waterlogged	29.84

The area had very little vegetation, with 5210.24 square kilo meters of cropland used only for seasonal cropping and a large portion of both districts covered in scrub forest (731.62 square kilo meters). The district's remaining portions are bordered by rocky land, stony wasteland, and quarry zones. There are very few river islands and water bodies totaling about 332.54 square kilo meters. The large cities Kolar and Chikkaballapura are large business areas. The built-up land is approximately 237.74 square kilo meters, and the mixed plantation area is 321.65 square kilo meters. The districts' cropping practices primarily involve growing commercial fruits like Mulberry Ragi, Mango, Finger Millet, and others during the rainy season. Figure 2.6 showed how the districts' LULC was represented in Table 2.
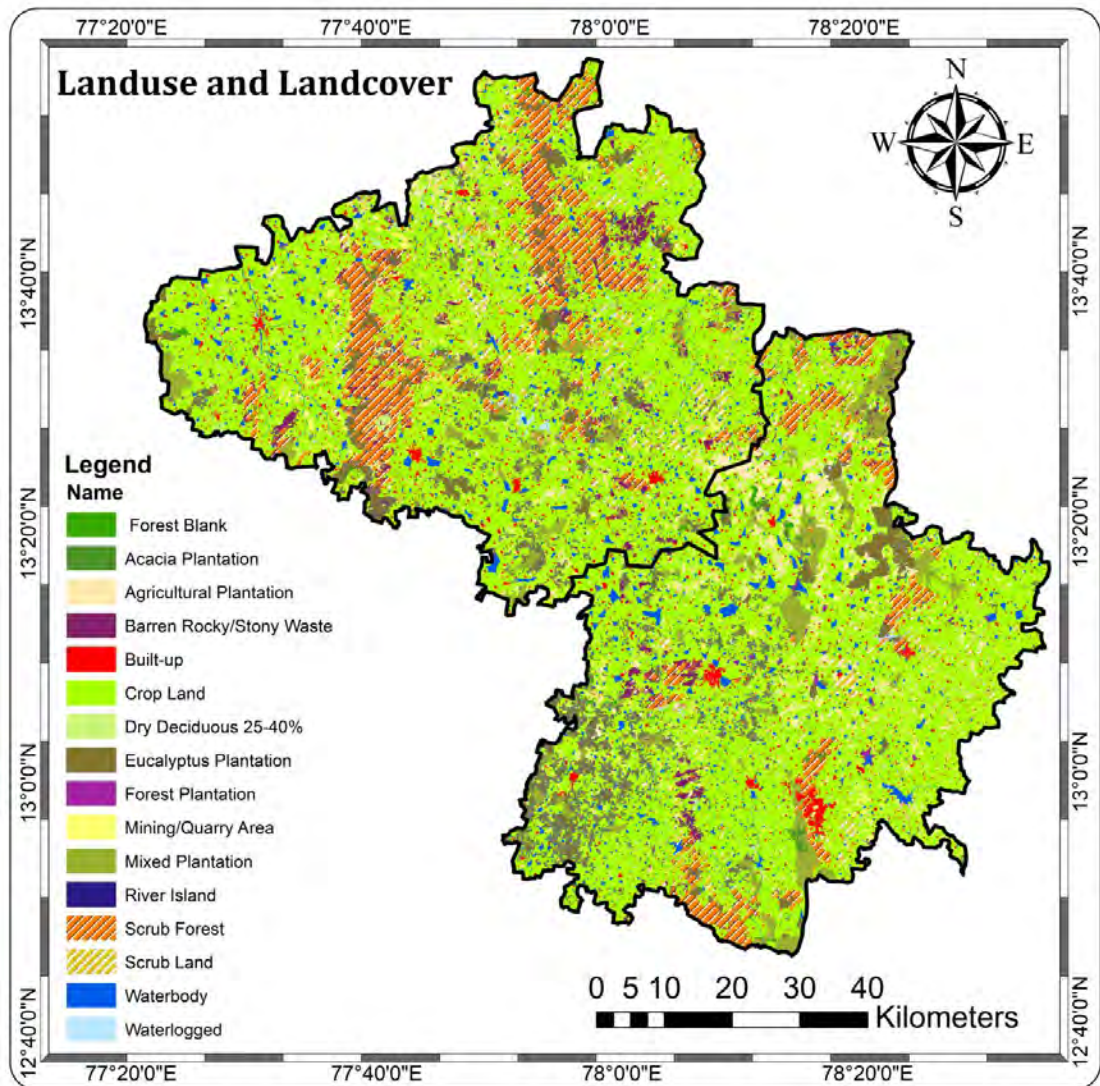
Figure.2.6 Land Use and Land Cover Map

2.8 The Climatic Parameters:

2.8.1 Rainfall and Temperature:

The region's south-eastern agro-dry climate is pleasant. 4 climatic seasons cover the entire year. The post-monsoon season, up until December to February, is when you'll find the dry months with sunny, with clear skies. The hottest months were from March to May during the pre-monsoon period, and from June to October during the southwest monsoon season. Northeast monsoon season begins in November. The districts in central India (2012) experienced a semi-arid climate, which was characterized by tropical weather with hot summers, mild winters, and a typical monsoon season.

Three seasons define the year: the pre-monsoon season (Jan.–May), the southwest monsoon (Jun.–Sept.), and the northeast monsoon season (Oct-Dec). The seasonal rainfall pattern shows that the highest amount of total precipitation, 58%, was received during the southwest monsoon, while the remaining 16% of total precipitation was obtained during the pre-monsoon and 26% during the northeast monsoon (Central Ground Water Board Ministry of Water Resources). Gauribidanur received an average of 840.1 mm of precipitation per year during the Southwest monsoon season, and Bagepalli station received an average of 546.3 mm.

Rainfall is very low in Bagepalli and Gudibande during the pre-monsoon season in all stations (79.7-80mm). The highest rainfall is in the Srinivasapura taluk (238.2mm/year) and Gudibande (165.1mm) during the northeast monsoon. IMD (India Meteorological Department) analyses the district's daily temperature data to determine how the temperature has changed daily, monthly, and annually. Chikkaballapura records 756 mm of annual precipitation, compared to 748 mm in the Kolar. The region's average annual temperature ranges from 14.5 to 35.7 degrees Celsius. Temperature and Rainfall both play a significant role in the hydrological cycle, which regulates seasonal variation in the various regions. This is particularly true in arid regions, where the temperature is much higher than the rainfall. The annual Temperature, Rainfall, and Relative Humidity variation in the area were shown in Figures 2.7, 2.8, 2.9, and 2.10, using the temperature data that was used in the research from 1951 to 2019.
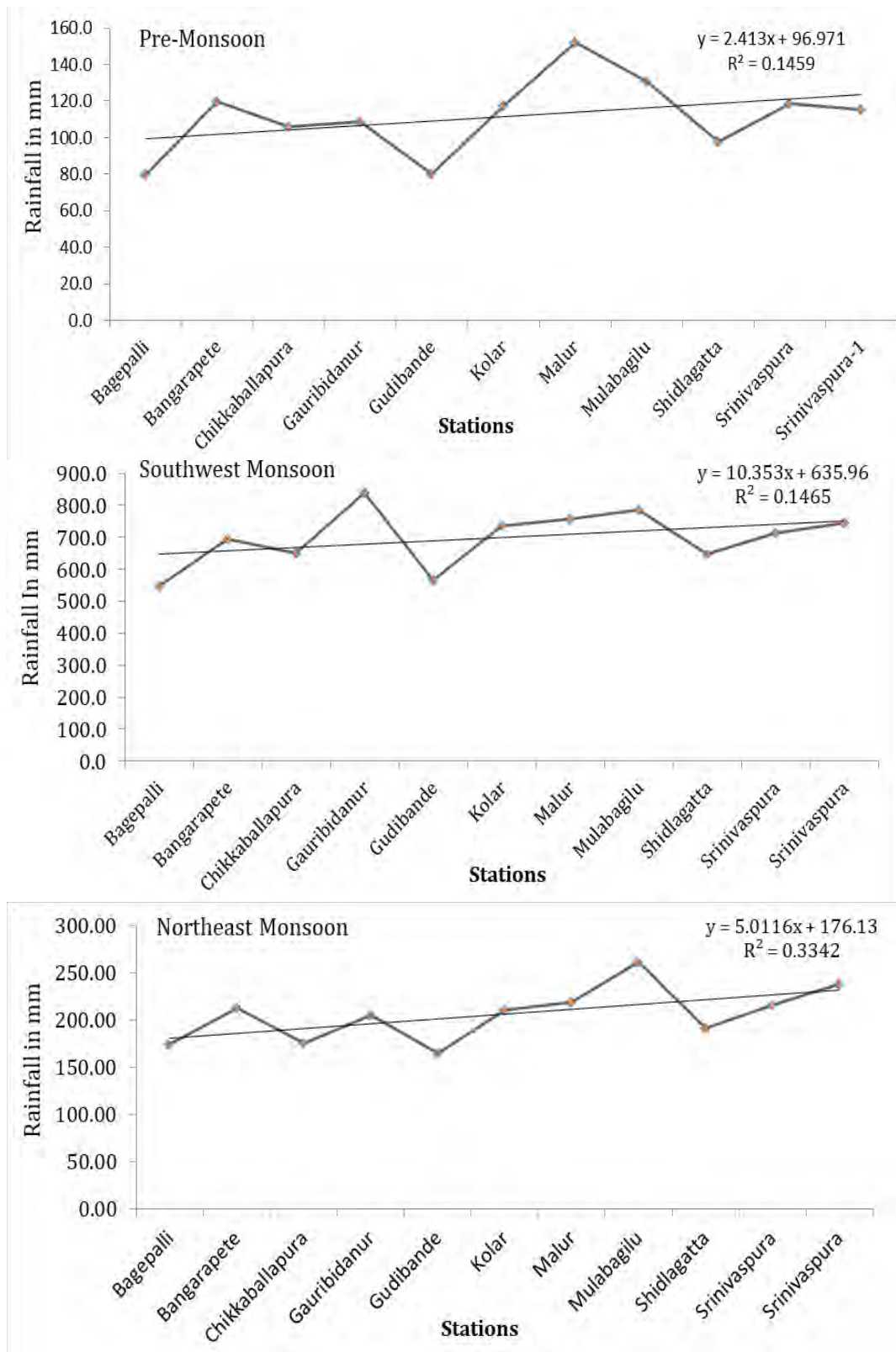
Figure 2.7 Average Rainfall Statistics of Seasons From 1951-2019
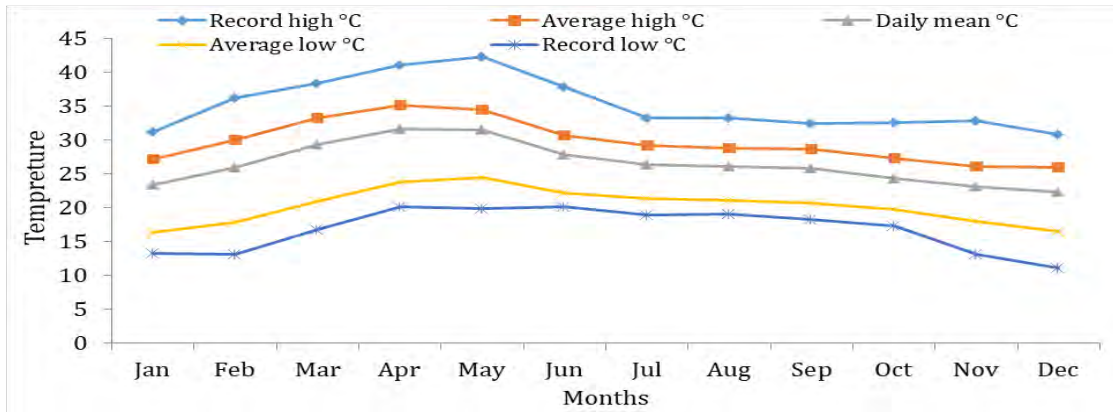
Figure 2.8 Monthly Temperature Statistics
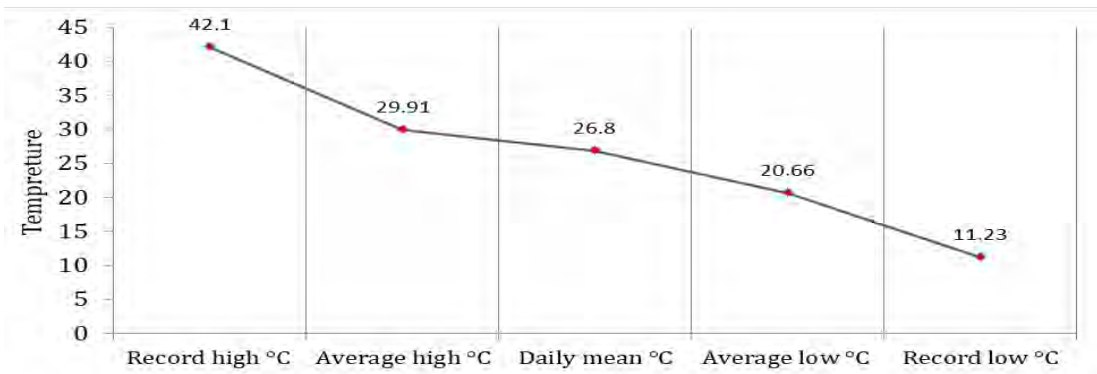
Figure 2.9 Annual Temperature Statistics
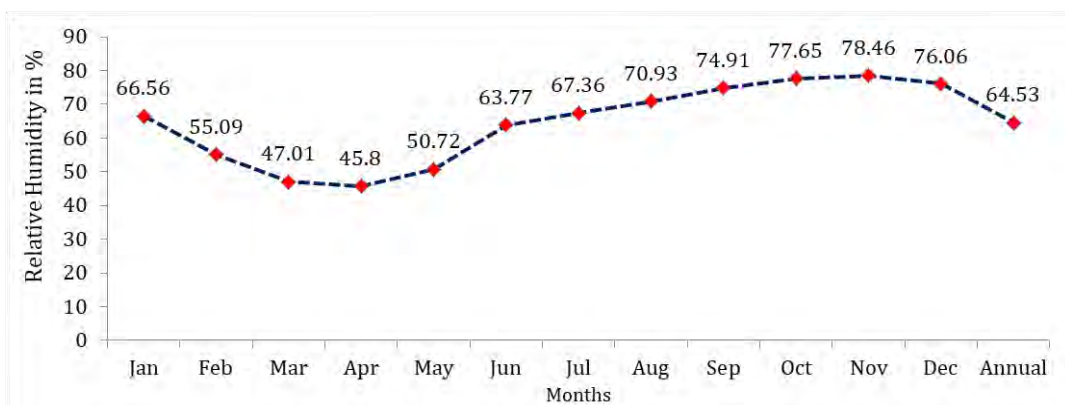
Figure 2.10 Monthly and Annual Relative Humidity Statistics

2.9 Conclusion

      The most important fundamental statistics and details about the research field were presented in this chapter. The research area, which is located in the southernmost region of the Indian state of Karnataka, has a variety of soil types, geomorphological features, lithological characteristics, drainage systems, slopes, land use, and land cover types. The hydrological cycle is greatly impacted by the study of rainfall, temperature, humidity, and other meteorological variables, which results in both excessive and insufficient rainfall. The semi-arid region always indicates less rainfall amount because of the climatic variation of the area. Gauribidanur station in the Southwest monsoon recorded average annual precipitation of 840.1 mm; while Bagepalli station recorded annual precipitation of 546.3 mm. Premonsoon season precipitation is very low across the board, especially in Bagepalli and Gudibande (79.7-80mm). Gudibande (165.1mm) recorded the highest annual rainfall in the Srinivasapura taluk (238.2mm/year) during the northeast monsoon. Mulberry, Graphs, Ragi, Pulses, and other Commercial Crops predominate in this region. The area was primarily dependent on agricultural practices, especially during the monsoon season.

CHAPTER -3
ASSESSMENT OF LONG-TERM DROUGHT

This Chapter is Based On:

Paper 1. Harishnaika N, S A Ahmed, Sanjay Kumar, Arpitha M (2022): Computation of the Spatio-Temporal Extent of Rainfall and Long-Term Meteorological Drought Assessment Using Standardized Precipitation Index Over Kolar and Chikkaballapura districts, Karnataka During 1951-2019, Remote Sensing Applications: Society and Environment: https://doi.org/10.1016/j.rsase.2022.100768:, 100768

Paper 2. Harishnaika N, S A Ahmed, Arpitha M (2022): Spatial and Temporal Assessment of Drought Condition, in Arid Steppe Hot (BSh) Regions of Karnataka State, India by Drought Indices.(Under review)

Chapter-3
Drought Assessment

3. Introduction

Global warming plays a crucial role in the climate change pattern which influences the land surface-atmosphere interactions and environmental variations. For decades, policymakers have been bothered with the issues of gradual climate changes, especially in temperature and precipitation. Such changes majorly impact the intensity, frequency, and Spatio-temporal pattern of precipitation resulting in various meteorological hazards (Arnell, 1999). A rise in global temperature and climate change has resulted in an alarming increase in disasters one of them being drought. Drought is known as a creeping environmental hazard phenomenon (Karavitis et al., 2011), caused by moisture deficiency within a region (Uddameri et al., 2019) that can bring severe causes to environmental, agricultural, and socio-economic consequences around the world (Piao et al., 2010; Jiang et al., 2020; Tirivarombo et al., 2018). In a semiarid and subhumid country such as India, precipitation is very precious in the sense of time and space; therefore, departure in precipitation trends leads to extreme natural hazards such as flood and drought that affect all the natural habitats (He et al., 2009). As per the American meteorological society, drought could be classified into three types of classes: agricultural, meteorological, and hydrological drought (Sona et al., 2012; Udmale et al., 2014; Bhunia et al., 2020). Meteorological drought is defined in terms of the magnitude of precipitation shortfall events as drought effects are noticed. Firstly, it indicates the scarcity of water storage in the reservoir than as a decrease in streamflow which results in depletion of groundwater table followed by a shortage of soil moisture. Agricultural drought is completely the result of a deficiency in soil moisture. Only the southwest monsoon receives nearly 80% share of the total rainfall over the country (Panda and Sahu 2019). Hydrological droughts are related to the precipitation shortfall on the surface and subsurface water supply and it becomes evident in the flow of stream water and deficiency in groundwater level (Haroon et al., 2016). Monitoring the occurrences of drought events and

understanding the suitable indices for the assessment of drought are necessary for reducing and avoiding the loss of property and lives during such events.

The study takes advantage of the standardized precipitation index (SPI) to arrive at sound performing and space-independent representation of rainfall anomaly. Convenience and robustness characteristics have let SPI evolve into a crucial tool on top of being simple to use in comparison to other indices as it requires only rainfall data as input. The study of dry and wet conditions is characterized by SPI which are previously demonstrated by many researchers in various countries such as the Republic of Korea (Kim et al., 2009), China (Pei et al., 2020), (Liu et al., 2021), Bangladesh (Mondol et al., 2017), Algeria (Bilel et al., 2021), Mongolia (Tong et al., 2017), India (Naresh Kumar et al., 2012), (Bhunia et al., 2019), (Das et al., 2020), Turkey (Dikici, 2020). Kolar district, which was recently bifurcated into two districts namely Kolar and Chikkaballapura, occupies the Karnataka table land immediately bounding on the Eastern Ghats. About 90–99% of the total agricultural area of the districts is irrigated by wells. Groundwater is the major source of irrigation in the lack of surface water. All the crop patterns are mostly dependent on the southwest monsoon (June–September) season. Since rainfall datasets are utilized to compute the SPI, a suitable interpolation technique should be used to generate the point values of SPI over the whole study area.

A spatial interpolated map of the standard precipitation index is very informative for assessing the severity level of drought. (Moghbeli et al., 2020; Akhtari et al., 2009). In this research, a geostatistical perspective has been adopted to compose the meteorological drought probability maps based on annual and seasonal SPI values. The analysis of SPI finds its application in drought assessment and provides a reliable solution to suppress the impacts of climate change on precipitation. A detailed approach and scope of this research are the following 1) to investigate the drought observation to elucidate dry and wet years at the district level and in turn evaluate the variability of the climatic conditions over the years 2) to analyze the variability of Spatio-temporal pattern of meteorological drought at seasonal and annual time scale from 1951 to 2019. In this region, no such study has been conducted previously.

3.1 Data

In this research, the daily precipitation dataset with a high spatial resolution ($0.25^0 \times 0.25^0$) gridded rain gauge data have been retrieved from the website of the India Meteorological Department, Pune, from 1951 to 2019. The 11 grid points/station spread across the districts is used for the analysis and preparation of maps. The spatial distribution of daily rainfall data has been converted into average monthly data and aggregated as per seasons such as pre-monsoon, southwest monsoon, northeast monsoon, and annual has been utilized to identify the wet and dry conditions of the study area. The study uses ALOS PALSAR – Radiometric Terrain Correction (RTC) (Laurencelle et al., 2015) DEM-Digital elevation model (Figure. 2) which has a high spatial resolution of about 12.5 m for procuring the elevation of all stations.

3.2 Methodology

SPI In this research, SPI was used to illustrate meteorological drought (Mckee et al., 1993), caused by a deficiency of rainfall. The standardized precipitation index was first initiated by (Mckee et al., 1993; Mallenahalli 2020) in the early 1990s using two-parameter quantification methods for "the purpose of the following discussion to propose an indicator and definitions of drought which could serve as a versatile tool in drought monitoring and analysis" (Cheval 2016). Firstly, the long-term series of rainfall data is defined by a probability function to calculate SPI. This distribution of rainfall data is utilized to compute the cumulative probability of the recorded rainfall amount. To accommodate the rainfall data in this research, a suitable gamma distribution function is chosen. SPI being a representative of the standard deviation is a z-score and portrays an event departure from the mean. SPI has become a famous method for drought computation across the world (Kazemzadeh and Malekian 2016). The real strength of the SPI lies in its ability to be calculated at different time scales showing the deficit or surplus in precipitation which in turn affects the various aspects of the hydrological cycle and makes it possible to deal with drought types. The characteristic of SPI allows for temporal flexibility in the evaluation of rainfall conditions concerning water supply (World Meteorological Organization, 1987). The standardized precipitation index represents the occurrence of

extreme wetness at ≥+2.0 and depicts the extremely dry condition at ≤ -2.0. A positive SPI value indicates more than mean rainfall and a negative SPI value indicates less than average rainfall, and the intensity of wet or dry conditions is indicated by the magnitude of the SPI values. The standardized precipitation index is calculated by using the following equation: function is incomplete(Edwards and Mckee 1997; Mckee, Doesken, and Kleist 1993). it was first fitted to a specified frequency distribution of rainfall series (Kazemzadeh and Malekian 2016). The standardized precipitation index ranged between -2.0 in indicating dry conditions and +2.0 in extremely wet conditions.
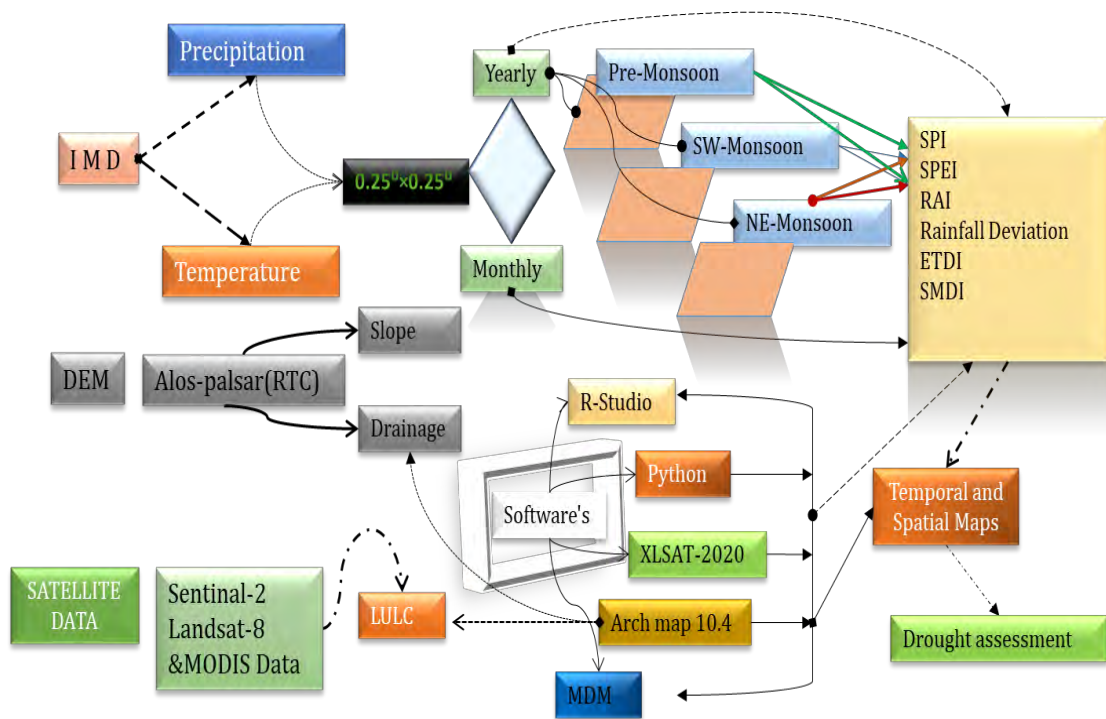
Figure 3. Flowchart of Methodology Adopted for Research

The standardized precipitation index is calculated by using the following equation:

$$g(x) = \frac{1}{\beta^{\alpha}\Gamma(\alpha)} x^{\alpha-1} e^{-\frac{x}{\beta}}(x0), \qquad 1)$$

Where α is indicated the shape parameter, and β denotes the Scale parameter, Γ(α) is a gamma function and x is the precipitation value and the gamma function is expressed as:

$$\Gamma(a) = \int_0^{\infty} x^{a-1} e^{-x} \, dx \qquad 2)$$

The maximum likelihood method is used to predict the optimal value of α and β (Diani et al. 2019)

$$\frac{1}{4A}\left(1 + \sqrt{1 + \frac{4A}{3}}\right) \qquad \qquad 3)$$

$$\beta \quad = \frac{\bar{x}}{\hat{\alpha}} \qquad \qquad 4)$$

$$A = 1\mathrm{n}\,(\bar{x}) - \frac{\Sigma\,1n(x)}{n} \qquad \qquad 5)$$

Where n is the number of rainfall series. The cumulative probability for a month then can be gotten by the following expression:

$$G(x) = \int_0^x g(x)dx = \frac{1}{\beta^\alpha \Gamma(\alpha)} \int_0^x x^{\alpha-1} e^{-\frac{x}{\beta}} dx \qquad \qquad 6)$$

Finally, SPI can be computed by the formula:

$$\mathrm{SPI} \quad = \frac{t - (C_2 t + C_1)\, t + C_0}{((d_3 t + d_2)t + d_1)\, t + 1.0} \qquad \qquad 7)$$

$$t = \sqrt{\ln \frac{1}{G\,(x)^2}} \qquad \qquad 8)$$

Where: n indicates the number of precipitation rainfall records, and x shows the average rainfall; finally SPI can be obtained by the following computation. (Edwards and Mckee 1997)

3.3 Composition of Spatial Maps Using IDW

To illustrate the spatial distribution of precipitation and severity level of drought, the Inverse Distance Weighted (IDW) technique has been used (Robinson and Metternicht 2006). This is based on the concept of distance weighting; The IDW technique estimates an average value for unknown locations using values from closer weighted locations. This interpolation method implements the assumption about those values which are very close to the nearest value. Precipitation grid stations are interpolated by the given nearest point data using weights that depend on the distance gap between rainfall grid stations. The IDW of the SPI dataset was computed by the interpolation method

using ArcGIS 10.8 software. The influence of the unknown point increases as higher weights are used for the value z at an unsampled location i.

$$Z_P = \frac{\sum_{i=1}^{n}\left(\frac{Z_i}{d_{iP}}\right)}{\sum_{i=1}^{n}\left(\frac{1}{d_{iP}}\right)} \qquad 9)$$

Where ZP represents the unknown point, Zi is the value of the known point, di indicates the Euclidean distance from the observation point and estimated point, and n is the user-selected exponential power of the exponent.

3.4 Results and Discussions

3.4.1 Analysis of SPI and Characteristics of Drought

SPI is a crucial tool that helps in understanding the Spatio-Temporal variability of precipitation and its deviation to characterize drought in different time scales. The drought classes based on the severity of dryness and wetness developed by (McKee et al., 1993) were adopted in this study (Table 3). SPI package of MDM software was employed to compute the SPI value. The study was devised to monitor drought events. The outcome of the study observed significant changes in terms of the spatial and temporal pattern of drought in Kolar and Chikkaballapura during the study period. Examination of the magnitude and frequency of drought at the time scale of pre-monsoon (January–May), southwest monsoon (June–September), northeast monsoon (October–December), and annual (January–December) periods has been observed. The study is conducted by calculating the SPI value for each month which was calculated considering the seasons. Overall results of eleven meteorological grid points are evidence of a clear returning pattern about both dryness and wetness conditions in 69 years.
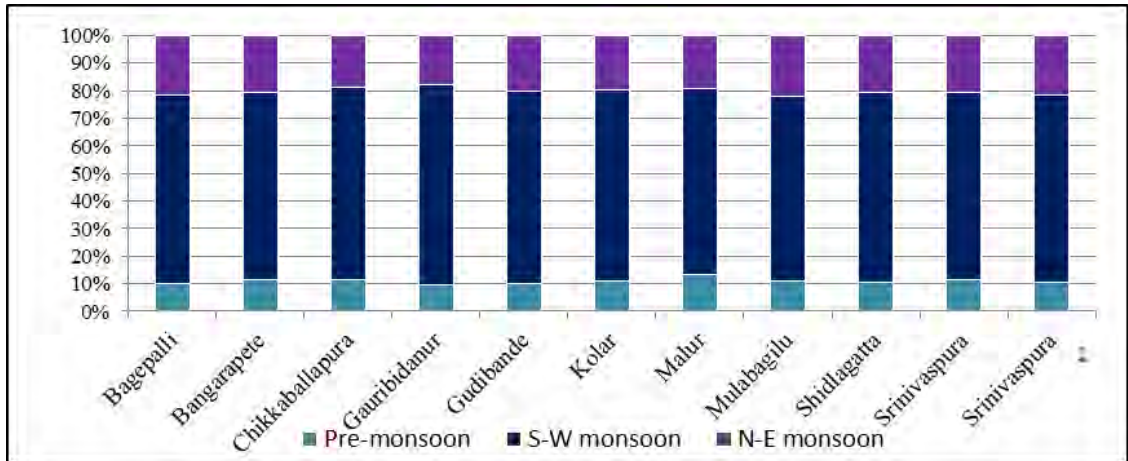
Figure 3.1 Average Rainfall Distributions of Pre, SW, and NE Monsoon in %

Table 3. Total Stations Used in this Study and the Corresponding Information.

Station name	Long	Lat	Time series	Elevation	Max(mm)	Min(mm)	Mean(mm)
Bagepalli	78	13.75	1951-2019	674	1027.4	221.1	531
Bangarapete	78.25	13	1951-2019	754	1447.6	237.4	684
Chikkaballapura	77.75	13.5	1951-2019	863	1153.4	171	611
Gauribidanur	77.5	13.5	1951-2019	663	1163.5	333.4	740
Gudibande	77.75	13.75	1951-2019	662	1068.6	68.2	532
Kolar	78	13.25	1951-2019	762	1199.4	401.7	701
Malur	78	13	1951-2019	783	1392.4	346.6	755
Mulabagilu	78.5	13.25	1951-2019	659	1442.0	271.0	790
Shidlagatta	78	13.5	1951-2019	769	1211.1	319.0	619
Srinivasapura	78.25	13.25	1951-2019	717	1293.2	331.8	696
Srinivasapura-1	78.25	13.5	1951-2019	673	1295.0	344.5	731

Table 3.1. Classification of SPI SPEI, and RAI range Values (Mckee, Doesken, and Kleist 1993)

Index	No-drought	Mild-drought	Moderate drought	Severe drought	Extreme drought
SPI	$-0.5 < SPI$	$-1.0 < SPI \leq -0.5$	$-1.5 < SPI \leq -1.0$	$-2.0 < SPI \leq -1.5$	$SPI \leq -2.0$
SPEI	$-0.5 < SPEI$	$-1.0 < SPEI \leq -0.5$	$-1.5 < SPEI \leq -1.0$	$-2.0 < SPEI \leq -1.5$	$SPEI \leq -2.0$
RAI	-0.49 to 0.49	-1.99 to -0.5	-2.00 to -2.99	-3.00 to -3.99	≤ -4.00

Table 3.2. Rain Gauge Stations with the Statistical Information From 1951-2019.

Bagepalli

Months	Observations	Minimum	Maximum	Mean	Std. deviation
January	69	0.0	28.8	1.8	5.7
February	69	0.0	72.3	3.8	11.2
March	69	0.0	88.6	5.8	13.5
April	69	0.0	90.1	15.9	19.3
May	69	0.0	181.0	52.5	38.5
June	69	0.7	327.6	50.6	47.2
July	69	2.2	196.9	53.3	44.7
August	69	0.2	189.8	61.6	46.3
September	69	5.6	267.9	111.5	67.7
October	69	2.4	333.1	121.0	73.2
November	69	0.0	391.2	52.3	63.6
December	69	0.0	2.8	0.5	0.7
Annual	69	220.1	1026.4	530.6	175.9

Chikkaballapura

Months	Observations	Minimum	Maximum	Mean	Std. deviation
January	69	0.0	27.9	1.6	4.9
February	69	0.0	45.1	3.2	9.1
March	69	0.0	128.9	6.9	19.1
April	69	0.0	112.0	25.7	25.1
May	69	0.0	160.9	68.5	46.3
June	69	0.0	238.7	57.8	45.4
July	69	0.0	280.5	71.9	58.7
August	69	0.0	218.6	77.8	54.9
September	69	0.0	302.4	122.2	76.1
October	69	0.0	596.9	130.4	105.9
November	69	0.0	310.0	44.5	55.6
December	69	0.0	2.2	0.4	0.6
Annual	69	178.0	1155.4	611.0	219.4

Bangarapete

Months	Observations	Minimum	Maximum	Mean	Std. deviation
January	69	0.0	37.7	2.5	6.3
February	69	0.0	62.2	3.9	12.2
March	69	0.0	57.5	9.4	14.9
April	69	0.0	187.2	27.0	32.1
May	69	0.8	197.4	76.7	51.8
June	69	0.3	233.9	62.6	49.6
July	69	4.4	259.6	73.5	57.9
August	69	0.2	238.5	79.7	60.4
September	69	9.2	351.4	136.7	81.2
October	69	4.6	452.5	135.1	86.4
November	69	0.0	394.6	76.4	75.7
December	69	0.0	5.1	0.8	1.0
Annual	69	237.5	1443.7	684.2	247.7

Gauribidanur

Months	Observations	Minimum	Maximum	Mean	Std. deviation
January	69	0.0	24.3	1.9	5.1
February	69	0.0	38.9	3.3	7.8
March	69	0.0	95.7	8.9	18.1
April	69	0.0	99.5	24.5	23.7
May	69	0.0	186.7	70.3	43.5
June	69	5.6	210.6	69.0	39.5
July	69	7.5	328.3	93.6	63.0
August	69	14.0	298.1	110.8	65.6
September	69	23.3	448.6	152.7	84.7
October	69	5.6	467.1	151.0	91.2
November	69	0.0	313.5	53.7	56.1
December	69	0.0	2.0	0.4	0.5
Annual	69	337.5	1168.6	740.1	205.6

38

Table 3.2. Continued…

Gudibande

Months	Observations	Minimum	Maximum	Mean	Std. deviation
January	69	0.0	50.6	2.1	8.2
February	69	0.0	37.6	1.8	6.5
March	69	0.0	127.6	6.9	21.5
April	69	0.0	78.4	17.3	18.4
May	69	0.0	185.2	51.9	41.5
June	69	0.2	221.7	45.4	41.6
July	69	1.1	337.7	58.9	57.6
August	69	0.0	324.3	71.4	65.0
September	69	1.3	303.4	110.7	73.0
October	69	0.5	457.5	121.1	105.5
November	69	0.0	280.1	43.7	56.8
December	69	0.0	3.0	0.3	0.6
Annual	69	68.9	1068.6	531.5	211.1

Kolar

Months	Observations	Minimum	Maximum	Mean	Std. deviation
January	69	0.0	37.0	2.3	5.4
February	69	0.0	48.8	4.1	10.0
March	69	0.0	48.5	8.5	13.6
April	69	0.0	84.2	27.0	24.0
May	69	0.8	163.0	75.3	42.1
June	69	0.8	207.7	63.1	47.7
July	69	0.2	324.9	76.3	64.1
August	69	4.0	250.2	90.7	62.1
September	69	5.2	337.5	142.9	76.5
October	69	15.5	403.6	152.1	89.3
November	69	0.0	389.9	58.2	58.3
December	69	0.0	3.2	0.6	0.7
Annual	69	240.6	1198.5	701.3	203.3

Malur

Months	Observations	Minimum	Maximum	Mean	Std. deviation
January	69	0.0	43.2	3.0	8.0
February	69	0.0	75.0	5.2	13.9
March	69	0.0	99.4	16.7	23.6
April	69	0.0	171.7	38.5	40.2
May	69	9.0	232.6	88.5	48.4
June	69	1.2	261.8	70.5	56.9
July	69	3.8	284.8	69.8	57.5
August	69	4.9	311.0	87.4	69.8
September	69	13.7	540.8	156.1	104.3
October	69	0.4	487.4	151.6	93.8
November	69	0.0	435.7	66.8	72.0
December	69	0.0	3.8	0.7	0.9
Annual	69	348.6	1398.5	754.7	224.8

Mulubhagilu

Months	Observations	Minimum	Maximum	Mean	Std. deviation
January	69	0.0	61.1	3.7	9.0
February	69	0.0	58.8	5.4	12.7
March	69	0.0	90.8	10.8	18.2
April	69	0.0	174.5	29.2	31.8
May	69	10.7	358.9	81.8	63.5
June	69	0.7	184.5	71.5	41.7
July	69	0.8	383.3	94.5	77.1
August	69	1.7	284.2	89.2	62.8
September	69	5.9	295.8	143.2	71.6
October	69	23.9	455.3	162.7	96.1
November	69	0.0	543.7	97.2	90.7
December	69	0.0	6.9	1.1	1.4
Annual	69	270.0	1447.0	790.3	209.5

Table 3.2. Continued…

Months	Observations	Minimum	Maximum	Mean	Std. deviation
January	69	0.0	21.8	1.9	4.0
February	69	0.0	33.0	3.6	7.3
March	69	0.0	72.0	8.1	16.4
April	69	0.0	83.2	23.3	22.7
May	69	1.8	149.1	61.0	38.6
June	69	0.2	180.5	56.6	41.9
July	69	0.4	216.7	66.2	55.3
August	69	4.5	217.6	76.8	51.7
September	69	3.4	267.8	129.6	63.9
October	69	8.1	403.7	132.3	89.8
November	69	0.0	423.4	58.9	76.3
December	69	0.0	2.0	0.4	0.5
Annual	69	316.0	1213.1	618.7	207.0

Sidhlaghatta

Months	Observations	Minimum	Maximum	Mean	Std. deviation
January	69	0.0	43.7	2.5	6.4
February	69	0.0	54.4	5.4	12.3
March	69	0.0	110.3	9.8	19.7
April	69	0.0	122.6	28.6	29.9
May	69	4.6	200.5	72.2	44.0
June	69	1.2	227.3	65.9	53.7
July	69	0.3	242.1	71.0	56.6
August	69	0.7	330.7	87.0	66.3
September	69	2.7	319.0	137.4	68.6
October	69	0.9	422.2	136.7	85.6
November	69	0.0	413.4	78.4	81.6
December	69	0.0	5.7	0.8	1.0
Annual	69	331.9	1297.3	695.6	213.7

Srinivasapura

Months	Observations	Minimum	Maximum	Mean	Std. deviation
January	69	0.0	0.0	45.4	4.4
February	69	0.0	0.0	77.9	6.4
March	69	0.0	0.0	117.8	9.7
April	69	0.0	0.0	111.1	25.7
May	69	1.8	1.4	201.8	69.3
June	69	0.2	16.9	323.4	71.3
July	69	0.4	7.3	276.6	81.6
August	69	4.5	4.9	283.1	96.0
September	69	3.4	17.3	263.5	128.6
October	69	8.1	8.3	431.1	148.1
November	69	0.0	0.2	513.8	89.1
December	69	0.0	0.0	3.9	1.0
Annual	69	316.0	347.5	1296.0	731.1

Srinivasapura-1

3.4.2 Precipitation Distributions From 1951-2019

The total mean rainfall over the study area from 1951 to 2019 is 671.81 mm with a standard deviation of 209.86 mm. In comparison, all the stations in the Chikkaballapura district apart from Gauribidanur with a mean rainfall of 740 mm and a standard deviation of 204.1 mm receive less rainfall than the stations in the Kolar district. Bagepalli and Gudibande stations which lie in the arid steppe hot (Aw) zone have recorded similar least mean rainfall of 531 mm and 532 mm respectively and standard deviations of 174.5 mm and 209.57 mm over the years. On average, the low-lying stations receive more rainfall as they are present in the windward face of the high elevation; the stations included are Mulabagilu, Gauribidanuru, and Srinivaspura. The low-lying station (659 m elevation) of Mulabagilu present in the tropical savanna (BSh) zone indicates the maximum mean rainfall of 790 mm and standard deviation of 207.9 mm over time. The adjacent stations of Chikkaballapura and Sidlagatta display almost similar mean rainfall values of 611 mm and 619 mm respectively. The corresponding standard deviation values are 245.9 mm and 205.5 mm respectively. The mean rainfall and the standard deviation of the remaining stations in the Kolar district are as follows: Bangarapete (684 mm and 245.9 mm), Kolar (701 mm and 201.7 mm), Malur (755 mm and 223.7 mm), Srinivaspura (696 mm and 212.1 mm), and Srinivaspura-1 (731 mm and 210.5 mm). There is variability in the rainfall distribution over the stations in the study area as indicated by rainfall data, elevation, and climatic zone (Table 3.2). The highest rainfall recorded in Mulabagilu station with a positive deviation of 83.16% in 1975 is 1447.01 mm. In 1983, Gudibande station experienced a record low rainfall of 68.92 mm with a negative deviation of − 87.04%. Seasonally, both districts demonstrate a homogenous pattern in rainfall distributions with the maximum amount in the south-west monsoon (June–September), minimum in the pre-monsoon (Jan–May), and moderate rainfall in the north-east monsoon (October–December). In the pre-monsoon season, Bagepalli and Gudibande stations show the least average rainfall. Bagepalli recorded an average rainfall of 79.7 mm with the least amount of 0.9 mm in 2003. Gudibande station received an average rainfall of 80.0 mm with 1.9 mm in 1964 being the least value. During the Kharif season (south-west monsoon), the maximum rainfall was seen in

Table 3.3 Annual Rainfall Deviations in Drought Years.

Stations	Deviation							Frequency		Duration %		Drought category	
	Extreme drought		Severe drought										
Bagepalli	1985	-58.54	2002	-46.88	2004	-32.26							
	1984	-54.60	1965	-46.15	1986	-31.52							
	1951	-52.24	2003	-38.76	1992	-29.75		0.07	0.15	7.24	15.94	ED	SD
	1983	-51.22	1980	-36.95	1952	-27.92							
	1982	-50.79	2006	-36.00	1998	-27.59							
					1959	-26.04							
Chikkaballapura	1959	-70.87	1989	-49.69	1983	-37.32							
	1995	-68.41	2006	-49.36	1992	-32.41							
	1990	-58.62	2003	-45.45	1957	-32.14							
			2002	-43.94	1985	-31.12		0.04	0.23	4.35	23.2	ED	SD
			1952	-42.74	1978	-30.71							
			1965	-40.84	2018	-28.40							
			1979	-40.82	1980	-27.15							
			1994	-39.84	1986	-26.85							
Gauribidanur	1965	-54.39	1952	-46.55	1985	-33.63							
			1990	-40.45	2012	-33.22							
			1957	-40.43	2014	-27.96							
			2018	-38.60	1999	-27.87		0.01	0.19	1.45	18.84	ED	SD
			2007	-38.05	2000	-27.87							
			2002	-37.99	1992	-25.55							
			1989	-36.66									
Gudibande	1983	-87.05	2002	-46.75	2001	-30.39							
	1971	-72.50	1977	-43.01	1992	-30.11							
	1987	-56.99	1985	-41.24	1976	-28.98							
	1999	-52.66	1998	-40.98	1978	-27.70		0.09	0.21	8.7	21.7	ED	SD
	2006	-52.40	1952	-40.50	2004	-27.58							
	1970	-50.86	1968	-40.26	1982	-27.48							
			1980	-38.74	1989	-25.24							
			2003	-34.27									
Kolar	1982	-65.68	1980	-47.85	2002	-30.73							
	1983	-53.82	1952	-42.69	1985	-30.20							
			1961	-40.85	1960	-28.93		0.03	0.16	2.90	15.94	ED	SD
			1965	-36.57	1995	-27.53							
			1957	-32.90	2016	-25.90							
			2018	-32.61									
Malur	1952	-53.81	1968	-43.93	1963	-32.70							
			1976	-42.71	1971	-28.22							
			2002	-40.55	1957	-27.88							
			1980	-40.02	1985	-27.44		0.01	0.17	1.45	17.39	ED	SD
			2016	-35.56	1965	-27.19							
			1961	-32.72	1982	-27.15							
Mulabhagilu	1957	-65.84	1980	-43.51	1965	-29.14							
	2006	-56.24	2007	-37.29	1987	-26.38		0.03	0.12	2.90	11.59	ED	SD
			1952	-32.87	2002	-25.38							
			1990	-30.83	1967	-25.17							

Table 3.3. Continued...

Stations	Deviation						Frequency		Duration %		Drought category	
	Extreme drought		Severe drought									
Bangarapete	1965	-65.28	1961	-49.29	1970	-37.69	0.06	0.16	5.80	13,67	ED	SD
	1959	-59.38	1980	-42.90	1958	-34.53						
	1967	-57.16	1957	-40.99	1986	-30.57						
	1971	-51.54	1952	-38.05	1976	-28.55						
			1960	-37.98	2007	-27.54						
					1982	-27.47						
Sidhlaghatta	-	-	1982	48.93	1996	-37.44	0.20	0.19	6.78	20.29	ED	SD
			2002	-46.02	1952	-33.28						
			2003	-46.02	1994	-33.08						
			1999	-45.27	2018	-33.01						
			1965	-42.79	1990	-31.58						
			1961	-42.10	2006	-29.81						
			1980	-39.48	1997	-26.96						
Srinivasapura	1965	-52.29	1967	-46.42	1961	-35.67	0.03	0.13	2.90	13.04	ED	SD
	1952	-51.89	1959	-45.77	1955	-31.49						
			2016	-45.39	1968	-28.98						
			1980	-44.09	1973	-28.85						
			1960	-36.80								
Srinivasapura-1	1965	-52.46	1980	-44.91	2016	-32.58	0.01	0.19	1.45	18.84	ED	SD
			2018	-40.85	1982	-32.18						
			1952	-38.69	2006	-29.28						
			1986	-38.66	1955	-27.14						
			1968	-38.62	1960	-27.12						
			1959	-34.93	1961	-25.34						
			1951	-33.58								

Gauribidanur and Mulabagilu with the average rainfall value being 426.1 mm and 398.3 mm respectively. Gauribidanur experienced 809.6 mm of rainfall in 1964 which was the Maximum during the season. Kolar and Gudibande displayed the least precipitation of 42.7 mm (1980) and 48.2 mm (1983) respectively. The average rainfall received in the study area during the northeast monsoon is 205.8 mm over the years. The overview of the highest and lowest rainfall distribution is listed in Table 3.5. Overall accounting for average rainfall, 8–10% of the precipitation was seen during the pre-monsoon, 55–60% of the rainfall during the southwest monsoon and 25–30% rainfall during the northeast monsoon (Figure 3.1 and Table 3.3).

3.4.3 Correlation of Standardized Precipitation Index and Yearly Rainfall

Using the range values of SPI classes, annual rainfall distribution (Table 2) values between 1951 and 2019 have been computed for grid stations over the entire district annually (Figure. 3.2). The relationship between the X and Y axes of rainfall is defined by R2 value for yearly precipitation. A positive rainfall deviation shows that there is more than normal rainfall and a negative value indicates less than normal rainfall value. The number of dry years is exhibited in Table 3.3. Bagepalli reveals significantly below normal rainfall and 17 deficient years below near-normal SPI value of 0.00. The station continuously received significantly low rainfall during the years 1982–1986 and the SPI value corresponding to these years also indicates negative values hence agreeing with the result. Similarly from 2000 to 2004, decreased precipitation can be seen which correlates with the low SPI value of − 0.38 in 2003. The R2 value for Bagepalli is 0.0476 representing a slight positive slope with the frequency of extreme drought being 0.07.

Table 3.4 A total number of Annual Drought Years During the Study Period.

Bagepalli	Bangarapete	Chikkaballapura	Gauribidanur	Gudibande	Kolar
1951,1952,1954, 1955,1957,1965, 1972,1980,1982, 1983,1984,1985, 1999, 2002,2004, 2006.	1951,1955,1956, 1957,1958,1959, 1960,1961,1962, 1963,1964,1967, 1968,1970,1971, 1972,1974,1976, 1980,1980,1982, 1983,1989,2002, 2003,2013.	1957,1959,1965, 1979, 1983, 1987, 1989, 1990, 1992, 1994, 1995, 2002, 2003, 2006.	1952,1957,1965, 1982,1987,1989, 1990,1992,1993, 1994,1999,2000, 2002,2003,2004, 2007,2012,2014, 2018.	1952.1960.1964, 1968,1969,1970, 1971,1972,1976, 1977,1979,1980, 1983,1987,1989, 1998,1999,2001, 2003,2006.	1951,1952,1954, 1957,1960,1961, 1965,1968,1970, 1974,1980,1982, 1983,1985,1989, 1995,1996,2002, 2003, 2006, 2016, 2018.
Malur	Mulabagilu	Shidlagatta	Srinivaspura	Srinivaspura-1	
1951,1952,1955, 1957,1961,1963, 1965,1968,1970, 1974,1976,1980, 1982,1985,1987, 1988,2002.	1951.1955,1957, 1959,1960,1965, 1974,1976,1980, 1982.1988,1989, 1990,1992,1994, 2002,2006,2007, 2014,2016.	1954,1960,1961, 1965,1980,1982, 1985,1989,1990, 1994,1996,1997, 1998,1999,2000, 2001,2002,2003, 2004,2005,2006, 20018.	1951,1952,1954, 1955,1957,1959, 1960,1961,1964, 1965,1968,1969, 1974,1980,1982, 2984,1985,1986, 1989,1992,1999, 2002,2003,2006, 2016,2018.	1951,1952,1954, 1955,1957,1959, 1960,1961,1964, 1965,1968,1969, 1970,1974,1976, 1980,1982,1885, 1986,1989,1992, 1999,2002,2003, 2006,2016,2018.	

The data points to a decrease in rainfall which is substantiated by a negative deviation of 57.37% which is associated with average SPI values from − 0.1 to − 0.5.15.94% of the time showing a deviation of − 25% to − 50% indicating a prominent reduction from normal precipitation (moderate to severe drought). Beyond − 50% deviation is seen in 7.24% of the duration of extreme drought. An increasing linear curve is seen in the stations Bangarapete, Malur, Srinivaspura, and Srinivaspura-1. Gauribidanur and Chikkaballapura have witnessed a decreasing curve in recent years. Bagepalli and Sidlaghatta stations receive relatively less rainfall than the others. The comparison of precipitation and SPI values is shown in Figure 3.2. To determine the spatial framework of rainfall and drought seriousness of stations IDW is used to plot the frequency and duration of drought.

3.4.4 Spatial Trend Pattern of Annual Drought

The spatial trend pattern and distribution of dry /wet conditions, the spatial extension of drought in annual standard precipitation index result, few of the major drought years found in the district were stated in Table.3.3. During 1955, 1978, 2009, and 2014, the annually whole two districts were generally bound with dryness. Moreover, the Kolar district dryness between 1952, 1955 to 1978, 1980, 1988, 2008 to 2011, 2013, 2014, and 2018. Similar to other parts of the whole Chikkaballapura district had an annual dry period in 1998, 2001, 2003, 2004,2006,2007,2009, and 2014 all gridded stations were recorded drought years in this study period with compared to the Kolar district, the area had the wettest year and less dry period, rest of the year are relatively near the normal value of drought. Figure 3.4 indicate the spatial trend of drought conditions majorly in 1955 the year that shows the maximum negative SPI value in the South eastern part of the district about -2.1 and north western part of the district has the normal wet condition.

The year 1974 and 2003 is the dry year because the actual rainfall is less than the average annual rainfall.
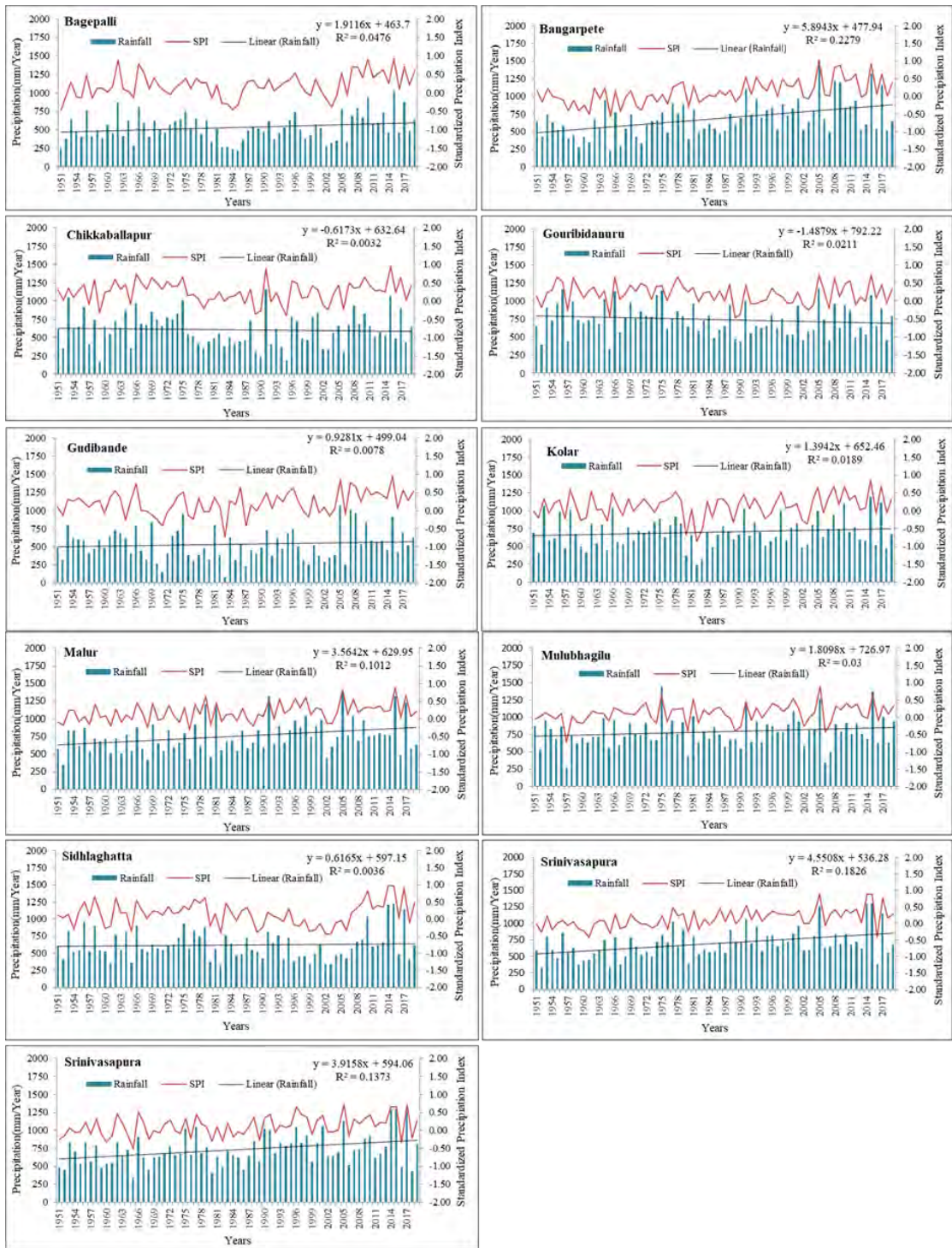
Figure 3.2 Temporal Variation of Annual Rainfall and SPI

3.4.5 Seasonal Characteristics of Standard precipitation index

The value of SPI has been computed for different seasons in a year to study the temporal trend in drought events which is graphically presented in Figure. 3.3. Noticeably, drought seriousness has changed and a mix of wet and dry years has been spotted. Further, SPI values were calculated based on monsoon seasons. There have been several years that show normal and moderate drought during the rabi and Kharif seasons. Apart from this, several years have witnessed nearly severe and extreme dry events happening in the midland late Kharif seasons.

3.4.5.1 Pre-Monsoon

For the pre-monsoon season, Bangarapete, Srinivaspura, and Mulabagilu rank top in terms of drought duration lasting 21.74%, 21.74%, and 24.64% respectively. In 1989, Bangarapete holds the least average SPI value of − 0.42 and Mulabagilu has − 0.43 in 1964. The other stations witnessed a quite relaxing scenario as the duration of drought during pre-monsoon seems minor when compared to the other seasons. The average drought duration of all the stations is 15.81% and has an average frequency of 0.157. In 1964, all stations apart from Chikkaballapura exhibited drought events. Bangarapete witnessed a prolonged drought from 1963 to 1965. Similarly, Mulabagilu station dealt with drought from 1964 to 1966.

Based on Figure 3.5 indicates the spatial variations of Drought and wet conditions in different meteorological years in 1974 the Kolar district shows more drought in that decade in the Southern part of the area.1981 suffers the huge drought condition in the northern part of the Chikkaballapura. Because January to May has less rainfall in the semi-arid regions. In the leeward part of the mountain regions, the air pressure will be high then the clouds form less amount of rainfall, and the atmospheric moist air moves to warm the surface of the region, especially in the arid environment.
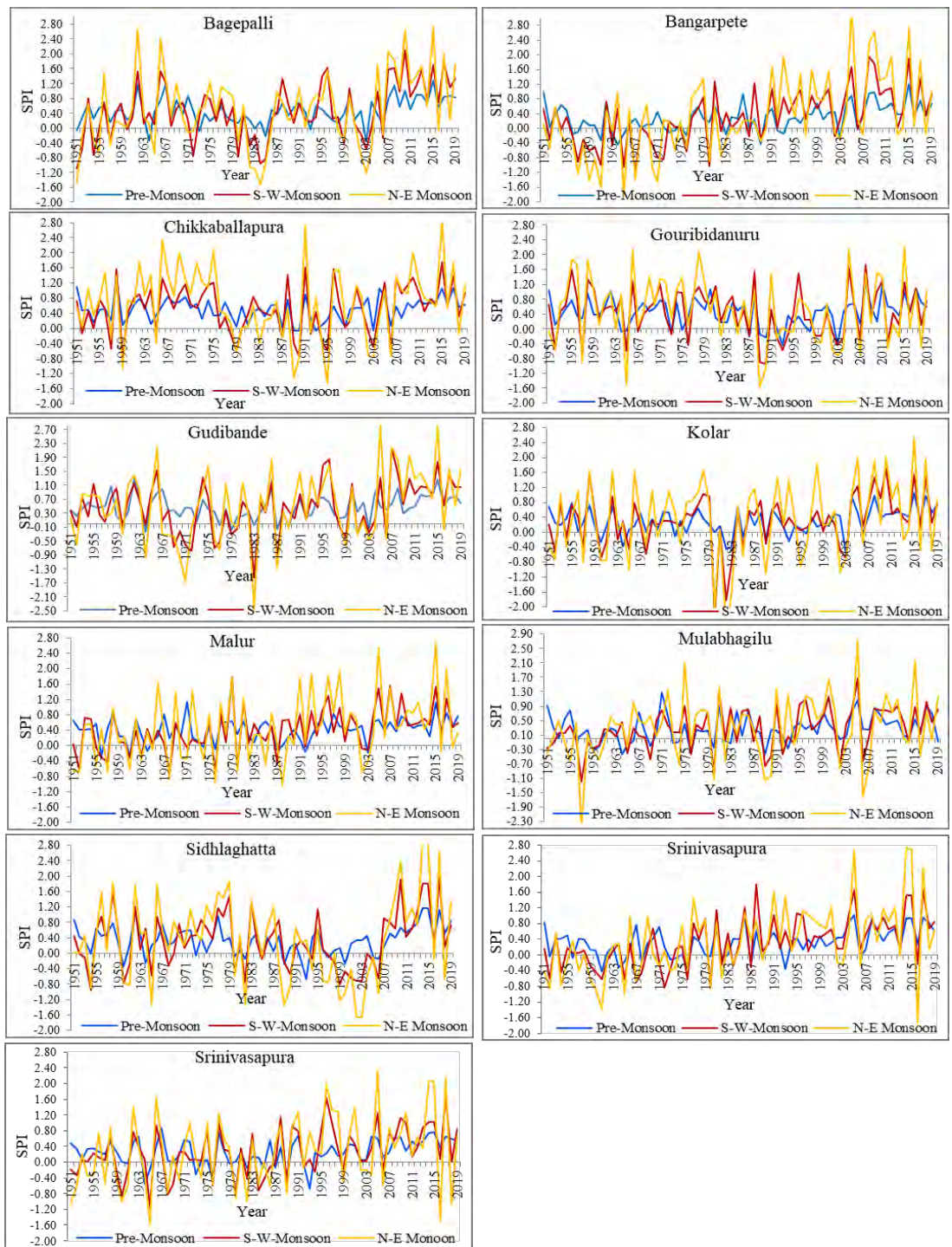
Figure 3.3 Temporal Distribution of SPI Series at Different Time Scales: Pre-Monsoon, SW Monsoon, NE Monsoon
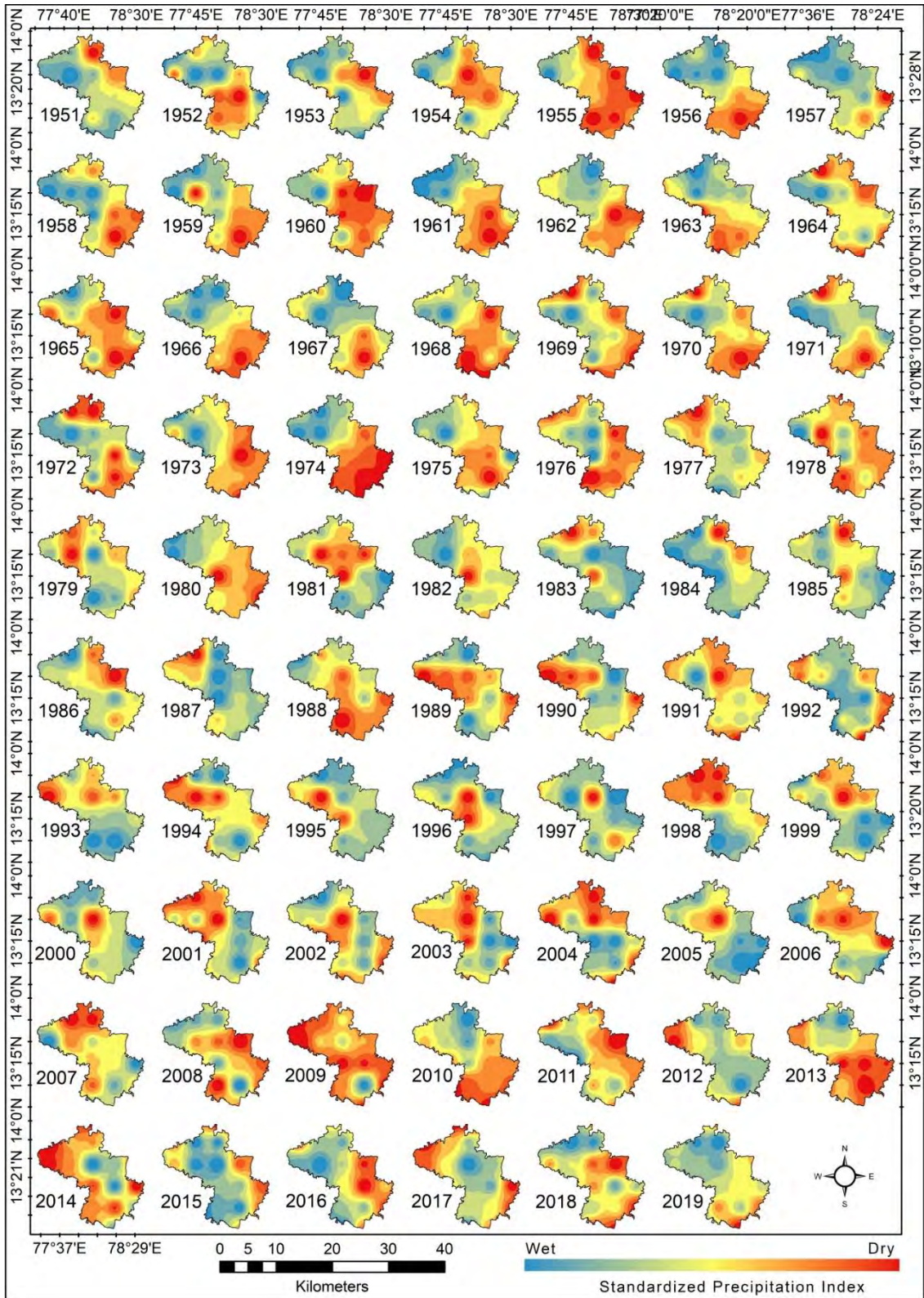
Figure 3.4 Spatial Representation of Yearly Average SPI Different Metrological Years

3.4.5.2 Southwest Monsoon

The study area though lacking any perennial rivers is completely dependent on the southwest monsoon to sustain agricultural activities. The deficiency of rainfall in this season has a large-scale impact on crop production and related activities. Shidlaghatta station experienced duration of 56.52% of drought during this season. Gauribidanur and Srinivaspura-1 show a similar frequency of 0.522 with duration of 52.17%. From 1954 to 1963 Bangarapete recorded long-term drought conditions with a total duration value of 49.28%. An extreme drought condition of − 2.22 SPI value was seen in 1980, at Kolar station. Shidlaghatta underwent a 9-year drought period from 1998 to 2006. There is a considerable improvement in the dry spell after the 1990s in the study area. Figure 3.6 shows the variation of dry conditions in every decade of the study period. The SW season in 1985 suffers a huge drought condition in the northern part of the Chikkaballapura district. The S-W monsoon has majorly more rainfall in the seasons compared to the pre-monsoon and Post monsoon seasons. The agricultural activities were done in this season, but when rainfall is very less compared to the normal rainy days the area is affected more by water scarcity then which leads to less crop pattern and less yield productivity.

3.4.5.3 Northeast Monsoon

The occurrence of drought in the northeast monsoon is relatively lower than in the southwest monsoon. Bangarapete dealt with 36 years amounting to 52.17% of drought duration whereas 1954 to 1962 had a continuous drought and in 1959 and 1965, the lowest SPI value of − 0.81 was recorded. Gauribidanur and Malur stations have 0.507 frequency values and drought duration of 50.72%. The temporal distribution of drought indicates that after 2003, there is a considerable decrease in drought frequency. Between 2002 and 2004, all the stations in the study area witnessed drought (Table 3.4 and Figure 3.7). Even though there is less extreme drought condition, the frequency of severe drought had increased over the years. Apart from the pre-monsoon drought in Mulabagilu station with an SPI value of − 0.06, none of the other stations experienced drought in 1966. In 1975, 1991, 2005, 2010, 2011, and 2017 had almost no drought events. 2015 was granted with absolutely no dry spell (Figure.

3.8 and Figure .3.9). The number of drought years along with the corresponding SPI values is listed in Table 3.6.

Rain grid stations	Pre-monsoon in (mm)			S-W monsoon in (mm)			N-E monsoon in (mm)		
	Avg	Max	Min	Avg	Max	Min	Avg	Max	Min
Bagepalli	79.7	201.0(1967)	0.9(2003)	277.1	624.5(1996)	100.3(1980)	173.8	497.8(2015)	10.8(2016)
Bangarapete	119.5	371.5(2015)	12.1(1964)	352.5	696.9(2008)	91.7(1980)	212.3	590.3(2005)	27.9(1983)
Chikkaballapur	106.0	241.3(1958)	0.0(1990)	329.7	635.4(1964)	125.2(2002)	175.3	596.9(1953)	0.0(1983)
Gauribidanur	109.0	267.7(2011)	1.5(2003)	426.1	809.6(1964)	180.1(1957)	205.1	551.5(1956)	27.0(2016)
Gudibande	80.0	265.5(2008)	1.9(1964)	286.4	787.4(2007)	48.2(1983)	165.1	554.6(2005)	6.0(2016)
Kolar	117.3	237.5(2004)	22.7(2003)	373.1	721.4(2010)	42.7(1980)	210.9	506.2(2015)	27.0(2016)
Malur	151.9	328.3(2015)	27.1(1956)	383.7	752.0(1979)	117.8(1952)	219.1	608.4(1991)	10.7(1988)
Mulabagilu	130.9	382.6(1999)	22.5(1989)	398.3	716.5(1964)	104.0(1957)	261.1	730.2(1975)	42.1(1998)
Shidlagatta	97.8	217.3(2014)	2.6(1993)	329.3	646.0(2010)	166.2(1994)	191.6	543.7(2014)	20.3(1988)
Srinivaspura	118.4	269.1(2004)	19.9(1961)	361.3	731.0(1988)	97.0(1967)	215.9	554.3(2014)	9.4(2016)
Srinivaspura-1	115.5	254.5(1977)	8.1(1993)	377.5	753.2(1996)	183.2(1980)	238.2	698.1(2015)	11.0(2016)

Table 3.5. Seasonal Share of Total Precipitation in 1951-2019
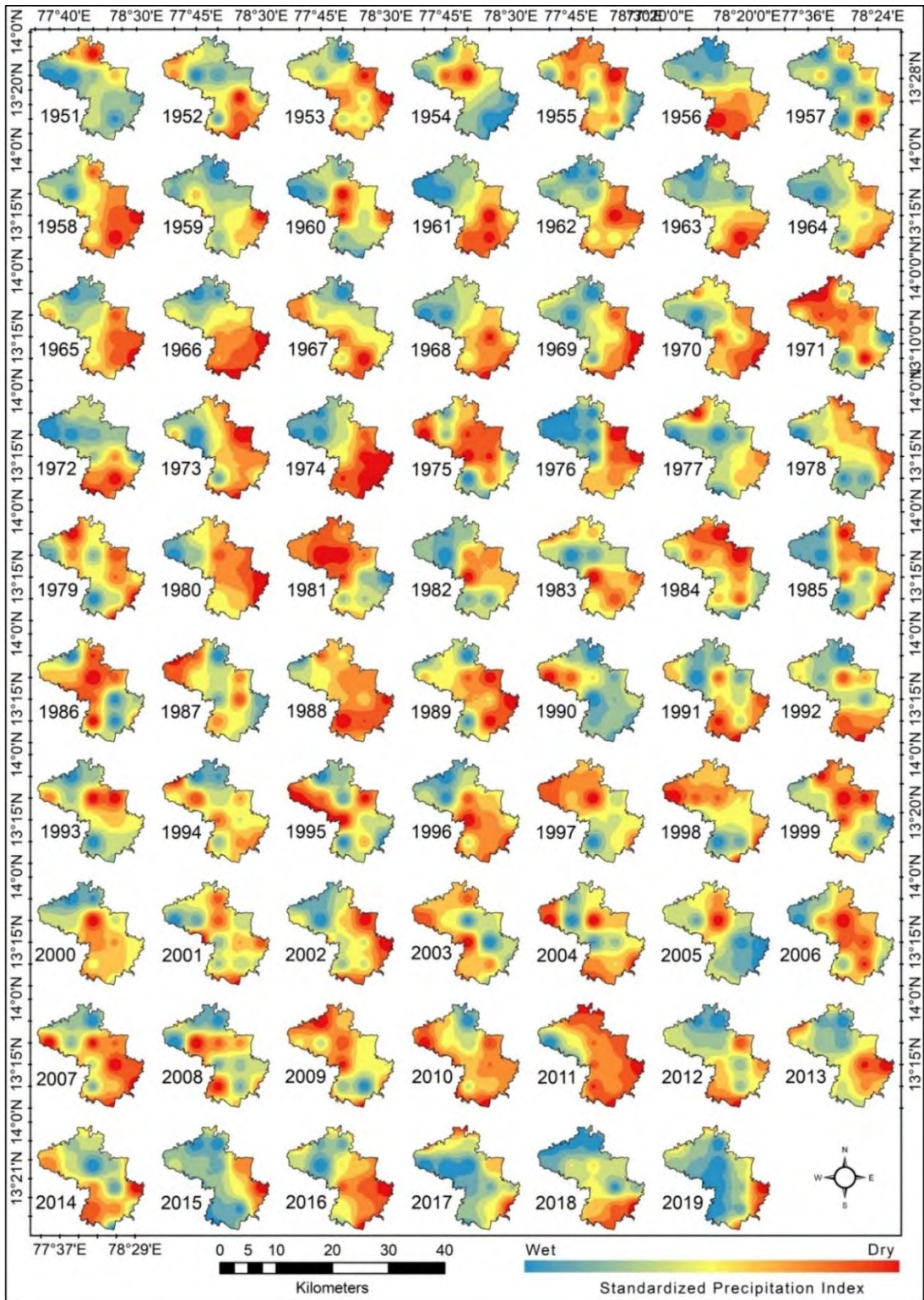
Figure 3.5 Spatial Representations of Pre-Monsoon Average SPI
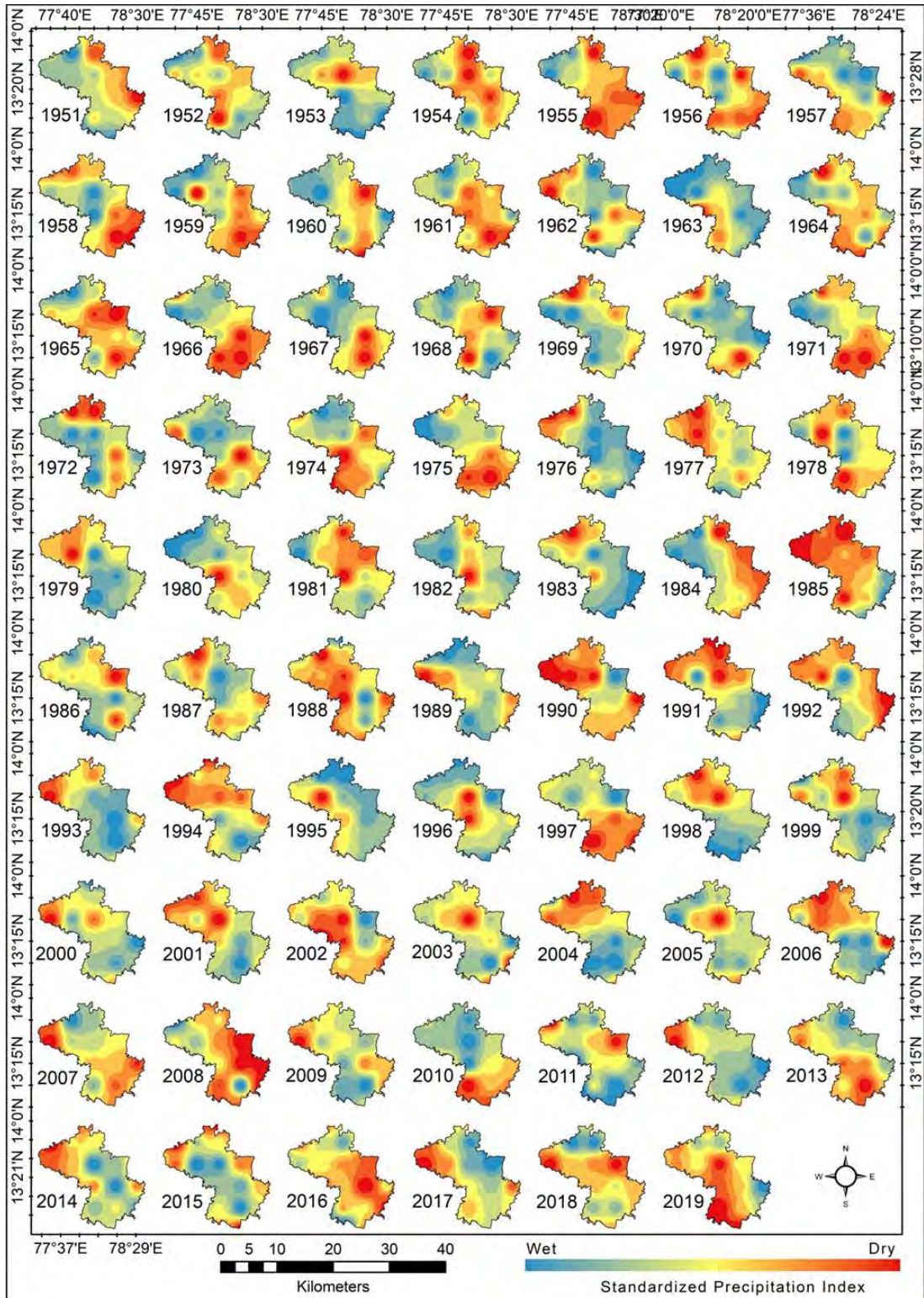
Figure 3.6. Spatial Representation of S-W Monsoon Average SPI
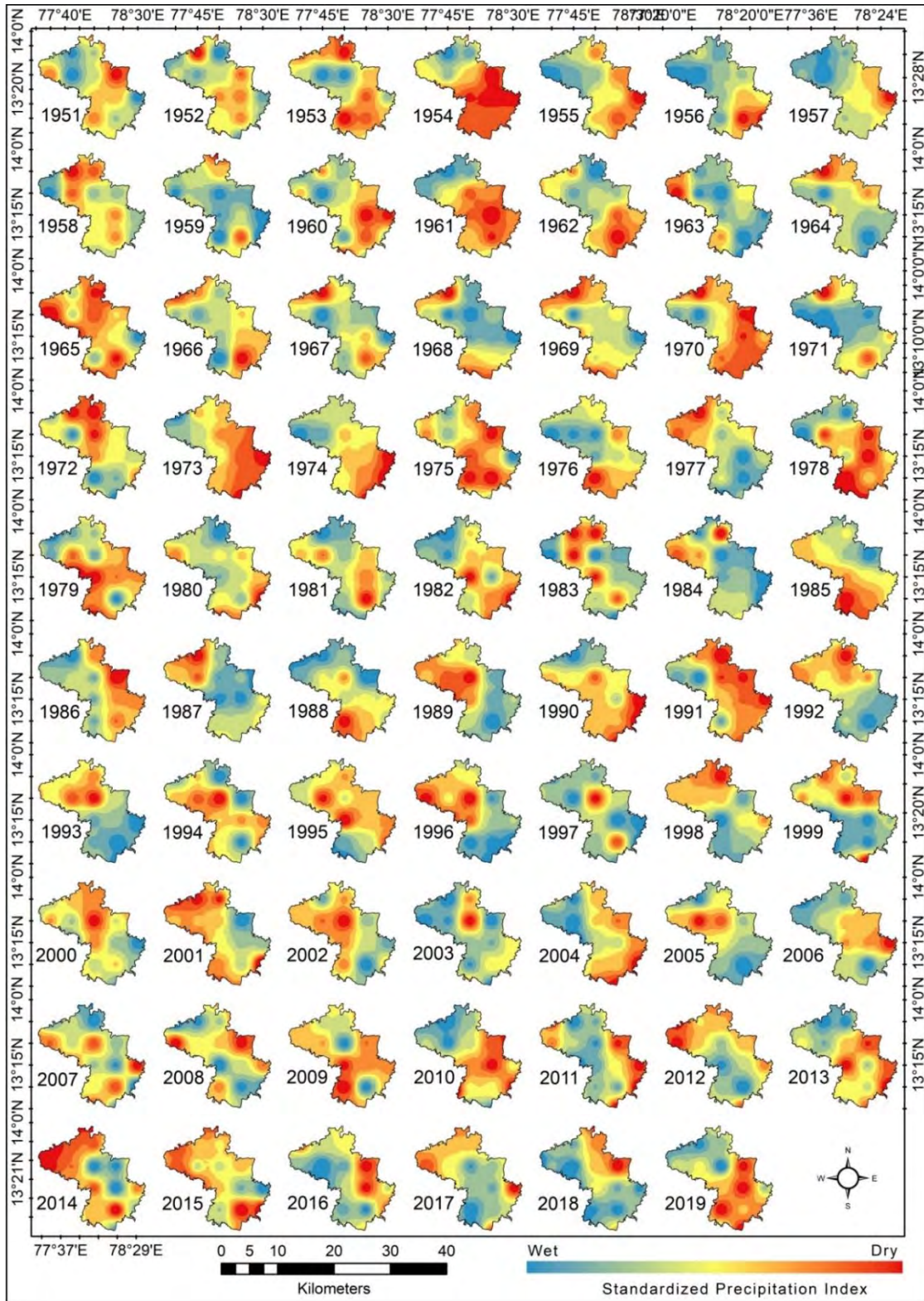
Figure 3.7 Spatial Representation of N-E Monsoon Average SPI

3.4.6 The spatial trend in the dry period across the district

The drought analysis is useful for determining the spatial variation of drought and evaluating the most affected areas of the districts. The spatial extent of dry conditions in the study area is depicted by the time series drought indices generated by employing the SPI values as input to ArcView/GIS. The maps of spatial distribution for seasonally average SPI values are generated using the IDW interpolation method and presented in Figure 3.8. The map representing the frequency of drought risk depicting its spatial pattern in the annual time reveals variation as complex and at a local scale. Under the severe drought situation, the stations of Chikkaballapura, Gudibande, and Sidlaghatta located mainly in the western part of the Chikkaballapura district showed very high-frequency values. Present in the southeaster part of the study area, the least value for frequency was recorded at Srinivaspura and Mulabagilu stations. Exhibiting the extreme drought conditions, the maximum frequency is seen prominently in the north of Chikkaballapura district at stations Bagepalli and Gudibande. The minimum of this value is held at Gauribidanur, Srinivaspura-1, Malur, and Sidlaghatta which are spread across the study area. For the pre-monsoon season, the maximum and minimum value of SPI is found in the year 1988 and 1964 respectively, and the average SPI for all the stations comes to 0.37.1980 and 1996 mark the maximum and minimum SPI value for southwest monsoon respectively with Kolar holding the record low SPI value of − 2.22 and 0.07 is the average value. Similarly, 2005 and 1998 exhibits the highest and lowest value in the northeast monsoon season and the mean value of SPI calculated is 0.05. The spatial distribution of frequency and duration of drought under extreme and severe conditions are represented in Figure 3.8. Spatially, there are distinct spatial differences in wet and dry conditions at seasonal time scales. The results indicated that there were significant changes in temporal and spatial conditions of drought in the Kolar and Chikkaballapura districts throughout the period. The results of the present study demonstrated that drought events are a recurrent process, and the vulnerability of dry events varies spatially and temporally. Significant changes were found in the SPI values in the seasonal and annual SPI average interface.

3.4.7 Standardized Precipitation Evapotranspiration Index

Standardized precipitation evapotranspiration index changes the precipitation in SPI with the variation between monthly potential evapotranspiration and monthly precipitation; it takes into the temperature factor And initiates the evaporation changes in the surface,

Table 3.6. Season-Wise Total Number of Drought Period

Sr. No	Stations	Pre-monsoon	Max Negative SPI Value	S-W Monsoon	Max Negative SPI Value	N-E Monsoon	Max Negative SPI Value
1	Bagepalli	7	-0.33(1964)	32	-1.20(1972)	29	-0.92(1983)
2	Bangarapete	15	-0.42(1982)	34	-1.49(1967)	36	-1.05(1988)
3	Chikkaballapura	4	-0.07(1993)	34	-0.87(2002)	34	-0.89(1989)
4	Gauribidanur	10	-0.44(1993)	35	-1.02(2002)	38	-0.91(1965)
5	Gudibande	7	-0.24(1964)	32	-1.51(1983)	30	-0.93(1964)
6	Kolar	12	-0.62(2003)	35	-2.22(1980)	32	-0.98(1995)
7	Malur	8	-0.26(1961)	33	-1.18(1981)	36	-1.67(1988)
8	Mulabagilu	15	-0.45(1964)	34	-1.20(1951)	34	-1.32(1957)
9	Sidlaghatta	14	-0.67(1993)	38	-1.05(2002)	29	-1.17(1988)
10	Srinivaspura	15	-0.30(1976)	36	-1.44(1967)	32	-1.50(2016)
11	Srinivaspura 1	13	-0.54(1993)	32	-0..95(1965)	33	-1.56(2016)

which is much sensitive to the reaction of drought caused by the temperature rise in the globe(Gao et al. 2017; Jia, Zhang, and Ma 2018; C. Liu et al. 2021).

To evaluate the SPEI value, the variation of the normalized log-logistic probability distribution in water balance. The probability density function expresses in the below equation

$$f\,(x) = \frac{\beta}{\alpha}\left(\frac{\chi - \lambda}{\alpha}\right)\left[1\,+\,\left(\frac{\chi - \lambda}{\alpha}\right)\right]^{-2} \qquad 10)$$

Where α, β, and γ indicate the parameters, origin, and shape, respectively. Hence, the distribution probability function can be intimated of the D series data is expressed by:

Therefore α, β, and γ indicates the parameters of scale, shape, and origin, individually. Hence, the distribution probability function is expressed by.

$$F(x) = \left[1 + \left(\frac{\alpha}{x - \gamma} \right)^{\beta} \right]^{-1} \tag{11}$$

Calculated the SPEI as follows (Vicente-Serrano, Beguería, and López-Moreno 2010).

$$SPEI = W - \frac{C_0 + C_1 W + C_2 W^2}{1 + d_1 W + d_2 W^2 + d_3 W^3} \tag{12}$$

Where $W = \sqrt{-2 \ln(P)}$, $P \leq 0.5$, and when $W = \sqrt{-2 \ln(1 - P)}$, $P > 0.5$, $C_0 = 2.515$, $C_1 = 0.8028$, $C_2 = 0.0203$, $D_1 = 1.4327$, $D_2 = 0.1892$, $D_3 = 0.0013$. The category of drought classified by the SPEI is shown in Table 3.1.
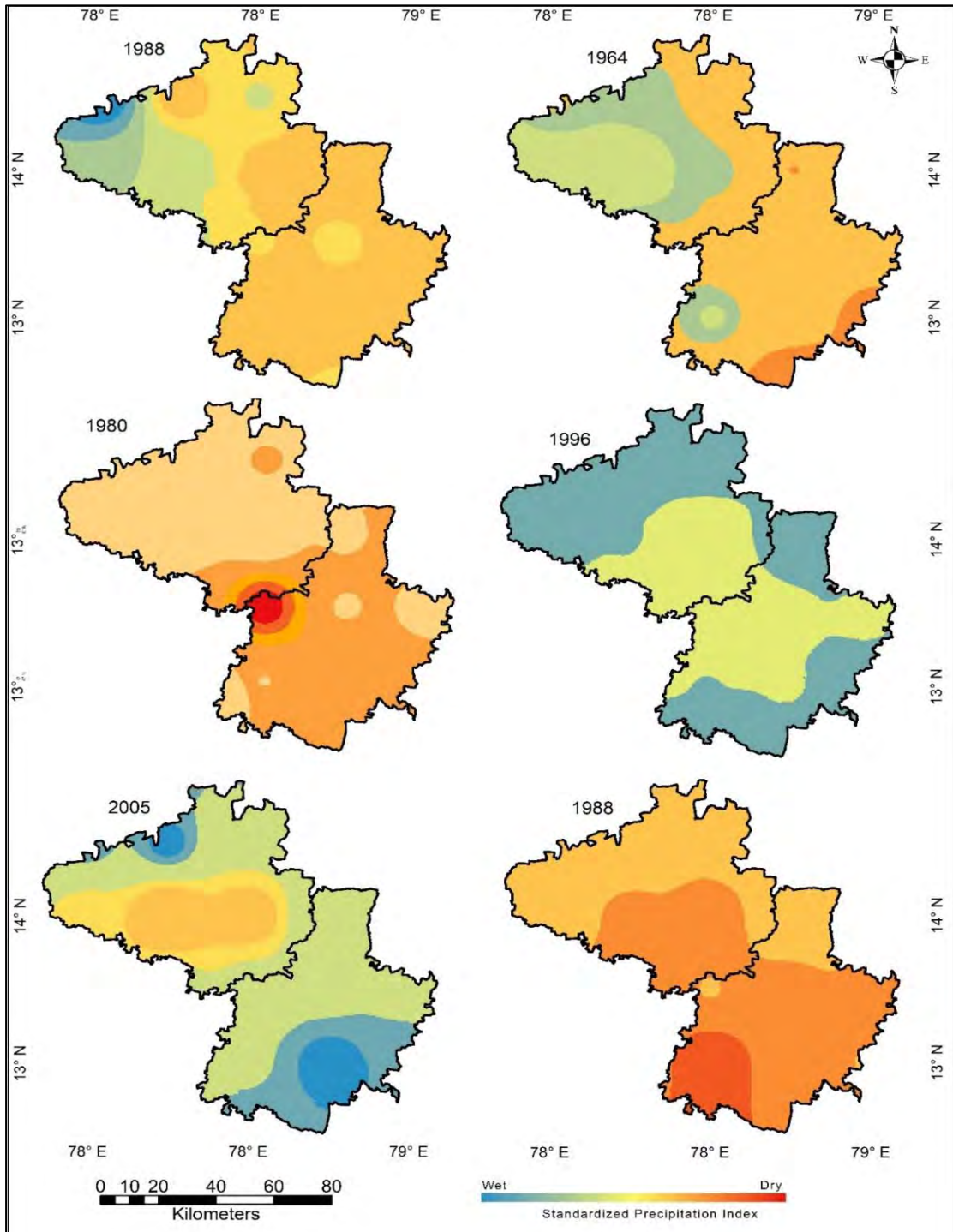
Figure 3.8 Spatial Distribution of Maximum and Minimum SPI of Pre-Monsoon (1988 & 1964), Southwest Monsoon (1980 & 1996), and Northeast Monsoon (2005 & 1998).
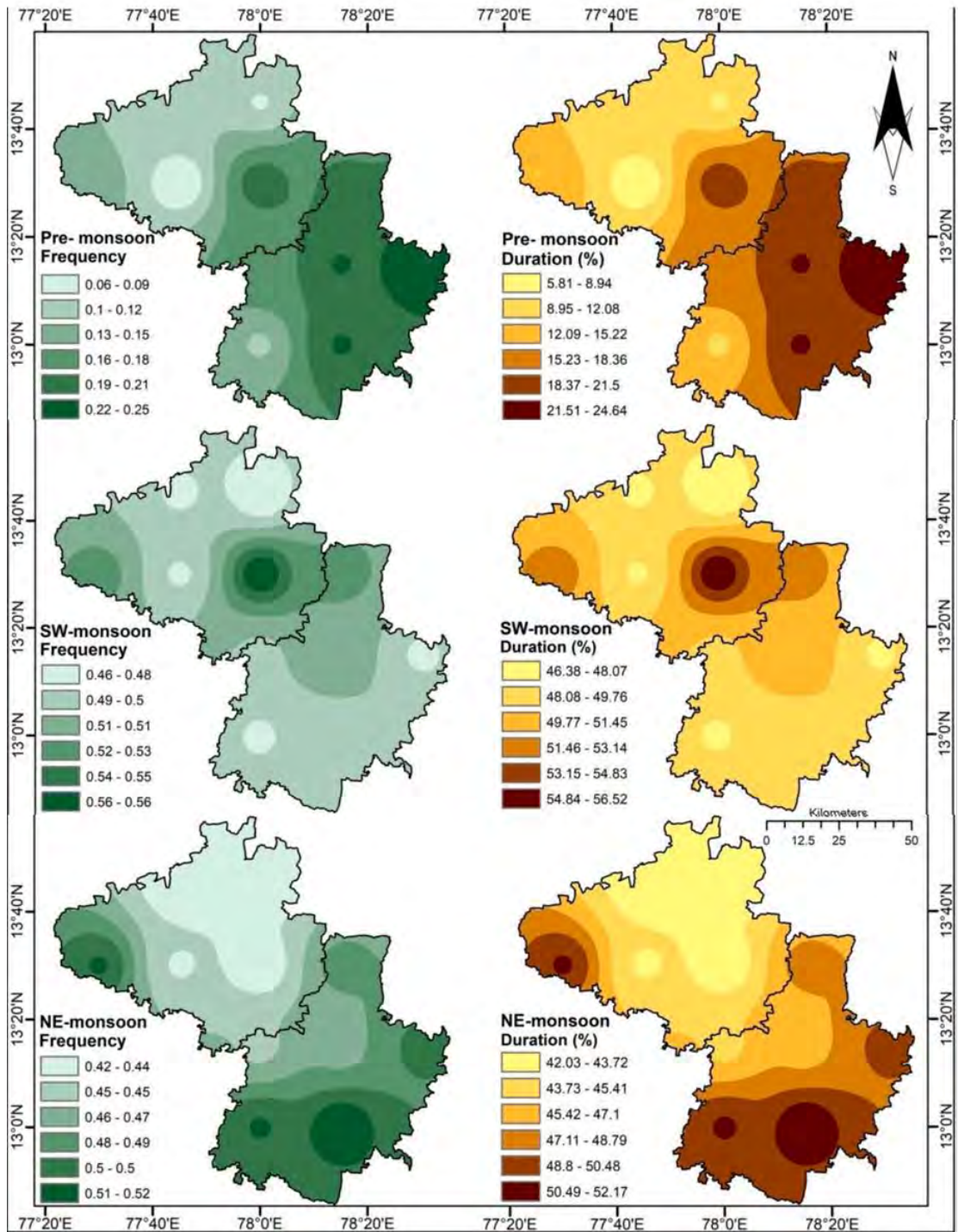
Figure 3.9 seasonal Distributions of SPI Duration and Frequency

3.4.8 Spatial and Temporal Variation of Drought in SPI and SPEI

By taking into account the temporal assessment of the SPEI and SPI in various areas and timelines, one may be better able to understand the temporal variance of drought. To calculate the trends and patterns of the SPI and SPEI, an analysis of the frequency, variations, and trends of the drought indexes was done for the SPEI and SPI time scale at the various prescribed timescales. To visualize the changes during the time, it is necessary to analyze the temporal assessment of the drought period. The number of droughts analyzed with each index from 1981 to 2019 for each station was computed separately and plotted into the different stations in Figures, 4, 4.1, and 4.2, R software is used. This resulted in both indices' 3 and 6-month scales showing a decline and both indices showing a significant number of droughts, ranging from 125 extreme drought months for the SPI-6 to 98 for the SPI 6-month scale. Research indicates the various drought categories

Classified by drought frequency it showed in spatial maps, based on SPI and SPEI monthly values of 11 meteorological grid stations from 1981 to 2019. These values were used to compute the drought duration and frequency of extreme and severe drought conditions. According to the findings, between 1981 and 2019 in grid stations, dry periods can occur between 9.7% and 17.8% of the time in the majority of Kolar and Chikkaballapura districts. The length and frequency of droughts have increased in both districts in recent years. Figures 4, 4.1, and 4.2 show the movement of the drought over a long period. Both SPEI and SPI frequently tend to 0 due to the influence of climate fluctuation on the short-term scale, which may indicate the precise variable in deprivation and water surplus at the 3-, 6-, 9.-12, and 24-month scales Table 3.8. By analysing the change of the inter-decadal and inter-annual features, which reveal long-term variation in the drought period, there is a modest difference between the SPEI and SPI. Inverse Distance Weighted (IDW) interpolation was used to create the maps of spatial distribution over the area for the annual average SPI and SPEI values, which are displayed in Figures 4.5 and 4.4. The maps represent the wet and dry parts of every grid station in both districts from 1979-2019.

3.4.9 Temporal Variation of Drought in the SPI and SPEI on a 3-Month Scale.

For the examination of short-term drought occurrences, SPI-3 and SPEI-3 are employed. This index provides seasonal rainfall estimation and short-term moisture conditions. There is evidence that the districts are frequently affected by the short-term drought oscillation on a three-month timeline. Because of insufficient precipitation, this type of drought oscillation directly affects crops and results in crop yield loss, Figures 4 and 4.3 shows spatial and temporal distribution of drought frequency in the percentage of SPI and SPEI Table 3.7 lists the occurrences of extreme and severe drought at the 3-month scale.

It shows how the study area's rainy and dry seasons vary from year to year. The Bagepalli station indicates both wet and dry periods in the first 10 years of the study period. The duration of drought is very long when compared to other decades, with the highest extreme drought occurring in 1992 (March), when the SPEI value was -2.48, as well as in 1983 (-2.49 in April and -2.29 in March), 2016 (-2.27 in December and -2.17 in November), and 2017 (-2.27 in December and -2.17 in November) (-2.04 in January). SPI revealed the worst drought in the years 1981 to 1991, with a high SPI score (-3.71 in 2003) and three consecutive months of drought. Compared to past droughts, the three-month drought experienced severe and extreme drought conditions for all grid stations. In SPI Gudibande, it was found that there were 17 extremely important drought months with 3.78% extreme drought events and 1.53% severe drought months. In SPEI Chikkaballapura, it was found that there were 10 extreme drought months with a total drought frequency of 2.19% and a maximum of 27 severe droughts with a frequency of 5.92%. The SPEI's lowest Extreme drought, located in Gudibande, had a 0.43% drought duration. Between terms of the 3-month scale, the SPEI showed that the highest extreme drought occurrences occurred more frequently in April and March. Throughout the entire study period, it often occurs between the years 1983 and 1992.

Kolar experienced dry occurrences in March 1983 with a maximum SPEI value of -2.73 compared to other stations. The months that experience the worst dry events during the SPI monsoon season are typically June through September.

According to Bagepalli, extreme drought events occurred in 2003 and 1984, with the highest negative SPI values of -3.71 in May and -3.46 in June, respectively.
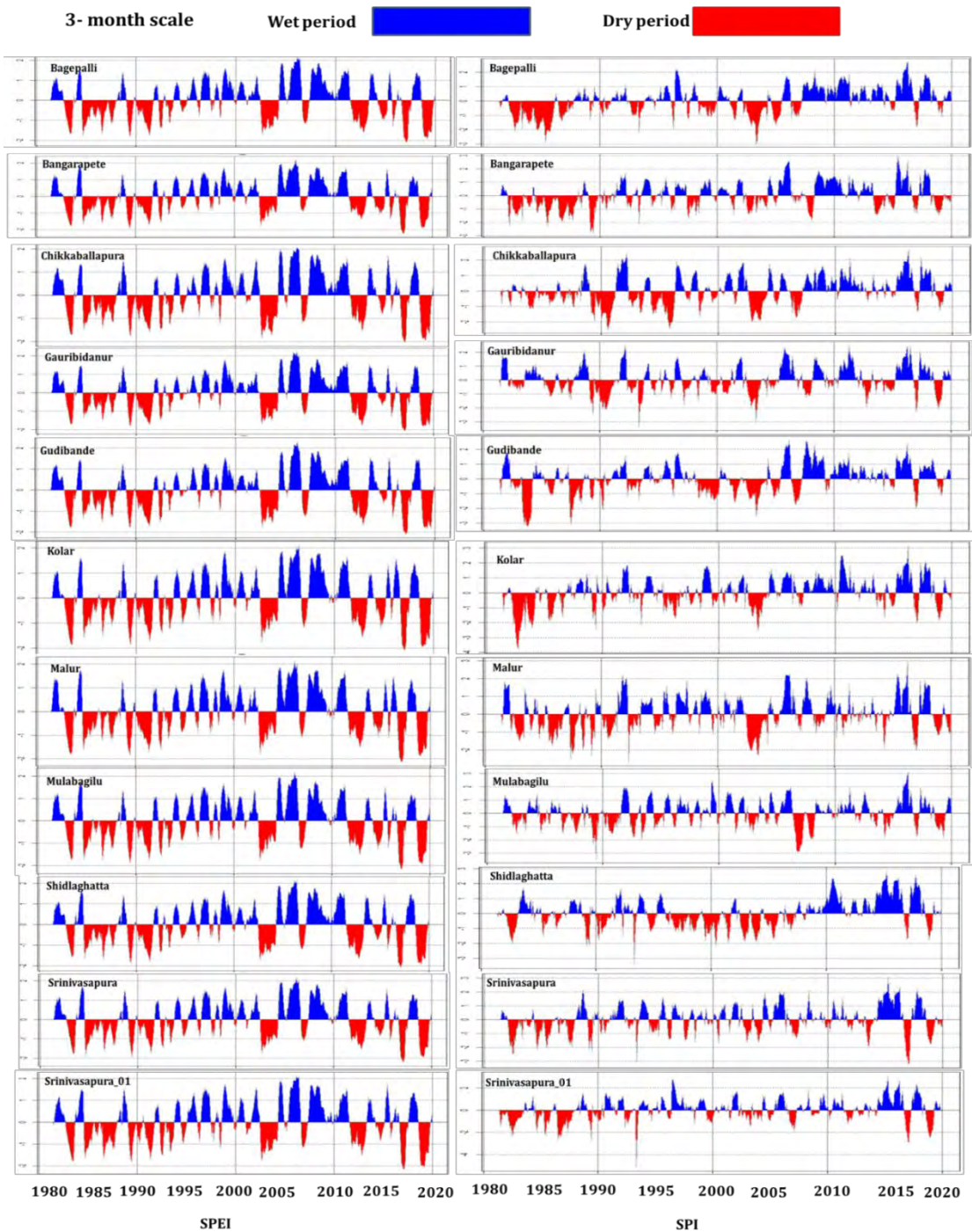
Figure 4. Temporal Evaluation of Drought at 3-Month Scale of SPI and SPEI

Table 3.7 Extreme and Severe Drought Events on the 3, 6, and 12 Monthly Scale

Station name	Intense drought		Extreme Drought months and Frequency in %				Severe Drought Months and Frequency in %			
	SPI-3	SPEI-3	SPI-3		SPEI-3		SPI-3		SPEI-3	
Bagepalli	2003 May (-3.71)	1992 April (-2.48)	10	2.1	7	1.5	18	3.9	17	3.7
Bangarapete	1985 July (-3.71)	1983 April (-2.58)	8	1.7	7	1.5	21	4.6	20	4.3
Chikkaballapura	1990 July(-2.10)	1983 April (-2.41)	4	0.8	10	2.1	10	2.1	10	2.1
Gauribidanur	2003 May (-2.46)	1992 April (-2.35)	5	1.0	8	1.7	10	2.1	19	4.1
Gudibande	2001 July (-2.91)	1983 April (-2.51)	17	3.7	2	0.4	7	1.5	27	5.9
Kolar	1982 April (3.80)	1983 March (-2.79)	12	2.6	6	1.3	18	3.9	18	3.9
Malur	1981June (-2.40)	1983 March (-2.79)	3	0.6	6	1.3	14	3.0	22	4.8
Mulabagilu	1989 June (-2.90)	1983 April (-2.54)	11	2.4	7	1.5	21	4.6	15	3.2
Shidlagatta	-	1992 April (-2.41)	7	1.5	8	1.7	21	4.6	17	3.7
Srinivasapura	2017 July (-2.33)	1983 April (-2.61)	7	1.5	8	1.7	20	4.3	17	3.7
Srinivasapura-1	1993 May (-3.92)	1983 April (-2.57)	14	3.0	9	1.9	15	3.2	11	2.4

Station name	Intense drought		Extreme Drought months and Frequency in %				Severe Drought Months and Frequency in %			
	SPI-6	SPEI-6	SPI-6		SPEI-6		SPI-6		SPEI-6	
Bagepalli	2003 May (-3.01)	2017 March (-2.06)	10	2.2	2	0.4	14	3.1	26	5.7
Bangarapete	1989 June (-2.83)	2017 Feb (-2.09)	7	1.5	0	0.0	14	3.1	21	4.6
Chikkaballapura	1980 July (-3.14)	2017 March (-2.05)	16	3.5	2	0.4	11	2.4	30	6.6
Gauribidanur	1993 May (-3.38)	2017 Feb (-2.07)	7	1.5	2	0.4	18	3.9	27	5.9
Gudibande	1983 Octo (-3.23)	2003 March (-2.31)	17	3.7	4	0.9	9	2.0	22	4.8
Kolar	1982 Octo (-3.77)	2017 Feb (-2.09)	13	2.9	3	0.7	17	3.7	25	5.5
Malur	1986 July (-3.11)	2017 Feb (-2.13)	6	1.3	3	0.7	16	3.5	26	5.7
Mulabagilu	1989 June (-3.46)	2017 April (-2.19)	11	2.4	3	0.7	20	4.4	23	5.0
Shidlagatta	1993 May (-3.44)	2017 March (-2.02)	4	0.9	2	0.4	19	4.2	26	5.7
Srinivasapura	2017 Feb (-3.13)	2017 March (-2.38)	11	2.4	1	0.2	18	3.9	20	4.4
Srinivasapura-1	1993 May (-5.14)	2017 March (-2.08)	16	3.5	4	0.9	13	2.9	25	5.5

Station name	Intense drought		Extreme Drought months and Frequency in %				Severe Drought Months and Frequency in %			
	SPI-12	SPEI-12	SPI-12		SPEI-12		SPI-12		SPEI-12	
Bagepalli	2003 June (-3.02)	No intense drought	10	2.2	0	0.0	28	6.1	30	6.6
Bangarapete	1987 Sept (-3.46)	No intense drought	3	0.7	3	0.7	16	3.5	20	4.4
Chikkaballapura	1990 July (-3.14)	2019 June (-2.04)	16	3.5	1	0.2	12	2.6	31	6.8
Gauribidanur	2003 June (-2.46)	No intense drought	5	1.1	0	0.0	5	1.1	31	6.8
Gudibande	1983 Nov (-3.47)	2017 June (-2.21)	10	2.2	4	0.9	16	3.5	27	5.9
Kolar	1982 Octo (-3.48)	2019 June (-2.06)	17	3.7	2	0.4	5	1.1	25	5.5
Malur	2015 Mar (-3.01)	No intense drought	7	1.5	0	0.0	10	2.2	26	5.7
Mulabagilu	2007 Mar (-3.07)	No intense drought	15	3.3	0	0.0	13	2.9	24	5.3
Shidlagatta	No intense drought	2019 June (-2.00)	0	0.0	1	0.2	7	1.5	24	5.3
Srinivasapura	2017 July (-2.33)	2016 Dec (-2.03)	5	1.1	2	0.4	11	2.4	25	5.5
Srinivasapura-1	1987April (-2.15)	2019 June (-2.08)	6	1.3	3	0.7	21	4.6	26	5.7

Based on 3 months, Table 3.7 summarises the drought characteristics for the stations in the region from 1981 to 2019. Every station has reported peak drought intensities of greater than 2, which is considered exceptional. The majority of these peak intensities took place in the 1980s, particularly in 1983. At Kolar Station, the highest high intensity (SPI 3.92) was detected in May

1993. The average duration month in SPI is 8.90 (98 months) and SPEI 7.09 (78 months) in extreme drought. In the severe drought condition, the total average month is SPI 15.90 (175 months) and SPEI 17.54 (193 months) respectively.

3.4.10 Temporal Variation of Drought in the SPI and SPEI on a 6-Month Scale

SPI -6 demonstrated a medium-term drought pattern in rainfall, and it may be very effectively demonstrated in seasonal precipitation. Anomalous circumstances in the storage reservoir and stream flow date back six months. In February and March of 2017, the SPEI index on a 6-month scale indicated that 2017 was a very critical, acute drought year. These months took the expanding research area and other numbers from a dry year into consideration. On the other hand, persistent drought conditions were noted in Gudibande and Srinivasapura-1 in March 2017 and were indicated by negative SPEI Values (-2.31) and (-2.38), respectively. With 4 drought months and a 0.9% drought frequency, Srinivasapura-01 had the driest months. In a severe drought, SPEI revealed that Chikkaballapura station had the most drought episodes, which resulted in 30 months with a 6.6% drought frequency. All of the stations reported 271 drought months, with an average monthly value of 24.63. (Figures 4.1 and 4.3). The years 1983, 1985, 1987, and 2003 are all completely dry years in the SPEI study period. The most severe drought in SPI, with a negative SPI value, was discovered in 1993 at Srinivasapura-1 in May. (-5.14). The Gudibande station revealed 17 months with a 3.7% drought frequency, which is the highest number of extreme drought months ever recorded. According to Mulubhagilu stations, there has been a severe drought for 20 months with a frequency of 4.4%. In ED, there were 118 drought months overall, with an average value of 10.72. However, in SD, there were a maximum of 169 drought months, with an average value of 15.36 dry months. Figures 4.1and 4.3, as well as Table 3.8, depict the drought's regional and temporal variance. Understanding the effects of drought on agricultural and other operations that depend on precipitation through temporary water sources is largely dependent on these figures.

Figure 4.1 Temporal Evaluation of Drought at 6-Month Scale of SPI and SPEI

3.4.11 Temporal Variation in the SPI and SPEI on a 12-Month Scale

Long-term droughts are less common than short- and medium-term ones, according to the analysis of SPI-12's assessment of them. Figures 4.2 and 4.4 depict a regional and temporal categorization, respectively, while Table 5 lists extreme and severe drought events over 12 months. Figures 4.2 demonstrate that the most extreme drought episodes, with a negative SPI value of -3.47, occurred in November 1983. However, during the study period, there were no severe, extreme drought episodes in Stations like Malur and Sidlghatta.

Total extreme drought months in the region were 94, with an average of 8.54 months. This shows that even though droughts were noted in the 1980s, particularly in 1983. In the studied region, there were hydrological long-term droughts in 1984, 1985, 1986, 2003, and 2007. The(Figure 4.5) 17-month ED was faced by SPI-12 Kolar with a 3.7%drought frequency. Gauribidanur, Bagepalli, Malur, and Mulubhagilu do not experience extreme drought, according to SPEI Gudibande station data, which shows a maximum ED of around 4 months with a frequency of 0.9%. However, another instance of severe drought (SD) that the station encountered in BagepallI demonstrates the lowest SD in Gauribidanur and Kolar stations is sharing about 10 months, with a maximum SD of around 28 months and a frequency of 6.1%. There have been 144 months' worth of SD revealed overall in SPI, with an average value of 13.09. However, the SPEI's maximum SD, which is 289 drought months with an average value of 26.7, is the greatest of the SPEI-3 and SPEI-6. The seasons with the longest droughts were recorded in 1983, 1985, 2003, 2007, and 2019.

In the current study, SPI, SPEI, and RAI are frequently utilized and may each evaluate drought features in space and time in drought regions. The southern peninsular region is home to Karnataka, the seventh-largest state in India. In the dry region, just 50 to 60 percent of the precipitation is used to grow crops. The districts of Chikkaballapura and Kolar are located in south India's eastern dry agro-climatic zone In the current study, SPI, SPEI, and RAI are frequently utilized and may each evaluate drought features in space and time in drought regions.

Figure 4.2 Temporal Evaluation of Drought at 12-Month Scale of SPI and SPEI
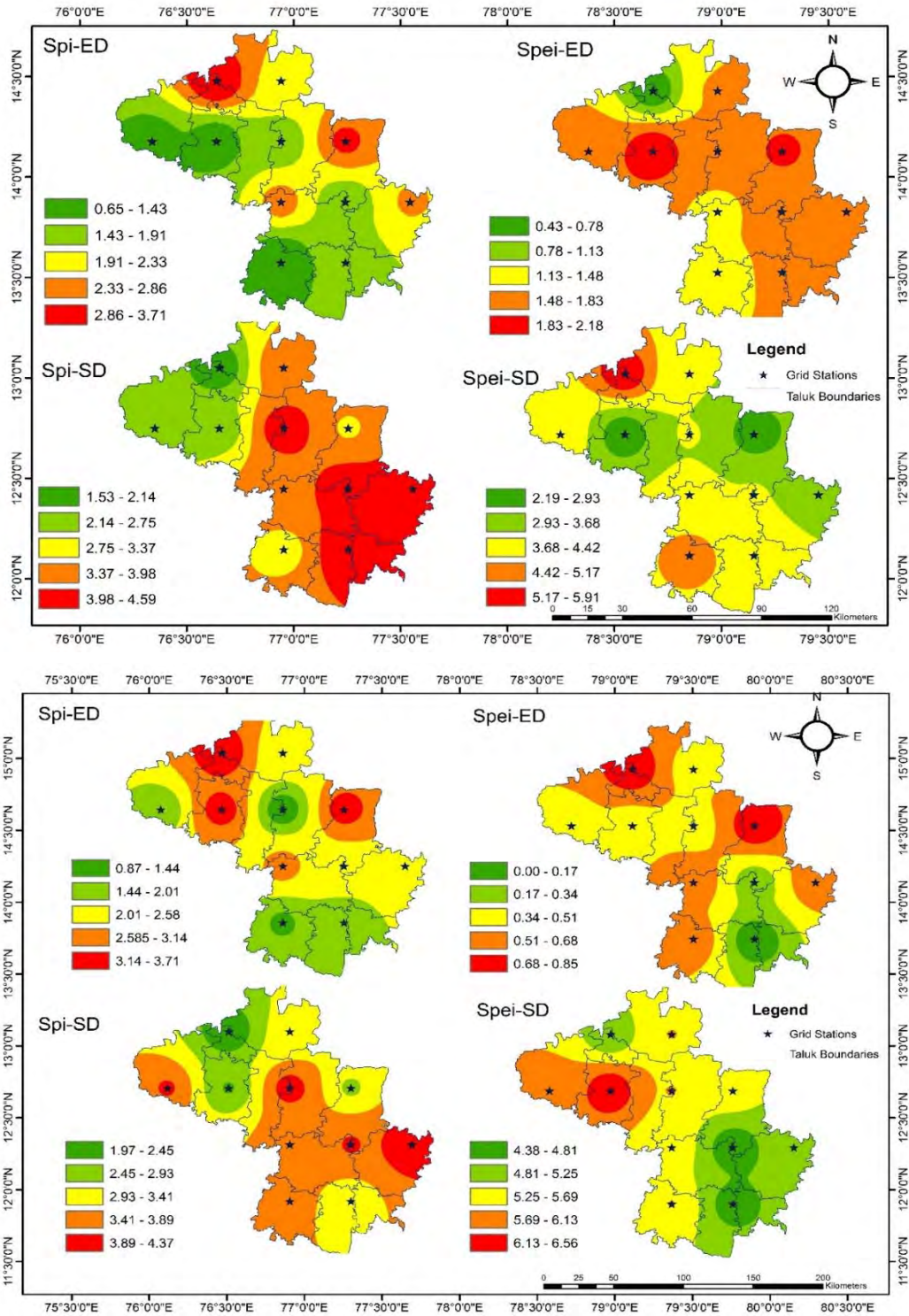
Figure 4.3. Spatial Distribution of Drought Frequency in a 3 and 6-Month Scale
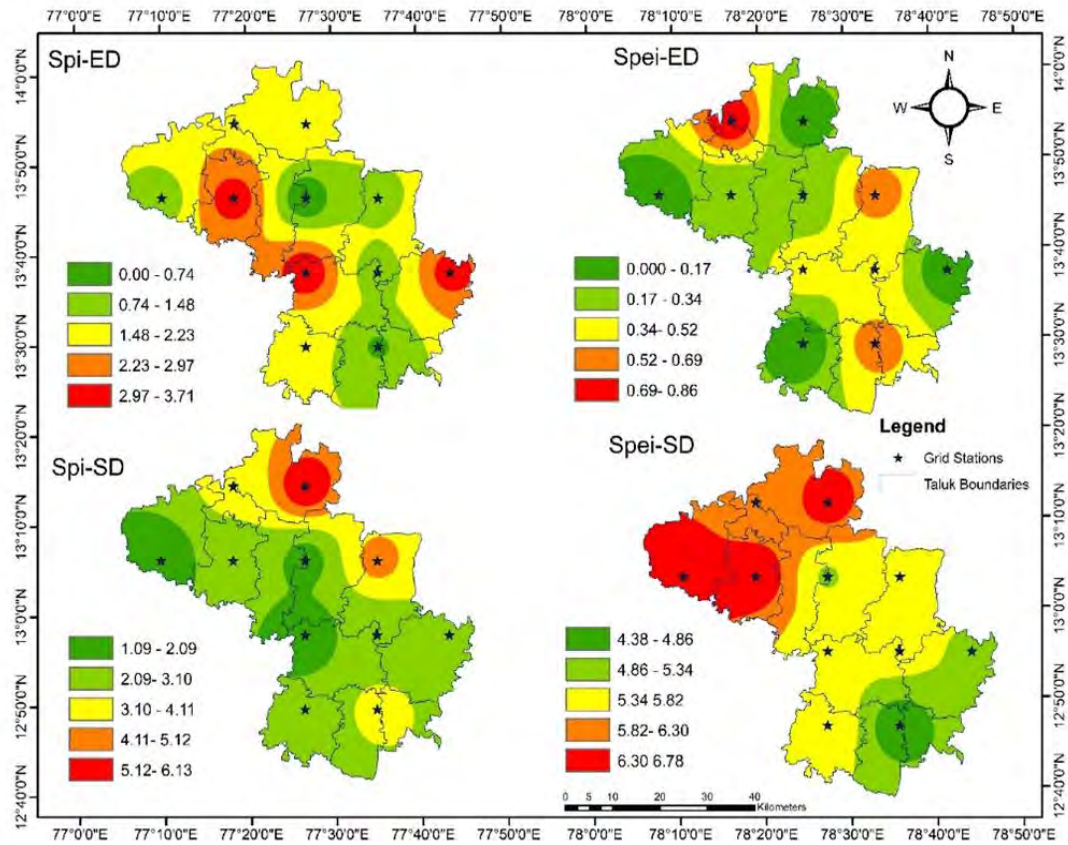
Figure 4.4. Spatial Distribution of Drought Frequency in a 12-Month Scale
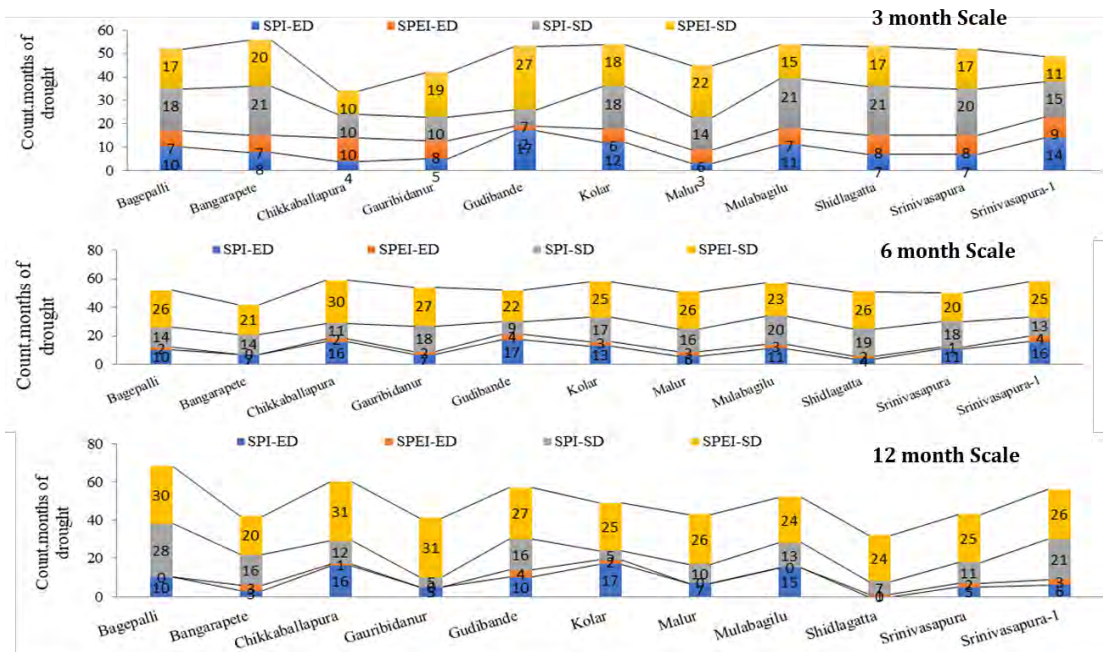
Figure 4.5. Number of Drought Months (1981-2015) at 3, 6, and 12-Month Scale

Table 3.8 Statistics and Drought years in Different Time Scales

Bagepalli

Time scale	Index	Mean	SD	Extreme dry period	Year	Wet Period	Year
1 month	SPI	0.34	1.12	-3,89 (September)	1983	2.78	2000
	SPEI	0.56	0.91	-2.78 (August)	1982	2.23	2007
3 month	SPI	0.69	0.66	-3.46 (June) / -3.71 (May)	1985 2003	2.80	1996
	SPEI	0.01	0.60	-2.48 (April)	2012	2.31	2004
6 month	SPI	0.21	0.74	-3.02 (June) / -2.89 (May)	2003 1985	2.72 (April)	2016
	SPEI	0.02	0.80	-2.09 (February)	2017	2.10	2006
9 month	SPI	0.23	-0.91	-2,39 (January)	1995	2.23	2016
	SPEI	0.34	0.91	-2.78 August)	1982	2.23	2007
12 month	SPI	0.16	0.91	-2.35 (June) / -2.34 (September)	2003 1985	2.35 (August)	2016
	SPEI	-0.15	0.85	-1.95 (June)	2019	2.08	2008
24 Month	SPI	0.03	0.29	-1.96 (March)	1981	2.93	2003
	SPEI	0.24	0.19	-2.89 (October)	2003	2.12	2005

Bangarapete

Time scale	Index	Mean	SD	Extreme dry period	Year	Wet Period	Year
1 month	SPI	0.37	1.23	-2.19 (September)	2003	2.12	2007
	SPEI	0.16	0.89	-2.28 (June)	2016	2.89	2006
3 month	SPI	0.21	0.51	-2.67 (July) / -2.38 (May)	1997 1989	2.85 (June)	2015
	SPEI	0.01	0.60	-2.48 (April)	2012	2.31	2004
6 month	SPI	0.03	0.60	-2.83 (March-June)	1989	2.95 (May August)	2015
	SPEI	0.21	0.74	-3.02 (June) / -2.89 (May)	2003 1985	2.72 (April)	2016
9 month	SPI	-0.11	0,13	-2,1 (June)	2003	2.0	2004
	SPEI	-0.34	-0.17	-2.29 (May)	2017	1.78	2004
12 month	SPI	0.01	0.30	-2.16 (May)	1987	2.39(September)	2006
	SPEI	0.11	0.63	-2.11 (August)	1993	2.48	2007
24 Month	SPI	0.85	0.57	-2.93 (November) / -2.86 (May)	1983 1983	2.63(December)	2017
	SPEI	0.12	0.3	-2.75 (August)	1993	2.72	2017

Chikkaballapura

Time scale	Index	Mean	SD	Extreme dry period	Year	Wet Period	Year
1 month	SPI	0.43	0.9	-3,12 (June)	1987	2.13	2007
	SPEI	0.89	0.78	-2.78 (August)	1983	2.56	1993
3 month	SPI	2.42	0.60	-2.10 (July) / -3.71 (May)	1990 2003	2.87 (January)	2016
	SPEI	-0.32	0.51	-2.40 (March) / -2.02 (January)	1983 2017	2.32(May)	2004
6 month	SPI	0.07	0.77	-3.24 (September) / -2.55 (August)	1990 2003	2.46 (July)	2016
	SPEI	-0.27	0.64	-2.05 (February) / -2.01 (March)	2017	2.07(March)	2006
9 month	SPI	0.39	0.9	-2.9 (June)	1987	2.13	2007
	SPEI	0.84	0.78	-2.38 (August)	1983	2.56	1993
12 month	SPI	0.17	0.83	-3.06 (August) / -3.13 (June)	1990 2003	2.28 (June)	2016
	SPEI	-0.14	0.79	-2.04 (June)	2019	2.24(September)	2008
24 Month	SPI	0.41	0.91	-3.08 (June)	1983	2.13	2007
	SPEI	0.78	0.34	-2.34 (August)	1987	2.56	1993

Gudibande

Time scale	Index	Mean	SD	Extreme dry period	Year	Wet Period	Year
1 month	SPI	0.31	1.63	-2.56 (September)	2017	2.09	2008
	SPEI	0.11	0.63	-2.11 (August)	1993	2.48	2007
3 month	SPI	0.85	0.57	-2.93 (November) / -2.86 (May)	1983 1983	2.63(December)	2005
	SPEI	0.12	0.3	-2.75 (August)	1993	2.72	2006
6 month	SPI	-0.27	0.65	-3.23 (October) / -3.15 (July)	1983 1983	2.65(March)	2006
	SPEI	0.32	0.92	-2.98 (August)	1993	2.66	2007
9 month	SPI	0,23	0.42	-2.1 (March)	2017	2.98	2007
	SPEI	0.78	0.42	-2.49 (June)	1983	2.13(June)	1995
12 month	SPI	0.02	0.77	-3.47 (November) / -3.33 (December)	1983 1983	2.30(April)	2008
	SPEI	0.34	0.95	-2.55 (August)	1993	2.98	2007
24 Month	SPI	-0.37	0,57	-2.1 (August)	1983	2.44	2006
	SPEI	-0.32	-0.86	-2.91 (May)	2003	2.89	2005

Table 3.8 Continued…

Kolar

Time scale	Index	Mean	SD	Extreme dry period	Year	Wet Period	Year
1 month	SPI	0.11	1.13	-2,76 (May)	2017	2.09	2008
	SPEI	0.12	0.93	-2.31 (June)	1983	2.12	2006
3 month	SPI	0.36	0.58	-3.80 (April) -3.20 (May)	1982 1982	3.10(Jan)	2016
	SPEI	-0.29	0.51	-2.73 (March)	1983	2.43(July)	2004
6 month	SPI	5.10	0.53	-3.77(October) -3.25(August)	1982 1982	3.56(September)	1982
	SPEI	-0.28	0.62	-2.0(February) -2.03(January)	2017 2017	2.11(June)	2006
9 month	SPI	-0.19	0.61	-2.19 (June)	2017	2.12	2007
	SPEI	0.36	0.33	-2,45 (June)	1983	2.13(June)	1995
12 month	SPI	4.99	0.63	-3.47(October)	1982	2.98(January)	1983
	SPEI	-0.06	0.83	-2.04 (June) -2.00 (April)	2019 2019	2.14(June)	2008
24 Month	SPI	-0.37	0.44	-2.91 (August)	2003	2.78	2006
	SPEI	-0.02	-0.4	-2.31 (May)	2003	1.89	2007

Gauribidanur

Time scale	Index	Mean	SD	Extreme dry period	Year	Wet Period	Year
1 month	SPI	0.91	0.46	-3,22 (October)	1983	2.35	2005
	SPEI	0.56	0.34	-2.34 (July)	1982	1.98	2007
3 month	SPI	0.92	0.51	-3.51 (May) -3.02 (May)	1989 1993	2.95(July)	2016
	SPEI	-0.60	0.53	-2.21 (December) -2.20 (March)	2016 1983	2.25(November)	2005
6 month	SPI	-0.35	0.62	-3.38 (May) -2.96 (May)	1993 2003	2.53 (March)	1992
	SPEI	-0.55	0.67	-2.06 (Feb) -2.03 (March)	2017	2.25 (March)	2006
9 month	SPI	0.62	0.42	-2.89 (October)	1983	2.35	2005
	SPEI	0.13	0.24	-2.35 (July)	1983	1.98	2007
12 month	SPI	0.17	0.69	-2.38 (August) -2.46 (June)	1990 2003	2.40(July)	2016
	SPEI	-0.25	0.85	-1.94 (July) -1.69 (May)	2019 1991	2.22(February)	2006
24 Month	SPI	0.04	0.47	-3,05 (October)	1984	2.35	2007
	SPEI	0.12	0.34	-2.60 (July)	1982	1.98	2017

Mulubhagilu

Time scale	Index	Mean	SD	Extreme dry period	Year	Wet Period	Year
1 month	SPI	0.14	1.44	-2.16(December)	2017	2.67	2016
	SPEI	0.89	0.32	-2.12 (June)	2016	1.89	2018
3 month	SPI	-0.29	0.42	-2.90 (June) -2.52(September)	1989 2006	2.99(January)	2016
	SPEI	-0.48	0.49	-2.54 (April) -2.51 (March)	1983 1983	2.34(July)	2004
6 month	SPI	-0.44	0.49	-3.46 (June) -2.92 (October)	1989 2006	3.09 (April)	2016
	SPEI	-0.46	0.61	-2.19 (February) -2.09 (March)	2017 2017	2.19 (March)	2006
9 month	SPI	0.14	0.23	-2,29 (April)	1985	2.13(June)	1998
	SPEI	0.78	-0.12	-2.16 (May)	2016 2017	2.76	2019
12 month	SPI	-0.05	0.70	-3.07 (Mar) -2.87 (December)	2007 2006	3.05 (August)	2016
	SPEI	-0.12	0.84	-1.95 (July) -1.92 (December)	2019 2016	2.10 (March)	2006
24 Month	SPI	-0.09	0.56	-2,21 (May)	2003	2,0	2007
	SPEI	-0.21	-0.1	-2.35 (August)	2003	1.78	2006

Malur

Time scale	Index	Mean	SD	Extreme dry period	Year	Wet Period	Year
1 month	SPI	1.9	2.1	-2,78 (October)	2016	2.1	1995
	SPEI	1.1	1.98	-2.12 (May)	2017	1.89	1987
3 month	SPI	1.7	1.76	-2,18 (September)	2016	2.1	1995
	SPEI	-0.50	0.51	-2.79 (Mar) -2.55 (April)	1983 1983	2.49 (July)	2004
6 month	SPI	1.1	1.12	-2,34 (September)	2017	2.12	1987
	SPEI	-0.48	0.63	-2.13 (February) -2.11 (January)	2017 2017	2.14 (March)	2006
9 month	SPI	0.17	0.98	-2,89 (April)	1983	2.1(July)	1996
	SPEI	0.35	-0.6	-3.46 (May)	2016 2019	2.78	2018
12 month	SPI	1.3	2.8	-2,08 (October)	2017	2.8	1995
	SPEI	-0.09	0.85	-1.98 (June) -1.97 (July)	2019 2017	2.03 (March)	2006
24 Month	SPI	-0.11	0.13	-2,1 (August)	2003	2.0	2004
	SPEI	-0.34	-0.17	-2.29 (May)	2017	1.78	2004

Table 3.8 Continued…

Sidhlaghatta

Time scale	Index	Mean	SD	Extreme dry period	Year	Wet Period	Year
1 month	SPI	0.45	0.98	-3.19 (June)	2017	2.09	2007
	SPEI	0.78	0.33	-3.12 (May)	2017	2.18	1997
3 month	SPI	0.2	0.5	-4.3 (November) -4.2 (October)	2016 2016	2.7 (January)	2015
	SPEI	-0.42	0.49	-2.61 (April) -2.53 (March)	1983 1983	2.46 (July)	2004
6 month	SPI	-0.14	0.57	-3.22 (January) -3.13 (February)	2017 2017	3.06 (April)	2015
	SPEI	-0.11	0.11	-2,1 (January) -2.13 (March)	2017	2.9(March)	2006
9 month	SPI	0.11	0.13	-2,32 (March)	1983	2.09(July)	1995
	SPEI	-0.12	0.11	-3.12 (August)	2017	2.18	2017
12 month	SPI	0.18	0.71	-2.33 (July) -2.23 (October)	2017 1982	2.39 (April)	2015
	SPEI	-0.11	0.83	-2.03 (December) -2.01 (January)	2016 2017	2.10 (March)	2006
24 Month	SPI	-0.03	0.43	-2.09 (July)	2003	2.78	2017
	SPEI	-0.12	0.23	-2.29 (February)	2003	2.99	2004

Srinivasapur

Time scale	Index	Mean	SD	Extreme dry period	Year	Wet Period	Year
1 month	SPI	-0.98	0.33	-3.18 (February)	2003	1.98	2007
	SPEI	-1.2	0.11	-3.12 (May)	2003	1.89	1987
3 month	SPI	0.67	0.60	-3.18(May) -2.88(June)	1993 2000	2.60 (January)	2015 2016
	SPEI	0.50	0.51	-2.41(April) -2.30 (April)	1992 1983	2.32 (July)	2004
6 month	SPI	0.43	0.69	-3.44 (May) -2.24 (June)	1993 2000	2.86 (April)	2015
	SPEI	0.46	0.64	-3.07 (February) -2.02 (March)	2017 2017	2.16 (Mar)	2006
9 month	SPI	0.01	0.23	-2,98 (March)	1983	2.1(July)	1996
	SPEI	-0.45	-0.1	-3.46 (August)	2017 2019	2.18	2017
12 month	SPI	0.40	0.79	-1.67 (May) -3.51 (September)	2000 2003	2.44 (September)	2015
	SPEI	0.23	0.83	-2.00 (June)	2019	2.12 (June)	2006
24 Month	SPI	-0.56	0.43	-3.97 (July)	2003	2.11	2017
	SPEI	-0.14	0.23	-4.79 (March)	2003	1.98	2004

Srinivasapur-1

Time scale	Index	Mean	SD	Extreme dry period	Year	Wet Period	Year
1 month	SPI	0.43	0.9	-3,12 (June)	1987	2.13	2007
	SPEI	0.89	0.78	-2.78 (August)	1983	2.56	1993
3 month	SPI	2.42	0.60	-2.10 (July) -3.71 (May)	1990 2003	2.87 (January)	2016
	SPEI	-0.32	0.51	-2.40 (March) -2.02 (January)	1983 2017	2.32(May)	2004
6 month	SPI	0.07	0.77	-3.24 (September) -2.55 (August)	1990 2003	2.46 (July)	2016
	SPEI	-0.27	0.64	-2.05 (February) -2.01 (March)	2017	2.07(March)	2006
9 month	SPI	0.39	0.9	-2.9 (June)	1987	2.13	2007
	SPEI	0.84	0.78	-2.38 (August)	1983	2.56	1993
12 month	SPI	0.17	0.83	-3.06 (August) -3.13 (June)	1990 2003	2.28 (June)	2016
	SPEI	-0.14	0.79	-2.04 (June)	2019	2.24(September)	2008
24 Month	SPI	0.41	0.91	-3.08 (June)	1983	2.13	2007
	SPEI	0.78	0.34	-2.34 (August)	1987	2.56	1993

3.5 Rainfall Anomaly Index:

The RAI (Rainfall Anomaly Index), created by Rooy(Kraus 1977), is employed to classify rainfall anomalies into negative and positive severities(Rafaela et al. 2022). Because it just requires precipitation data, it is also characterized as an index of notable procedural efficiency (like SPI). The RAI concept was utilized by Arajo et al (Aryal, Maharjan, and Talchabhadel 2022) to assess the meteorological drought in the Semi-arid region of Karnataka. Employed the RAI approach to examine the variability of rainfall variation throughout more than decades (1979-2019). According to the outcomes of these studies, RAI may be an important tool for assessing the rainfall data over the study region. Table 3.1 shows the RAI index's severity level. From -4 (extreme dry) to +4 (highly humid/wet), there are different severity levels. Equations were used to calculate the RAI values in Microsoft Excel.

For positive (+) anomalies: $\qquad RAI = 3\left[\frac{(P-\bar{P})}{(\bar{M}-\bar{P})}\right]$ $\qquad$ 13)

For negative (+) anomalies: $\qquad RAI = -3\left[\frac{(P-\bar{P})}{(\bar{X}-\bar{P})}\right]$ $\qquad$ 14)

$\bar{P}$ -Is the mean monthly, seasonal, and annual rainfall of a historical period

$\bar{M}$ -Is the mean the ten highest monthly, seasonal, and annual rainfall?

$\bar{X}$ -Is the mean of the ten lowest monthly, seasonal, and annual rainfall.

P– $\bar{P}$ -Indicate the positive and negative anomaly based on negative or positive values.

Drought indices, notably SPI and RAI, are simple to operate but effective(Aryal, Maharjan, and Talchabhadel 2022). Furthermore, they just require rainfall data. SPI has been widely used in a variety of studies both internationally and regionally(Wu et al. 2007). SPI offers several benefits over other drought indicators, such as data requirements for temporal and spatial aspects of the application. The SPI has also been employed to examine projection outcomes, but RAI has received less scrutiny. Many studies have been done to evaluate SPI and RAI. Standardized precipitation anomalies can be used to compare model findings to observed data. RAI has a higher level of transparency

and is less complex in arithmetic operations than SPI. RAI can also be calculated at the same periods as SPI with a corresponding algorithm(Q. Zhang et al. 2013) the relationship between different hydrological droughts with their parameter.

3.6 Temporal Characteristics of RAI and SPI.

Figures 5 and 5.1 depict the drought and rainy years based on a time series of the rainfall anomaly index (RAI) over Kolar and Chikkaballapura for 40 years (1979-2019). It can depict the times when drought and precipitation events happen over a given time. RAI is positive (>0) for the majority of the year, with some years before 2003 and 2004 experiencing a dry year. The majority of the years after 2003 were dry, with only two exceptions (1987 and 2011) being humid. Figure 5 shows positive values for rainy or wet years, while negative values, with varying degrees of intensity, show dry years. 14 years with a positive RAI have occurred, ranging from very wet to There were 27 years with a negative RAI, ranging from very dry to dry, and they were humid. In other words, the number of dry years and wet years is roughly equal. For the previous 40 years. According to an analysis of the 40 years, there were three years of drought. Before 2003, 2004, and 2005, the drought year climbed to a maximum of four years (1973–1978). But none of the years had a particularly dry year, as indicated by RAI > 4. Additionally, as the dryness grew over time, it prompted water scarcity after 1983. Figures 5.1 and 5.2 displays the yearly distribution of RAI based on the wet and dry years in every station.
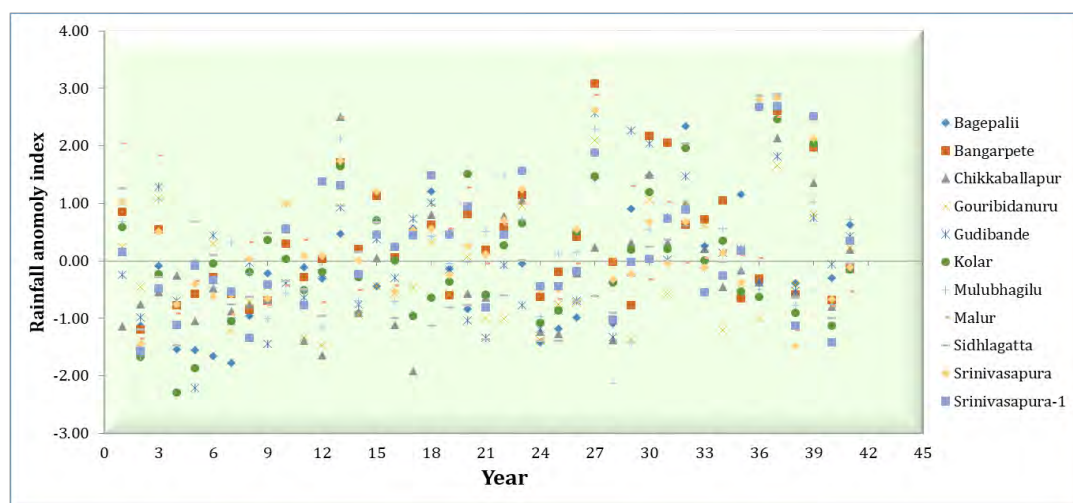
Figure 5. Rainfall Anomaly Index in 1979-2019
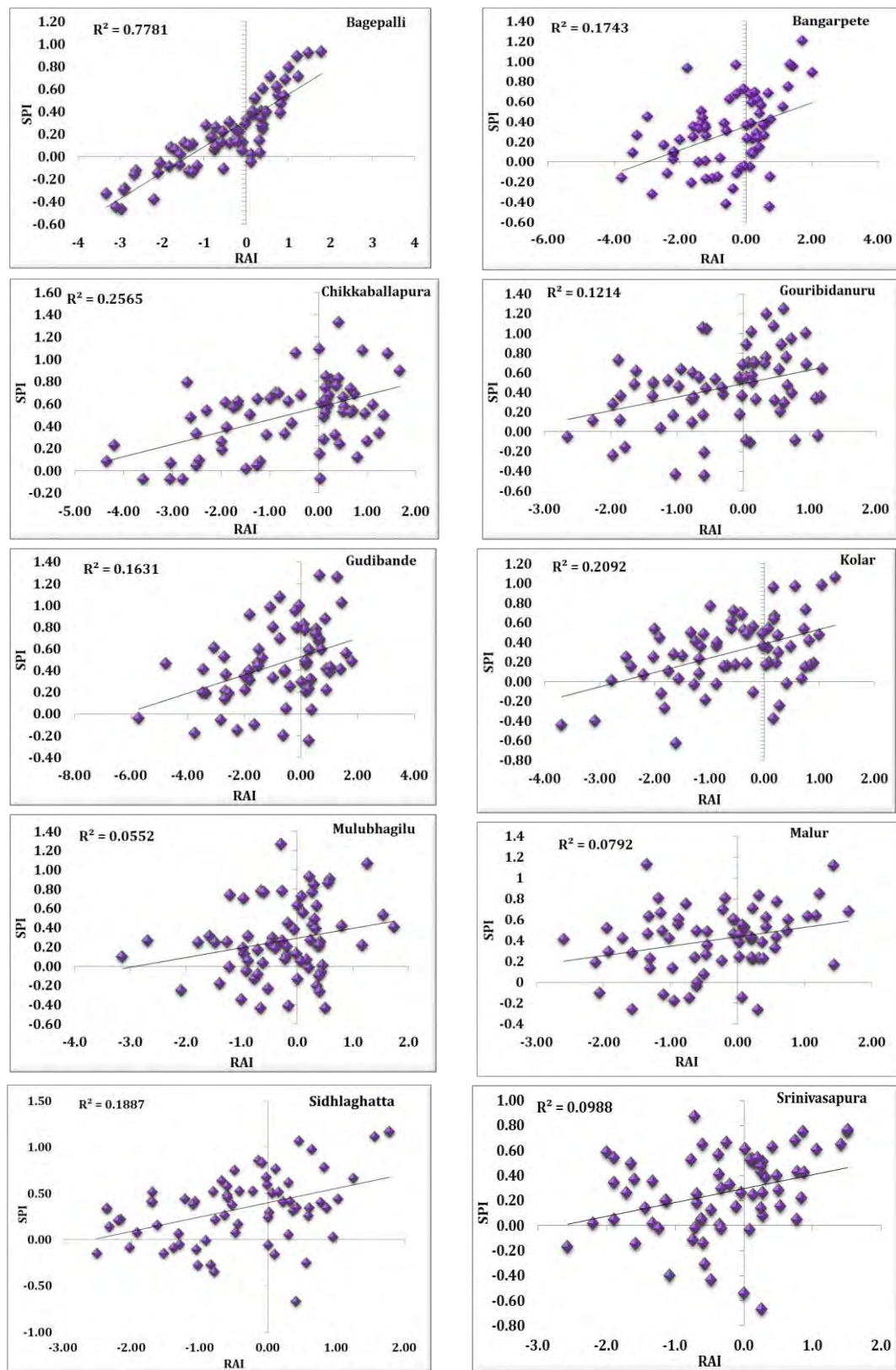
Figure 5.1 Correlation of Dry and Wet Conditions of yearly SPI and RAI value
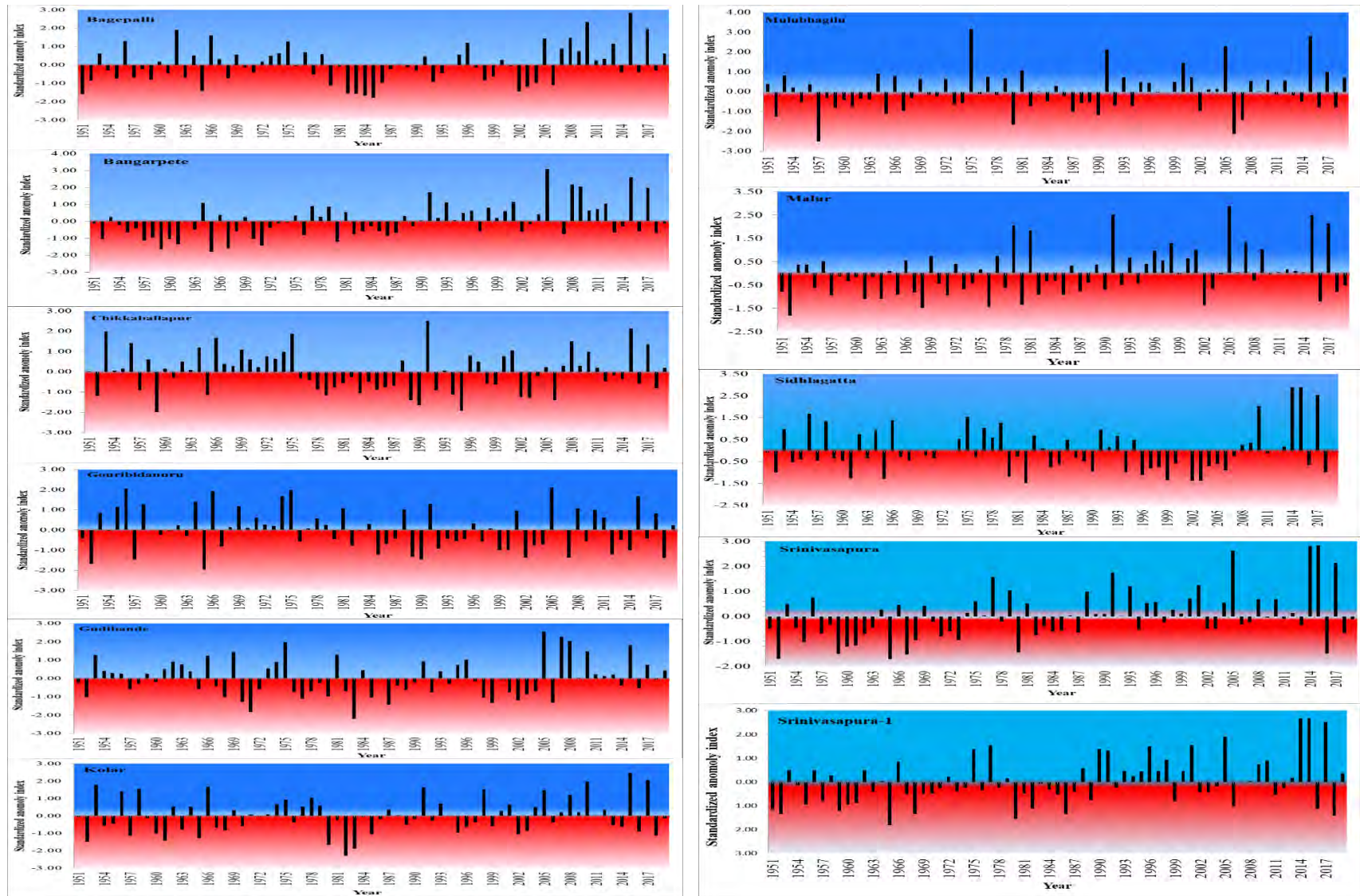
Figure 5.2: Standardized Anomaly Index (-2 dry and +2 Wet Periods)

76

3.7. Agricultural Drought Assessment

3.7.1 Introduction

Rainfall deficit is a major factor in drought assessment and quantification. It is examined to be an indicator of increased drought risk in the conditions of climate change. Drought indices representing rainfall deficit have required valuable information about global meteorological and hydrologic drought. The two major indices are the SPI standardized precipitation index (Mckee, Doesken, and Kleist 1993)which is a factor based only on rainfall, and the PDSI-Palmer drought severity index (Palmer, 1965), which is a factor based on air temperature and precipitation (T_{air}) SPI and PDSI indices have been discussed in detail elsewhere. (Chemeda, Mukand, and Babel 2010; X. Liu et al. 2016; Y. Liu et al. 2016)

The other climatic factors, such as humidity, solar radiation, and wind speed, may be the primary factors causing the soil moisture to decrease. Conversely, the consistency and evolution of the Palmer drought severity index, calculated using the Tair-based potential PET (ET) estimate, significantly influence the direction and magnitude of short- and long-term drought event trends, particularly in areas with limited access to energy. They fail to take into account the rate at which dry periods are globally inclining and increasing.

The difference in potential evapotranspiration (PET) calculated using the Tair-based on Thornthwaite and Penman-Monteith (PM) methods gave rise to the discussion of drought trends over a global region. Long-period PET has not necessarily gradually increased along with the rise in air temperature. Even though the local air temperature is rising, physical factors other than the air temperature, such as atmospheric humidity, wind speed, and reduced radiation, can cause a reduction in potential evapotranspiration (PET). There is a potential increase in evapotranspiration that could result in VWS when there is low soil moisture (vegetation water stress).

Different drought indices are based on PET (potential evapotranspiration), which is a useful parameter in quantifying and rising the severity of drought. For instance, the index SPEI, which is obtained by

standardizing the variation between PET and rainfall at different periods (scales), has shown better performance than SPI. A further application and formulation of the EDDI (evaporative demand drought index) based solely on potential evapotranspiration have been made.

Water supply and demand are taken into account by the reconnaissance drought index (RDI) and demand-sensitive drought index (DSDI). Since a positive anomaly does not necessarily indicate the severity of a drought, the compliance of drought indexes takes into consideration inappropriate regions with adequate soil moisture conditions. Some drought indices, including the ET deficit index (EDI), the Evaporative stress index (ESI), the DSI (drought severity index), the SEDI (standardized ET deficit index), and the ETDI, were developed; the differences or ratios have been accepted for quantifying drought severity (ET deficit index). Table 1 condenses the drought indices along with their relative advantages and disadvantages. Estimates of evapotranspiration are subject to various sources of uncertainty derived from essentially straightforward Tair-related physical models.

The availability of remote sensing products has impacted station remark ET meteorological data's low temporal resolution and spatial coverage. Due to soil heterogeneity, vegetation conditions (VI), and interactions between the atmosphere, plants, and soil, some remotely sensed (evapotranspiration) ET conditions may contain a significant amount of uncertainty. The modelling methods frequently distinguish irrigation in the water cycle, which causes significant biases in the modelled ET. ETDI is a useful indicator to assess short-term agricultural drought, as is to be expected, and remotely sensed ET estimates are further better quality to analyse and monitor drought.

Using this simulated data set for monitoring the drought indices like Soil Moisture Deficit Index (SMDI) and Evapotranspiration Deficit Index (ETDI) were advanced based on monthly or weekly soil moisture deficit and evapotranspiration deficit, respectively. SMDI (Soil Moisture Deficit Index) was calculated at 4 different leveling measures, using soil water accessible in the whole soil profile level, then soil water obtainable at the top 2 feet, 4 feet, and 6 feet in the ground(Mishra and Singh 2010; Narasimhan and Srinivasan 2005).

This was agreed upon because of the potentiality of the agricultural crop to take out water from various depths during particular stages of growth of the crop and also by crop types. ETDI and SMDI had very less autocorrelation lag, designated that they can be used as a very good indicator of drought in a short-term period. The advanced drought index indicates high spatial variability up to a Standard deviation of ~ 1.00 in the research area, primarily due to very high spatial variability of rainfall events. The major crop yields were good correlated with r > 0.75 with the SMDI and ETDI during the period of critical crop growth stages, showing that the advanced drought index can be utilized for agricultural drought assessment(Vicente-serrano et al. 2012; Vicente-Serrano, Beguería, and López-Moreno 2010). The analysis of the SPI, SPEI, ETDI, and SMDI, identifies dry and wet seasons in the region and can be used to evaluate droughts and address the effects of climate change on rainfall. This paper's detailed study and focus are on the evaluation of the drought, the clarification of wet and dry years at the district level, and the analysis of the spatial-temporal pattern of meteorological, agricultural, and hydrological drought at the annual time scale.

3.7.2 Data

The IMD (India Meteorological Department) Pune website provided temperature and precipitation data with a spatial resolution of 0.250 0.250 for the years 1951 to 2019. For statistical interpretation, the 11 grid points collected from the districts are used. To identify trends and conditions for rainfall variability, the spatial distribution was converted into total annual data. With a spatial resolution of 500 m, the soil moisture, evapotranspiration (ET), and potential evapotranspiration (PET) datasets were obtained from 2001 to 2019 in LPDAAC (https://lpdaac.usgs.gov/).

3.8 Methodology

3.8.1 Soil Moisture Deficit Index (SMDI)

SMDI Each grid station's daily data model result for soil water at the root zone was averaged over 7 days to obtain weekly soil water for 52 weeks between the years 2010 and 2019. The mean of the available soil water for that week time during 10 years was taken to obtain the long-term soil moisture data for each specific week in years (2010-2019). The median is more stable and is unaffected

by some outliers because the average value was chosen over the median as a measure of typical, attainable soil water. From the 10 years of data, the minimum and maximum soil water for each week also predominated. Using this median, long-term, minimum, and maximum soil water, the weekly % soil moisture excess or deficit for 10 years (2010-2019) was computed as:

$$SD_{i,j} = \frac{SW_{i,j} - MSW_j}{MSW_j - minSW_j} \times 100 \quad \text{if } SW_{I,j} \leq MSW_j \tag{15}$$

$$SD_{i,j} = \frac{SW_{i,j} - MSW_j}{maxSW_j - MSW_j} \times 100 \quad \text{if } SW_{i,j} > MSW_j \tag{16}$$

Where:

$SD_{i,j}$ = Soil water deficit in %

$SW_{i,j}$ = Average weekly soil water data available in the soil profile in mm,

MSW_j = Long-term average obtainable soil water in the soil profile in mm,

$maxSW_j$ = Long-term maximum obtainable soil water in the soil profile in mm,

$minSW_j$ = Long-term minimum obtainable soil water in the soil profile in mm.

(Where j = 1 to 52 weeks and i = 1901 to 1998)

Table 3.9 Summary of the drought indices used in this research.

Indices	Data	Strengths	Index values
SPI(McKee et al., 1993)	precipitation	Calculated for multiple time scales/periods; like both wet and dry spells	≥2.0 Extremely wet
SPEI	Precipitation, PET	Multiscalar properties with the capacity to include the effects of Air temperature variability on drought Evaluation; equally sensitive to PET and precipitation	2.0 to 1.5 (Severely wet) 1.49 to 1 (Moderately wet) 1 to -1(Near Normal) -1 to -1.49 (Moderate dry) -1.5 to -1.99 (Severe dry)
ETDI(Narasimhan and Srinivasan 2005)	ET, PET, water stress ratio	Indicators of short-term agricultural drought assessment. importance of LAI and vegetation type	≤ – 2.0 (Extreme dry)
SMDI(Narasimhan and Srinivasan 2005)	Soil Moisture	Soil moisture on the surface	

Equation 2 eliminated the seasonality of the data that was crucial for understanding soil water. As a result, the deficit range values can be distinguished between seasons. The soil water deficit (SD) values range from +100 to -100 in a week, indicating extremely wet to extremely dry conditions. The soil water deficit values for all grid stations ranged from +100 to -100, making them spatially approximate in both humid and arid climate zones. When compared to long-term historical metrological data, the SD range for each week provides the amount of moisture and dryness during that week. Only when an area's dryness lasts for a protracted period and has an impact on crop growth do drought events occur. As the limitation of (SD) values ranged between +100 and -100, the worst event of drought can be described by a straight line and the equation is:

$$\sum_{t=1}^{j} Z_t = -100t - 100 \qquad \qquad 17)$$

Where time in weeks t. If this line describes the worst severe drought value -4 for the drought index value to be comparable with the palmar drought severe index (PDSI), then SMDI for any week can be computed by:

$$SMDI_j = \frac{\sum_{t=1}^{j} SD_t}{(25\,t+25)} \qquad \qquad 18)$$

Therefore, we fail to complete the Taff task of choosing the weeks (period) over the area where the dryness range needs to be collected to determine the length of the drought. To overcome this and time into considering indirectly, the index of the drought was computed on a basis as suggested by Palmer (1965):

$$SMDI_j = SMDI_{j-1} + \Delta SMDI_j \qquad \qquad 19)$$

To calculate the addition of each month of the drought severity, we can set t = 1 and i = 1 in Equation 5 and we have:

$$SMDI_1 = \frac{SD_1}{50} \qquad \qquad 20)$$

Since these are the initial months:

$$SMDI_1 - SMDI_0 = \Delta SMDI_1 = \frac{SD_1}{50} \qquad \qquad 21)$$

If consecutive months are close to normal or normal, the drought won't progress to the severe and extreme category. As a result, the rate at which the soil water deficit (SD) must increase to manage value depends on the SMDI value that needs to be maintained. For this purpose, Equation 6 should include an additional term for all specific months that follow a first initial drought month.

$$SMDI_J = \frac{SD_1}{50} + cSMDI\,j_1 \qquad \text{22)}$$

Where

$$SMDI_J = SMDI_J - cSMDI\,j\_1$$

23)

Equation 7 can be solved no for c. By taking over Soil Moisture Deficit Index are 4 during time steps, then SDI should be 100 values:

$$\Delta SMDI_j = \frac{-100}{50} + c(-4.0)$$

$$0 = -2 - 4c \qquad \text{24)}$$

$$c = -0.5$$

Hence, drought severity given week is by:

$$SMDI_j = SMDI_{j-1} + \frac{SD_j}{50} - 0.5SMDI_{j-1}$$

$$\text{25)}$$

$$SMDI_j = 0.5SMDI_{j-1} + \frac{SD_j}{50}$$

SMDI will range from +4 to -4 during any given week, depending on whether it is wet or dry. It was calculated using water from the soil that was available at four different levels: the whole soil profile level, the top two feet, the top four feet, and the top six feet, which are represented by SMDI. This occurred as a result of the crop's potential to withdraw water from a variety of depths depending on the crop type and crop growth stage.

3.8.2 ETDI- (Evapotranspiration Deficit Index)

The water stress ratio specified by Equation 1 was used to calculate the evapotranspiration deficit index rather than using evaporation and transpiration as it was for the SMDI. Each sub-weekly station's potential and actual

evapotranspiration for each of the 52 weeks in a year was calculated using the daily model product of potential and actual evapotranspiration. The ratio of water stress for every week is computed as:

$$WS = \frac{PET - AET}{PET}$$ 26)

WS = Water stress ratio in a week

PET= potential evapotranspiration in weekly

AET= Actual evapotranspiration in weekly

Water stress values range from 0 to 1, with 0 designating evapotranspiration occurring at the same rate as potential evapotranspiration and 1 designating no evapotranspiration. By averaging the water stress for that week over the previous 10 years, one can determine the length of the water stress for each week of the entire year (2010-2019). The minimum and maximum water stress ratio for every week was obtained from the 10-year data from long period maximum, minimum and median water stress, % of anomaly water stress during a week for 10 years (2010-2019) is calculated as:

$$WSA_{i,j} = \frac{MWS_j - WS_{i,j}}{MWS_j - minWS_j} \quad \text{If WSi,j} \leq \text{MWSj}$$ 27)

$$WSA_{i,j} = \frac{MWS_j - WS_{i,j}}{maxWS_j - MWS_j} \times 100 \text{ if WS}_{i,j} > \text{MWS}_j$$ 28)

Where

WSA = Water stress Anomaly for week

WSJ = Long-period average water stress of week (j),

Max, WSJ = Long-period maximum water stress of week (j),

Min, WSJ = Long period minimum water stress of week (j),

WS = water stress ratio on a Weekly.

The water stress anomaly during any week ranges from -100 to +100 indicating very dry to very wet conditions concerning evapotranspiration. Adopting a similar cumulating procedure. The valve of EDTI and SMDI is presented in Table 3.9.

3.9 Result and Discussions

3.9.1 Surface Soil Moisture

The surface soil moisture of the districts in 2010 experienced maximum in the first week of November and September is about 20 to 23mm and lowest in March in is about only 2 mm, rest of the period of pre-monsoon time the value is negligible. In 2017 and 2019 the soil moisture become more compared to the other study year about 25-27 mm. In the pre-monsoon season of 2018 experience maximum length of soil moisture content on the surface even in the March, April, and May months is about 4 to 23. Figure 6 and 6.1 shows variations in the weekly surface soil moisture.
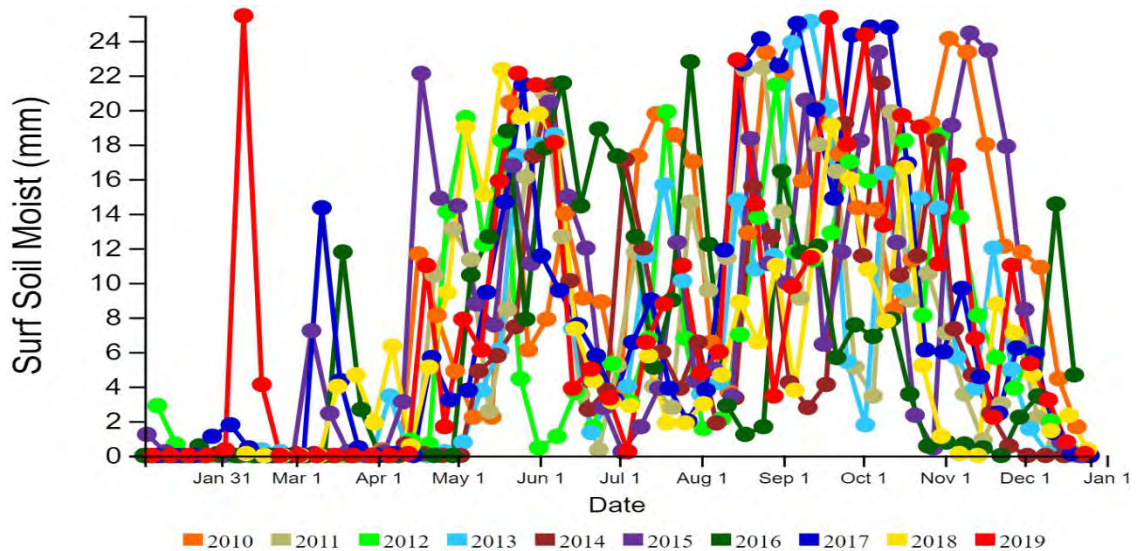
Figure 6. Weekly Surface Soil Moisture in all Stations (8 Days)
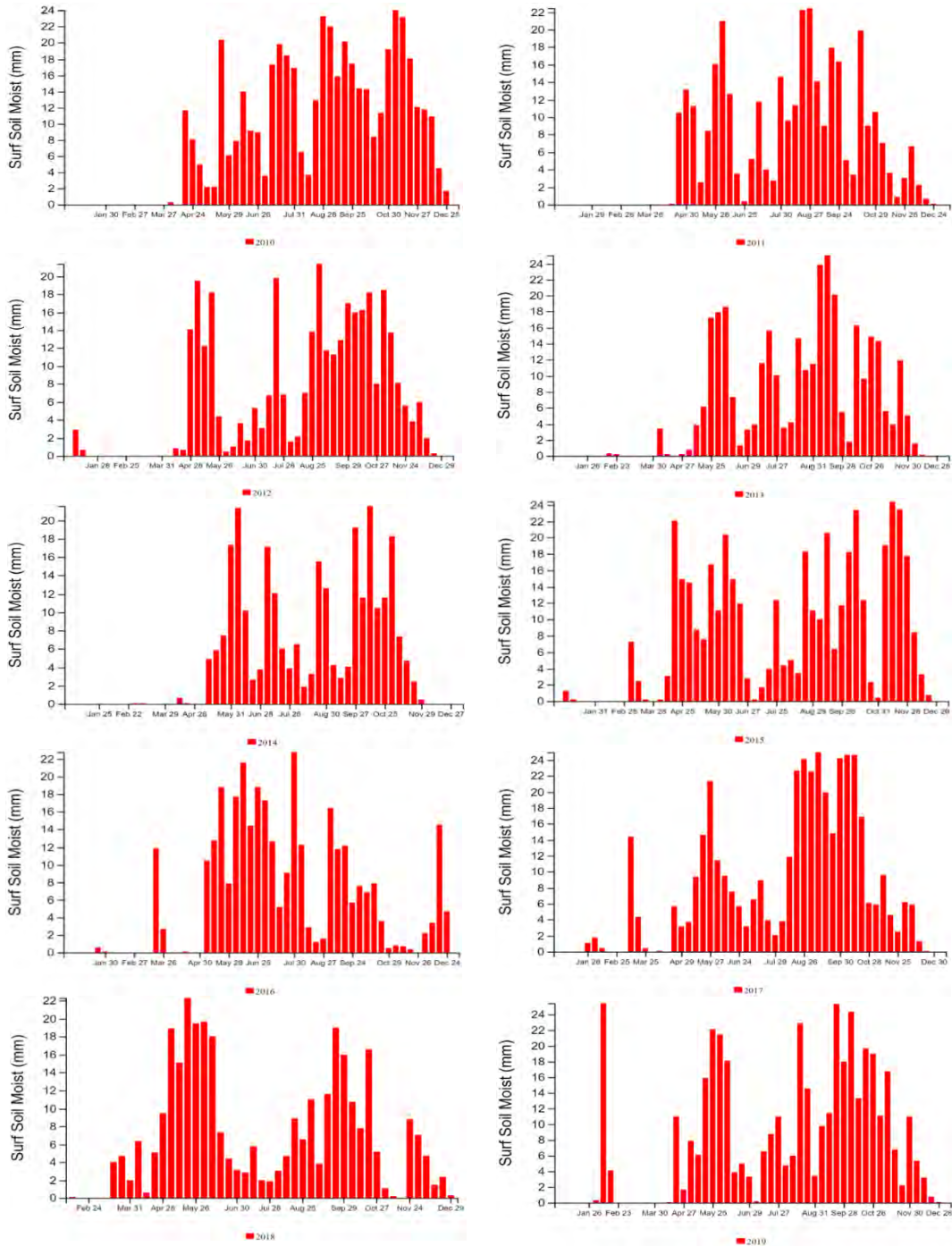
Figure 6.1 Weekly Surface Soil Moisture From 2010-2019 (8 Days)

3.9.2 ETDI, SMDI Analysis, and Characteristics of Drought

The ED can be used for both the atmospheric evapotranspiration demand and the water emitted into the atmosphere by vegetation and soil in terms of eco-physiological and terrestrial agronomic systems. This physiological describes how vegetation behaves and functions (Kim & Rhee, 2016). Table 3.10 showed that as the duration of the temporal scale gradually increased at all 11 stations in both districts, the number of dry events decreased. Except for Bangarapete and Srinivasapura grid stations, where differences between monthly and yearly temporal scales were

Figure 6.1. Weekly Surface Soil Moisture in all year (8 days)

Significant (Figure 6.2) the disparity in the number of drought occurrences over successive temporal scales was primarily between ETDI, SMDI, and SPI index (About 6 drought events). The Bagepalli stations indicate that 2015 was the wettest year during the study period, with an annual rainfall of approximately 1026.4 mm and EDTI values of approximately 4.5 SMDI 2.1. Additionally, 2018 was the driest year in comparison to other stations, with an average rainfall of 456 mm. nearly all stations indicate that 2015 is the wettest year this year, with the station mulubhagilu showing the highest rainfall. The ETDI is approximately 4.88 and the SMDI is approximately 2.67 (Figure 6.3).

In the year 2018, there were extreme drought events in Sidhghatta, which received 414 mm of rain (EDTI-1.41, SMDI-0.71), and Srinivasapura, which received 432.1 mm (EDTI-1.92, SMDI-1.22). The figure and Table show the correlation matrix (R) value of the ETDI, SMDI, and SPI with annual rainfall for the elevation grid stations. Major drought events measured by the ETDI and SMDI Index occurred in 2011, 2012, 2016, and 2018. ETDI was compared to SPI to assess the long-term drought events using SPI's yearly average. Value If the temperature is high and the amount of rainfall is significantly below average, drought will occur over a longer period. These dry and wet events were picked to compare the various drought indices because they varied over time across all grid stations and had a strong correlation with each grid station.
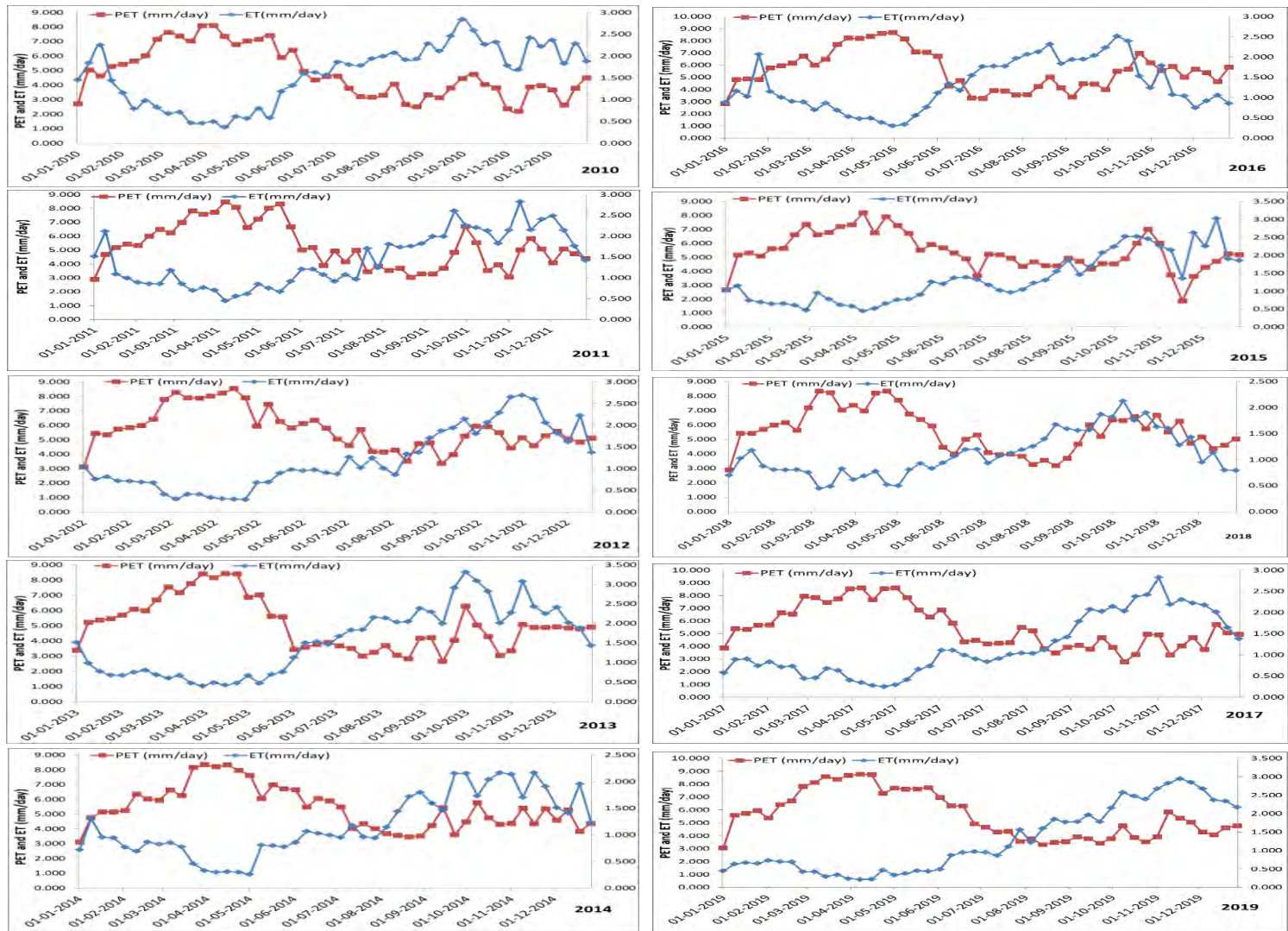
Figure 6.2 Weekly MODIS Potential evapotranspiration and Evapotranspiration

3.9.3 Drought Variation in the Different Indices.

All 11 stations' ETDI and SMDI values were calculated for the periods of 2010–2019 and 1981–2019 for the drought indices like SPI and SPEI. Figure 2 depicts the results of SPI and SPEI measurements taken at each grid station for further analysis in this section. Typically, the two stations display the downstream and upstream portions of the study area. Show the effectiveness of the drought indices in displaying historical drought periods. Except for occasionally indicating a bounce between the drought period and normal situation at a very lower time scale at 1- and 3-month scale, the majority of the drought indices consistently indicated the historical drought years (1973–1974, 1983–1984, 1994–1955, 2003–2004, 2008–2009, 2012, and 2018).

The historical drought period was highlighted in the SPI and SPEI indices at time scales of six, nine, twelve, and twenty-four months. The majority of the stations' meteorological drought indexes indicate severe drought in the years 1983, 2003, and 2018, while other drought indices failed to adequately reflect the severity of this condition. The patterns of the 1-month and 3-month time scales for the agricultural and meteorological drought indexes were comparable. Additionally, the agricultural drought indices demonstrated a decreased magnitude of drought severity in several of the stations when compared to other drought indices. The most likely reason is that, in comparison to other input variables like evapotranspiration and rainfall, river flow variation is rather gradual.

Table 3.10 Dry spell years in the ETDI, SMDI, and SPI along with the Rainfall

Stations	Rainfall and Drought Parameters										
Bagepalli	Year	2010	2011	2012	2013	2014	2015	2016	2017	2018	2019
	Rainfall	940.6	574.8	589.9	733.0	462.8	1026.4	463.1	873.1	479.5	639.7
	ETDI	1.7	0.4	0.5	1.4	-1.6	4.5	-1.4	1.6	-1.2	1.0
	SMDI	0.5	0.8	1.0	0.5	-1.7	2.0	-2.1	-1.4	-0.4	-1.2
	SPI	0.92	0.41	0.52	0.62	0.26	1.30	0.09	0.71	0.22	0.61
Bangarapete	Rainfall	838.9	861.4	941.3	523.2	607.8	1324.8	538.5	1169.1	517.2	650.4
	ETDI	0.91	1.31	1.58	-1.09	-0.64	5.17	-0.82	3.04	-1.00	-0.43
	SMDI	1.99	0.29	0.36	-0.20	-0.42	4.13	1.85	-1.06	0.13	0.39
	SPI	0.44	0.48	0.63	-0.01	0.07	0.94	0.06	0.64	0.02	0.39
Chikkaballapura	Rainfall	827.4	656.8	511.7	575.1	529.3	1075.7	486.3	907.1	437.5	654.2
	ETDI	1.59	0.11	-0.80	-0.32	-0.44	4.10	-0.95	2.56	-1.34	0.25
	SMDI	0.6	1.6	1.6	-0.4	0.1	2.7	-2.2	-0.4	-0.8	-0.4
	SPI	0.66	0.44	0.29	0.30	0.26	0.94	0.24	0.64	0.03	0.42
Gauribidanur	Rainfall	941.9	864.6	494.2	639.2	533.1	1079.5	654.2	905.8	454.4	786.5
	ETDI	2.08	1.13	-1.70	-0.78	-1.49	4.82	-1.15	1.32	-2.16	0.25
	SMDI	0.89	1.03	-0.25	0.79	-0.54	2.27	1.87	0.27	0.82	-0.05
	Rainfall	941.9	864.6	494.2	639.2	533.1	1079.5	654.2	905.8	454.4	786.5
Gudibande	Rainfall	841.1	577.0	559.7	574.0	452.5	911.7	421.3	687.8	519.4	622.6
	ETDI	1.31	0.50	-0.21	-0.78	-0.49	2.64	1.82	-0.87	-1.69	-0.55
	SMDI	1.10	-0.51	0.74	-0.22	-1.39	2.09	1.98	-0.42	0.77	-0.02
	SPI	0.64	0.44	0.51	0.44	0.32	0.95	0.05	0.57	0.28	0.53
Kolar	Rainfall	1098.0	703.1	772.0	594.3	574.5	1198.5	519.5	1113.6	472.4	670.5
	ETDI	3.1	0.3	0.6	-1.2	-1.4	4.9	-1.9	4.2	-2.0	-1.0
	SMDI	2.0	-0.5	-0.1	-1.1	-1.2	3.2	-1.9	2.6	-1.0	-0.2
	SPI	0.69	0.30	0.44	0.02	0.08	0.86	-0.08	0.69	-0.06	0.34
Malur	Rainfall	ETDI	SMDI	SPI	Rainfall	ETDI	SMDI	SPI	Rainfall	ETDI	SMDI
	746.5	0.1	0.22	0.33	746.5	0.1	0.22	0.33	746.5	0.1	0.22
	766.2	0.1	2.10	0.30	766.2	0.1	2.10	0.30	766.2	0.1	2.10
	790.8	-0.1	-0.50	0.37	790.8	-0.1	-0.50	0.37	790.8	-0.1	-0.50

Table 3.10. Continued…

Mulabagilu	**Rainfall**	**918.0**	**762.4**	**908.3**	**754.2**	**688.6**	**1374.9**	**629.6**	**1002.0**	**631.6**	**941.1**
	ETDI	2.10	0.22	2.00	0.16	-0.40	4.88	-2.15	1.06	-1.05	2.16
	SMDI	0.57	0.04	0.04	0.10	0.81	2.00	1.18	-1.34	-0.58	0.62
	SPI	0.40	0.28	0.39	0.05	-0.04	0.66	-0.10	0.35	0.09	0.35
Sidhlagatta	Rainfall	1037.5	592.0	615.8	656.4	1210.0	1213.1	486.3	1140.3	414.5	609.2
	ETDI	3.75	-0.32	0.35	0.11	5.74	5.80	-0.70	4.42	-1.41	0.66
	SMDI	1.38	1.22	1.29	-1.76	2.60	2.77	-1.27	0.13	-0.76	0.27
	SPI	1.81	0.29	0.40	0.34	1.99	1.97	0.01	1.91	-0.11	0.47
Srinivasapura	Rainfall	840.5	673.2	724.7	616.7	1292.0	1297.3	379.9	1147.3	553.1	672.7
	ETDI	0.67	0.00	-0.04	-0.34	4.74	5.10	-2.75	2.99	-0.66	0.13
	SMDI	-0.48	0.25	-0.35	0.03	2.12	2.37	-1.21	1.59	-1.59	-0.36
	SPI	0.40	0.32	0.42	0.02	0.89	0.88	-1.43	0.77	0.16	0.28
Srinivasapura-1	Rainfall	919.3	616.7	677.1	767.5	1293.6	1296.0	492.9	1260.3	432.4	806.2
	ETDI	1.07	-0.66	-0.55	0.31	4.14	4.23	-2.39	4.39	-1.92	0.45
	SMDI	1.32	-1.29	0.19	-0.85	2.51	2.21	1.72	2.14	1.22	-0.15
	SPI	0.42	0.10	0.22	0.21	0.66	0.66	-0.34	0.73	-0.22	0.28

SPI and SPEI indices showed that the historic drought period was more prominent at time scales of six, nine, twelve, and twenty-four months. The majority of drought indicators demonstrated the severity of the prior drought condition at various severity levels, ranging from mild to serious drought conditions. Therefore, using each drought indicator, it is possible to assess a portion of the historic drought period in the Kolar and Chikkaballapura districts. Other drought indicators currently in use, such as the SPI and SPEI, were compared to the SMDI and ETDI drought indices developed in this work (Mckee et al., 1993). The SPEI and SPI data are displayed at the spatial scale of the climatic divisions.

3.10 Monitoring Agricultural Drought Using MODIS Remote Sensing Data

3.10.1 ET and PET

A vegetated surface's evapotranspiration (ET) is influenced by climate variability, crop variables, and environmental factors. The procedure depends on the available energy, whose primary source is solar radiation, as well as on environmental factors like air temperature.
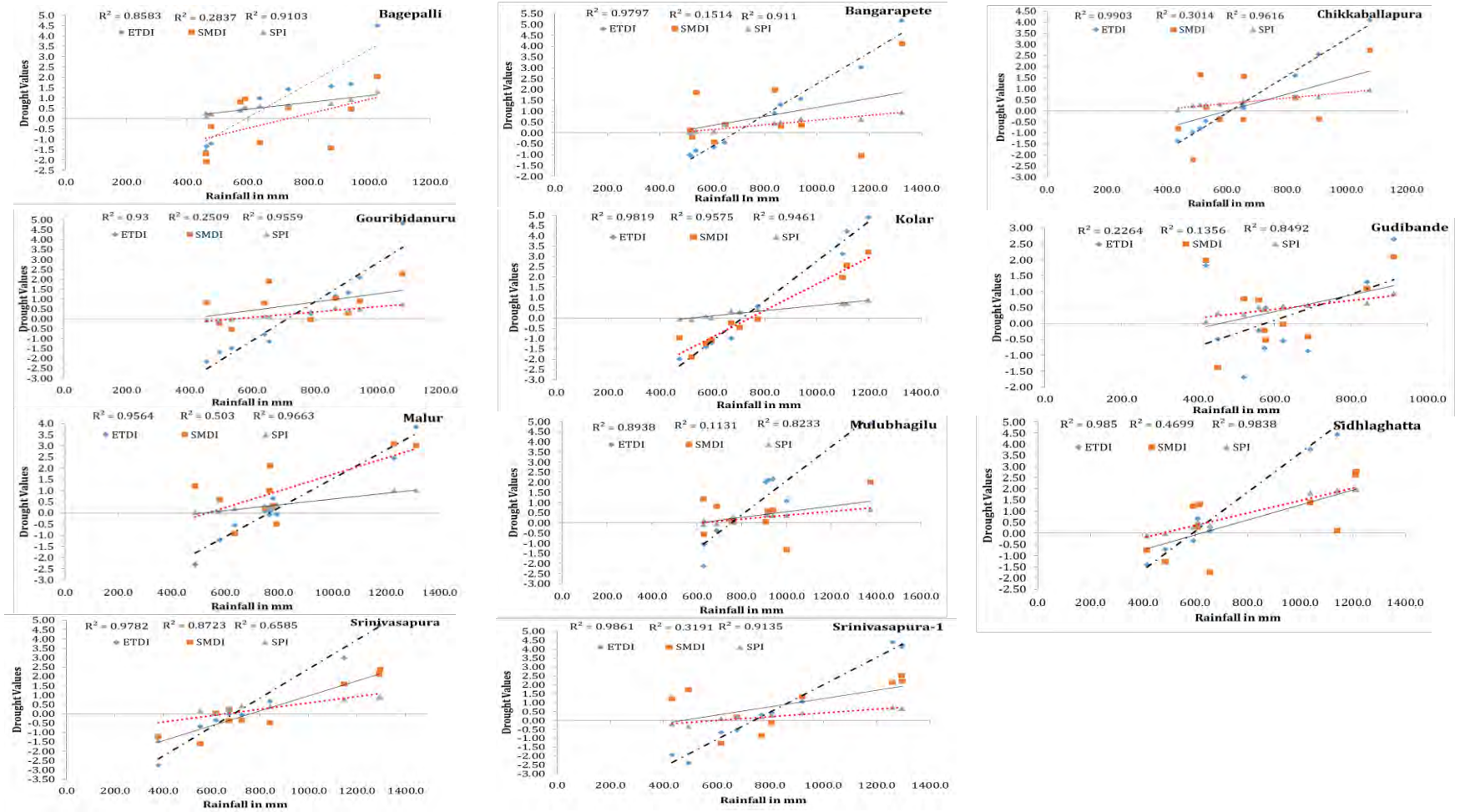
Figure.6.3 The Correlation of ETDI, SMDI, and SPI

The pressure differential between the water vapor on the evaporating surface and the water vapor in the surrounding atmosphere is what elevates this process. Since its accurate estimation enables to lower the cost of irrigation projects, the ET has a huge economic impact on several Taluks in the semi-arid region (Kolar and Chikkaballapura). As a result, it is a research area that is actively being studied in the fields of hydrology, agriculture, and meteorology, which has resulted in the creation of several empirical designs that can be used with satellite data.

The recent advances in Earth observation technology provide the possibility to use a new viewpoint for PET estimation on both a global and local scale. The dual Terra and Aqua satellites' mission should be mentioned as a remarkable example. The datasets required for the final PET product are provided with an 8-day (interval) temporal resolution and a 500 m spatial resolution by the MODIS modules installed on the previously mentioned satellite systems. The Penman-Monteith concept formed the basis for the MODIS algorithm. It makes perfect sense to combine satellite data into the national system for monitoring agricultural drought given its advantages, particularly its spatial and temporal resolution. Evapotranspiration investigates the ecosystem, which further investigates the water, energy, and carbon cycles. Water availability in a terrestrial environment is determined by the ratio of ET to PET, which also aids in understanding local dry seasons.

3.10.2 Datasets

In this study, the MODIS satellite terra sensor evapotranspiration (ET) and potential evapotranspiration (PET) 8-Day Global 500 m datasets, both of which are freely available, were used. And MODIS (Terra) NDVI 16-Day Global 250 m Resolution While the NDVI dataset is available from February 2015 to the present, the ET and PET datasets are available from January 2010 to the present. Therefore, drought mapping and monitoring are done for this study from 2010 to 2019.

3.10.3 Methodology

Data from MODIS Terra are analyzed and computed in this study. ET (Evapotranspiration), PET (potential evapotranspiration), and NDVI (normalized difference vegetation index) are the parameters used in this index(Gong et al. 2015). Before calculating drought conditions, datasets are modified to remove shadows, reduce cloud coverage, smooth the timeframe of our study, scale values to monthly data, and mask vegetation statistics (Astuti et al. 2022). The following is the computation methodology: The ratio between AET is first calculated. The ratio is standardized in the following stage. Thirdly, the NDVI pre-computed product from MODIS is uniform(Evapotranspiration, Sensing, and Application n.d.).

3.11 Results and Discussions

3.11.1 Spatial-Temporal Differences of Monthly PET and ET

The statistical median is calculated for spatial maps' final product for the annual outcome. Since the results are displayed more clearly when using the mean rather than the median, this decision was not made. The performance increased to r value ranges using only the native MODIS16A2-006 PET and the average 8-day temperature from MODIS's land surface temperature. The performance increased to r value ranges of 0.12 to 0.64 using only the native MODIS16A2-006 PET and the average 8-day temperature from MODIS's land surface temperature(Degano et al. 2018). To examine the Spatio-temporal differences of monthly PET within the Kolar and Chikkaballapura, ET data from MODIS-16MODIS16A2-006 PET from 2010 to 2019 were used. Figure 6 shows that the watershed had been in a variable condition concerning the element of water loss. When the PET indicates the combined loss of water from 1) the plant's mechanism of transpiration through its vascular system & 2) The evaporation of moisture from the ground surface, the average value in the district in 2010 during the pre-monsoon season reveals a 5 to 12mm. Both are affected by wind, sunlight, and temperature. PET readings show how much water has been lost and must be restored, either through irrigation or rainfall. The future is predicted to see enhanced PET throughout Kolar and Chikkaballapura,

including in the semi-arid region of Karnataka. By 2025, the amount of change will have increased by 3% to 5% (Figure 6.4 and Table 3.11).
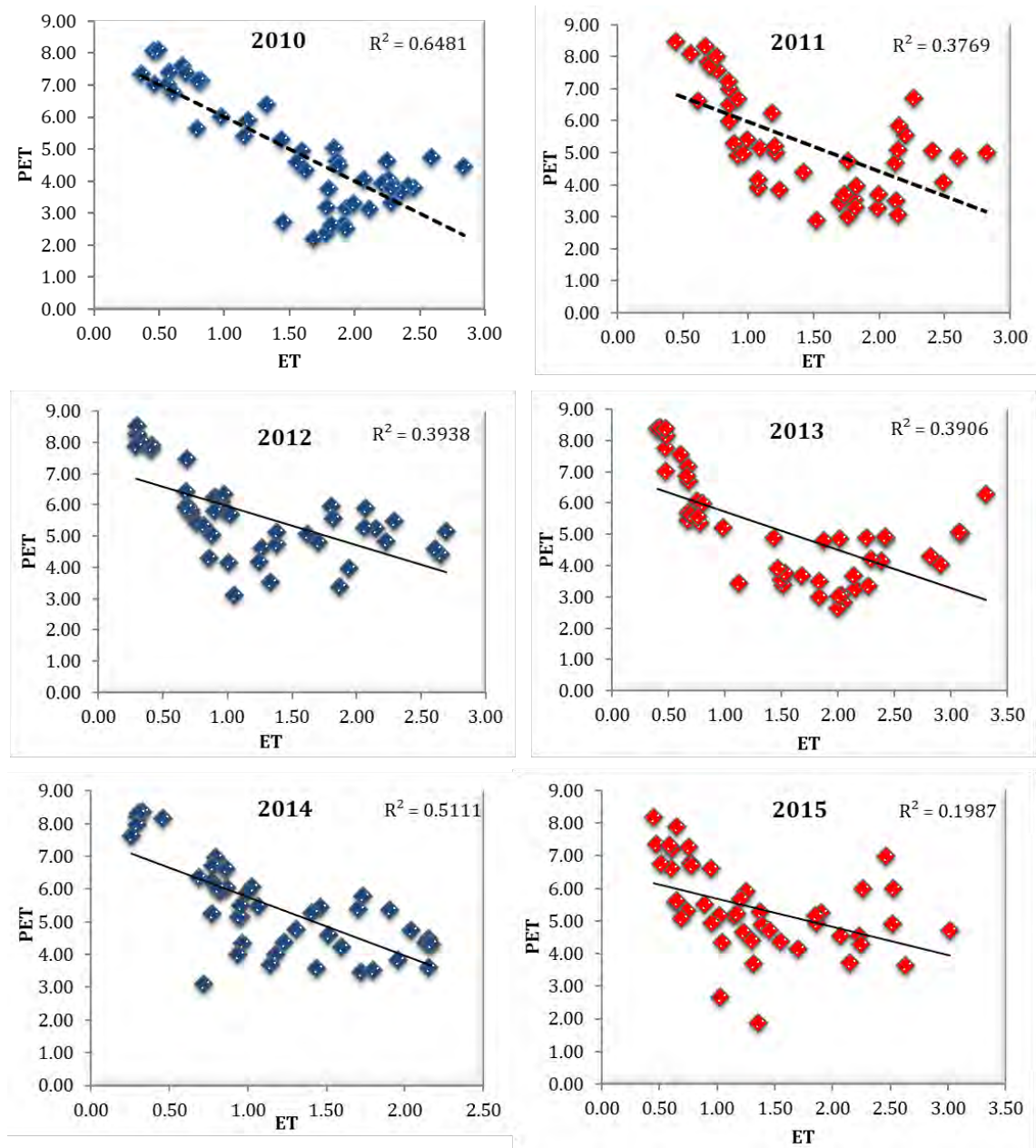
Figure 6. 4 Correlations of PET and ET
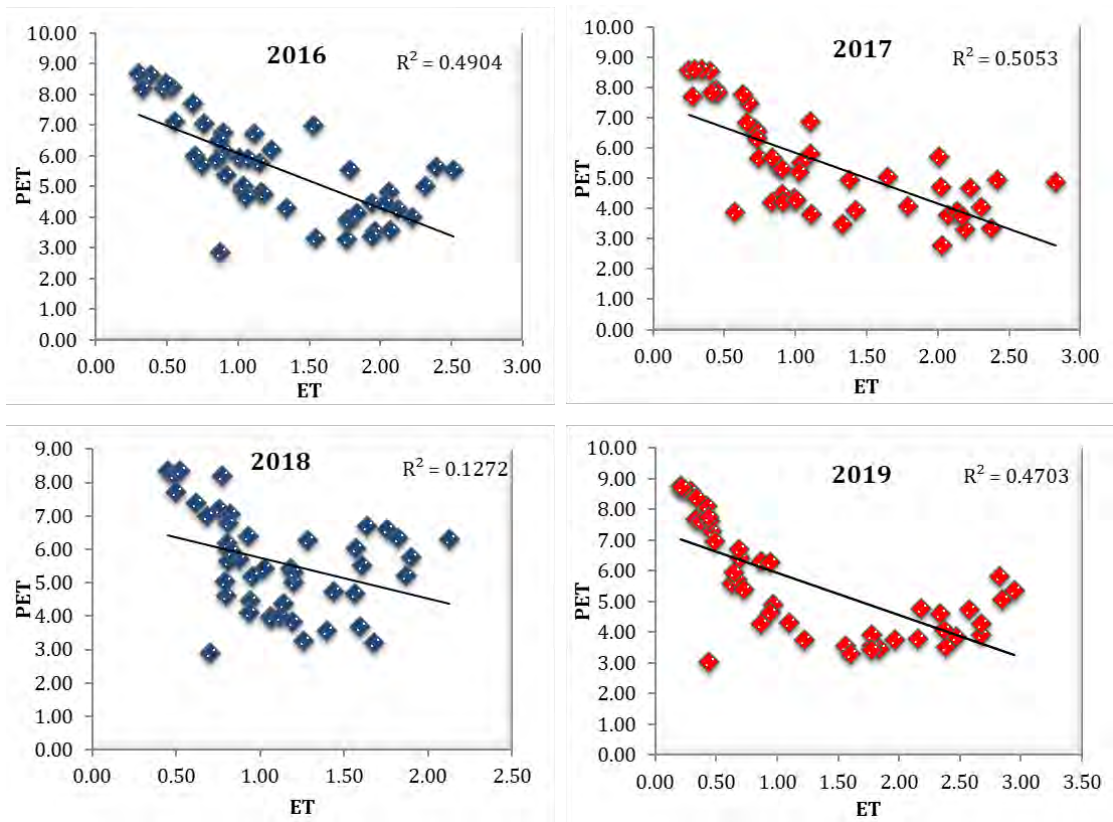
Figure 6. 4 Correlations of PET and ET

This rise in PET will have a stronger propensity to lower soil moisture levels overall in the districts than one might anticipate from increases in rainfall alone. Due to rising temperatures and probable evapotranspiration, there will be a greater disparity between water supply and demand in the southern Basin. This disparity will widen as a

Result of climate change. The possibility for greater evapotranspiration across Kolar would also be increased, and the opportunity for the back burner to control load capacity would be smaller due mostly to rising temperatures. These modifications are similarly affected by variations in rainfall, and they would be most noticeable in those regions. A useful indicator of the moisture health of an ecosystem during a season or year is the shortfall in moisture consumption when actual ET is less than PET. This index is occasionally used as a difference and other times as a ratio. With potential and actualdistinction.

Table 3.11 Monthly PET and ET in mm

2010					2011				
Months	Average of ET	Average of PET	ET in Month (mm/day)	PET in Month (mm/day)	Months	Average of ET	Average of PET	ET in Month (mm/day)	PET in Month (mm/day)
Jan	13.95	35.29	1.74	4.41	Jan	11.44	36.35	1.43	4.54
Feb	13.95	35.29	1.74	4.41	Feb	7.56	48.10	0.95	6.01
Mar	13.95	35.29	1.74	4.41	Mar	6.04	60.23	0.75	7.53
Apr	3.91	59.23	0.49	7.40	Apr	4.31	61.87	0.54	7.73
May	6.24	54.95	0.78	6.87	May	6.37	60.49	0.80	7.56
Jun	12.20	40.52	1.52	5.07	Jun	8.80	38.06	1.10	4.76
Jul	14.76	29.46	1.85	3.68	Jul	9.96	32.89	1.24	4.11
Aug	15.82	25.08	1.98	3.13	Aug	14.25	27.06	1.78	3.38
Sep	19.37	29.38	2.42	3.67	Sep	17.70	37.02	2.21	4.63
Oct	19.12	33.53	2.39	4.19	Oct	16.43	34.71	2.05	4.34
Nov	16.69	29.14	2.09	3.64	Nov	19.04	37.95	2.38	4.74
Dec	16.69	29.14	2.09	3.64	Dec	15.63	36.61	1.95	4.58

2012					2013				
Months	Average of ET	Average of PET	ET in Month (mm/day)	PET in Month (mm/day)	Months	Average of ET	Average of PET	ET in Month (mm/day)	PET in Month (mm/day)
Jan	6.68	39.27	0.83	4.91	Jan	7.90	38.82	0.99	4.85
Feb	4.97	52.07	0.62	6.51	Feb	5.84	48.88	0.73	6.11
Mar	2.90	64.16	0.36	8.02	Mar	4.32	61.76	0.54	7.72
Apr	2.39	65.74	0.30	8.22	Apr	3.70	66.54	0.46	8.32
May	6.49	50.95	0.81	6.37	May	5.20	50.15	0.65	6.27
Jun	7.40	46.60	0.93	5.82	Jun	11.26	29.38	1.41	3.67
Jul	9.07	37.28	1.13	4.66	Jul	15.00	26.84	1.87	3.35
Aug	10.55	34.65	1.32	4.33	Aug	17.21	27.44	2.15	3.43
Sep	15.52	37.04	1.94	4.63	Sep	21.03	34.37	2.63	4.30
Oct	18.70	42.16	2.34	5.27	Oct	21.10	32.98	2.64	4.12
Nov	18.36	41.16	2.30	5.14	Nov	20.04	36.37	2.51	4.55
Dec	13.93	39.96	1.74	5.00	Dec	7.90	38.82	0.99	4.85

Table 3.11 Continued...

	2014					2016			
Months	Average of ET	Average of PET	ET in Month (mm/day)	PET in Month (mm/day)	Months	Average of ET	Average of PET	ET in Month (mm/day)	PET in Month (mm/day)
Jan	7.84	36.35	0.98	4.54	Jan	10.26	34.63	1.28	4.33
Feb	6.29	47.14	0.79	5.89	Feb	7.90	49.20	0.99	6.15
Mar	4.82	58.74	0.60	7.34	Mar	5.55	56.83	0.69	7.10
Apr	2.39	65.29	0.30	8.16	Apr	3.61	67.07	0.45	8.38
May	5.26	54.70	0.66	6.84	May	3.91	61.99	0.49	7.75
Jun	7.88	48.14	0.99	6.02	Jun	10.36	38.06	1.30	4.76
Jul	8.06	35.67	1.01	4.46	Jul	14.56	29.19	1.82	3.65
Aug	12.20	28.45	1.52	3.56	Aug	16.69	33.94	2.09	4.24
Sep	14.72	35.51	1.84	4.44	Sep	16.29	32.53	2.04	4.07
Oct	15.84	39.54	1.98	4.94	Oct	17.18	48.32	2.15	6.04
Nov	15.82	38.97	1.98	4.87	Nov	10.26	45.25	1.28	5.66
Dec	12.20	36.18	1.53	4.52	Dec	7.15	43.11	0.89	5.39

	2015					2017			
Months	Average of ET	Average of PET	ET in Month (mm/day)	PET in Month (mm/day)	Months	Average of ET	Average of PET	ET in Month (mm/day)	PET in Month (mm/day)
Jan	7.21	36.39	0.90	4.55	Jan	6.21	40.45	0.78	5.06
Feb	4.73	50.35	0.59	6.29	Feb	5.44	53.55	0.68	6.69
Mar	5.82	55.84	0.73	6.98	Mar	4.31	63.12	0.54	7.89
Apr	4.30	60.87	0.54	7.61	Apr	2.32	66.25	0.29	8.28
May	7.35	50.74	0.92	6.34	May	4.18	59.16	0.52	7.40
Jun	10.56	39.10	1.32	4.89	Jun	8.21	43.02	1.03	5.38
Jul	8.38	39.32	1.05	4.91	Jul	7.59	36.39	0.95	4.55
Aug	11.88	36.72	1.49	4.59	Aug	9.79	32.79	1.22	4.10
Sep	14.91	35.86	1.86	4.48	Sep	16.04	32.93	2.01	4.12
Oct	20.02	47.68	2.50	5.96	Oct	18.20	29.56	2.28	3.69
Nov	16.78	30.42	2.10	3.80	Nov	19.09	33.81	2.39	4.23
Dec	18.04	38.80	2.26	4.85	Dec	14.41	38.84	1.80	4.86

Table 3.11 Continued...

2018

Months	Average of ET	Average of PET	ET in Month (mm/day)	PET in Month (mm/day)
Jan	7.57	38.87	0.95	4.86
Feb	6.35	50.02	0.79	6.25
Mar	4.76	61.98	0.60	7.75
Apr	5.29	62.78	0.66	7.85
May	6.13	53.60	0.77	6.70
Jun	8.81	37.52	1.10	4.69
Jul	8.64	31.74	1.08	3.97
Aug	11.85	27.41	1.48	3.43
Sep	13.66	44.46	1.71	5.56
Oct	15.44	49.71	1.93	6.21
Nov	11.92	46.43	1.49	5.80
Dec	7.37	38.38	0.92	4.80

2019

Months	Average of ET	Average of PET	ET in Month (mm/day)	PET in Month (mm/day)
Jan	4.77	40.59	0.60	5.07
Feb	5.07	52.59	0.63	6.57
Mar	2.59	67.49	0.32	8.44
Apr	2.39	66.10	0.30	8.26
May	3.19	61.29	0.40	7.66
Jun	6.52	48.95	0.82	6.12
Jul	8.94	33.59	1.12	4.20
Aug	12.88	28.14	1.61	3.52
Sep	15.35	29.76	1.92	3.72
Oct	19.82	32.29	2.48	4.04
Nov	22.59	40.32	2.82	5.04
Dec	19.11	35.47	2.39	4.43

The 2010 to 2019 datasets showed the inter-annual variations of total PET. According to the correlation between PET and ET from 2010 to 2019, the watershed may experience a deficiency state where total precipitation is less than total PET. The majority of whole district areas within the districts indicate that the district experienced a sustained deficiency in 2012, 2014, and 2016. The 2010 to 2019 datasets showed the inter-annual differences in total PET. According to the correlation between PET and ET from 2010 to 2019. The majority of orange to red (red indicates an area experiencing a 12-month deficiency) places within the districts indicate that the district experienced a sustained deficiency in 2013. Spatial distributions of PET characteristics are found through the analysis of long-term datasets. The topographic setting is spatially connected to the PET differences in the district. Mountainous areas have relatively low PET across all categories—both annually and seasonally. These patterns imply that topography and other climate variables regulate PET dynamics. The gradients in elevations and orographic precipitations within the watershed have been shaped by several mountain complexes. This explains the wide heterogeneity in PET in part.

Mountainous areas have relatively low PET across all categories—both annually and seasonally. These patterns imply that geography and other climate variables regulate PET dynamics. The gradients in altitude and orographic precipitations within the watershed have been shaped by several mountain complexes. This explains the wide heterogeneity in PET in part. A very dry season is presently prevailing across more than half of Chikkaballapura and Kolar district highest average ET was in November 2019 is about 22.59 and PET was 66.10 the yearly ET and PET shown in Table 1. Regarding persistent droughts, two North-Eastern districts come to mind: While Kolar and the Chikkaballapura district have a warm, dry climate to the north with an annual rainfall of less than 570 mm; the district has a wet tropical climate to the south with annual rainfall exceeding 970 mm. Our findings show that water shortages in the district are typical of an extreme nature and tend to occur more frequently in the country's north. The various climatic and surface parameters show their differences, these parameters are dependent and they cause the flood and drought, it indicated in Figures 6.5 and 6.6.
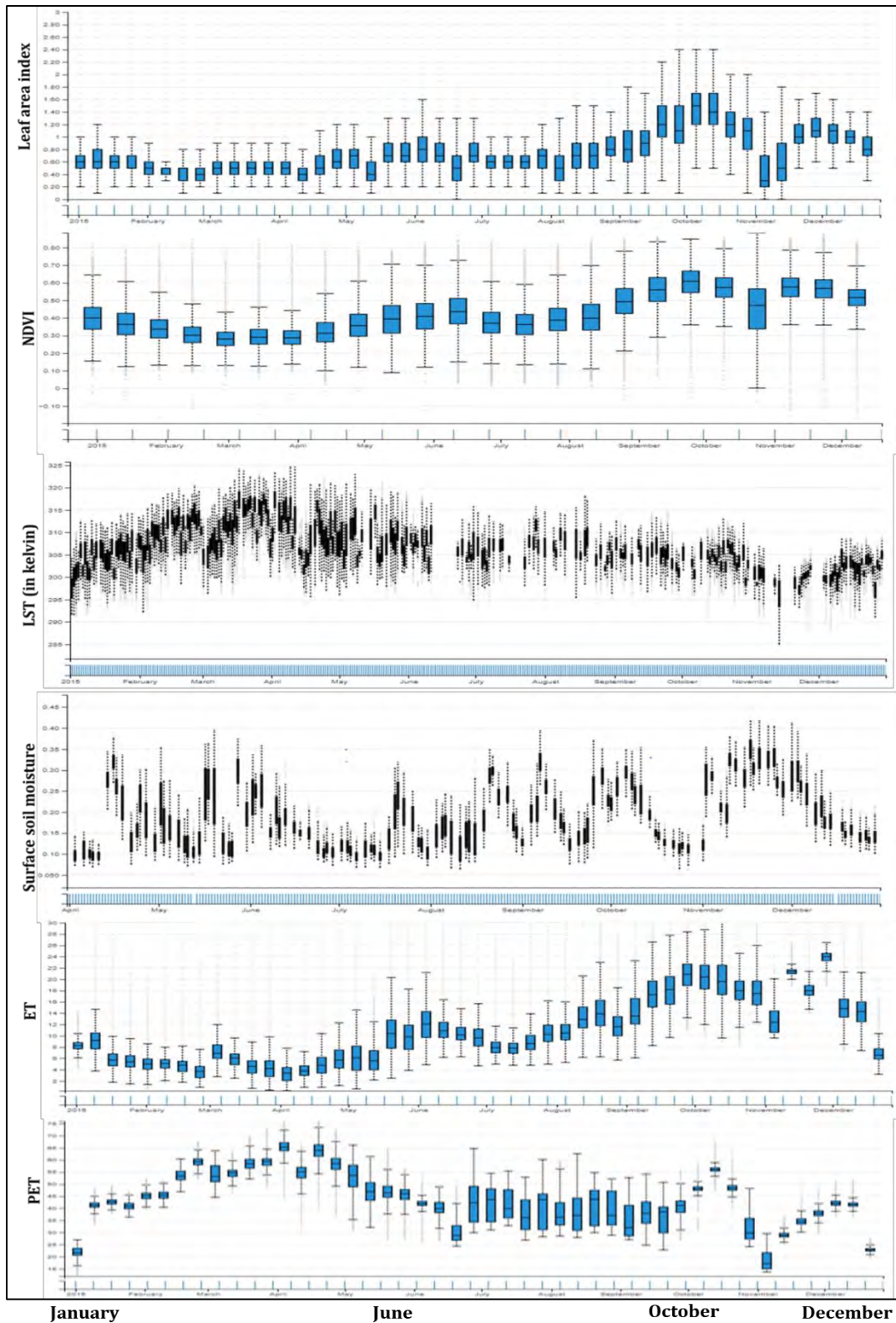
Figure 6.5 Modis Surface Parameter 2015
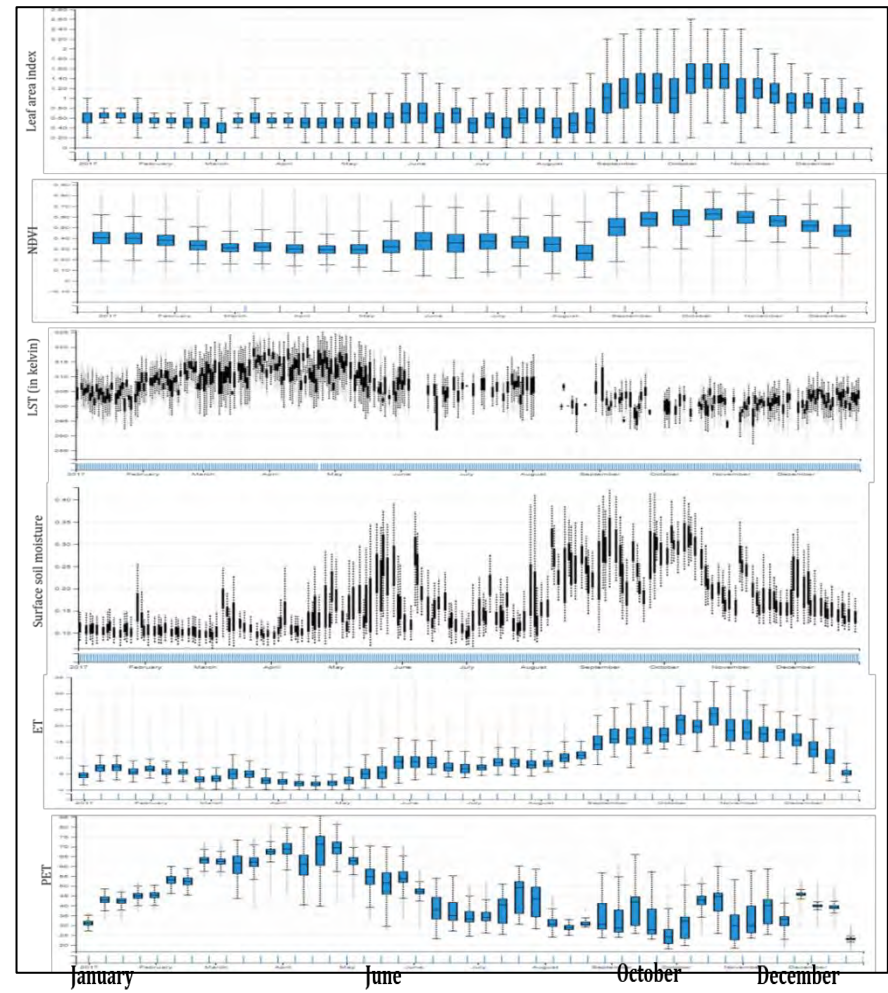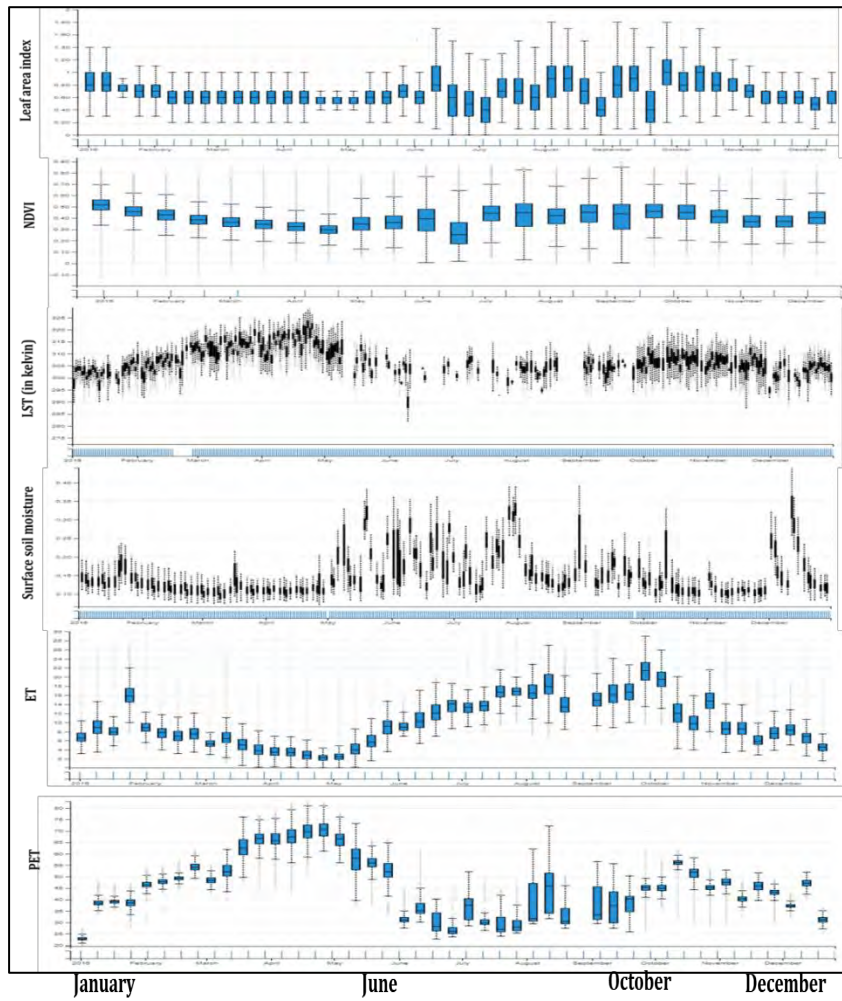
Figure 6.5 (continued). Modis Surface Parameter 2016 and 2017
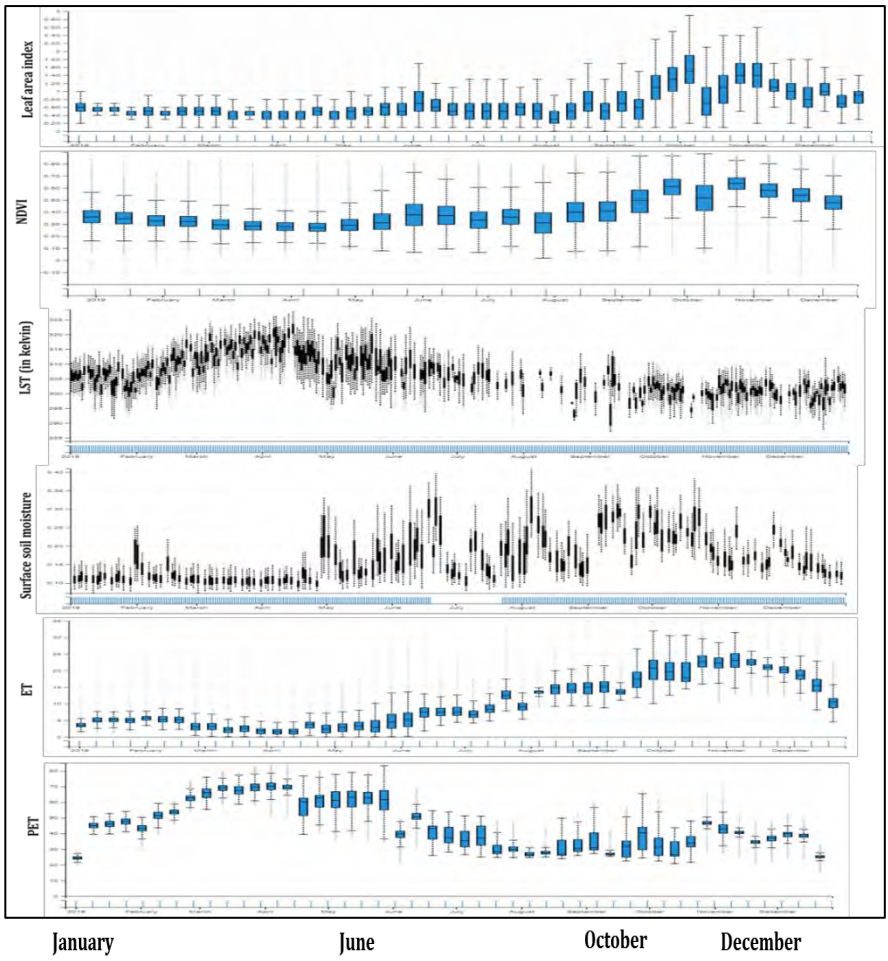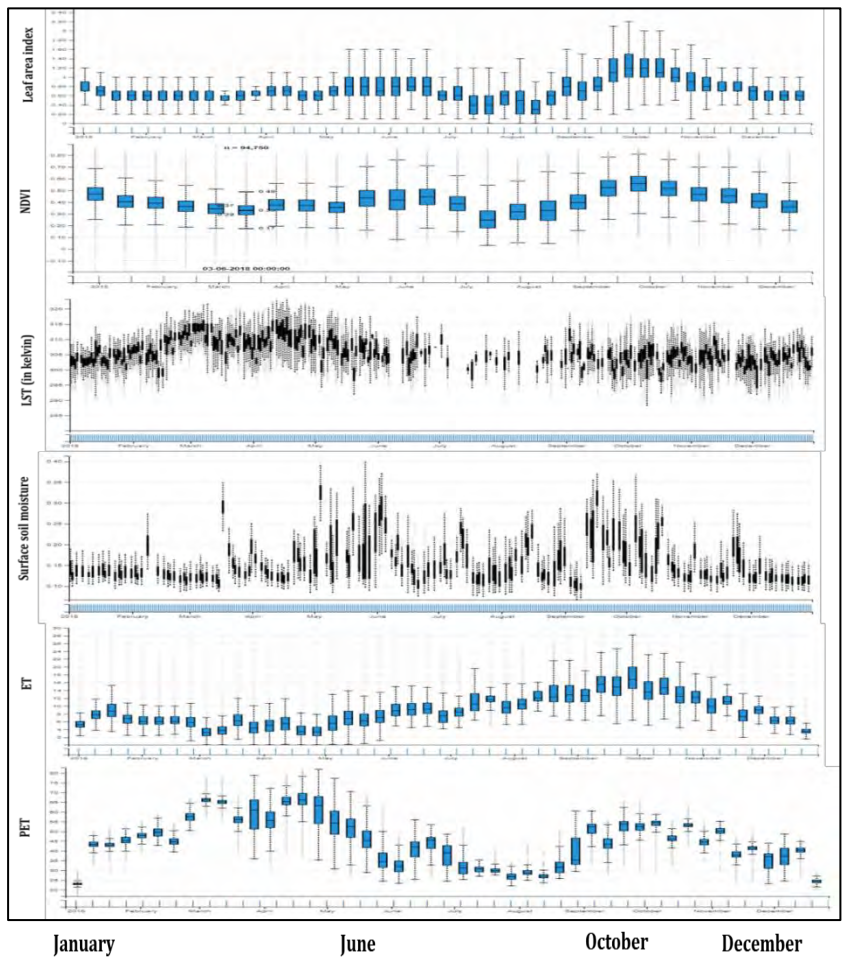
Figure 6.5 (continued). Modis Surface Parameter 2018 and 2019
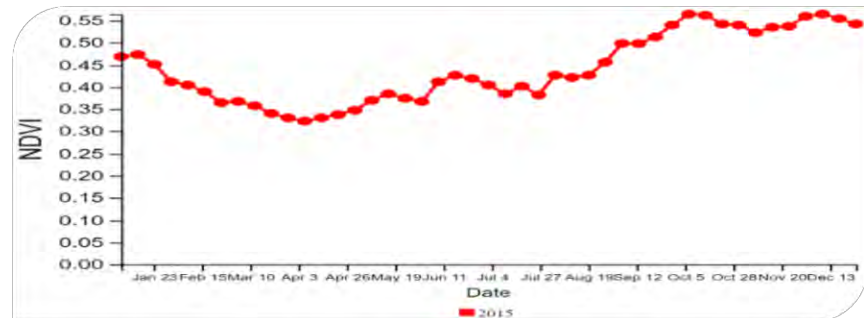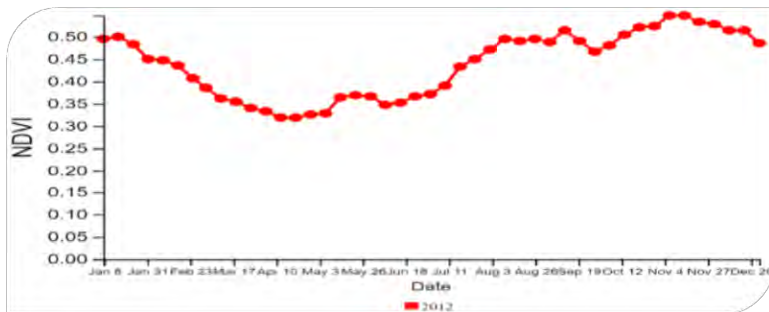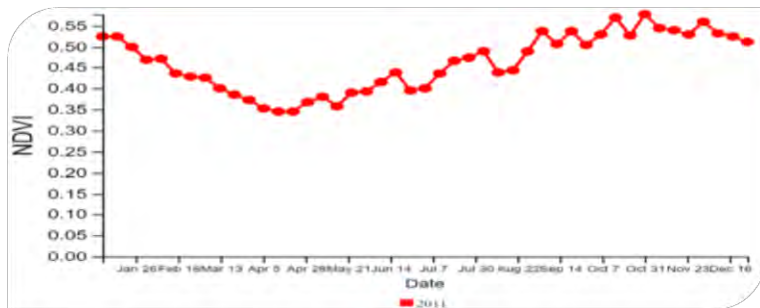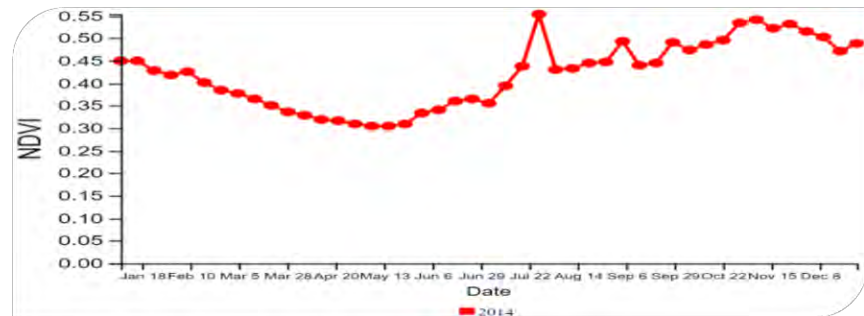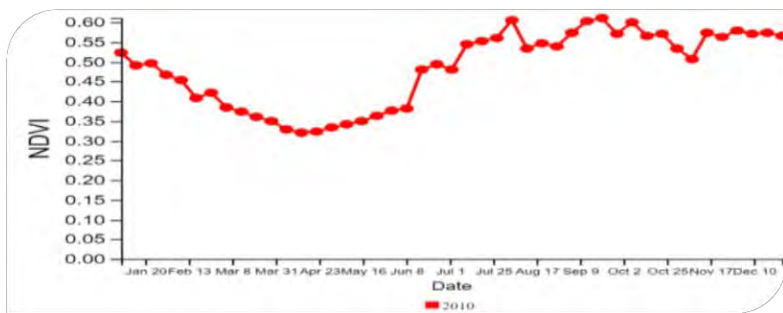
Figure 6.6. Weekly NDVI (Vegetation) Trend from 2010-2019
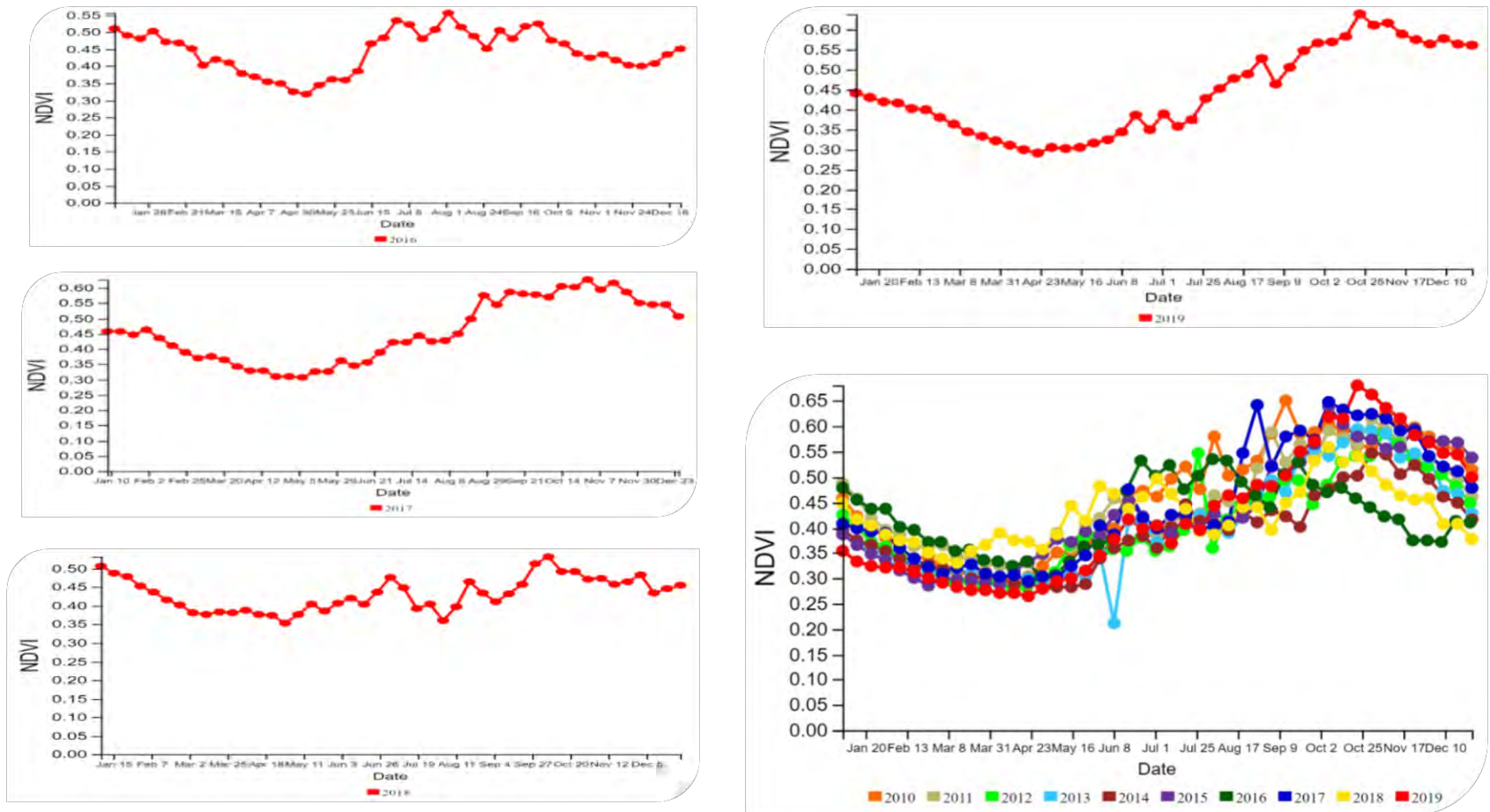
Figure 6.6. (continued)...

3.12 Conclusions

Human intervention coupled with population explosion has created emergencies of climatic disasters such as drought. There is a crucial societal need to provide immediate attention to deal with the variation in the Spatio-temporal aspects of drought leading to a worldwide water shortage. Forecasting dry and wet events is of the highest importance in the dry parts of districts for the planning of water utilization, agriculture activity, and economic activity, which is highly dependent on precipitation. Characterization and assessment of droughts in the area at seasonal time scales will be useful for developing short, medium, and long-term planning needed to negate such calamities in the future.

The present study is concerned with analyzing the spatiotemporal characters of various time drought indices such as SPI in the dry semi-arid region of Kolar and Chikkaballapura in Karnataka, India. The analysis results mirror the actual situation proving that the SPI is suitable to study drought events. SPI not only acts as a tool to understand the temporal and spatial variation of drought but more importantly creates a basis for prediction, prevention, monitoring, and mitigation paired with engineering construction concerning the drought. This work utilized three drought indices, namely SPI, SPEI, and RAI, to assess semi-arid region meteorological drought conditions both spatially and temporally. RAI has been given less attention in previous studies than SPI, although being extensively used for mapping drought. As a result, 11 stations' rainfall from 40 years (1979-2019) was distributed unevenly over a study area. This research employed the conditional probability approach to computing the changes in drought attributes between SPI and SPEI in some grid stations at various times to examine the drought and wet period in SPI and SPEI indices. In the districts from 1979 to 2019, if the SPI consistently declines in value while the SPEI rises,

All grid stations demonstrated that SPEI accurately reflected wet and dry conditions in more complicated locations and was more evaluation-sensitive than SPI. The north-eastern (N-E) portion of the districts' hilly regions experienced a greater SPI and SPEI drought trend. Based on the frequency and length of droughts, we discovered that Chikkaballapura experienced more severe drought conditions than the Kolar district. Drought frequency in the N-E region

gradually grew from 1.56 to 2.5, while the S-W region exhibited a weakened drought period average value of 0.98 to 1.52. With a frequency value of roughly 3.1%, the More Extreme Drought Period has mostly affected the Gudibande station for about 17, 18, and 10 months in SPI (3, 6, and 12-month scales, respectively). In the SPEI time scale, Chikkaballapura displayed a more severe drought at a frequency value of roughly 2.4.

Overall consistent years of drought were reported in 1983, 1985, 2003, 2007, and 2019. Therefore, this assessment of dry occurrences is crucial in dry areas for the planning of agricultural activity, water use, and economic activity, all of which are heavily reliant on rainfall. Characterizing and evaluating the region's droughts at different time scales will aid in creating the short-, medium-, and long-term plans required to prevent similar catastrophes in the future.

The Bagepalli stations show that 2015 is the wettest year in the study period that annual rainfall is about 1026.4 and the EDTI is about 4.5 SMDI 2.1 values respectively, and also 2018 is the dry year compared to the other stations with an average rainfall of 456mm. the station Mulubhagilu shows the highest rainfall in the year 2015 the ETDI is about 4.88 and SMDI is about 2.67 it indicates the 2015 is the wettest year this year almost all station shows positive wet events. Extreme drought events occurred in the Sidhghatta is about 414 mm rainfall (EDTI-1.41, SMDI—0.71) and Srinivasapura is about 432.1 mm (EDTI-1.92, SMDI—1.22in the year 2018. the correlation matrix (R) value of the ETDI and SMDI and SPI with annual Rainfall for the elevation grid stations. The primary goal of this study is to compare the current drought conditions in both districts. The spatiotemporal categorization of drought using various methodologies is important in this setting for crop management, irrigation management, irrigation infrastructure construction, and irrigation facility design. This information is useful to governments, farmers, and researchers in that region for crop development, calendar planning, and irrigation management. Furthermore, careful design could increase food supply while protecting the environment. rural residents and urge them to become involved in agriculture As a result, the SPI, SPEI, and RAI techniques are employed in this study to characterize the drought using long-term rainfall data.

References

1. Akhtari, R., Morid, S., Mahdian, M.H., Smakhtin, V., 2009. Assessment of areal interpolation methods for spatial analysis of SPI and EDI drought indices. Int. J. Climatol. 29, 135–145. https://doi.org/10.1002/joc.1691.

2. Aryal, Anil, Manisha Maharjan, and Rocky Talchabhadel. 2022. "Characterizing Meteorological Droughts in Nepal : A Comparative Analysis of Standardized Precipitation Index and Rainfall Anomaly Index." : 409–32.

3. Arnell, N.W., 1999. Climate change and global water resources. Global Environ. Change 9, S31–S49. https://doi.org/10.1016/S0959-3780(99)00017-5.

4. Astuti, Ike Sari et al. 2022. "An Application of Improved MODIS-Based Potential Evapotranspiration Estimates in a Humid Tropic Brantas Watershed — Implications for Agricultural Water Management."

5. Beck, Hylke E et al. 2018. "Present and Future Köppen-Geiger Climate Classification Maps at 1-Km Resolution." *Scientific Data* 5(1): 180214. https://doi.org/10.1038/sdata.2018.214.

6. Bilel, Z., Chettih, M., Abda, Z., Mesbah, M., Santos, C., Brasil Neto, R., da Silva, R., 2021. Spatiotemporal meteorological drought assessment in a humid Mediterranean region: case study of the Oued Sebaou basin (northern central Algeria). Nat. Hazards 108. https://doi.org/10.1007/s11069-021-04701-0.

7. Caloiero, T., G. Buttafuoco, R. Coscarelli, and E. Ferrari. 2015. "Spatial and Temporal Characterization of Climate at Regional Scale Using Homogeneous Monthly Precipitation and Air Temperature Data: An Application in Calabria (Southern Italy)." *Hydrology Research* 46(4): 629–46.

8. Caloiero, Tommaso. 2020. "Evaluation of Rainfall Trends in the South Island of New Zealand through the Innovative Trend Analysis (ITA)." *Theoretical and Applied Climatology* 139(1–2): 493–504.

9. Chen, Wenhua, Juan Xu, and Shuangcheng Li. 2020. "Prediction of Meteorological Drought in the Lower Nu River by Statistical Model." *American Journal of Climate Change* 09(02): 87–99.

10. Chemeda, Desalegn, Edossa Mukand, and Singh Babel. 2010. "Drought Analysis in the Awash River Basin , Ethiopia." : 1441–60.

11. Cheval, S., 2016. The Standardized Precipitation Index – an Overview.

12. Das, J., Gayen, A., Saha, P., Bhattacharya, S.K., 2020. Meteorological drought analysis using standardized precipitation index over Luni River Basin in Rajasthan, India. SN Appl. Sci. 2, 1530. https://doi.org/10.1007/s42452-020-03321-w.

13. Diani, K., Kacimi, I., Zemzami, M., Tabyaoui, H., Haghighi, A.T., 2019. Evaluation of meteorological drought using the standardized precipitation index (SPI) in the high ziz River basin , Morocco. https://doi.org/10.2478/limre-2019-0011, 125-135.

14. Dikici, M., 2020. Drought analysis with different indices for the Asi Basin (Turkey). Sci. Rep. 10 https://doi.org/10.1038/s41598-020-77827-z.

15. Edwards, Daniel C, and Thomas B Mckee. 1997. *CHARACTERISTICS OF 20TH CENTURY DROUGHT IN THE UNITED STATES AT MULTIPLE TIME SCALES*.

16. Evapotranspiration, Potential, Remote Sensing, and Data Application. "Agricultural Drought Monitoring by MODIS Potential Evapotranspiration Remote Sensing Data Application."

17. Gao, Xuerui et al. 2017. "Temporal and Spatial Evolution of the Standardized Precipitation Evapotranspiration Index (SPEI) in the Loess Plateau under Climate Change from 2001 to 2050." *Science of the Total Environment* 595: 191–200. http://dx.doi.org/10.1016/j.scitotenv.2017.03.226.

18. Gong, Z et al. 2015. "MODIS Normalized Difference Vegetation Index (NDVI) and Vegetation Phenology Dynamics in the Inner Mongolia Grassland." (November).

19. Harishnaika, N, S A Ahmed, Sanjay Kumar, and M Arpitha. 2022. "Remote Sensing Applications : Society and Environment Computation of the Spatio-Temporal Extent of Rainfall and Long-Term Meteorological Drought Assessment Using Standardized Precipitation Index over Kolar and Chikkaballapura Districts Karnataka during 1951-2019."*Remote Sensing Applications: Society and Environment* 27(January): 100768https://doi.org/10.1016/j.rsase.2022.100768.

20. Haroon, M.A., Zhang, J., Yao, F., 2016. Drought monitoring and performance evaluation of MODIS-based drought severity index (DSI) over Pakistan. Nat. Hazards 84, 1349–1366. https://doi.org/10.1007/s11069-016-2490-y.

21. Huang, Jin, Shanlei Sun, Jinjian Li, and Jinchi Zhang. 2014. "Spatial and Temporal Variability of Precipitation and Dryness / Wetness During 1961 – 2008 in Sichuan." : 1655–70.

22. He, Y., Wetterhall, F., Cloke, H.L., Pappenberger, F., Wilson, M., Freer, J., 2009. Tracking the uncertainty in flood alerts driven by grand. Meteorol. Appl. 101, 91–101. https://doi.org/10.1002/met.

23. Ionita, M., P. Scholz, and S. Chelcea. 2016. "Assessment of Droughts in Romania Using the Standardized Precipitation Index." *Natural Hazards* 81(3): 1483–98.

24. Jia, Yanqing, Bo Zhang, and Bin Ma. 2018. "Daily SPEI Reveals Long-Term Change in Drought Characteristics in Southwest China." *Chinese Geographical Science* 28(4): 680–93.

25. Jiang, W., Wang, L., Feng, L., Zhang, M., Yao, R., 2020. Drought characteristics and its impact on changes in surface vegetation from 1981 to 2015 in the Yangtze River Basin, China. Int. J. Climatol. 40, 3380–3397. https://doi.org/10.1002/joc.6403.

26. Kalisa, Wilson et al. 2020. "Spatio-Temporal Analysis of Drought and Return Periods over the East African Region Using Standardized Precipitation Index from 1920 to 2016." *Agricultural Water Management* 237(January): 106195.

https://doi.org/10.1016/j.agwat.2020.106195.

27. Karavitis, C.A., Alexandris, S., Tsesmelis, D.E., Athanasopoulos, G., 2011. Application of the standardized precipitation index (SPI) in Greece. Water (Switzerland) 3, 787–805. https://doi.org/10.3390/w3030787.

28. Kazemzadeh, Majid, and Arash Malekian. 2016. "Spatial Characteristics and Temporal Trends of Meteorological and Hydrological Droughts in Northwestern Iran." *Natural Hazards* 80(1): 191–210.

29. Khan, Muhammad Imran et al. 2016. "Recent Climate Trends and Drought Behavioral Assessment Based on Precipitation and Temperature Data Series in the Songhua River Basin of China." *Water Resources Management* 30(13): 4839–59.

30. Kraus, E B. 1977. "Subtropical Droughts and Cross-Equatorial Energy Transports." *Monthly Weather Review* 105(8): 1009–18. https://journals.ametsoc.org/view/journals/mwre/105/8/1520-0493_1977_105_1009_sdacee_2_0_co_2.xml.

31. Kumar, Sanjay, and S A Ahmed. 2022. "Spatial and Temporal Pattern Assessment of Meteorological Drought in Tumakuru District of Karnataka during 1951-2019 Using Standardized Precipitation Index." 98: 822–30

32. Kim, D.-W., Byun, H.-R., Choi, J.-W., 2009. Evaluation, modification, and application of the effective drought index to 200-year drought climatology of Seoul, Korea. J. Hydrol. 378, 1–12. https://doi.org/10.1016/j.jhydrol.2009.08.021.

33. Laurencelle, J., Logan, T., Gens, R., 2015. Alaska Satellite Facility (ASF) - radiometrically terrain corrected ALOS PALSAR products. ASF-Alaska Satell. Facil. 1 (2), 12.

34. Lettenmaier, Dennis P, Eric F Wood, and James R Wallis. 1994. 7 586 JOURNAL OF CLIMATE *Hydro-Climatological Trends*. https://about.jstor.org/terms.

35. Liebmann, Brant et al. 2014. "Understanding Recent Eastern Horn of Africa Rainfall Variability and Change." *Journal of Climate* 27(23): 8630–45.

36. Liu, Changhong, Cuiping Yang, Qi Yang, and Jiao Wang. 2021. "Spatiotemporal Drought Analysis by the Standardized Precipitation Index (SPI) and Standardized Precipitation Evapotranspiration Index (SPEI) in Sichuan Province, China." *Scientific Reports* 11(1): 1–14. https://doi.org/10.1038/s41598-020-80527-3.

37. Liu, Xianfeng et al. 2016. "Agricultural Drought Monitoring: Progress, Challenges, and Prospects." *Journal of Geographical Sciences* 26(6): 750–67. https://doi.org/10.1007/s11442-016-1297-9.

38. Liu, Yibo et al. 2016. "Recent Trends in Vegetation Greenness in China Significantly Altered Annual Evapotranspiration and Water Yield." *Environmental Research Letters* 11(9): 94010. https://doi.org/10.1088/1748-9326/11/9/094010.

39. Maity, Rajib, Mayank Suman, and Nitesh Kumar Verma. 2016. "Drought

Prediction Using a Wavelet Based Approach to Model the Temporal Consequences of Different Types of Droughts." *Journal of Hydrology* 539: 417–28. http://dx.doi.org/10.1016/j.jhydrol.2016.05.042.

40. Mallenahalli, Naresh K. 2020. "Comparison of Parametric and Nonparametric Standardized Precipitation Index for Detecting Meteorological Drought over the Indian Region." *Theoretical and Applied Climatology* 142(1–2): 219–36.

41. Mckee, T.B., Doesken, N.J., Kleist, J., 1993. THE RELATIONSHIP OF DROUGHT FREQUENCY AND DURATION TO TIMESCALES.

42. Mishra, Ashok K., and Vijay P. Singh. 2010. "A Review of Drought Concepts." *Journal of Hydrology* 391(1–2): 202–16.

43. Min, Seung Ki, Xuebin Zhang, Francis W. Zwiers, and Gabriele C. Hegerl. 2011. "Human Contribution to More-Intense Precipitation Extremes." *Nature* 470(7334): 378–81. http://dx.doi.org/10.1038/nature09763

44. Mu, Qiaozhen, Maosheng Zhao, and Steven W Running. 2011. "Remote Sensing of Environment Improvements to a MODIS Global Terrestrial Evapotranspiration Algorithm." *Remote Sensing of Environment* 115(8): 1781–1800. http://dx.doi.org/10.1016/j.rse.2011.02.019.

45. Moghbeli, A., Delbari, M., Amiri, M., 2020. Application of a standardized precipitation index for mapping drought severity in an arid climate region, southeastern Iran. Arabian J. Geosci. 13 https://doi.org/10.1007/s12517-020-5201-7.

46. Mondol, M.A.H., Ara, I., Das, S.C., 2017. Meteorological drought index mapping in Bangladesh using standardized precipitation index during 1981–2010. Adv. Meteorol., 4642060 https://doi.org/10.1155/2017/4642060, 2017.

47. Narasimhan, B, and R Srinivasan. 2005. "Development and Evaluation of Soil Moisture Deficit Index (SMDI) and Evapotranspiration Deficit Index (ETDI) for Agricultural Drought Monitoring." 133: 69–88.

48. Naresh Kumar, M., Murthy, C.S., Sesha Sai, M.V.R., Roy, P.S., 2012. Spatiotemporal analysis of meteorological drought variability in the Indian region using standardized precipitation index. Meteorol. Appl. 19, 256–264. https://doi.org/10.1002/met.277.

49. Nguyen, Luong Bang, and Trieu Anh Ngoc. 2015. "Drought Assessment in Cai River Basin , Vietnam : A Comparison with Regard to Drought Assessment in Cai River Basin , Vietnam : A Comparison With." (September).

50. Park, Junehyeong, Jang Hyun Sung, Yoon Jin Lim, and Hyun Suk Kang. 2019. "Introduction and Application of Non-Stationary Standardized Precipitation Index Considering Probability Distribution Function and Return Period." *Theoretical and Applied Climatology* 136(1–2): 529–42.

51. Pai, D.S., Sridhar, L., Rajeevan, M., Sreejith, O.P., Satbhai, N.S., Mukhopadyay, B., 2014. Development of a New High Spatial Resolution (0 . 25 ∘ × 0 . 25 ∘) Long Period (1901-2010) Daily Gridded Rainfall Data Set over India and its

Comparison with Existing Data Sets over the Region Data Sets of Different Spatial Resolutions and Time Period 1, pp. 1–18.

52. Panda, A., Sahu, N., 2019. Trend analysis of seasonal rainfall and temperature pattern in Kalahandi, Bolangir and Koraput districts of Odisha, India. Atmos. Sci. Lett. 20 https://doi.org/10.1002/asl.932. Pei, Z., Fang, S., Wang, L., Yang, W., 2020. Comparative analysis of drought indicated by the SPI and SPEI at various timescales in inner Mongolia. China Water 12. https://doi.org/10.3390/w12071925.

53. Piao, S., Ciais, P., Huang, Y., Shen, Z., Peng, S., Li, J., Zhou, L., Liu, H., Ma, Y., Ding, Y., Friedlingstein, P., Liu, C., Tan, K., Yu, Y., Zhang, T., Fang, J., 2010. The impacts of climate change on water resources and agriculture in China. Nature 467, 43–51.

54. Rafaela, Tarciana et al. 2022. "Climate Indices-Based Analysis of Rainfall Spatiotemporal Variability in Pernambuco State , Brazil." : 1–26.

55. Revadekar, J V, Hamza Varikoden, P K Murumkar, and S A Ahmed. 2018. "Science of the Total Environment Latitudinal Variation in Summer Monsoon Rainfall over Western Ghat of India and Its Association with Global Sea Surface Temperatures." *Science of the Total Environment* 613–614: 88–97. http://dx.doi.org/10.1016/j.scitotenv.2017.08.285.

56. Robinson, T. P., and G. Metternicht. 2006. "Testing the Performance of Spatial Interpolation Techniques for Mapping Soil Properties." *Computers and Electronics in Agriculture* 50(2): 97–108

57. Rafaela, Tarciana et al. 2022. "Climate Indices-Based Analysis of Rainfall Spatiotemporal Variability in Pernambuco State , Brazil." : 1–26.

58. Revadekar, J V, Hamza Varikoden, P K Murumkar, and S A Ahmed. 2018. "Science of the Total Environment Latitudinal Variation in Summer Monsoon Rainfall over Western Ghat of India and Its Association with Global Sea Surface Temperatures." *Science of the Total Environment* 613–614: 88–97. http://dx.doi.org/10.1016/j.scitotenv.2017.08.285.

59. Robinson, T. P., and G. Metternicht. 2006. "Testing the Performance of Spatial Interpolation Techniques for Mapping Soil Properties." *Computers and Electronics in Agriculture* 50(2): 97–108.

60. Sona, N.T., Chen, C.F., Chen, C.R., Chang, L.Y., Minh, V.Q., 2012. Monitoring agricultural drought in the lower mekong basin using MODIS NDVI and land surface temperature data. Int. J. Appl. Earth Obs. Geoinf. 18, 417–427. https://doi.org/10.1016/j.jag.2012.03.014.

61. Tirivarombo, S., Osupile, D., Eliasson, P., 2018. Drought monitoring and analysis: standardised precipitation evapotranspiration index (SPEI) and standardised precipitation index (SPI). Phys. Chem. Earth 106, 1–10. https://doi.org/10.1016/j.pce.2018.07.001.

62. Tong, S., Quan, L., Zhang, J., Bao, Y., Lusi, A., Qiyun, M., Li, X., Zhang, F., 2017. Spatiotemporal drought variability on the Mongolian Plateau from 1980–2014 based on the SPE I-PM, intensity analysis and Hurst exponent. Sci.

Total Environ. 615 https://doi.org/10.1016/j.scitotenv.2017.09.121.

63. Tran, Thuong V. et al. 2019. "Assessing Spatiotemporal Drought Dynamics and Its Related Environmental Issues in the Mekong River Delta." *Remote Sensing* 11(23)

64. Uddameri, V., Singaraju, S., Hernandez, E.A., 2019. Is standardized precipitation index (SPI) a useful indicator to forecast groundwater droughts? — insights from a karst aquifer. J. Am. Water Resour. Assoc. 55, 70–88. https://doi.org/10.1111/1752-1688.12698.

65. Udmale P, D., Ichikawa Y, Kiem A, S., Panda S, N., 2014. Drought impacts and adaptation strategies for agriculture and rural livelihood in the Maharashtra state of India. Open Agric. J. 8, 41–47. https://doi.org/10.2174/1874331501408010041.

66. Vicente-Serrano, Sergio M., Santiago Beguería, and Juan I. López-Moreno. 2010. "A Multiscalar Drought Index Sensitive to Global Warming: The Standardized Precipitation Evapotranspiration Index." *Journal of Climate* 23(7): 1696–1718.

67. Vicente-serrano, Sergio M et al. 2012. "Challenges for Drought Mitigation in Africa : The Potential Use of Geospatial Data and Drought Information Systems." *Applied Geography* 34: 471–86. http://dx.doi.org/10.1016/j.apgeog.2012.02.001.

68. World Meteorological Organization (WMO), 1987. Standardized precipitation index user Guide. J. Appl. Bacteriol. 63, 197–200.

69. Wu, Hong et al. 2007. "Appropriate Application of the Standardized Precipitation Index in Arid Locations and Dry Seasons." 79(June 2006): 65–79.

70. Wang, Qianfeng et al. 2015. "The Alleviating Trend of Drought in the Huang-Huai-Hai Plain of China Based on the Daily SPEI." *International Journal of Climatology* 35(13): 3760–69.

71. Wambura, Frank Joseph. 2021. "Sensitivity of the Evapotranspiration Deficit Index to Its Parameters and Different Temporal Scales."

72. Wilhite, Donald A., Mark D. Svoboda, and Michael J. Hayes. 2007. "Understanding the Complex Impacts of Drought: A Key to Enhancing Drought Mitigation and Preparedness." *Water Resources Management* 21(5): 763–74.

73. Wu, Hong et al. 2007. "Appropriate Application of the Standardized Precipitation Index in Arid Locations and Dry Seasons." 79(June 2006): 65–79.

74. Zerouali, Bilel et al. 2021. "Spatiotemporal Meteorological Drought Assessment in a Humid Mediterranean Region : Case Study of the Oued Sebaou Basin (Northern Central Algeria)." *Natural Hazards*. https://doi.org/10.1007/s11069-021-04701-0.

75. Zhang, Anzhi, Gensuo Jia, and Hesong Wang. "Improving Meteorological Drought Monitoring Capability over Tropical and Subtropical Water-

Limited Ecosystems : Evaluation and Ensemble of the Microwave Integrated Drought Index Improving Meteorological Drought Monitoring Capability over Tropical and Subtropical Water-Limited Ecosystems : Evaluation and Ensemble of the Microwave Integrated Drought Index."

76. Zhang, Qiang, Mingzhong Xiao, Vijay P Singh, and Xiaohong Chen. 2013. "Copula-Based Risk Evaluation of Droughts across the Pearl River Basin, China." *Theoretical and Applied Climatology* 111(1): 119–31. https://doi.org/10.1007/s00704-012-0656

CHAPTER -4
SPATIAL-TEMPORAL RAINFALL TREND ASSESSMENT

This Chapter is Based On:

Chapter-4
Rainfall Trend Assessment

4. Introduction

Climate variation is admittedly one of the worldwide complications of the twentieth century for health, food security, and livelihoods (Ghosh 2018; Campbell-Lendrum et al. 2007; Mina et al. 2018; Rautela and Karki 2015). Precipitation is a prime part of the hydrological cycle, and its elements affect the temporal and spatial patterns of water bodies (Islam et al. 2012). The hazards like floods and drought are dangerous events that can happen periodically, because of the greatest transformation in precipitation pattern (Srivastava et al. 2015; Gupta et al. 2014). Every nation in the world is facing distinct modifications in precipitation patterns. Nowadays, India, Ethiopia, Australia, Scotland, Nigeria, Iran, and Spain are affected by the rising temperature (Huang et al. 2015). Asian continent nations like India, China, Korea, and Taiwan are continuously studying rainfall variability. India has faced seasonal variation in rainfall due to its topography (Guhathakurta and Rajeevan 2008). In India, the monsoon seasons play a major task in agriculture production. Sixty-eight percent of agricultural land is involved in irrigated agronomy, which helps human beings for livelihood (Meshram et al. 2017). The study of climatic change particularly variation in the dispersal of precipitation is mandatory for reliable water assets (Praveen et al. 2020). Above all, a total perception of the precipitation analysis in the adapted ecology will reduce the risk of extreme climate conditions.

Karnataka is India's seventh-largest state located in the south peninsular part. Only 40% to 50% of precipitation is presently used to grow crops in the region. Kolar and Chikkaballapura districts fall in the south-eastern dry agro-climatic area. It practices a semiarid climate, tropical weather, monsoon with mild summers, and mild winters. The year is split into 3 seasons, namely, pre-monsoon (January to May), Southwest (June–September), and Northeast (October–December). Based on the rainfall data about the districts, there are 11 grid stations. This study shows the effective variation of rainfall trends with the temporal distribution. In the literature, more learning is obtainable through on-trend observations in the meteorological (Chatterjee et al. 2016; Talaee 2014;

Yang et al. 2017) time data of distinct divisions of the nation. In an immense work, trends were marked by non-parametric and parametric processes (Sonali and Nagesh Kumar 2013) such as the Mann-Kendall (Mann 1945) and Sen's slope assessment (Kumar Sen 1968; Şen 2017). Many researchers have conducted numeral studies all over the world to ascertain and execute rainfall trend analysis and climate adaptation. In the current research, the MK test is normally applied to detect a positive or negative trend in a sequence of meteorological data. MK test is usually applied as the universal technique for trend assessment (Hipel et al. 1988; Van et al. 1984). Sen's estimator method is an alternate non-parametric test to manage the trend assessment of hydro-meteorological data (Lettenmaier et al. 1994; Partal and Kahya 2006; Yue and Hashino 2003), and it is used to recognize the trending moment. Accordingly, this test calculates the undeviating speed of change in the slope (Kumar Sen 1968). The tests for trend series are divided into two categories of absolute and relative approaches; in the relative procedure (Kiat Chang n.d.), the nearest grid stations are utilized in the testing process, while the test was actually for every station as an individual in the absolute method. Using the relative method, we can easily detect the homogeneity of data (Peterson et al. 1998); however, this homogeneity procedure did not examine how real changes can be determined from random oscillation (Buishand1982). The absolute method operates statistical examination to check the inhomogeneity of data. Different statistical methods have been continuously used by researchers to inspect inhomogeneity and break years in rainfall data series. The change detection procedure includes the Pettitt test (Pettitt 1979), SNHT test (Moberg and Alexanderson 1997), and Buishand test (Buishand1982, n.d.). This test assesses the homogeneity, followed by the change detection analysis (Praveen et al. 2020). The outcome from these approaches is more suitable and reliable for trend detection. The target of this inquiry is to detect the variation of rainfall in Kolar and Chikkaballapura by employing Sen's estimates and the MK test. The homogeneity tests such as Pettitt, Buishand, and SNHT tests glance at the result of climate variability in the study area. There have been a few studies to investigate the yearly trend in Kolar and Chikkaballapura. This research will consider the overall tendency of precipitation using the MK test, and Sen's slope test was detecting the magnitude

(slope) of the trend line in annual rainfall data. The nonparametric Pettit, SNHT, and Buishand range test was applied to detect the change point (shift year) in time series that divide the whole study period into the disturbed and undisturbed periods. This research is useful for the appraisal and planning of drought management and water assets in the location.

4.1 Methods and Materials

4.1.1 Data source and Analysis Tools

The daily precipitation dataset with a spatial resolution of 0.25°×0.25° has been procured from the website of the India Meteorological Department (IMD) Pune, from 1951 to 2019. The 11 grid points obtained across the districts are used for statistical interpretation. The spatial distribution of daily rainfall data has been converted into the total sum of monthly and annual data, which have been utilized to identify the trends and rainfall variability conditions of the study area. The radiometric terrain correction (ALOS PALSAR DEM) digital elevation model (Fig. 1), which possesses a high spatial resolution of about 12.5 m, is used in bringing about the elevation of all stations. The data inspection tools such as the MK test, Sen's test, Pettitt test, SNHT, and Buishand tests were used to calculate the trend assessment of precipitation. These tests were computed using XLSTAT 2020; conversely, the interpretive statistical approach such as mean, maximum, minimum, standard deviation (std), skewness, kurtosis, and also yearly rainfall graph was enumerated utilizing Microsoft excel

Table 4. Statistical Information for Study (1951-2019)

Station name	Long	Lat	Ele	Max(mm)	Min (mm)	Mean (mm)	STD	Skew	Kurto
Bagepalli (a)	78	13.75	674	1026.4	220.1	531	174.5	0.489	-0.030
Bangarapete (b)	78.25	13	754	1443.6	237.4	684	245.9	0.799	0.675
Chikkaballapura (c)	77.75	13.5	863	1155.4	178	611	217.1	0.298	-0.415
Gauribidanur (d)	77.5	13.5	663	1168.5	337.4	740	204.1	0.275	-0.705
Gudibande (e)	77.75	13.75	662	1068.6	68.92	532	209.5	0.421	-0.178
Kolar (f)	78	13.25	762	1198.4	401.7	701	201.7	0.314	-0.264
Malur (g)	78	13	783	1398.4	348.6	755	223.7	0.852	0.553
Mulabagilu (h)	78.5	13.25	659	1447.0	270.0	790	207.9	0.598	1.399
Shidlagatta (i)	78	13.5	769	1213.1	316.0	619	205.5	0.972	0.711
Srinivasapura (j)	78.25	13.25	717	1297.2	331.8	696	212.1	0.827	0.832
Srinivasapura-1(k)	78.25	13.5	673	1296.0	347.5	731	210.5	0.731	0.303
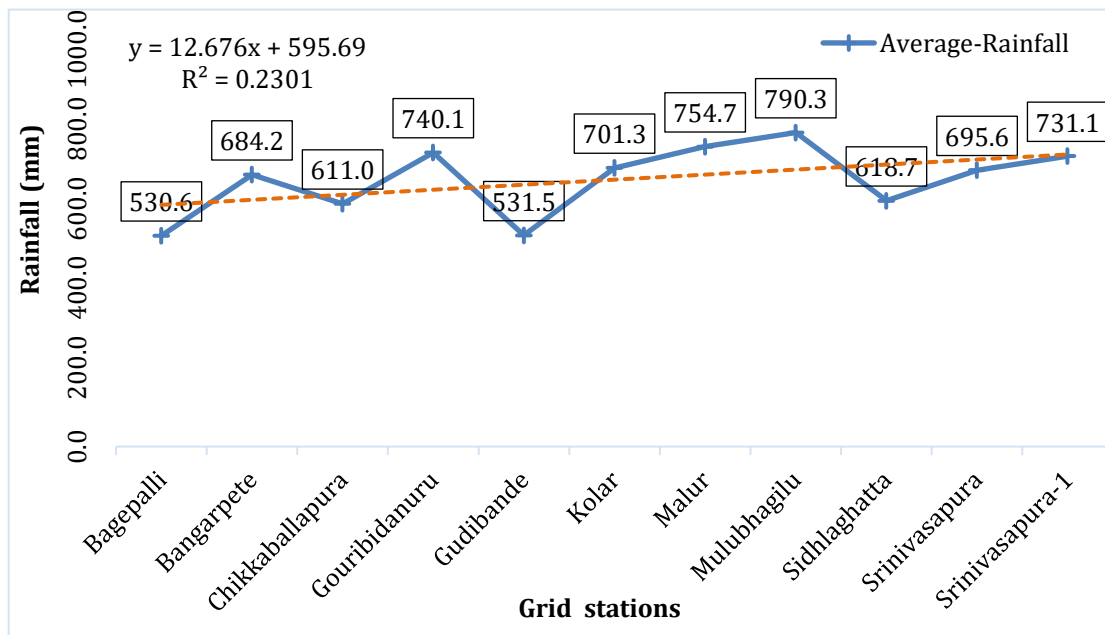
Figure.7 Mean Annual Rainfall (1951–2019)

4.1.2 Mann-Kendal Test for Trend Analysis

The M-K test is generally operating to resolve the trends of hydrometeorological studies (Gedefaw et al., 2018). This analysis has been suggested usually by the WMO-World Meteorological Organization for notable significance (Gajbhiye et al., 2016). This research reveals significant trends, based on positive or negative signs. In this analysis, the alternate hypothesis (Ha) denoted a trend (upward or downward) over time series, and the null hypothesis (H0) presented no trend in precipitation over time (Ahmad et al., 2015). To handle this test requires evaluating the existence of serial correlation inside the long-

117

term data series, the effect of the trend, the magnitude, size, and adaptation of rainfall data. Monthly and annual rainfall series are utilized for the trend, a particular station of rainfall is differentiated with all relative years. The Mann–Kendall statistics "S" is then written down as:

$$S = \sum_{i=1}^{n-1} \sum_{j=i+1}^{n} \text{sign} \left(x_j - x_i \right) \tag{29}$$

These two common sequential data x_i and x_j values for the ith and j the idiom; total length of data n.

sign $\left(x_j - x_i \right)$ conclude the ensuring values:

$$\text{sign}(x_j - x_i) = \begin{cases} +1, & \text{if } x_j - x_i > 1 \\ 0, & \text{if } x_j - x_i = 0 \\ -1, & \text{if } x_j - x_i < 1 \end{cases} \tag{30}$$

Under this test, the statistic S has roughly allotted Gaussian n=18 with the Var(S) and average E(S) of the integer S stated by the bearing assess as follows: MK test specified by a distributed normally along with the average E(S) = 0

$$E(S) = 0, \text{Variance } (S) = \frac{n(n-1)(2n+5)}{18} \tag{31}$$

For Var (S) has to be modified and becomes:

$$\text{Var}(S) = \frac{\{n(n-1)(2n+5) - \sum_{p=1}^{q} t_p(t_p-1)(2t_p+5)\}}{18} \tag{32}$$

Where, n is the length of data, the variable t_p the tied categories of number and q number of values of pth category in Equation (4) were individual.

The standardized static for the Mann–Kendall test (Z) can be deliberate; S is given as observed shown in Equation (5):

$$Z_{mk} = \begin{cases} \dfrac{S-1}{\sqrt{\text{Var } (S)}} & \text{if } S > 0 \\ 0 & \text{if } S = 0 \\ \dfrac{S+1}{\sqrt{\text{Var } (S)}} & \text{if } S < 0 \end{cases} \tag{33}$$

The sign of Z_{mk} desirable negative and positive values of in a test, statistics return the decreasing and increasing trend, individually, although Z_{mk} comprises

values 0, stipulates a normally distributed. At the level, of 5% significance, the change in annual and monthly rainfall trends was evaluated with significance by employing the Mann-Kendal.

4.1.3 Sen's Estimator

Sen's estimation is another non-parametric method to evaluate the magnitude of rainfall trends (Weldegerima et al., 2018). To recognize a trend existing in the data series or nill, a framework called slope estimate β, (Hirsch et al. 1982) is employed. These equations are as suggested in 1968 by Sen (Alemu & Dioha, 2020). A positive statistics of β exhibits 'upward trend', whiles negative statistics show a downward trend'. Here slope (β) connecting any two data points of a series x can be estimated as specified by the equation, computed as:

$$\beta = \frac{x_j - x_i}{j - i} \qquad\qquad 34)$$

Then x_j and x_i inspect as data statistics for i and j time of period ($j > i$), individually. $N = n(n-1)/2$ is the average of N statistics of β is act as Sen's slope, but a single datum feasible in every time, n is number of interval values of T_i that can be deliberate if the data sequence in every year. Next$N < (n-1)/2$; n is the total observations. The N statistics of the estimation of the slope are ordered from lower to highest, generally, slope estimator Q$_t$ is thus enumerated as:

$$Q_t = \begin{cases} T_{(N+1)/2} & N \text{ is uneven} \\ \frac{1}{2}\left(T_{N/2} + T_{(N+2)/2}\right) & N \text{ is even} \end{cases} \qquad\qquad 35)$$

A positive Q_t in the statistics constitute an increasing trend; a negative Q_t statistics constitute a decreasing trend over time. When data series were identified significant trends at intervals of 95% confidence, were intended to operate a non-parametric approach as expressed by a similar procedure (Weldegerima et al., 2018).

4.1.4 Pettitt Test:

This test is utilized broadly to recognize the variation noticed in weather data (Zhang & Lu, 2009). Following Pettitt's, if $x_1.x_2.x_3, \dots x_n$ is and perceive data that has a variation point at t, project as $x_1.x_2.\dots,x_t$ have a function

distribution $F_1(x)$ which is distinct by the function distribution $F_2(x)$ 2nd part $(x_t +1)$, (x_t+2), (x_t+3) …, (x_n). The Pettitt statistics U_t for trial is expressed as:

$$U_t = \sum_{i=1}^{t} \sum_{j=t+1}^{n} \text{sign} \ (x_t - x_j) \qquad 36)$$

$$\text{sign} \ (x_t - x_j) = \begin{bmatrix} 1 & \text{if } (x_i - x_j) > 0 \\ 0 & \text{if } (x_i - x_j) = 0 \\ -1 & \text{if } (x_i - x_j) < 0 \end{bmatrix} \qquad 37)$$

The K statistic and related level confidence (ρ) and the sampling extent (n) express as:

$$K = \text{max } |U_t| \qquad 38)$$

$$\rho = \text{Exp} \left(\frac{-K}{n^2 + n^3} \right) \qquad 39)$$

ρ −value is less than the specific level of confidence and rejected the null hypothesis. The estimated probability (ρ) for a change-point was expressed as:

$$p - 1 - \rho \qquad 40)$$

The K statistic also is evaluated with standard statistics at distinct confidence levels noticing of change point and the analytic of K at a 5 % level of confidence for this test is utilized in the examination (Jaiswal et al., 2015).

4.1.5 SNHT Test

The statistic (Tk) makes use to contrast the average of the first n observations, with the average of (n-k) remaining observations, and n is data time (Alexanderson 1986)

$$T_k = kZ_1^2 + (n - k)Z_2^2 \qquad 41)$$

$$Z_1 = \frac{1}{k} \sum_{i=1}^{k} \frac{(x_i - \bar{x})}{\sigma x} \qquad 42)$$

$$Z_2 = \frac{1}{n - k} \sum_{i=k+1}^{n} \frac{(x_i - \bar{x})}{\sigma x} \qquad 43)$$

σx and $\bar{x}$ are the average and standard deviation. Annual k can be appraised as shift point and comprise a break of the series of T_k reach out maximum statistics.

4.1.6 Buishand's Test

The S_k (*Buishand1982*) is a modified sum of the cumulative divergence from the average of kth observations of a data $x_1, x_2, \dots \dots x_k \dots \dots x_n$ with average ($\bar{x}$) is enumerated using the formula:

$$S_k = \sum_{i=1}^{k} (x_i - \bar{x}) \qquad \qquad 44)$$

Data is needed homogeneously at any shift point then Sk$\cong$ 0 since in random data; the departure from average desire is to diffuse both parts of the average of the data. The shift adjusted range of significance (r) utilizes the given equation:

$$r = \frac{\text{Max } (S_k) - \text{Min }(S_k)}{\bar{x}} \qquad \qquad 45)$$

Then calculate statistics of $R/\sqrt{n}$ is in contrast with interpretive values.

4.1.7 Calculation of Magnitude Change

Change % is set by calculating the linear trend. This will be equivalent to (β) median slope multiplied by total length divided by the corresponding average, communicate as a % PC (Yue and Hashino 2003)

$$(\%) \text{ change } = \frac{\beta \times \text{ total period}}{\text{average}} \times 100 \qquad \qquad 46)$$

4.2 Results and Discussion

4.2.1 Descriptive Analysis of Annual Precipitation

The preliminary evaluation of the data that has been computed includes maximum, minimum, mean, skewness, standard deviation (SD), and kurtosis in the yearly rainfall data for every station (Table 4). The mean amount of annual rainfall in Bagepalli was 531 mm with a standard deviation of 174.5 followed by Bangarapete (684 mm and 245.9 mm), Gauribidanur (740 mm and 204.1 mm), Kolar (755 mm and 201.7 mm), Chikkaballapura (611 mm and 245.9 mm), Malur (755 mm and 223.7 mm), Gudibande (532 mm and 209.57 mm), Mulabagilu (1447.01 mm and 207.9 mm), Sidlaghatta (619 mm and 205.5 mm), Srinivaspura (696 mm and 212.1 mm), and Srinivaspura-1 (731 mm and 210.5 mm). Mulabagilu recorded an enormous rate of the annual rainfall of about 1447.01 mm in 1976; Gudibande admits the lowest amount of annual rainfall about 68.92

mm observed in 1982. The skewness deviates between 0.275 and 0.972 mm. Generally, positive skewness with a mean of about 0.597 reveals that yearly precipitation is dissimilar and exists to mean above thoroughly of the station's data, and kurtosis diversity range from –0.030 to 1.399. The initial interpretation of annual precipitation has indicated that stations that have higher precipitation show more variability and the lower precipitation shows lesser variability. The annual average rainfall graph shows the variability of the rainfall (Fig. 7).

LOWESS curves were used to shorten the local fluctuations (Cleveland 1979, 1984; Helsel and Hirsch n.d.) on monthly and yearly precipitation using statistical regression curves over the study period. The results of rainfall were initiated statistically notable at a significant level of 5% throughout the study period. The non-parametric regression test for annual rainfall exhibits a different outline from eleven grid stations (Fig. 7.1), which expresses a decline to trend during the 1st decade of study time, particularly in 1954. In the 2nd and 3rd decades, the trend steadily increased up to 1969. The least point in the LOWESS curve was noticed from 1980 to 1990, and then it increases highest up to the year 2019. Overall, the annual rainfall data indicate an increasing and decreasing precipitation variation in the stations individually.

Annual precipitation for Bangarapete (Fig. 7.1) manifests a regular rise from 1951 to 2019; after achieving its highest value in 2018, the value will be above the first to last decade, the lowest value was noticed in 1964. In Chikkaballapura station (c), the 1st and 3rd decades are slightly decreasing up to 1990, and it reached the lowest in the year 1991; after that, an increasing trend was observed up to 2019. In station Gauribidanur (d), there was a slightly decreasing trend from the year 1970 to 1995 and then increased up to 2019. In the Gudibande (e), the declining trend has been detected from 1970 to 1990, and then dipped to the lowest value in 1981. Overall rainfall pattern is a gently increasing trend throughout the study time of some stations (Fig. 7.1 f, g, h, j, and k). Kolar grid station (f) exhibits little fluctuation with the lowest value in the year 1953 and the highest in 2019. Malur (g), Srinivaspura (j), and Srinivasapura-1 (k) stations have the minimum LOWESS curve value revealed in 1953 and excessive in 2002, 2016, and 2018, respectively. Mulabagilu (h) holds

the highest value in 2018 and the lowest in the year 1951. But in the Sidlaghatta (i) station, the annual precipitation LOWESS curve demonstrates a decline between 1951 and 1998 and the highest in 2018. The LOWESS curve demonstrates the variations of annual rainfall time series in every particular decade of the study time, but the general trend was constant in some decades, and little variation throughout the time series. The fitted series at the annual LOWESS test (predicted line) of rainfall showed a significant outcome at all grid stations. The determination of coefficient value (R^2) in Srinivaspura (j) R^2 = 0.9505 > Bangarapete (b) R^2 = 0.949 > Srinivasapura-1(k) R^2 = 0.9404 > Malur (g) R^2 = 0.8682 > Mulabagilu (h) R^2 = 0.7455 > Kolar (f) R^2 = 0.476 > Bagepalli (a) R^2 = 0.3867 > Gauribidanur (d) R^2 = 0.3194 > Gudibande (e) R^2 = 0.1211 > Sidlaghatta (i) R^2 = 0.0803, and finally very least value of coefficient is > Bagepalli (a) R^2 = 0.3867. The values of the determination of coefficient show a correlation connecting the predicted and observed rainfall data.
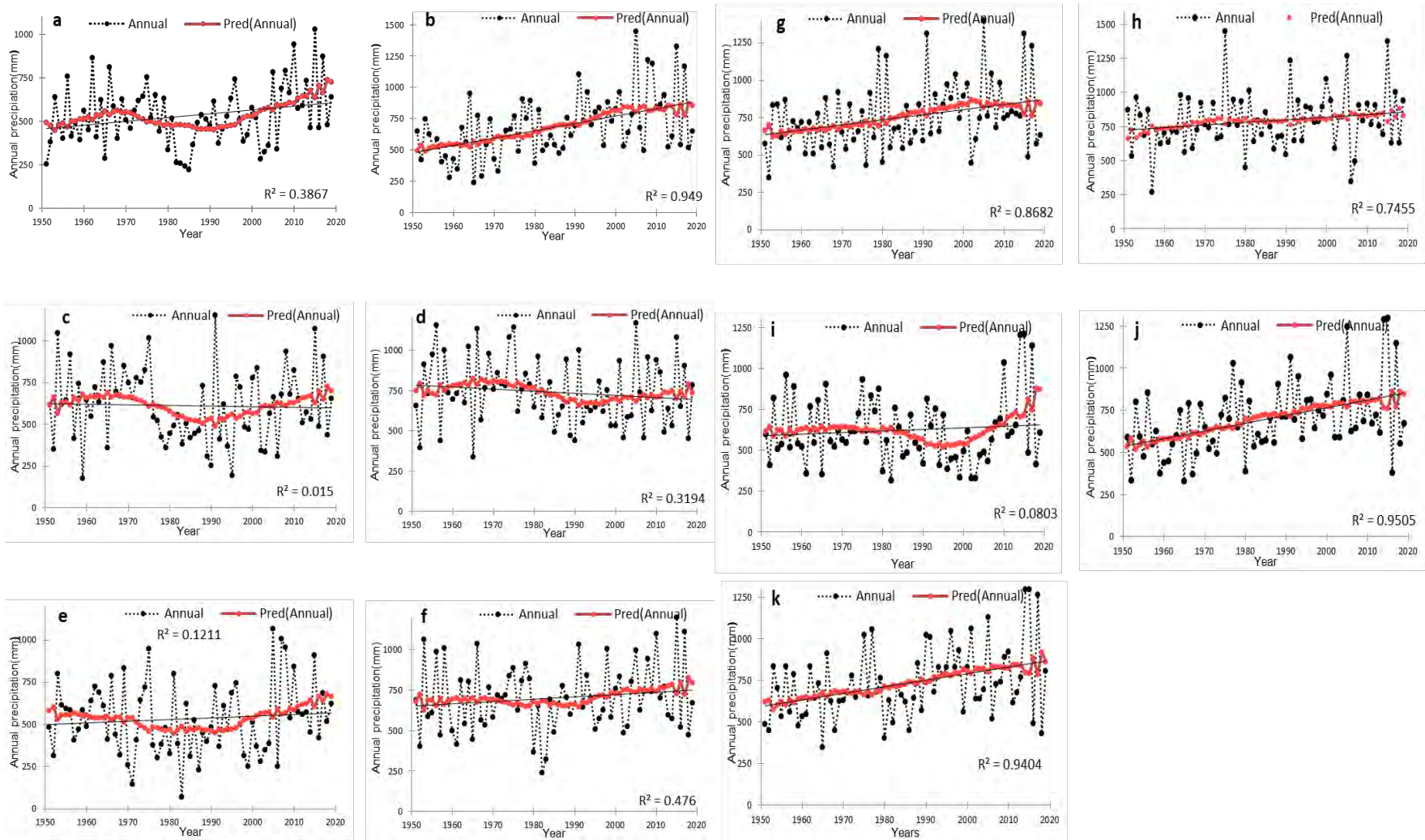
Fig. 7.1 LOWESS Regression Lines for Annual Rainfall in Rain Grid Station (Prediction)

4.2.2 Monthly Precipitation Trend

The MK test was applied on a monthly time to inspect the trends of rainfall (Table 4.1). The monthly rainfall trend established a blend of negative and positive trends. The seven meteorological stations unveil positive rainfall trends with statistically significant for June. In October it was noticed a significant negative trend at Shidlagatta. All the stations exhibit positive trends in March and June but show that more stations have negative trends in October at six stations and December at four stations shown in Table 4.1. A blend of notably positive and negative tendencies is beginning to be found in several months, which are January, February, April, May, July, August, September, November, and December. The magnitudes of trend have an insignificant level on a monthly scale; Sen's slope method reveals the trends are quick (Incline/decline) from July to October and November. Bagepalli, Bangarapete, Gudibande, Kolar, Malur, Mulabagilu, Sidlagatta, Srinivasapura, and Srinivasaura-1 show corresponding to maximum positive and less negative growth during some months (Fig. 7.3). Chikkaballapura and Gauribidanur show a maximum negative and less positive growth shown in Table 4.1.

Table 4.1 expresses the monthly trend in rainfall that proposes a positive trend in January, February, March, April, May, June, August, September, and December, and a large number of stations show a negative trend for July, October, and December months across the districts. The results show a maximum positive value in monthly precipitation found during March, April, May, June, August, and September and a maximum negative value occurred during July and October. No significant negative trend happened in the early monsoonal months and a decreasing trend was observed in the post-monsoonal months.Trend and drought severity has changed with time and a mix of wet and dry years has been detected. There have been several months that show a normal trend during Rabi (January to May) and Kharif seasons (June to September). Along with this, several months have to view extreme trend events during the mid-and late Kharif seasons. Figure 7.3 reveals the spatial difference in the rainfall data series for more significant positive and negative trend months like June and October in the study area from 1951 to 2019.

Station name	January		February		March		April		May		June	
	M-K trend (Z)	slope estimate	M-K trend (Z)	slope estimate	M-K trend (Z)	slope estimate	M-K trend (Z)	slope estimate	M-K trend (Z)	slope estimate	M-K trend (Z)	slope estimate
Bagepalli	1.515	0.00	0.481	0.00	0.968	0.000	1.730	1.227	1.227	0.308	2.952*	0.626
Bangarapete	0.676	0.00	1.376	0.00	2.462*	0.010	1.730	0.190	2.201*	0.731	4.029*	0.956
Chikkaballapura	1.004	0.00	-0.470	0.00	1.710	0.000	1.105	0.100	-0.694	-0.175	1.098	0.237
Gauribidanur	-0.403	0.00	0.981	0.00	0.442	0.000	-0.404	-0.036	0.124	0.039	0.217	0.039
Gudibande	0.715	0.00	1.509	0.00	1.179	0.000	1.616	0.132	0.269	0.056	1.999*	0.392
Kolar	1.043	0.00	0.976	0.00	1.566	0.000	0.492	0.055	0.999	0.255	1.605	0.424
Malur	0.988	0.00	0.806	0.00	1.780	0.000	2.212*	0.349	1.289	0.412	2.247*	0.570
Mulabagilu	0.289	0.00	0.807	0.00	1.919	0.003	1.372	0.170	1.046	0.263	2.108*	0.503
Shidlagatta	1.256	0.00	0.012	0.00	1.245	0.000	0.145	0.009	0.554	0.145	1.574	0.358
Srinivasapura	1.453	0.00	2.039*	0.00	1.549	0.000	1.782	0.213	1.781	0.468	3.382*	0.894
Srinivasaura-1	0.265	0.00	0.945	0.00	1.776	0.000	0.683	0.069	1.864	0.418	2.962*	0.678

Station name	July		August		September		October		November		December	
	M-K trend (Z)	slope estimate	M-K trend (Z)	slope estimate	M-K trend (Z)	slope estimate	M-K trend (Z)	slope estimat	M-K trend (Z)	slope estimat	M-K trend (Z)	slope estimate
Bagepalli	0.818	0.159	2.071*	0.467	0.227	0.121	-1.455	-0.706	0.802	0.152	0.354	0.000
Bangarapete	1.616	0.500	2.154*	0.763	1.533	0.741	0.813	0.427	1.310	0.399	1.602	0.005
Chikkaballapur	-0.098	-0.016	0.450	0.150	0.150	0.055	-1.735	-0.853	-0.290	-0.003	-0.571	0.000
Gauribidanur	-1.118	-0.309	-0.828	-0.314	-0.626	-0.306	-1.439	-0.734	-0.409	-0.082	-0.266	0.000
Gudibande	0.165	0.041	1.320	0.412	0.502	0.183	-0.305	-0.145	1.476	0.118	1.428	0.000
Kolar	0.347	0.089	0.875	0.275	0.160	0.109	0.279	-0.134	0.176	0.033	0.566	0.001
Malur	1.134	0.300	1.434	0.513	1.196	0.665	0.108	0.076	0.637	0.175	0.830	0.000
Mulabagilu	0.000	0.002	1.460	0.488	1.072	0.573	-0.341	-0.233	-0.315	-0.119	0.046	0.000
Shidlagatta	-0.554	-0.128	1.087	0.334	0.341	0.139	-2.201*	-0.988	0.336	0.087	-0.083	0.000
Srinivasapura	0.652	0.144	1.351	0.429	1.010	0.526	0.414	0.182	1.310	0.411	1.108	0.002
Srinivasaura-1	0.264	0.068	1.662	0.481	1.300	0.522	0.124	0.036	0.450	0.159	-0.896	-0.003

Table. 4.1 Outcome of the Z Value (5%) Significance Level and Sens Estimate for Rainfall in Monthly data1951–2019 * Stand for Significant Trend

4.2.3 Annual Scale of Rainfall Trend Analysis during 1951– 2019

The MK approach was used to recognize trends in yearly precipitation (Table 4.2). Similar to the monthly inspection, a blend of positive and negative trends is recognized at particular stations. For the yearly series (Fig. 7.3), positive trends with significant levels were found at Bangarapete, Malur, Srinivasapura, and Srinivasapura-1 grid stations, whereas Chikkaballapura, Gauribidanur, and Shidlagatta exhibited a statistically negative trend. The magnitude of yearly precipitation data is extracted to utilize Sen's slope estimator, and the output shows the yearly precipitation is gradually rising in Bangarapete with a percentage change of 53.22%, Malur (29.32%), Srinivasapura (40.18%), Bagepalli (22.62%), and Srinivasapura-1 (35.08%). The precipitation remains nearly stable at Gudibande (6.01%), Kolar (12.37%), and Mulabagilu (13.51%). Annual rainfall is slightly decreasing, whereas, in Chikkaballapura grid station, it is –10.52%, Gauribidanur –8.96%, and Shidlagatta –3.56%.

4.2.4 Inspection of Homogeneity of Annual Rainfall Trends

The homogeneity test permits finding homogeneity in the data. Pettit's is a non-parametric test that needs no presumption about the dissemination of rainfall data. Table 4.3 displays the outcome of change points in yearly precipitation is enumerated using a test like Pettitt's, SNHT, and Buishand tests were used for the analysis of the data to find out the homogenous series (H0) and heterogeneous series (Ha) of precipitation. Using homogeneity analysis of (H0) represents that Malur (0.034), Bangarapete (0.000), Srinivasapura (0.003), and Srinivasapura-1 (0.014) show to be the immensely expected change point year in Pettit's test analysis, with comparison to the 5% significance level. P 0.05 accepts the H0. SNHT outcome shows a (T0) value more in the stations like Bagepalli (12.58), Bangarapete (17.10), Srinivasapura (12.82), and Srinivasapura-1 (11.75) stations indicate that more significant shift point year, but other stations display a homogeneity in series of data. In the Buishand (Q) value analysis, the outcome indicates a significant change point year in 5 stations, like Bagepalli (11.95), Bangarapete (17.12), and Malur (12.27),

Srinivasapura (14.87), and Srinivasapura-1 (14.22), and then remaining stations are continuously homogenous series of data.
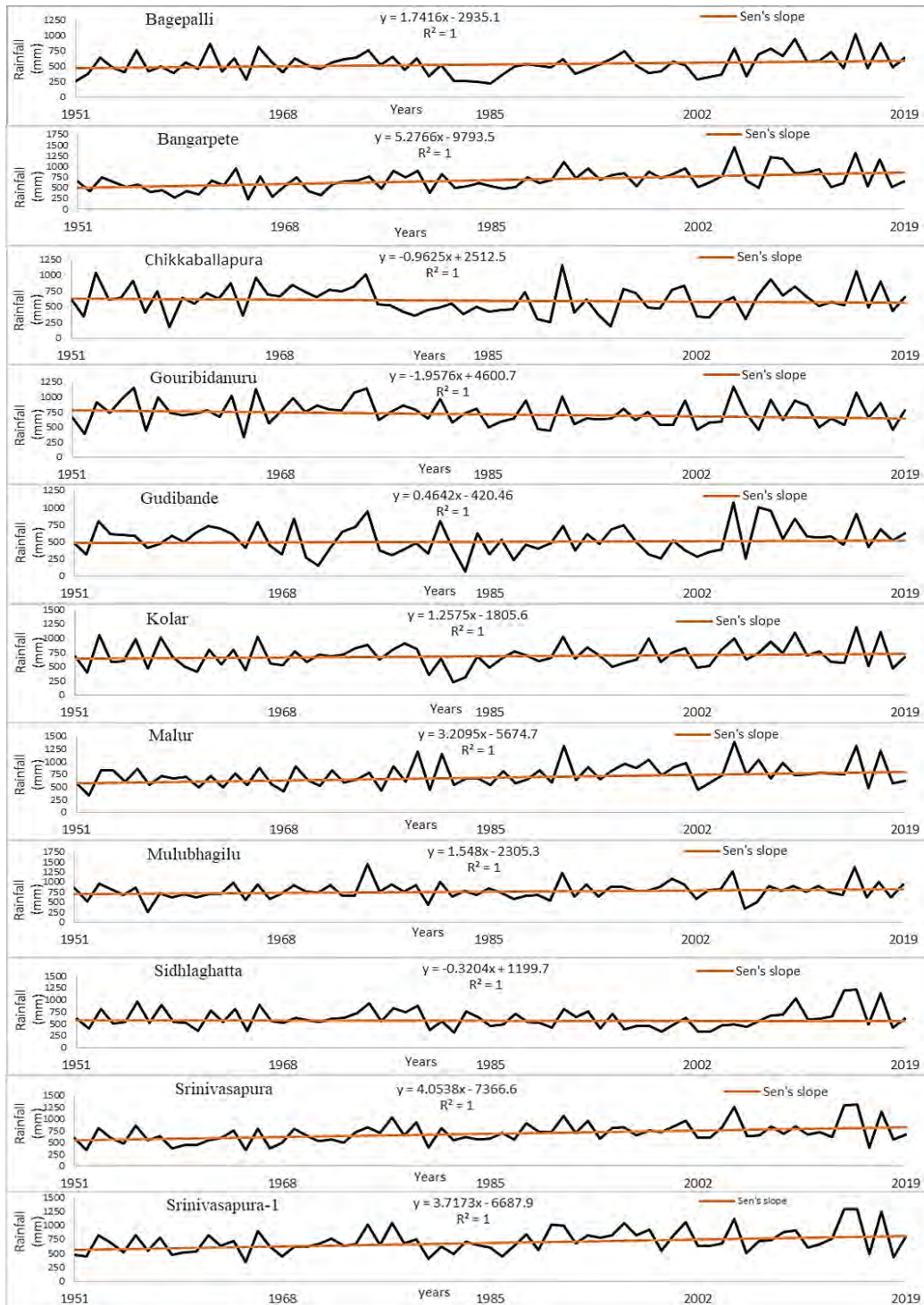
Figure. 7.2 Slope Estimates for the Monthly Time Data in Grid Stations 1951–2019 Using Sen's Test

Table-4.2 Outcome of the Man Kendal test, 1) Bagepalli, 2) Bangarapete, 3) Chikkaballapura and 4) Gauribidanur

1.MONTHS	Kendall's(s)	Kendall's tau	Var.(S)	P-value	α-Value	Sen's slope	2.MONTHS	Kendall's (S)	Kendall's tau	Var.(S)	P-value	α-Value	Sen's slope
January	192.0	0.138	17720.6	0.151	0.05	0.000	January	89.0	89.0	29831.	0.610	0.05	0.000
February	55.0	0.035	22229.0	0.717	0.05	0.000	February	196	196.0	23796	0.206	0.05	0.000
March	200.0	0.110	27762.0	0.232	0.05	0.000	March	502.0	502.0	32546	0.005	0.05	0.016
April	299.0	0.132	35656.3	0.115	0.05	0.110	April	401	401.0	35669.	0.034	0.05	0.237
May	184.0	0.081	35686.6	0.333	0.05	0.252	May	470	470.0	35688.6	0.013	0.05	0.829
June	507.0	0.223	35685.6	0.007	0.05	0.588	June	747	747.0	35687.6	< 0.0001	0.05	0.969
July	201.0	0.088	35685.6	0.290	0.05	0.200	July	343	343.0	35685.6	0.070	0.05	0.588
August	397.0	0.174	35687.6	0.036	0.05	0.477	August	383	383	35687.6	0.043	0.05	0.734
September	-23.0	-0.010	35685.6	0.907	0.05	-0.042	September	239	239.0	35687.6	0.208	0.05	0.647
October	-318.0	-0.140	35686.6	0.093	0.05	-0.837	October	154	154	35688.6	0.418	0.05	0.438
November	164.	0.072	35684.0	0.388	0.05	0.166	November	262	262	35686.6	0.167	0.05	0.429
December	16.0	0.007	35277.3	0.936	0.05	0.000	December	89	89	29831.7	0.610	0.05	0.000

3.MONTHS	Kendall's (S)	Kendall's tau	Var.(S)	P-value	α-Value	Sen's slope	4.MONTHS	Kendall's (S)	Kendall's tau	Var.(S)	P-value	α-Value	Sen's slope
January	120.0	0.089	16712.6	0.357	0.357	0.000	January	-67.0	-0.050	16713.6	0.610	0.05	0.000
February	-89.0	-0.057	21397.0	0.547	0.547	0.000	February	127	0.084	20530.3	0.379	0.05	0.000
March	338.0	0.191	26557.3	0.039	0.039	0.000	March	143	0.072	31134.3	0.421	0.05	0.000
April	273.0	0.123	35194.3	0.147	0.147	0.165	April	-29.0	-0.013	35677.0	0.882	0.05	-0.010
May	-79.0	-0.035	35669.0	0.680	0.680	-0.094	May	75	0.033	35687.	0.695	0.05	0.109
June	167.0	0.073	35671.0	0.379	0.379	0.199	June	3.00	0.001	35685.2	0.992	0.05	0.001
July	24.0	0.011	35684.0	0.903	0.903	0.040	July	-159	-0.070	35687.6	0.403	0.05	-0.226
August	38.0	0.017	35686.6	0.845	0.845	0.08	August	-223	-0.098	35687.6	0.240	0.05	-0.475
September	18.0	0.008	35682.0	0.928	0.928	0.023	September	-150	-0.066	35684.0	0.430	0.05	-0.386
October	-316	-0.139	35670.0	0.095	0.095	-0.860	October	-307	-0.135	35687.6	0.105	0.05	-0.822
November	-83.0	-0.037	35521.6	0.664	0.664	-0.037	November	-126	-0.055	35678.0	0.508	0.05	-0.138
December	120.0	0.089	33125.6	0.422	0.422	000	December	-103	-0.047	35092.3	0.586	0.05	0.000

Table 4.2 Continued…

5.MONTHS	Kendall's (S)	Kendall's tau	Var.(S)	P-value	α-Value	Sen's slope	6.MONTHS	Kendall's (S)	Kendall's tau	Var.(S)	P-value	α-Value	Sen's slope
January	80.0	0.062	15668	0.528	0.05	0.000	January	150.0	0.084	27173.3	0.366	0.05	0.000
February	200.0	0.136	19627	0.155	0.05	0.000	February	137.0	0.079	25912.3	0.398	0.05	0.000
March	271.0	0.147	28319	0.109	0.05	0.000	March	315	0.149	33628.3	0.087	0.05	0.000
April	313.0	0.138	35649	0.098	0.05	0.134	April	160.0	0.070	35676.0	0.400	0.05	0.100
May	61.0	0.027	35687	0.751	0.05	0.070	May	244.0	0.107	35686.6	0.198	0.05	0.379
June	427	0.188	35683	0.024	0.05	0.456	June	247.0	0.108	35687.6	0.193	0.05	0.357
July	83.0	0.036	35685	0.664	0.05	0.93	July	118.0	0.052	35688	0.536	0.05	0.170
August	198.0	0.087	35688	0.297	0.05	0.306	August	120.0	0.053	35688.6	0.529	0.05	0.182
September	74.0	0.032	35688.6	0.699	0.05	0.136	September	24.0	0.011	35688.6	0.903	0.05	0.060
October	-82.0	-0.036	35688.6	0.668	0.05	-0.199	October	-55.0	-0.024	35687.6	0.775	0.05	-0.138
November	294.0	0.129	35668.0	0.121	0.05	0.125	November	-3.000	-0.001	35687.6	0.992	0.05	-0.005
December	225.0	0.104	34577.6	0.228	0.05	0.000	December	53.0	0.024	35519.6	0.783	0.05	0.000

7.MONTHS	Kendall's (S)	Kendall's tau	Var.(S)	P-value	α-Value	Sen's slope	8.MONTHS	Kendall's (S)	Kendall's tau	Var.(S)	P-value	α-Value	Sen's slope
January	130	0.084	21396	0.378	0.05	0.000	January	335.0	0.28	13465.0	0.004	0.05	0.000
February	103	0.067	21397.0	0.486	0.05	0.000	February	129.0	0.114	12305.0	0.249	0.05	0.000
March	337.0	0.165	32545.0	0.063	0.05	0.000	March	411.0	0.272	20528.3	0.004	0.05	0.000
April	427.0	0.190	35475.0	0.024	0.05	0.380	April	60.0	0.027	35544.6	0.754	0.05	0.001
May	314.0	0.138	35686.6	0.098	0.05	0.502	May	-45.0	-0.020	35674.3	0.816	0.05	-0.020
June	377.0	0.166	35687.1	0.047	0.05	0.516	June	12.0	0.005	35676.0	0.954	0.05	0.004
July	278.0	0.122	35688.6	0.143	0.05	0.379	July	-179.0	-0.079	35687.6	0.346	0.05	-0.162
August	220.0	0.097	35688.6	0.246	0.05	0.418	August	438.0	0.192	35684.6	0.021	0.05	0.573
September	188.0	0.083	35688.6	0.322	0.05	0.586	September	-138.0	-0.061	35686.6	0.468	0.05	-0.282
October	-12.0	-0.005	35686	0.954	0.05	-0.022	October	-91.0	-0.040	35685.6	0.634	0.05	-0.125
November	80.0	0.035	35678.0	0.676	0.05	0.128	November	204.0	0.095	34252.0	0.273	0.05	0.000
December	108.0	0.049	35193.0	0.568	0.05	0.000	December	335.0	0.281	13465.0	0.004	0.05	0.000

In the Buishand (Q) value analysis, the outcome indicates a significant change point year in 5 stations, like Bagepalli (11.95), Bangarapete (17.12), and Malur (12.27), Srinivasapura (14.87), and Srinivasapura-1 (14.22), and then remaining stations are continuously homogenous series of data. Bangarapete indicates the expected change year in Pettitt's analysis in 1987, SNHT in 1990, and Buishand's showed in 1996, these trend series are heterogeneous in all three tests. Because the data indicate more average rainfall compared to the homogeneity in different stations showed shift change point years shown in Table 4.4. It conveys there is an indicative shifting in the average of earlier and after they perceive the change point in Pettit's, Buishand's, and SNHT is known to search change points. Pettit's tests and Buishand's are located the changes in the center of sequence. Investigation over the tests indicates 4 common stations, where all 3 tests show around the change shift year. The 4 grids indicate the change point year except for the Malur station, where the SNHT test and Pettit's test is homogenous in Bagepalli stations. Figure 7.4 indicates perceptible changes in the precipitation series and earlier the change point in the total grid station. The spatial distribution of the p-value of homogeneity tests is highlighted in Fig. 7.5.

Table 4.3 Outcome of the Z-value of MK test, at Significance Level (5%) and Sen's Slope in Annual Rainfall.

Station name	M-K trend (Z)	Sen's slope	Change (%)	Trend status
Bagepalli	1.559	1.741	**22.62**	Positive
Bangarapete	**3.734***	5.276	**53.22**	↑ Increasing
Chikkaballapura	-0.548	-0.932	-10.52	Negative
Gauribidanur	-0.541	-0.962	-8.96	Negative
Gudibande	0.336	0.464	6.01	No trend
Kolar	0.927	1.257	12.37	No trend
Malur	**2.579***	3.209	**29.32**	↑ Increasing
Mulabagilu	1.269	1.547	13.51	Positive
Shidlagatta	-0.155	-0.320	-3.56	Negative
Srinivasapura	**3.470***	4.053	**40.18**	↑ Increasing
Srinivasapura-1	**2.838***	3.717	**35.08**	↑ Increasing

Table 4.4 Prettitt's, SNHT, and Buishand Trend Test Statistics

Station name	Pettit's test			SNHT			Buishand's test		
	K	P	Trend	T_o	P	Trend	Q	P	Trend
Bagepalli (a)	430	0.092	Ho	**12.58**	**0.007**	**Ha** (2006)	**11.95**	**0.019**	**Ha** (2004)
Bangarapete (b)	**662**	**0.000**	**Ha** (1987)	**17.10**	**0.001**	**Ha** (1990)	**17.12**	**0.000**	**Ha** (1988)
Chikkaballapura (c)	402	0.160	Ho	5.343	0.270	Ho	9.29	0.121	Ho
Gauribidanur (d)	388	0.183	Ho	4.547	0.368	Ho	8.87	0.164	Ho
Gudibande (e)	336	0.401	Ho	7.788	0.078	Ho	9.63	0.099	Ho
Kolar (f)	216	0.613	Ho	3.582	0.565	Ho	6.70	0.427	Ho
Malur (g)	**487**	**0.034**	**Ha** (1990)	8.838	0.059	Ho	**12.27**	**0.015**	**Ha** (1990)
Mulubagilu (h)	284	0.752	Ho	2.890	0.716	Ho	7.02	0.389	Ho
Shidlagatta (i)	278	0.790	Ho	8.758	0.058	Ho	9.31	0.119	Ho
Srinivasapura (j)	**602**	**0.003**	**Ha** (1987)	**12.82**	**0.012**	**Ha** (1972)	**14.87**	**0.002**	**Ha** (1987)
Srinivasapura-1 (k)	**532**	**0.014**	**Ha** (1987)	**11.75**	**0.014**	**Ha** (1987)	**14.22**	**0.003**	**Ha** (1989)

Ha- Heterogeneous Series, **Ho**-Homogenous Series
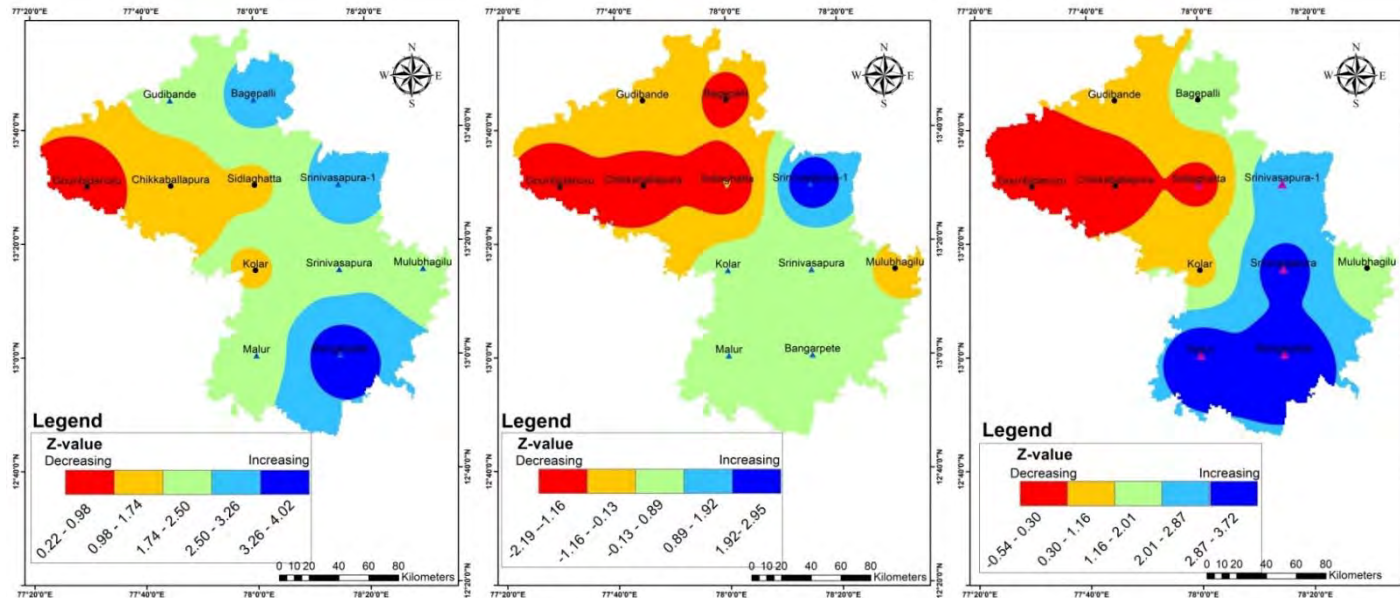
Figure7.3 Spatial Distribution (MK) Z Value of Location with Decline and Increasing Trends at Significance Level 5%, for a,) June, b. October, and c. Annual.
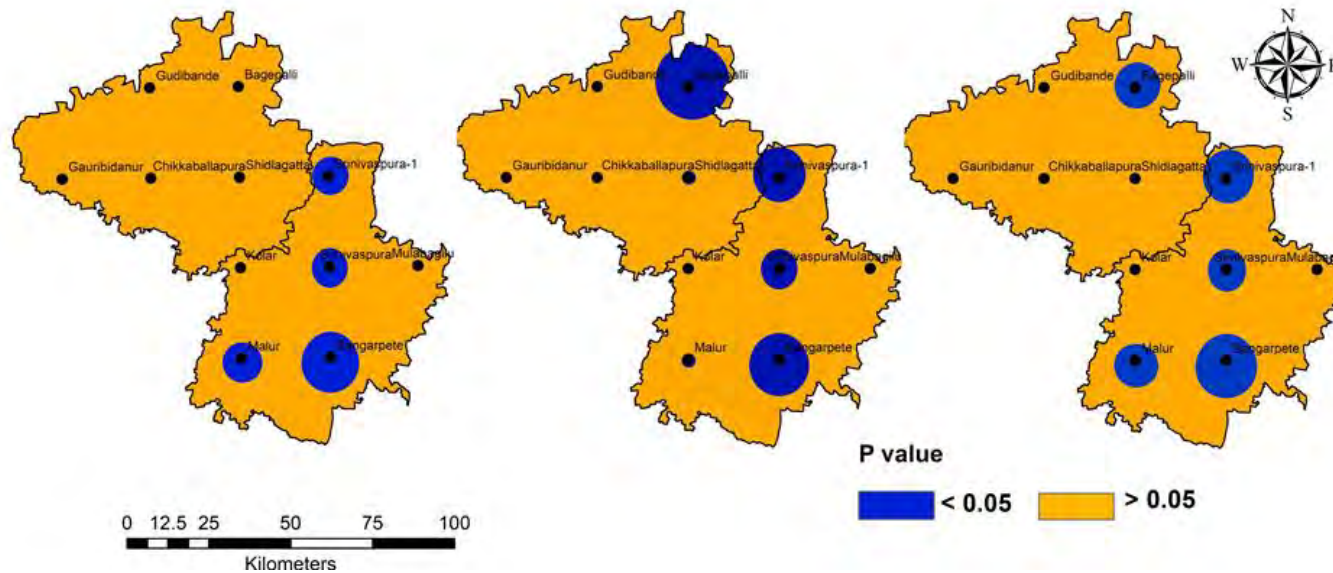
Figure.7.4 Change Point Year in Annual Precipitation in Different Tests a) Pettit's b) SNHT c) Buishand's Test Where <0.05 Indicate the Acceptance of Ha, and >0.05 Accept the H0

1) Pettit's Test Change Points Year
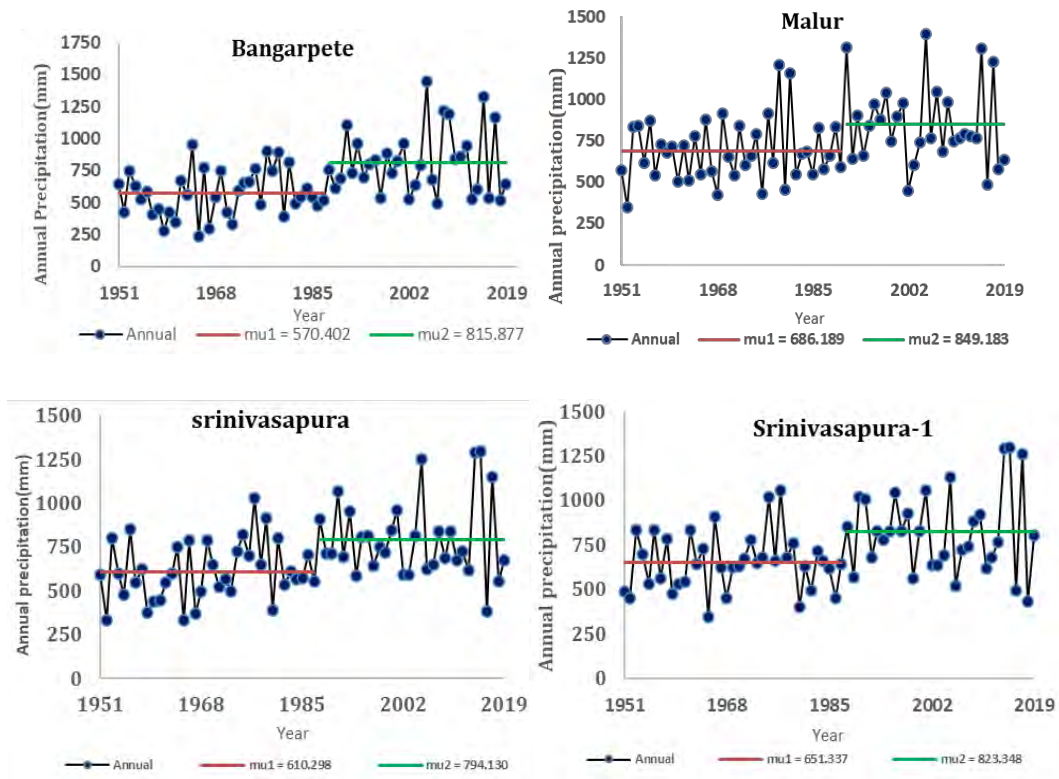
2) SNHT Test Change Year Points
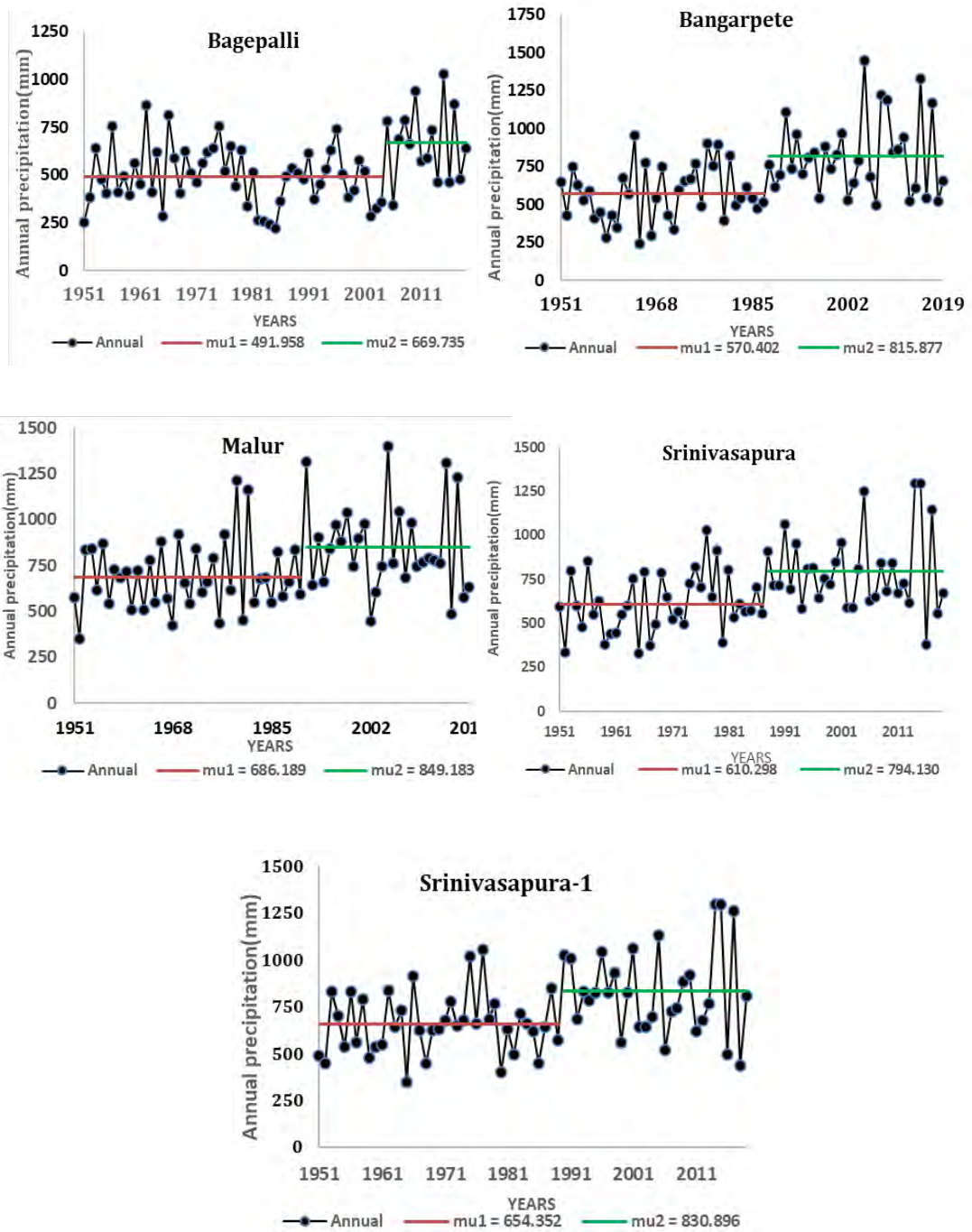
Figure.7.5 Change Point Year in Annual Precipitation Data (a) Bagepalli, (b) Bangarapete, (g) Malur, (j) Srinivasapura, (K) Srinivasapura-1 (mu1 and mu2 Depict the Average Precipitation Before and After)

4.3 Conclusions

The current study analyses precipitation trends across the last 7 decades in the circumstances of climate change for the Kolar and Chikkaballapura districts. The pattern of precipitation trends is represented along with a territorial explanation, statistical tables, and interpretive figures by applying the scientific methodology. The evaluation seems to enhance our interpretation of rainfall trends in these districts. This work finds out there is a noticeable monthly and annual trend using eleven meteorological grid stations in 69 years of the study period. The fitted line LOWESS curve for annual rainfall trends manifests that statistically, results were initiated for the determination of coefficient (R^2) highest in the Srinivaspura (j) (R^2 = 0.9505) and lowest coefficient in the Bagepalli (R^2 = 0.3867) grid stations. The LOWESS curve demonstrates the difference in annual rainfall time sequence in each decade, but the overall tendency was almost nearly constant in considerable decades. The outcome of M-Kendall and Sen's slope estimator trend for every station exhibits increasing and decreasing trends. The coefficient values of an output display an extreme correlation between the predicted and observed data. The rainfall trend was inspected at 5% statistical significance levels or 95% confidence level. The maximum grid stations at monthly rainfall were appearing statistically significant ($P < 0.05$), the 7 meteorological grid stations show statistically significant positive trends for June, and significant negative trends were noticed in October at Shidlagatta. The yearly precipitation output indicates an upward trend, whereas the highest percentage changes in Bangarapete (53.22%) and the lowest in Shidlagatta (–3.56 %). The change point in annual precipitation is computed using Pettitt's, SNHT, and Buishand's methods were used to test the homogenous and heterogeneous series of precipitation. An inspection of these tests reveals that 4 common stations show the change point year. Bangarapete indicates the expected change year in SNHT (1990) with Pettitt's analysis (1987), and Buishand's showed in (1996), followed by the Bagepalli, Malur, and both stations of Srinivasapura. The spatial variability map of precipitation and homogeneity was prepared for Mann Kendall (Z) value to detect the significant increasing and decreasing trend, and homogeneity. The earth's climate change and reallocation of rainfall circulation in monsoon seasons may affect the long-

term rainfall variations. The spatial-temporal variability and heterogeneous trends in precipitation are responsible for drought or foods affecting the agricultural cropping patterns. The source of these changes is essential for the next study to relate the perceived trends with climate variability. Overall, the findings of the research will be beneficial for the arrangement and implications of water resource controlling strategies and drought management in the study area.

4.4 Reference

1. Ahmad I, Tang D, Wang T, Wang M, Wagan B (2015) Precipitation trends over time using Mann-Kendall and spearman's Rho tests in a swat river basin, Pakistan. Adv Meteorol 2015. https://doi.org/ 10.1155/2015/431860
2. Alemu ZA, Dioha MO (2020) Climate change and trend analysis of temperature: the case of Addis Ababa, Ethiopia. Environ Syst Res 9(1). https://doi.org/10.1186/s40068-020-00190-5
3. Campbell-Lendrum, D., Corvalán, C., & Neira, M. (2007). Global climate change: implications for international public health policy. In Bulletin of the World Health Organization (Vol. 85, Issue 3). https://data.giss.nasa.gov/
4. Chatterjee S, Khan A, Akbari H, Wang Y (2016) Monotonic trends in Spatio-temporal distribution and concentration of monsoon precipitation (1901–2002), West Bengal, India. Atmos Res 182:54– 75. https://doi.org/10.1016/j.atmosres.2016.07.010
5. Cleveland WS (1979) robust locally weighted regression and smoothing scatterplots. In Journal of the American Statistical Association (Vol. 74) Cleveland WS (1984) Graphs in Scientifc Publications (Vol. 38, Issue 4) Gajbhiye S, Meshram C, Singh SK, Srivastava PK, Islam T (2016) Precipitation trend analysis of Sindh River basin, India, from the 102-year record (1901-2002). Atmos Sci Lett 17(1):71–77. https:// doi.org/10.1002/asl.602
6. Gedefaw M, Yan D, Wang H, Qin T, Girma A, Abiyu A, Batsuren D (2018) Innovative trend analysis of annual and seasonal rainfall variability in Amhara Regional State, Ethiopia. Atmosphere 9(9). https://doi.org/10.3390/atmos9090326
7. Ghosh KG (2018) Analysis of rainfall trends and its spatial patterns during the last century over the Gangetic West Bengal, Eastern India. J Geovisual Spat Anal 2(2). https://doi.org/10.1007/ s41651-018-0022-x
8. Guhathakurta P, Rajeevan M (2008) Trends in the rainfall pattern over India. Int J Climatol 28(11):1453–1469. https://doi.org/10.1002/ joc.1640 Gupta M, Srivastava PK, Islam T, Ishak AM, Bin. (2014) Evaluation of

TRMM rainfall for soil moisture prediction in a subtropical climate. Environ Earth Sci 71(10):4421–4431. https://doi.org/10. 1007/s12665-013-2837-6

9. Helsel, D. R., & Hirsch, R. M. (n.d.). Techniques of water-resources investigations of the United States Geological Survey Book 4, Hydrologic analysis and interpretation statistical methods in water resources. https://water.usgs.gov/pubs/twri/twri4a3/

10. Hipel KW, Mcleod AJ, Weller RR (1988) Water Resources Bulletin Data Analysis of Water Quality Time Series in Lake Erie' Huang YF, Puah YJ, Chua KC, Lee TS (2015) Analysis of monthly and seasonal rainfall trends using Holt's test. Int J Climatol 35(7):1500–1509. https://doi.org/10.1002/joc.4071

11. Islam T, Rico-Ramirez MA, Han D, Srivastava PK (2012) A JossWaldvogel disdrometer derived rainfall estimation study by collocated tipping bucket and rapid response rain gauges. Atmos Sci Lett 13(2):139–150. https://doi.org/10.1002/asl.376

12. Jaiswal RK, Lohani AK, Tiwari HL (2015) Statistical analysis for change detection and trend assessment in climatological parameters. Environ Process 2(4):729–749. https://doi.org/10.1007/ s40710-015-0105-3

13. Kiat Chang C (n.d.) HOWTION PUAY (3) & MAZLINA ALANG OTHMAN (4) (1, 2, 3, 4) River Engineering and Urban Drainage Research Centre (REDAC) (Issue 2)

14. Kumar Sen P (1968) Estimates of the regression coefcient based on Kendall's Tau. In Journal of the American Statistical Association (Vol. 63, Issue 324)

15. Lettenmaier DP, Wood EF, Wallis JR (1994) Hydro-climatological trends. In 586 Journal of Climate (Vol. 7). Https://about.jstor. org/terms

16. Mann HB (1945) Nonparametric Tests Against Trend (Vol. 13, Issue 3). Https://www.jstor.org/stable/1907187

17. Meshram SG, Singh VP, Meshram C (2017) Long-term trend and variability of precipitation in Chhattisgarh State, India. Theor Appl Climatol 129(3–4):729–744. https://doi.org/10.1007/ s00704-016-1804-z

18. Mina U, Singh D, Kumar P (2018) Climate change impacts on plants population and Community Ecological Attributes, Mitigation Strategies and Policy Interventions-A Review. Appl Ecol Environ Sci 6(3):84–92. https://doi.org/10.12691/aees-6-3-3

19. Moberg A, Alexanderson H (1997) Homogenization of Swedish temperature data. Part ii: homogenized gridded air temperature compared with a subset of global gridded air temperature since 1861. In an international journal of climatology (vol. 17)

20. Partal T, Kahya E (2006) Trend analysis in Turkish precipitation data. Hydrol Process 20(9):2011–2026. https://doi.org/10.1002/hyp. 5993

21. Peterson TC, Easterling DR, Karl TR, Groisman P, Nicholls N, Plummer N, Torok S, Auer I, Boehm R, Gullett D, Vincent L, Heino R, Tuomenvirta H, Mestre O, Tama T, Szentimrey T, Salinger J, Førland EJ, Hanssen-Bauer I, ... Parker D (1998) Homogeneity adjustments of in situ atmospheric climate data: a review. In International Journal of Climatology Int. J. Climatol (Vol. 18)

22. Peterson TC, Easterling DR, Karl TR, Groisman P, Nicholls N, Plummer N, Torok S, Auer I, Boehm R, Gullett D, Vincent L, Heino R, Tuomenvirta H, Mestre O, Tama T, Szentimrey T, Salinger J, Førland EJ, Hanssen-Bauer I, ... Parker D (1998) Homogeneity adjustments of in situ atmospheric climate data: a review. In International Journal of Climatology Int. J. Climatol (Vol. 18)

23. Praveen B, Talukdar S, Shahfahad, Mahato S, Mondal J, Sharma P, Islam ARMT, Rahman A (2020) Analyzing trend and forecasting of rainfall changes in India using non-parametrical and machine learning approaches. Sci Rep 10(1). https://doi.org/10.1038/ s41598-020-67228-7

24. Rautela P, Karki B (2015) Impact of climate change on life and livelihood of indigenous people of Higher Himalaya in Uttarakhand, India. Am J Environ Protect 3(4):112–124. https://doi.org/10. 12691/env-3-4-2

25. Rautela P, Karki B (2015) Impact of climate change on life and livelihood of indigenous people of Higher Himalaya in Uttarakhand, India. Am J Environ Protect 3(4):112–124. https://doi.org/10. 12691/env-3-4-2

26. Sonali P, Nagesh Kumar D (2013) Review of trend detection methods and their application to detect temperature changes in India. J Hydrol 476:212–227. https://doi.org/10.1016/j.jhydrol.2012.10. 034

27. Srivastava PK, Mehta A, Gupta M, Singh SK, Islam T (2015) Assessing impact of climate change on Mundra mangrove forest ecosystem, Gulf of Kutch, western coast of India: a synergistic evaluation using remote sensing. Theor Appl Climatol 120(3–4):685–700. https://doi.org/10.1007/s00704-014-1206-z

28. Talaee PH (2014) Iranian rainfall series analysis by means of nonparametric tests. Theor Appl Climatol 116(3–4):597–607. https://doi. org/10.1007/s00704-013-0981-2

29. Van G, And B, Hughes JP (1984) Nonparametric tests for trend in water quality. In Water Resources Research (Vol. 20, Issue 1)

30. Weldegerima TM, Zeleke TT, Birhanu BS, Zaitchik BF, Fetene ZA (2018) Analysis of Rainfall Trends and Its Relationship with SST Signals in the Lake Tana Basin, Ethiopia. Adv Meteorol 2018. https://doi.org/10.1155/2018/5869010

31. Yang P, Ren G, Yan P (2017) Evidence for a strong association of short-duration intense rainfall with urbanization in the Beijing urban area. J Clim 30(15):5851–5870. https://doi.org/10.1175/ JCLI-D-16-0671.

32. Yue S, Hashino M (2003) Temperature trends in Japan: 1900-1996. Theor Appl Climatol 75(1–2):15–27. https://doi.org/10.1007/ s00704-002-0717-1

33. Zhang S, Lu XX (2009) Hydrological responses to precipitation variation and diverse human activities in a mountainous tributary of the lower Xijiang, China. Catena 77(2):130–142. https://doi.org/ 10.1016/j.catena.2008.09.001

CHAPTER -5
VEGETATION HEALTH ANALYSIS

Chapter-5

Vegetation Health and Drought Analysis

5. Introduction

In semi-arid regions, the production of rain-fed agricultural activity is a majorly risky operation because sensitivity is very high to climate extremes, including drought and other calamities (Choi et al. 2013; He et al. 2021). Several researchers have noticed that drought events cause a serious decline in agricultural productivity and production all over the globe. This can happen with no caution, without identified economic or borders and political differences (KOGAN 1990). For example, during the time of periods 2001–2012, extreme-exceptional (EE) covered about 1–7% of Severe-exceptional (SE) 8–16%, moderate to-exceptional (ME) 18–36%, of the total land area of the globe, respectively. Respectively(Kogan, Adamenko, and Guo 2013), For instance, the droughts period in Russia from 2010 and 2011 to 12 in the United States of America produced substantial global and local economic impacts (Kogan and Guo 2016). As an outcome, the balance of food demand and supply was affected significantly due to extreme and severe droughts (SD) at global, regional, and local scales level (Hoolst et al. 2016). In semi-dry regions, where the precipitation pattern is extremely variable, the susceptible collapse is realized (Maybank et al. 1995). Different regions of the globe, mainly the grain-growing nations like the USA, China, Russia, India, and the European Union thus encountered an incline in the intensity and frequency of droughts events (Owrangi et al. 2011).

In developed nations, drought mitigation, monitoring, and early warning structure are situated on earth observation data products and it is most effective, while in most Asian countries (including India) the location depends highly on the in-situ climatic data format only, which largely affects the smallholder farmers of the countries. It also scarcity the continuous temporal and spatial range needed to monitor and characterize the detailed temporal pattern and spatial extent of drought events (Gu et al. 2007). Karnataka is one of the main revenue states of India; some regions of the state were affected by frequent

drought periods and events due to erratic and poor precipitation variability where the problem is extreme and severe in the south-eastern parts of the state. Some researchers reported that the occurrence of El Nino climate event droughts and dry events has also been regularly occurring over the several decades triggering different threats to the agriculture sector. Particularly the semi-arid area has been majorly affected by recurrent droughts events (Harishnaika et al. 2022). The duration, cessation, severity, frequency, and spatial extent of drought in the regions are high. Despite the substantial growth and health in the major crop types maize, wheat, barley, sorghum, and other crops). which were noticed in terms of area and productivity coverage, these yields are low when assess by international standards. Because production is largely susceptible to weather events, particularly dry events, and drought. Agricultural cultivation and production, majorly in the poor regions have endured highly dependent on the climate and weather (A. Zhang, Jia, and Wang n.d.). The challenges stand up May also in the future as the natural resources are highly overexploited due to increasing population growth. Agriculture is the sector firstly affected by the hydro-meteorological period droughts because it negatively affects vegetation growth as well as crop production (Bhuiyan, Singh, and Kogan 2006), but behind move on to other water resource-dependent sectors (Komuscu 2001).

Agricultural drought is expressed by the depletion of crop productivity and production due to a shortfall of precipitation as well as insufficient soil moisture to the zone of crop root (Sruthi and Aslam 2015). However, the dependency on weather and climate data alone is not enough to monitor and prediction in the region of drought events, especially when these data are sparse, untimely, and incomplete (Peters et al. 2002). The conventional ways of dry events monitoring which highly depend only on weather grid stations lack repeated spatial coverage to monitor and characterize the spatial pattern of dry incidences in-depth (Gu et al. 2007). Monitoring the health of vegetation status of the research area is significant to describe the events of agricultural drought, then it requires 5 years of satellite data observation suitable drought indices Furthermore, the monitoring, mitigating, and understanding of drought are become a difficult aspect because of the natural phenomenon (Vicente-serrano et al. 2012). Yet, satellite data observations have some limitations to meteorological

142

observations, giving the possibility for cost-effective, spatially and temporarily dynamic and explicit scale drought monitoring (Zhang et al. 2016).

Satellite product observation like NDVI, eMODIS, and MOD11A2 LST supported with highly advanced remote sensing drought indexes such as VHI (Vegetation Health Index) can help to evaluate the occurrence of agricultural droughts events. Kogan and Liu (1996) express that the seasonal and inter-annual drought events can be represented by using the VCI (Vegetation Condition Index) and TCI-Temperature Condition Index (L. Zhang et al. 2019) because both indexes can help to calculate and generate VHI (Rhee, Im, and Carbone 2010). Vegetation Health Index has been the accepted agricultural drought indices. but, it needs both LST and NDVI data (Gidey et al. 2018). The target of this research was to monitor the agricultural drought for 5 years period of duration, onset, cessation, severity, frequency, and spatial and temporal extent utilizing the Vegetation Health Index (VHI) which combines NDVI, LST, VCI, and TCI in Kolar and Chikkaballapura district area of Karnataka state. The study is conclusive for understanding, monitoring, and managing the events of droughts through meteorological and satellite earth observation data.

5.1 Methodology and Analysis

5.1.1 Data Acquisition

5.1.1.1 Expedited MODIS (EMODIS) -TERRA NDVI

Tsiros et al. (2004) describe that remote sensing data should effectively be used to monitor drought events, vegetation response, and cessation of the drought period. In this research, the agricultural drought of the research region was inspecting the historical EROS Moderate Resolution Imaging Spectroradiometer and real-time Earth observation data products. A multi spatial-temporal monthly and weekly, Terra eMODIS-NDVI, (advance Moderate Resolution Imaging Spectora diameter Normalized Difference Vegetation Index) data from the period of 2015 to 2019, at 250 m spatial resolution. The data (Terra eMODIS-NDVI) are finer for agricultural drought understanding and monitoring than Aqua.

5.1.1.2 Land Surface Temperature (LST)

In this research, the MOD11A2 Emissivity and LST Terra 16 days temporal resolution (later aggregated into Monthly days bases) data were acquired from the NASA (National Aeronautics and Space Administration) — USGS (United States Geological Survey) Lands and Processes allocate LP DAAC (Active Archive Centre). The intention to use the LST daytime (Terra) data exists in its temporal extension. (Frey, Kuenzer, and Dech 2012) describe that the temporal-spatial evolution of Land Surface Temperature gets during the daytime is finer to get in details than the Aqua because a change in LST can be observed during the night-time. Yet, in the nighttime, LST remains stable as an outcome, and the limitation on time differences could be mitigated. The MODIS Land Surface Temperature introduces a quality of LST than the AVHRR satellite sensor due to its spatial and temporal differences and updated algorithms such as satellite view zenith, azimuth angle, and time of acquisition quality for interpretation of the products are easy. This satellite data was utilized to compute the Temperature condition index (TCI) and VHI, which is an integrated and latest drought monitoring model in agriculture.

5.1.1.3 Rainfall

Rainfall data are highly useful meteorological components in drought-related research. In this study, the long-term daily rainfall data were obtained from the India Meteorological Department (IMD) 2015–2019. The rainfall data were primarily used to examine the response of drought to precipitation,
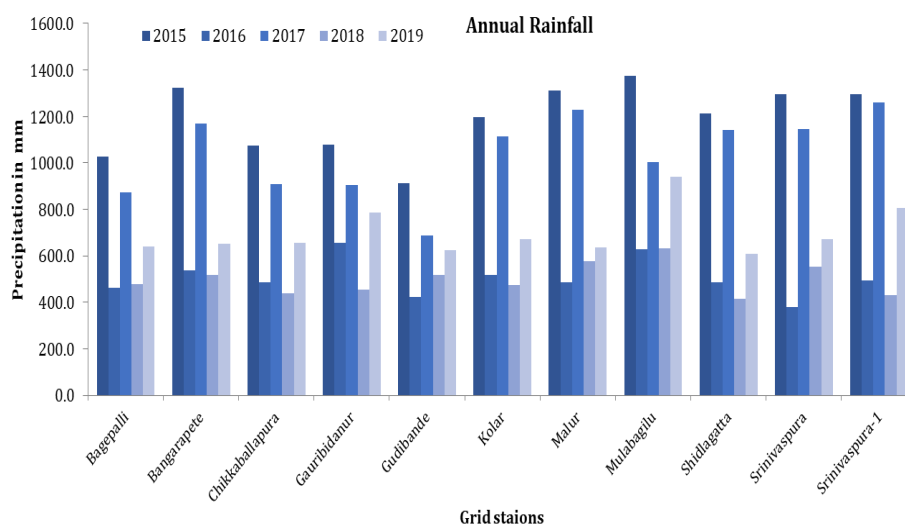
Figure 8. Showed an annual rainfall from 2015-2019

5.2 Data Analysis and Processing

5.2.1 Expedited MODIS (eMODIS) -TERRA NDVI

E MODIS is a procedure for creating a specific suite-community of vegetation examination products based on the NASA (National Aeronautics and Space Administration's), EOS (Earth Observing System) MODIS (Moderate Resolution Imaging Spectroradiometer) and produced in the USGS (U.S. Geological Survey's), EROS (Earth Resources Observation and Science) Center (Jenkerson and Schmidt 2008). Jenkerson et al. (2010) described that the eMODIS (NDVI) data are a match for vegetation-related research because the remote sensing data were captured with a repeated frequent cycle.

Rhee et al. (2010) suggested that the NDVI has been used for drought detection and monitoring. But Normalized Difference Vegetation Index data cannot show the severity and magnitude of the drought (Kogan et al. 2013; Kogan and Guo 2016). Hence, the multi-temporal investigation of eMODIS (NDVI) supported by TCI and VCI can notably correct the early warning systems and drought monitoring. (Barbosa, Huete, and Baethgen 2006)suggested that the NDVI can be calculated based on the band red, which has NIR high reflectance and reflectance is low value for portions of the wavelength. mainly, in non-drought times, vigorous and green vegetation reflects very little light in the visible spectrum due to large absorption by chlorophyll in the light and more reflection in the NIR (near-infrared) part due to the precision of scattering light by water content and internal leaf. In this study, the healthy vegetation (VI) greatly absorbed the red (visible incident solar) and it reflects less amount of solar radiation in the VS (visible spectrum). Hence, the unhealthy vegetation highly reflects the NIR (near-infrared light). Consequently, dense and healthy vegetation has a high normalized difference vegetation index value generally > 0.5 than the unhealthy. The eMODIS NDVI data is better to calculate the chlorophyll density confined in vegetative cover (Frey, Kuenzer, and Dech 2012). (Kogan and Guo 2016) suggest that normalized difference vegetation index data helps to calculate the Vegetation health index (VCI) development reflects both precipitation and temperature conditions. The NDVI was statistically computed as follows equation (47):

$$NDVI = (NIR - RED)/(NIR + RED) \qquad 47)$$

Where RED=visible red reflectance and NIR=near-infrared reflectance. In this research, the row eMODIS NDVI data were rescaled, processed, and analyzed in ArcGIS 10.8 and 10.4.1 package to find the real normalized difference vegetation index value of the research area as following equation (Eq. 48):

E -MODIS NDVI = Float (Smoothed e-MODIS NDVI – 100) / 100 $\qquad$ 48)

The value of NDVI (e-MODIS) ranges from −1.0 to + 1.0. The unit of NDVI is the NDVI ratio. The NDVI negative ratio indicates less unhealthy or vigorous vegetation cover majorly appeared in a rock outcrop (barren rock), and sand, and positive NDVI values indicate healthy vegetation. NDVI values are high indicating dense and healthy vegetation than Water, bare soil, and rocks (Kogan 1995). Comparable, grasslands, and shrubs/bushes are sparse vegetation cover may result in NDVI values moderate between 0.2 to 0.5. Higher NDVI values between 0.6–0.9 indicated dense health vegetation in the tropical and temperate crops or forests at their peak high growth stage. The NDVI data were utilized as a component to calculate the VCI (vegetation condition index) only

5.2.2 Vegetation Condition Index (VCI)

Different drought indexes have been advanced for monitoring the drought event's characteristics such as duration, intensity, spatial extent, and severity (Mishra and Singh 2011). The vegetation condition index which is calculated from remote sensing satellite data has been used with vegetation cover and state. The indices are applicable for monitoring the response of vegetation and vegetation stress. The VCI allows not only the explanation of vegetation but also and calculation of temporal and spatial weather impacts on vegetation and vegetation changes (Kogan 1990). In this research, the smoothed 16 days NDVI data was used as a parameter, to compute the vegetation condition index model. The VCI was applied to calculate the agricultural drought events status of the research area as following Equation 3:

$$VCI = 100 \times (NDVI_i - NDVI_{min})/(NDVI_{max} - NDVI_{min}) \qquad 49)$$

146

Where NDVI=the smoothed value of I [the] month, NDVI max and NDVI min are from (2015– 2019) absolute maximum and minimum value (NDVI) for different pixels at a specific period. The VCI value is measured in % between 0 - 100. A big value of VCI indicates unstressed vegetation and healthy condition, this region is free from agricultural drought events. The value of VCI 50–100 shows above wet or normal conditions. This indicates that there are no events of drought, then between 35 - 50 % indicates the area under the moderate drought (MD) condition and VCI between 20 - 35 % indicates severe drought (SD) events. Moreover, the annual and seasonal VCI values of 0 to 20 % are showing very severe drought events (SD). Hence, the combination of both TCI and VCI calculate from MOD11A2 (LST and NDVI) Terra data are to calculate agricultural droughts.

5.3 Temperature Condition Index (TCI)

5.3.1 Land Surface Temperature (LST)

Land Surface Temperature expresses the radiative temperature of the land obtained from solar radiation. The MOD11A2 LST and emissivity measure the temperature of the earth's surface. These assess soil moisture, vegetation health status, and the impact of thermal (Parviz 2016; Karnieli et al. 2010). In this research, the MOD11A2 Terra 16 days LST data was acquired at a 1-kilometer spatial resolution get in HDF–EOS Format (Hierarchical Data–Earth Observing System). Hence, the MODIS Tool Re-projection (MRT) v 4.1 evolves in 2011 March to resample the 1 km resolution LST MOD11A2 data in 250 m resolution jointly with the NDVI data. The MRT (Re-projection) is also used to turn the HDF (Hierarchical Data Format) into a Geo-TIFF format to conduct interpretations and better analysis of the MOD11A2 (LST) and NDVI (eMODIS). In this research, the land surface temperature data were rescaled and then converted into °C degree Celsius units as following equation

$$LST = (\varpi \times 0.02) - 273.15 \hspace{3cm} 50)$$

Where LST-Land Surface Temperature (Degree Celsius), ϖ= SDS (Row Scientific data). The temperature condition index accepts that higher temperature has a movement to cause failure or drought during the growth period of vegetation; while temperatures are low it is The TCI was evaluated using the following expression:

$$TCI = 100 \times (LST_{max} - LST_i)/(LST_{max} - LST_{min}) \qquad \text{51)}$$

Where LST$_i$=LST value of ith-month, LST min, and LST max are the smoothed several-year minimum and maximum LST.

5.3.2 Vegetation Health Index (VHI)

Rhee et al. (2010) noticed that the newly developed drought indices like NDWI, NMDI, and NDDI did not execute better than the normalized difference vegetation index (NDVI) with a 1-kilometer resolution in the semi-arid area. The Research indicates NDVI only is not able to depict non-drought or drought conditions. The Vegetation Health Index model has existed in robust Agricultural monitoring drought indices and it has the efficiency to inspect the temporal and spatial scale of agricultural extreme and severity drought period. In the semi-arid area, VHI was exceptionally correlated to the situ variables (Mishra and Singh 2011), suggesting that the Vegetation Health Index (VHI) combination of VCI and TCI is main to specify the spatial-temporal extent, the severity, and the magnitude of agricultural droughts in a fine agreement with rainfall patterns. The vegetation stress caused due to wetness and the dry situation was assessed to investigate the agricultural drought severity in the research area. Both the TCI and VCI index specified an equal weight due to the temperature and moisture contribution during the period of vegetative growth (Kogan 2001). The lack of more correct information on the effect of TCI and VCI on the VHI in the Kolar and Chikkaballapura districts, the coefficient of the vegetation health index was fixed at 0.5. The vegetation health index was mathematically calculated as the following equation:

$$VHI = a \times VCI + (1 - a) \times TCI \qquad \text{52)}$$

Where VHI (Vegetation Health Index), a = 0.5 (TCI and VCI), VCI (Vegetation Condition Index), TCI (Temperature Condition Index).

148

Table 5. The Severity of Agricultural Drought by VHI (Source: Kogan 2001)

Severity level	VHI values
Extreme drought	<10
Severe drought	<20
Moderate drought	<30
Mild drought	<40
No drought	>50

5.3.3. Drought Period Assessment Using Satellite-Based Vegetation Health Index (VHI).

The satellite data-based VHI data product can be used to monitor thermal conditions, moisture stress conditions, vegetation health conditions, and regional drought. The time, duration, affected region, and drought intensity can be computed based on various ranges of VHI values. The ranges of VHI including TCI, VCI, and VHI started from extreme stress (0) to the most favorable condition (100), with normal drought conditions ranging from 25–40 corresponding to the mean cumulative moisture content, vegetation health conditions, and temperature. Higher ranges of values showed better moisture area, vegetation condition, or thermal. For Example, VCI < TCI 50 indicates moisture conditions favorable for the crop. A decrease in VHI value from 35 to 0 indicates sufficient vegetation stress and for VHI from 50 to 100 and vice versa, the value of the drought conditions in VHI was shown in Table 5.

5.4 Results and Discussion

5.4.1 Agricultural Drought Assessment

Figure 9 indicates the multi-temporal sequence of NDVI- LST, TCI-VCI, and rainfall— VHI for the period 2015 to 2019. The low-land region of districts reveals that the average NDVI was between 0.27 and 0.31 and this scattered value of NDVI is extremely low when it is calculated by mathematically accepted threshold values, while the Land Surface Temperature was very high and it is between 37.4 and 42.91 °C. Therefore, the value of low NDVI is reached at very

149

high LST ranges because the thick vegetation is under very high water stress assets.

The west and south areas of the study areas showed relatively better NDVI ranges between 0.39 and 0.58 was indicated, although the Land Surface Temperature (LST) was between 31.3 and 35. 79 °C. In this region, the LST ranges were comparatively less than the low-land region expresses but it is quite an unfavorable situation for the thick vegetation and very high moisture water stress. In the high region, well coverage NDVI ranges between 0.52 and 0.59 were indicated. Other than that, very low LST between 21.3 and 23.9 °C was shown in the same region. Very High LST directs the vegetation growing time may happen vegetation stress. Thus, the gradual increase in surface temperature (ST) may influence vegetation evaluation (Karnieli et al. 2006). Singh et al. (2003) describe that NDVI is the most important tool for monitoring vegetation cover and growth of vegetation analysis. Especially, this research indicated that NDVI presented during the major rainy season declined by 5–9 % in all regions of both districts. Yet the LST has increased by 0.49–1.16 °C.

Overall agro regions as well as both districts in the last 6 years. The increase in land surface temperature and the decrease in NDVI provide extensive moisture stress that can cause the occurrence of agricultural drought. The results indicate that the vegetation stress was caused due to rising surface temperature (ST). In the low area, the ranges of Vegetation Condition Index were between 39.12 and 43.13, So the TCI was high between 36.18 and 38.12. In the middle area of the district, the value ranges of VCI were 49.76 and 63.18, although TCI was 48.59–62.3. In the high area, the VCI ranged values between 58.91 and 65.13, and then TCI was 63.113–65.85. Furthermore, VHI and precipitation value was diminished in the main rainy season.

This showed that the occurrence of agricultural drought enhances more severe and frequent because of the sensitivity to soil moisture, especially in the low region, and several parts of the high and midland area were affected seriously. For example, the VHI of the low area was between 34.39 and 41.53, although the precipitation was about 345.41–467.89. The station-wise seasonal

150

drought mean to value and total area of square Kilometre in the Pre-monsoon season from 2015-2019 showed in Tables 5.1and 5.2.

4.2 Temporal and Spatial variation of vegetation growth, based on VHI.

To reveal the temporal and spatial difference in the vegetation growth process in past decades, the Geographical area's average values of the TCI, VCI, and VHI throughout the growing season were researched for each grid station between 2015 and 2019 in Kolar and Chikkaballapura districts. As represented in Figures 9,9.1, and 9.2. the average values of VCI throughout the growing period for each grid station were between 33 and 59 in the pre-monsoon season (Figure 10), in contrast with the Temperature condition Index within the ranges of 26–79 and the Vegetation health index from 45 to 84 (Figure 9.2), respectively. The different VHIs and different stations with the maximum (83) and minimum (3) values in VCI were found (Figure 9.2), and the Vegetation health index (VHI) had a relatively small variation in value in pre-monsoon (Figure 10).

Spatially, the study results showed that 65% of the Kolar and Chikkaballapura regions had a positive value for VCI, and the remaining 35% was negative based on the TCI and 63 % for VHI. Indicating that the vegetation had increased in the majority of the study area for both VHI and VCI. Hence the regions with increasing vegetation stress based on the VHI were wider than that of VCI.

This was evident in big semi-arid districts such as Kolar and Chikkaballapura districts. Comparable with that of VCI showed that the area might sustain more water moisture stress for seasonal vegetation growth. In the case of the Temperature Condition Index, the decreasing value detected in the north-eastern part of both districts suffered from moisture conditions for vegetation growth, especially in semi-arid regions. Most of the northern part of the study region showed increasing temperature based on TCI and VCI in Pre monsoonal season, showing that the southwest part of the area province might happen to less thermal stress.

Drought is a natural hazard with far-reaching effects including economic losses, and soil damages, and threatens the health of residents and livelihood. The present research aimed to observe the vegetation health index across the semi-arid regions of Karnataka state in 2015-2019 using GIS and remote sensing techniques. Landsat-8 dataset images, with a 30 m spatial resolution and from various platforms were used to recognize the Vegetation Condition Index (VCI) and Temperature Condition Index (TCI). The VCI is dependent on the NDVI (Normalized Difference Vegetation Index) datasets. The Temperature Condition Index used LST (land surface temperature datasets). As an outcome, the Vegetation Health Index (VHI) was generated and classified into 5 categories of drought: no drought, mild, moderate, severe, and extreme drought. The results indicate that the highest % of the extreme agricultural drought found in Chinthamani taluk is about 740.20 squares Km (20%) area. In the S-W monsoon showed Bagepalli is about 397.70 squares Km (18%), and Sidhlaghatta taluk is 26 % (338.55 squares Km). In the North-east Monsoon extreme drought severity was affected in Malur at 22% (704.05 squares Km), Mulubhagilu at 26 % (909.99 squares Km), and Bangarapete at 21% (879.64 sq. km) of the area have severely affected the agriculture and vegetation from 2015-2019 respectively. Severe to moderate drought occurred in the north–east part of both areas of Kolar and Chikkaballapura districts. 2016 and 2017 experienced a less level of drought % compared to the other study years using the CDI.
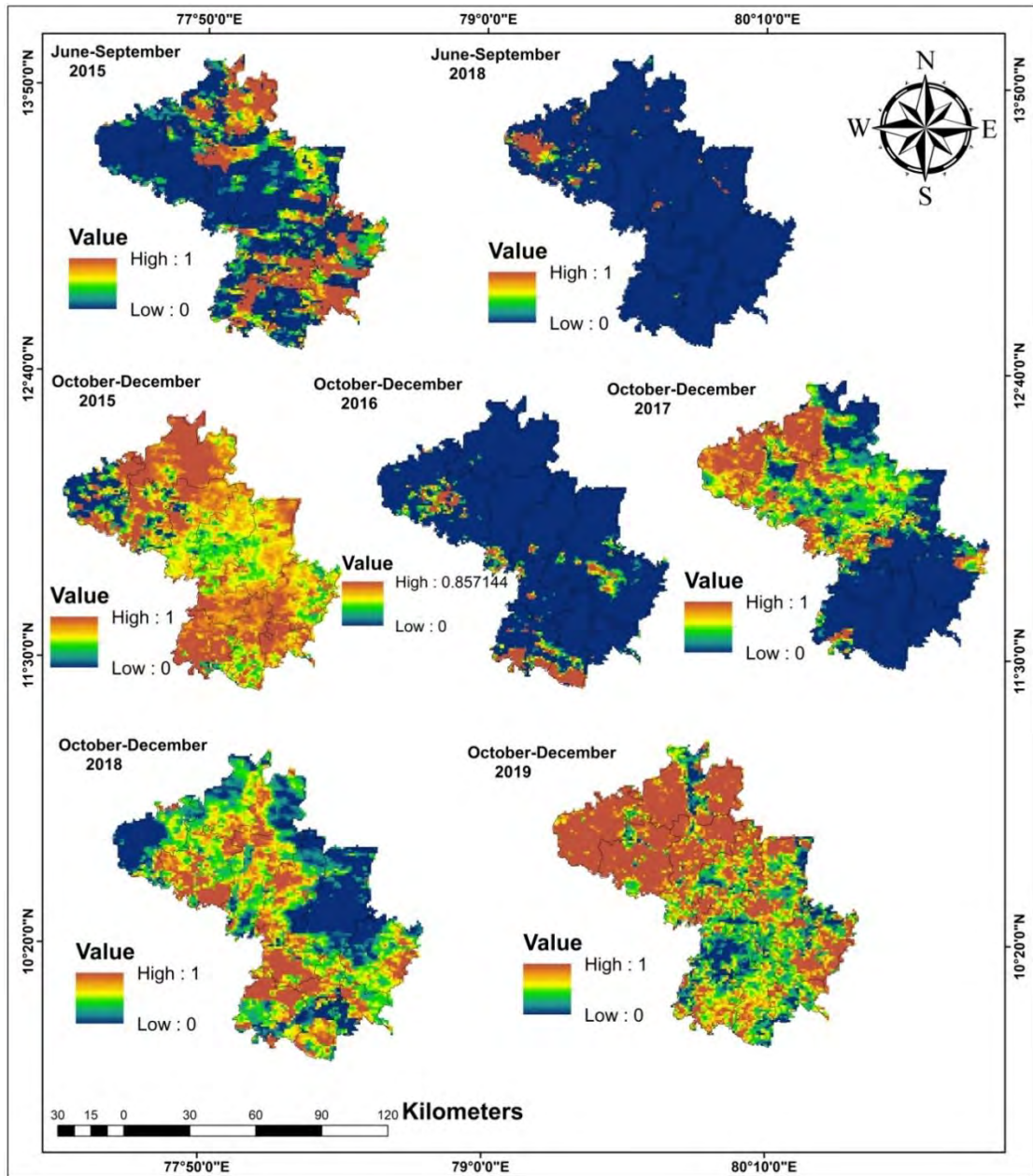
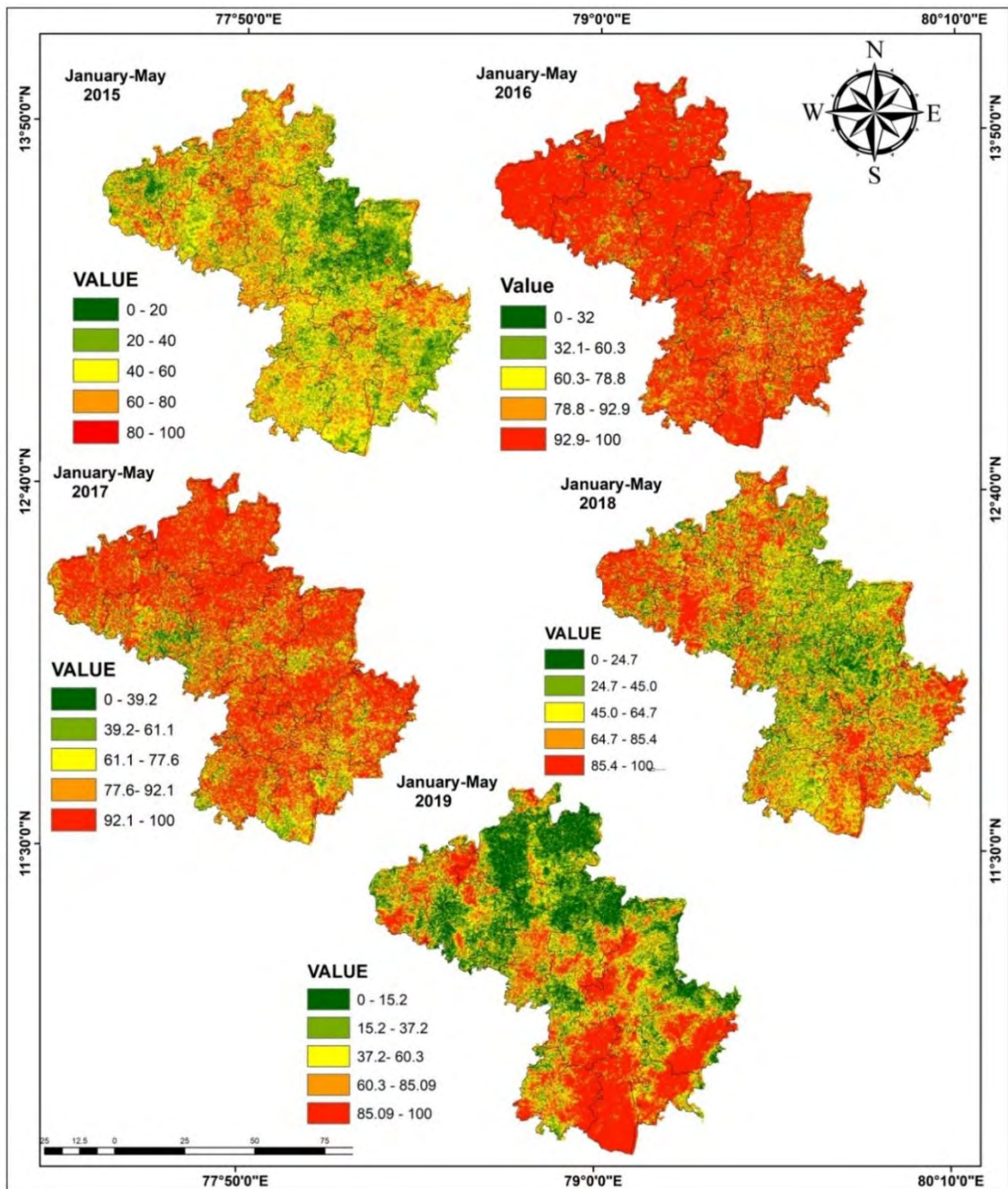**Figure 9.** TCI in S-W and N-E Monsoonal Period

Figure 9.1 VCI in Pre Monsoonal Period
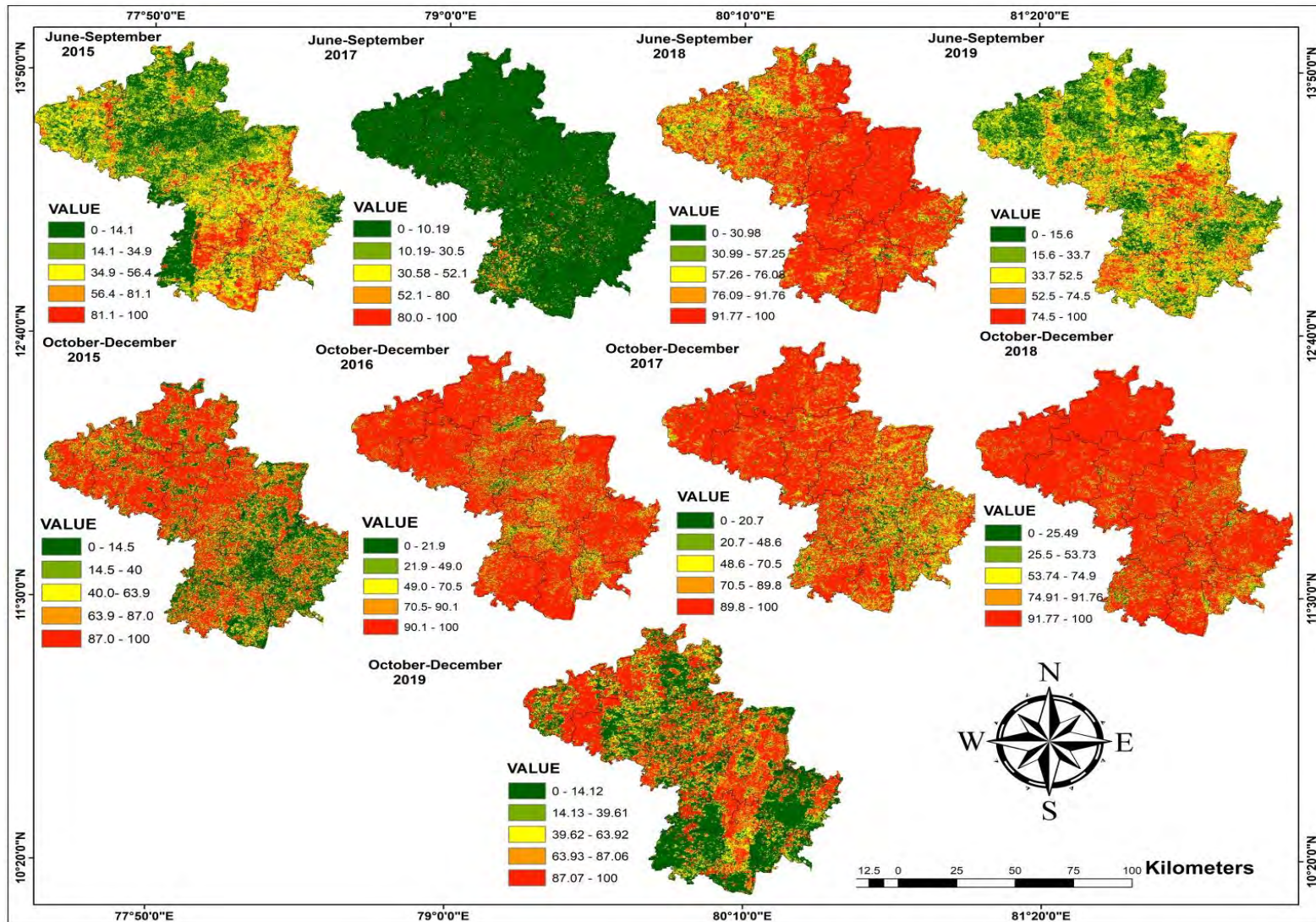
Figure 9.2 VCI Spatial Patterns in the South-West and North-East Monsoonal Period

155
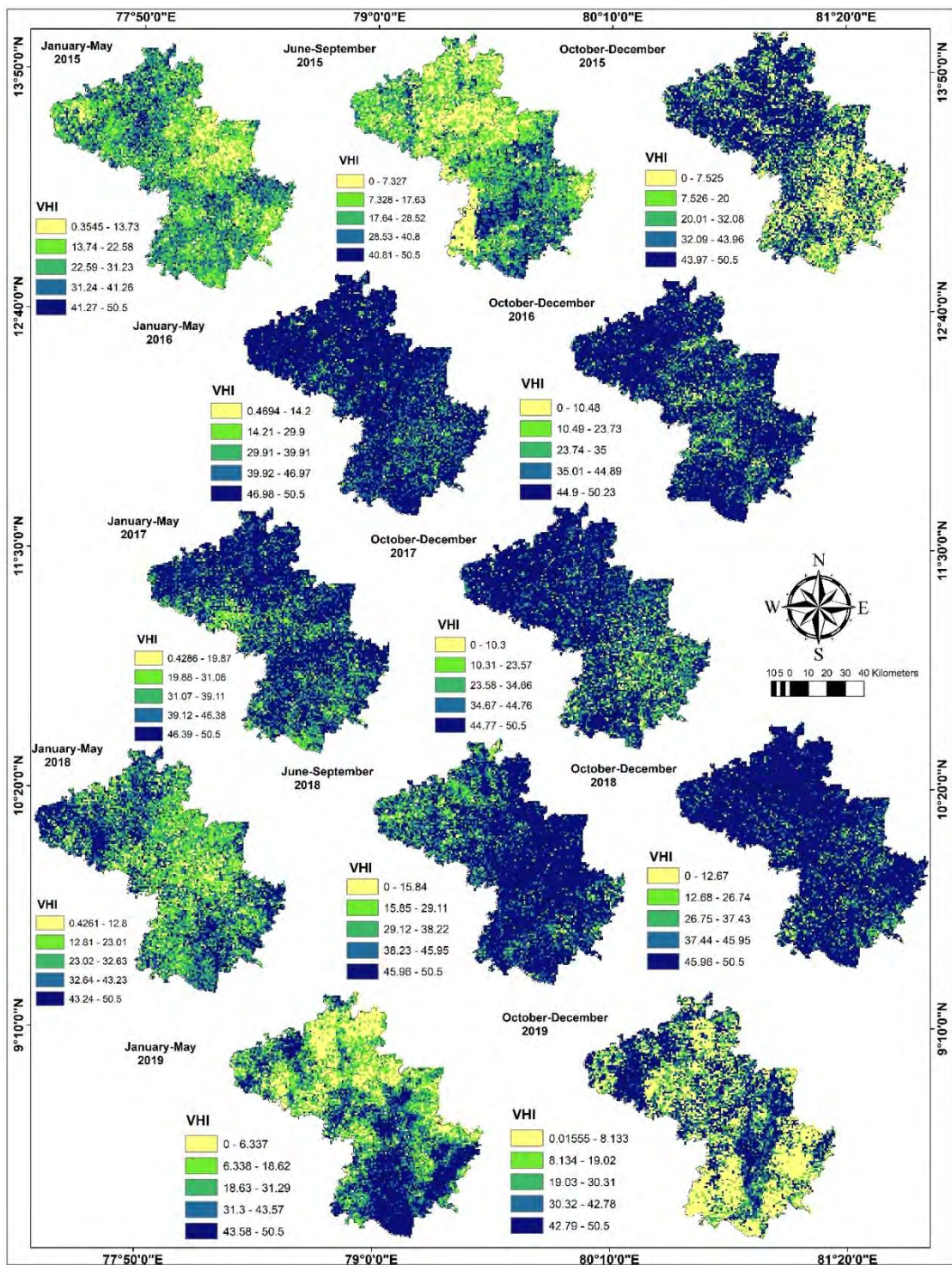
Figure 10. VHI Spatial Pattern Pre, South-West, and North-East Monsoonal
Period

The percentage of area changes showed vegetation stress is VHI < 40, normal vegetation health condition 40 < VHI< 60, and favorable vegetation condition > 60 were further researched, as shown in Figure 4. Again, the % of the area with vegetation stress VHI < 40 decreased from 2015 to 2019, and at the same time, the % of the area with normal vegetation conditions and favorable vegetation conditions increased from 2015 to 2019.

Overall, the study indicated that the Average values of % of the area affected by extreme drought in Bagepalli grid station were 14 % affected area as flowed by Chintamani station was affected with the highest percentage in the Pre-monsoon season about 17 % of the area Srinivasapura also affected 15 % Gudibande effected 10 % so the overall station was affected the extreme condition of the drought showed in Figure 10. For the S-w monsoon season, the Shidlaghatta area suffered 26% of the Extreme drought Condition; Malur station recorded 22 % of the ED, and Gudibande, Bagepalli, and Chikkaballapura top in terms of drought % duration lasting 22.14%, 22.85%, and 22.64% respectively. Srinivasapura and Kolar hold 5 % and 6% of the agricultural drought respectively in the least position all the stations show a drought % in Figures 11, 11.1, and 11.2.

The occurrence of VHI drought in the northeast monsoon is relatively lowered than in the southwest monsoon season. Mulubhagilu dealt with 5 years amounting to 23.17% of VHI Extreme drought duration whereas 2015 to 2019. The lowest ED was happened in Gudibande station with 3 %. Gauribidanur and Malur stations have 25 % of values and a drought duration of 50.72% Overall the stations in the study area witnessed drought in the whole study period shown in Figure 11.3.

We see that the vegetative drought Index assessment in terms of TCI and VCI shows different results over some stations of Kolar and Chikkaballapura. hence, useful to apply such an index for drought which takes into cause both the TCI and VCI i.e., surface moisture as well as thermal stress of vegetation. This is completed utilizing the VHI for drought monitoring. In Figure 8 we show the Vegetation health index for the total area affected in different grid station in square kilometers in the pre-monsoon season the Srinivasapura and Chintamani

157

taluks was affected by more than 300 square Kilometre in the Extreme drought Category. Severe drought in the Bangarapete and Gauribidanur suffered 200 square Kilometres affected in the severe drought category and different stations indicate the affected area in square Kilometre in Figure 8.

In the same area, mild to moderate severity of the drought was also indicated in the rest of the areas. Moreover, the outcome of the VHI as a drought severity detection index depends on the acceptance that LST and NDVI at a given pixel value in satellite images will differ inversely over the period, with variations in TCI and VCI operating by local surface moisture conditions. This research also exhibited that the occurrence of the agricultural drought was due to a deficit of Precipitation leading to a peak level of surface moisture stress caused by the drought conditions.

Table 5.1 Drought in Pre-monsoon season from 2015-2019

| Grid Stations | Drought Category in Area of square Km in Pre-Monsoon | | | | | Mean rainfall inmm |
	Extreme	Severe	Moderate	Mild	No drought	
Bagepalli	633.21	605.41	664.49	639.05	2003.57	79.7
Bangarapete	106.83	477.97	818.26	717.27	2164.07	119.5
Chikkaballapur	331.23	535.08	568.39	530.94	1194.58	106.0
Gauribidanur	369.44	564.07	631.91	621.59	2155.49	109.0
Gudibande	123.97	150.90	146.12	141.80	565.06	80.0
Kolar	225.12	553.53	777.73	720.57	1661.06	117.3
Malur	129.30	416.68	732.76	634.30	1199.70	151.9
Mulabhagilu	314.08	581.11	740.94	703.11	1693.17	130.9
Shidlaghatta	305.67	526.49	606.26	531.83	1332.63	97.8
Srinivaspura	606.69	863.13	705.80	581.34	1497.69	118.4
Chinthamani	740.20	985.54	696.35	450.76	1555.57	115.5
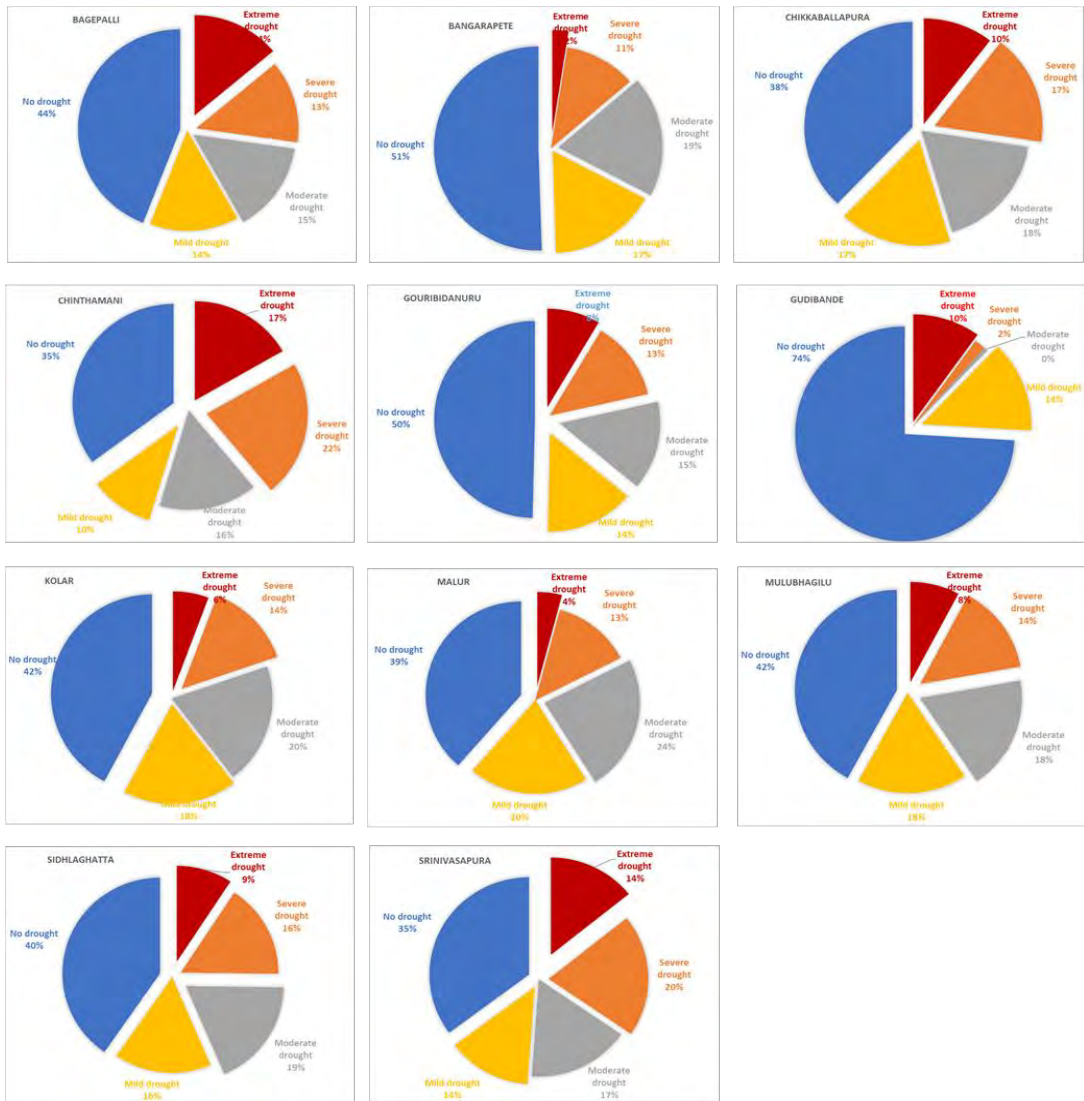
Figure 11. Agricultural Drought Areas to km2 in Pre-Monsoon Period
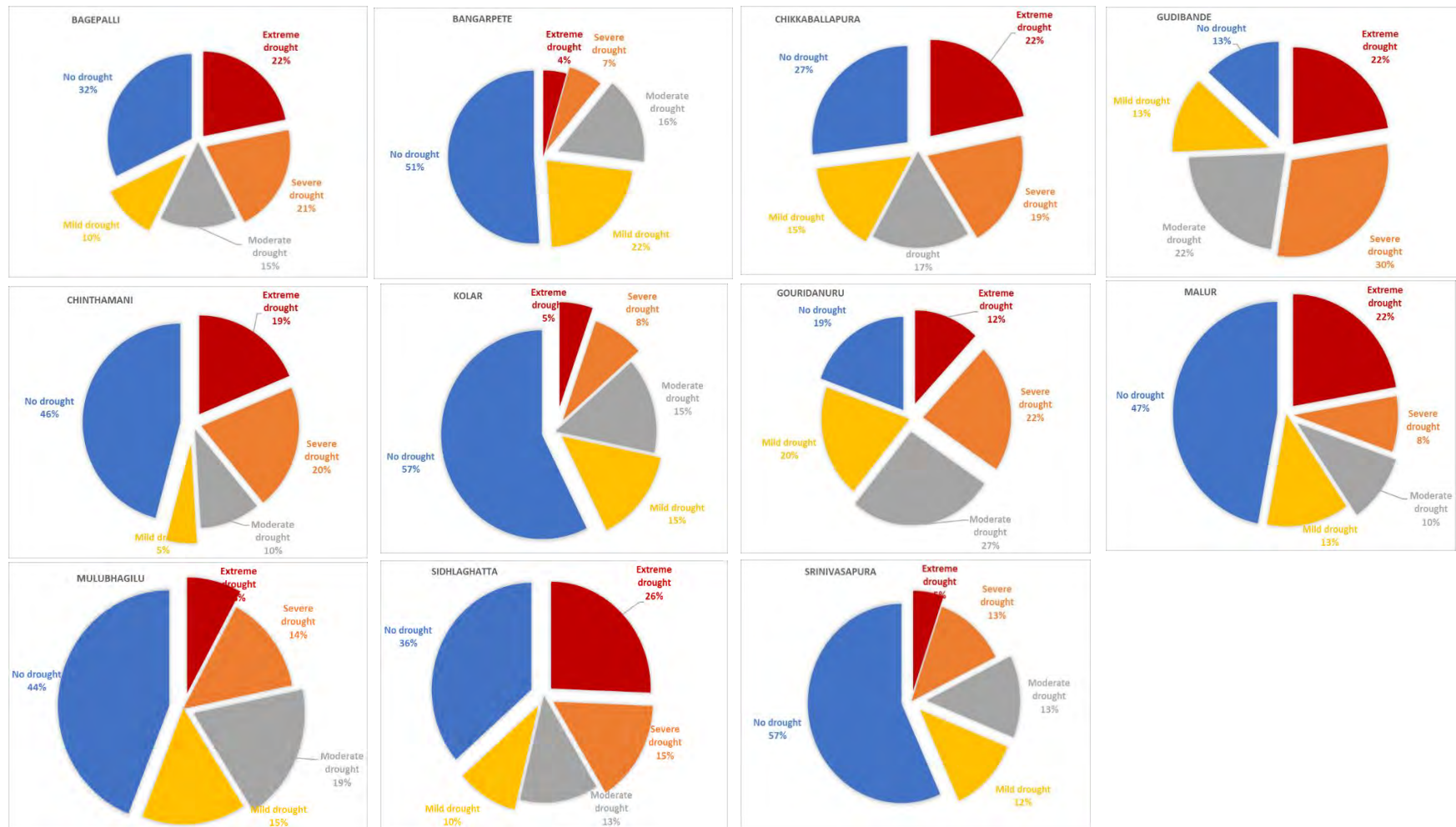
Figure 11.1 Agricultural Drought Areas to km2 in SW-Monsoon Period

160
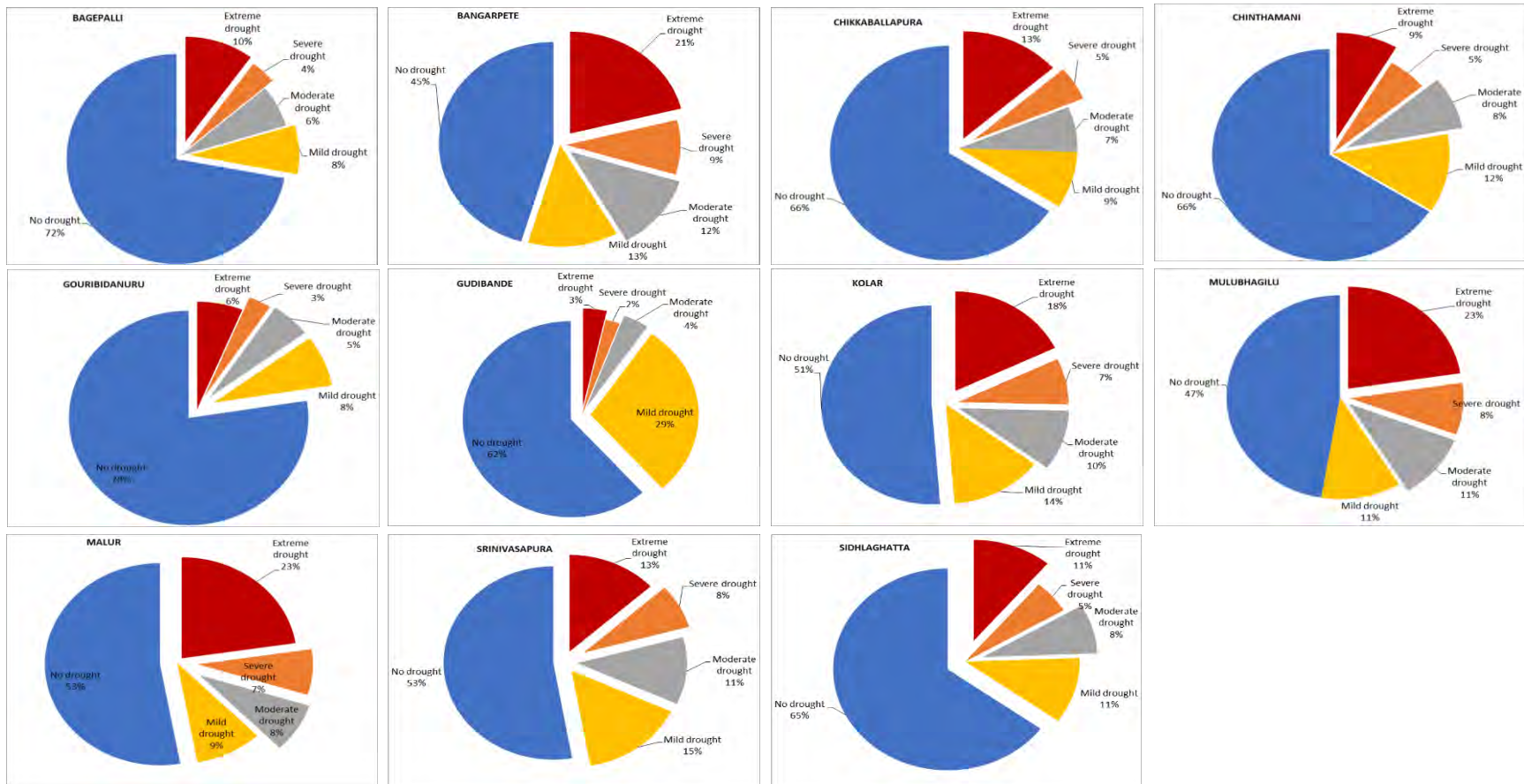
Figure 11.2 Agricultural Drought Areas to km2 in NE-Monsoon Period
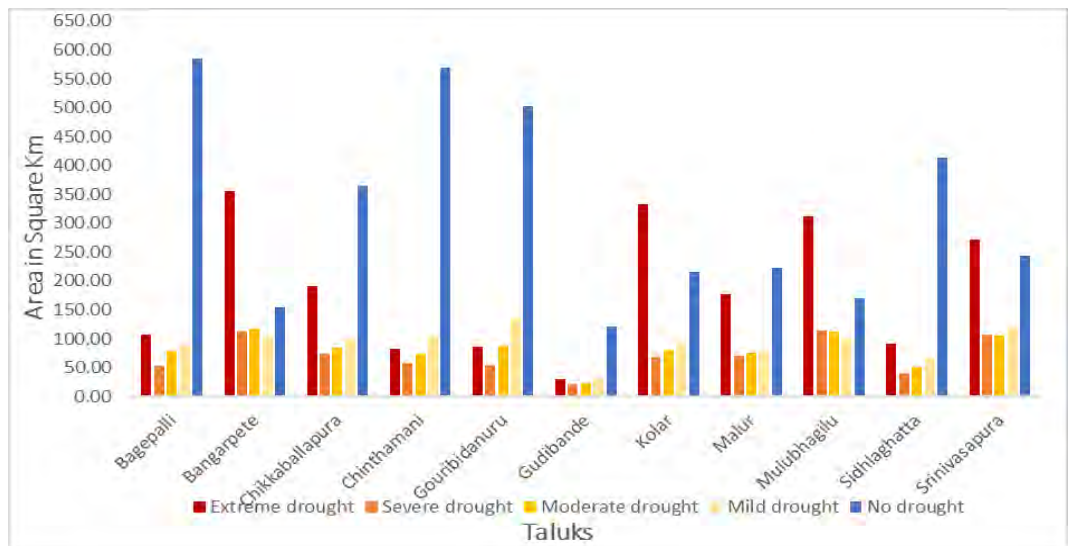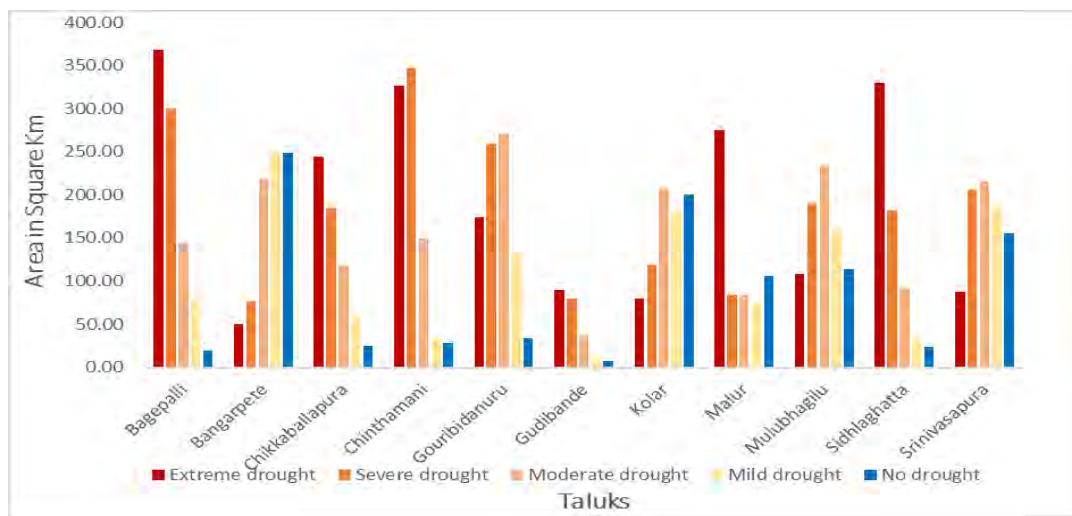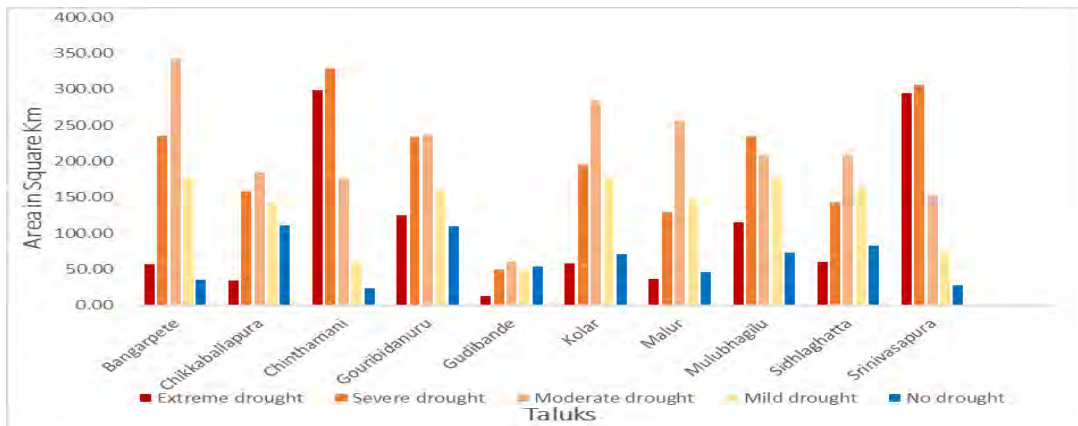
Figure 11.3 Agricultural Drought Areas in Square Kilometres According to the Severity

162

Table 5.2 Drought in S-W and N-E monsoon season from 2015-2019

Grid Stations	Drought Category in Area of square Km in S-W Monsoon					Mean rainfall inmm
	Extreme	Severe	Moderate	Mild	No drought	
Bagepalli	397.70	375.53	270.11	189.91	587.17	546.3
Bangarapete	73.61	108.54	272.55	370.80	859.08	694.9
Chikkaballapura	273.63	247.31	210.25	190.81	341.48	650.1
Gauribidanur	209.27	388.38	463.10	339.74	338.92	840.1
Gudibande	99.77	134.19	97.91	56.75	58.01	564.6
Kolar	83.62	128.93	233.08	227.00	903.35	735.5
Malur	278.22	100.21	124.95	158.32	587.36	756.5
Mulabhagilu	127.87	222.55	309.82	242.52	710.03	785.2
Shidlaghatta	338.55	205.54	167.27	129.72	480.12	649.2
Srinivaspura	89.16	211.38	226.86	206.99	964.68	712.4
Chinthamani	330.55	361.08	176.07	89.67	812.47	744.2

Grid Stations	Drought Category in Area of square Km in N-E Monsoon					Mean rainfall inmm
	Extreme	Severe	Moderate	Mild	No drought	
Bagepalli	460.14	172.88	292.46	342.84	3275.63	173.79
Bangarapete	879.64	361.94	505.70	531.76	1899.63	212.3
Chikkaballapura	451.57	171.28	227.55	285.32	2196.78	175.25
Gauribidanur	267.65	133.45	238.98	334.07	3369.76	205.05
Gudibande	31.94	19.39	34.88	260.85	555.65	165.1
Kolar	704.60	296.54	387.46	534.53	2020.10	210.9
Malur	704.05	227.74	245.18	293.00	1645.96	219.10
Mulabhagilu	909.99	332.48	421.82	459.57	1907.58	261.1
Shidlaghatta	367.58	177.40	261.61	348.69	2147.78	191.6
Srinivaspura	562.10	315.73	478.60	650.25	2240.44	215.9
Chinthamani	374.79	241.99	356.82	530.89	2921.74	238.2

5.5 Conclusion

GIS and remote sensing-based agricultural drought can be improved and monitored by the Vegetation Health Index composed of TCI and VCI agricultural drought indices. This Research showed the duration, severity, and spatial extent of agricultural drought areas using TCI, NDVI, VCI, and VHI at different grid stations in both districts during the Pre, Southwest, and Northeast monsoon season. The Vegetation Health Index model indicate that the year 2019 and 2015 was extremely drought (ED) period whole the study area where the average VHI value range was less than 10. Our outcome in this research provides the evaluation of regional growth of vegetation activity and drought time and area estimation, which shall be useful for vegetation growth productivity management, Drought prevention, and detection to help agriculture assessment for decision-makers and farmers. Especially, the yearly drought model income showed the drought severity status at the different spatial resolutions, which is considered by drought management decision-makers and former at regional levels. If all spatial maps can be evaluated by the local communities, these maps also help estimate land conditions. Drought severity like extreme stress, moderate stress, and severe stress, near normal, poor vegetation, good vegetation, fair healthy vegetation, very good healthy vegetation, and excellent healthy vegetation was appraised in terms of % area coverage.

This study reveals that the effect of agricultural drought could be lessened by requiring smallholder farmers to a range of on-farm practices. The research may also contribute implementation and formulation of drought mitigation and coping programs in the Kolar and Chikkaballapura Districts.

5.6 References

1. Barbosa, H., Huete, A., & Baethgen, W. (2006). A 20-year study of NDVI variability over the Northeast Region of Brazil. *Journal of Arid Environments*, *67*, 288–307. https://doi.org/10.1016/j.jaridenv.2006.02.022

2. Bhuiyan, C., Singh, R. P., & Kogan, F. N. (2006). Monitoring drought dynamics in the Aravalli region (India) using different indices based on ground and remote sensing data, *8*, 289–302. https://doi.org/10.1016/j.jag.2006.03.002

3. Choi, M., Jacobs, J., Anderson, M., & Bosch, D. (2013). Evaluation of drought indices via remotely sensed data with hydrological variables. *Journal of Hydrology*, *476*, 265–273. https://doi.org/10.1016/j.jhydrol.2012.10.042

4. Frey, C. M., Kuenzer, C., & Dech, S. (2012). Quantitative comparison of the operational NOAA-AVHRR LST product of DLR and the MODIS LST product V005. *International Journal of Remote Sensing*, *33*(22), 7165–7183. https://doi.org/10.1080/01431161.2012.699693

5. Gidey, E., Dikinya, O., Sebego, R., Segosebe, E., & Zenebe, A. (2018). Analysis of the long - term agricultural drought onset , cessation , duration , frequency , severity and spatial extent using Vegetation Health Index (VHI) in Raya and its environs , Northern Ethiopia. *Environmental Systems Research*. https://doi.org/10.1186/s40068-018-0115-z

6. Gu, Y., Brown, J. F., Verdin, J. P., & Wardlow, B. (2007). A five-year analysis of MODIS NDVI and NDWI for grassland drought assessment over the central Great Plains of the United States, *34*, 1–6. https://doi.org/10.1029/2006GL029127

7. Harishnaika, N., Ahmed, S. A., Kumar, S., & Arpitha, M. (2022). Remote Sensing Applications : Society and Environment Computation of the spatio-temporal extent of rainfall and long-term meteorological drought assessment using standardized precipitation index over Kolar and Chikkaballapura districts , Karnataka during 1951-2019. *Remote Sensing Applications: Society and Environment*, *27*(January), 100768. https://doi.org/10.1016/j.rsase.2022.100768

8. He, X., Yan, J., Huang, A., Zhou, H., Wu, Y., Yang, L., & Paudel, B. (2021). *Households' Climate Change Adaptation Strategies for Agriculture on the Eastern Tibetan Plateau*. https://doi.org/10.21203/rs.3.rs-607815/v1

9. Hoolst, R. Van, Eerens, H., Haesen, D., Royer, A., Bydekerke, L., Rojas, O., et al. (2016). FAO's AVHRR-based Agricultural Stress Index System (ASIS) for global drought monitoring. *International Journal of Remote Sensing*, *37*(2), 418–439. https://doi.org/10.1080/01431161.2015.1126378

10. Kogan, F., Adamenko, T., & Guo, W. (2013). Global and regional drought dynamics in the climate warming era. *Remote Sensing Letters*, *4*(4), 364–372. https://doi.org/10.1080/2150704X.2012.736033

11. Kogan, F., & Guo, W. (2016). Early twenty-first-century droughts during the warmest climate. *Geomatics, Natural Hazards and Risk*, *7*(1), 127–137. https://doi.org/10.1080/19475705.2013.878399

12. KOGAN, F. N. (1990). Remote sensing of weather impacts on vegetation in non-homogeneous areas. *International Journal of Remote Sensing*, *11*(8), 1405–1419. https://doi.org/10.1080/01431169008955102

13. Komuscu, A. U. (2001). Using the SPI to Analyze Spatial and Temporal Patterns of Drought in Turkey, (February 1999).

14. Maybank, J., Bonsai, B., Jones, K., Lawford, R., O'Brien, E. G., Ripley, E. A., & Wheaton, E. (1995). Drought as a natural disaster. *Atmosphere-Ocean*, *33*(2), 195–222. https://doi.org/10.1080/07055900.1995.9649532

15. Mishra, A. K., & Singh, V. P. (2011). Drought modeling – A review. *Journal of Hydrology*, *403*(1–2), 157–175. https://doi.org/10.1016/j.jhydrol.2011.03.049

16. Owrangi, A., Adamowski, J., Rahnemaei, M., Mohammadzadeh, A., & Sharifan, A. (2011). Drought monitoring methodology based on AVHRR images and SPOT vegetation maps. *Journal of Water Resource and Protection*, *335041*, 325–334. https://doi.org/10.4236/jwarp.2011.35041

17. Peters, A. J., Walter-Shea, E. A., Ji, L., Viña, A., Hayes, M. J., & Svoboda, M. D. (2002). Drought Monitoring with NDVI-Based Standardized Vegetation Index. *Photogrammetric Engineering and Remote Sensing*, *68*, 71–75.

18. Rhee, J., Im, J., & Carbone, G. J. (2010). Monitoring agricultural drought for arid and humid regions using multi-sensor remote sensing data. *Remote Sensing of Environment*, *114*(12), 2875–2887. https://doi.org/https://doi.org/10.1016/j.rse.2010.07.005

19. Sruthi, S., & Aslam, M. A. M. (2015). Agricultural Drought Analysis Using the NDVI and Land Surface Temperature Data; a Case Study of Raichur District. *Aquatic Procedia*, *4*, 1258–1264. https://doi.org/https://doi.org/10.1016/j.aqpro.2015.02.164

20. Vicente-serrano, S. M., Beguería, S., Gimeno, L., Eklundh, L., Giuliani, G., Weston, D., et al. (2012). Challenges for drought mitigation in Africa : The potential use of geospatial data and drought information systems. *Applied Geography*, *34*, 471–486. https://doi.org/10.1016/j.apgeog.2012.02.001

21. Zhang, A., Jia, G., & Wang, H. (n.d.). Improving meteorological drought monitoring capability over tropical and subtropical water- limited ecosystems : evaluation and ensemble of the Microwave Integrated Drought Index Improving meteorological drought monitoring capability over tropical and subtropical water-limited ecosystems : evaluation and ensemble of the Microwave Integrated Drought Index.

22. Zhang, L., Yao, Y., Bei, X., Jia, K., Zhang, X., Xie, X., et al. (2019). Assessing the Remotely Sensed Evaporative Drought Index for Drought Monitoring over Northeast China. *Remote Sensing*, *11*(17).

CHAPTER -6

LONG-TERM RAINFALL FORECASTING AND PREDICTION USING ADVANCED MACHINE LEARNING MODELS

Chapter -6

Linear Multiple Regression Model for Long-Term Rainfall Forecasting

6. Introduction

Weather forecasting is the most crucial use of meteorology and one of the most difficult global scientific topics(Liyew and Melese 2021). The primary focus of weather forecasting is predicting the weather for a specific period. Environment, Climate observation, drought detection, agricultural and production, aviation industry planning, communication, pollution dispersion, and many other things are the key goals of weather prediction(Gowtham, Ganesh, and Ali 2021). There is a significant time in history when weather conditions affected military operations and changed the outcome of battles. The effort of accurately predicting weather conditions is challenging since the weather is a non-linear and dynamic process, meaning that it changes. Even from minute to minute, from day to day(Gandhi et al. 2015). Knowing past weather conditions over a wide area and for a long time is necessary for a prediction to be accurate. The forecasting department offers crucial information regarding the upcoming weather(Gobierno de Colombia 2017). There are numerous methods for predicting the weather, ranging from exceedingly easy highly intricate computational mathematical models to sky observation(Yashasathreya 2021).

6.1 Methods

6.1.1 Linear Multiple Regression Modelling (LMR)

The LMR is a method of linear statistical modeling that seeks the strongest connection between a measure (Year Precipitation) and several other variables (climate indices). The following equation can be used to define the general formula for LMR models. The size of the meteorological station's data set was appropriate for this study's use of multivariate linear regression, a machine learning approach that can estimate the area's daily rainfall totals. This technique can demonstrate the degree to which each environmental factor affects the daily rainfall intensity(Karama 2021)

Any established model considers evaluation to be a crucial component in deciding whether the project is worthwhile in terms of producing the desired results. It is generally accepted that statistical correlation tests are used to evaluate empirical models. Several error metrics and statistical performance tests were used in this study to evaluate the developed LMR models' performances it shows in Figure12 and 13

There are two types of linear regression: multivariate, in which several independent variables are utilized as input features, and simple, in which there is only one variable or input feature. One dependent variable in each linear regression can be projected or anticipated using the input features(Ahmed and Mohamed 2021; Prabakaran, Kumar, and Tarun 2017). This study used multivariate linear regression to predict the dependent variable, daily rainfall amount, which was dependent on several environmental variables or features. Using the known environmental factors as input, the supervised machine learning technique of linear regression is utilized to forecast the uncertain daily rainfall amount. According to the linear regression concept, p quantitative explanatory variables, such as X1, X2... Xp, are combined linearly to describe a quantitative dependent variable, Y. For observation I the equation of linear regression is expressed as follows(Chellaian and Engineering 2019):

$$y_i = a_1 x_{1\,i} + a_2 x_{2i} + \ldots \ldots + a_p x_{pi} + e_i \qquad 53)$$

Where e_i is the model error, xki is the value taken by variable k for observation I, and y_i is the variable observed for the dependent variable for observation i.

Many people ask if OLS and linear regression are the same because the model is obtained using the ordinary least squares (OLS) method (the sum of squared errors, ei2, is minimized). OLS just refers to the technique that allows us to identify the regression line equation.

The e_i errors are independent and share the identical normal distribution N (0, s), according to the linear regression hypothesis(Hou, Liu, and Zou 2004).

6.1.2 Choosing Variables for Linear Regression

Not every variable in the model of linear regression is significant. Utilizing any of the four approaches used for forecasting, it is feasible to choose only the most crucial ones (Gleixner et al. 2017; k k, R, and Gouda 2015).

6.2 Results and Discussion

The major goal of this chapter was to employ machine learning techniques to identify the pertinent atmospheric variables that generate precipitation and predict the severity of daily precipitation. As a result, the research findings are listed below. The ability of monsoon rainfall to anticipate annual precipitation has been examined in this study. Utilizing both non-linear and linear modeling techniques. This is because annual rainfall at various stations has the highest correlation with the 12-month average values of climate indices. Results provide the projected values of the numerical data for both the forecast and actual rainfall in millimeters. Actual values are derived from test data sets, whereas predicted values are the result of the trained algorithm, and the error rate is different. The data and the outcomes of the various machine learning methods are described in this chapter. The acquired results have been examined using several parameter kinds. The outcome is displayed as a bar diagram. Here, we'll focus more on the data description. Develop the model, Model Assessment(Ehsan et al. 2021) as shown in Figures 12 and 13.

The figure shows the predicted future rainfall at each station throughout the study period of 1951–2050. With their historical mean rainfall data set, the Bagepalli, Bangarapete, and Malur stations demonstrated a future prediction of rainfall that gradually increases. The lowest drop rainfall value is at the Chikkaballapura station at roughly R 0.0032, while the Bangarapete station exhibited very big incline changes in the future prediction in comparison to the other Grid stations with R-value 0.2279 (about 700-900mm) rest of the station experience various rainfall trend in future forecasting.
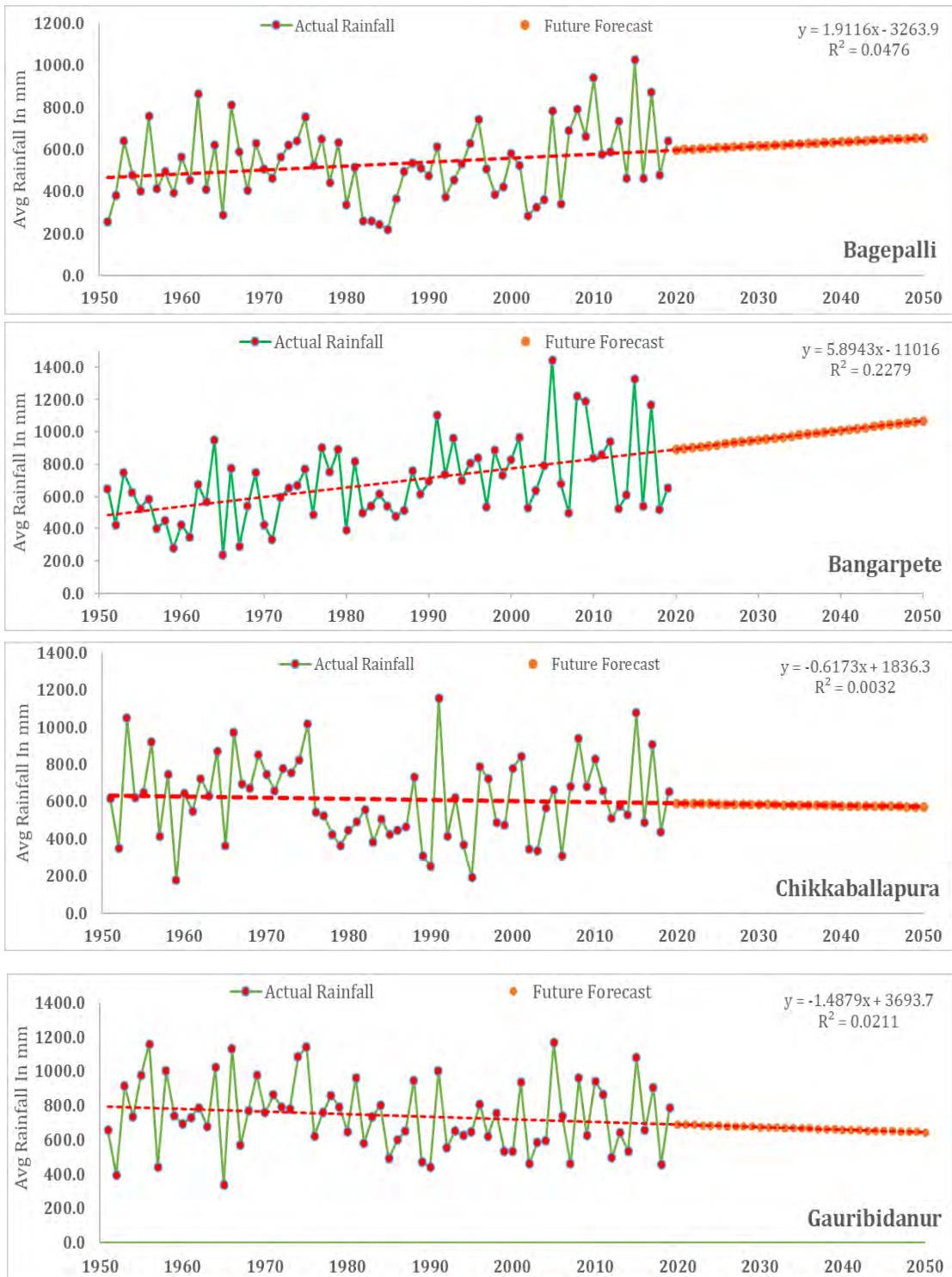

169
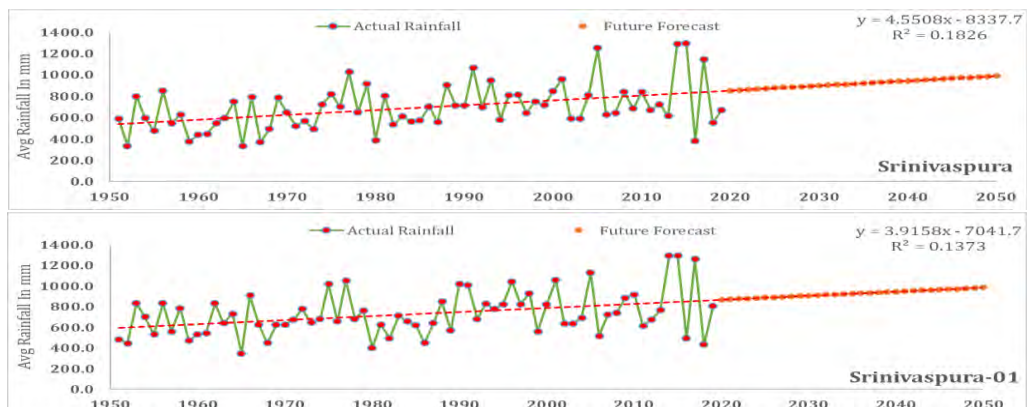
Figure 12. Performance and Forecasting of Rainfall in LMR Modelling with Annual Mean Data Sets

170
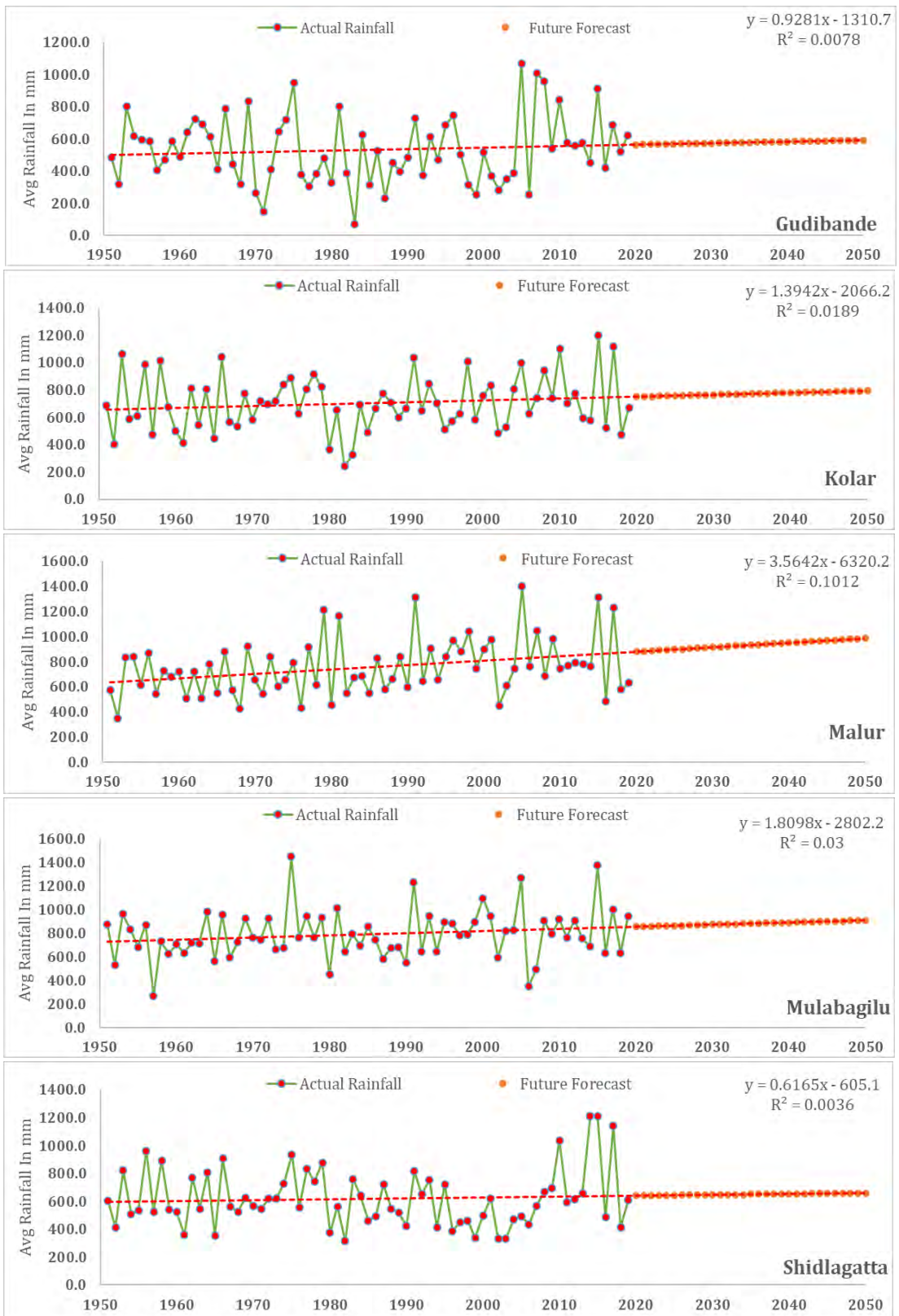
Figure 12. Continued...

6.2.1 Best Model Using for Future Forecasting of Rainfall:

Using this method, you can choose the model that can manage the greatest number of variables, ranging from Max Variables to Min Variables among all the models. Additionally, the user has a variety of "criteria" to choose from when deciding on the best model: Mean Square of Errors (MSE), Amemiya's PC, Schwarz's SBC, Mallows Cp, and Akaike's AIC(Liyew and Melese 2021).

Beginning with the variable that contributes the most to the model, the candidate is chosen (Student's t statistic is used as the criterion). A second variable is included in the model if the probability connected to its t is lower than that of the "Probability for admission." Another variable's situation is the same(Gowtham, Ganesh, and Ali 2021). The effects of deleting each variable from the model after it has been included are assessed once the third variable is added (using the t statistic). The variable is eliminated if the likelihood exceeds the Probability of removal Up until no further variables may be added or removed, the process is repeated(Gandhi et al. 2015).

6.2.2 Evaluate the Premises of Linear Regression.

Regarding the residuals, there are two key requirements for linear regression that must be verified:

1. They have to adhere to a normal distribution.
2. They must be autonomous

Utilize the numerous tests shown in the results of the linear regression to check, in retrospect, that the fundamental hypotheses have been successfully confirmed.

6.2.3 List of the Variables Chosen

The selection summary is shown by statistic tables once a methodology has been selected(Jiang et al. 2006). The statistics related to the various steps of a stepwise selection are shown. When the best model for a set of variables with values ranging from p to q has indeed been chosen, the prediction fit for each set of variables is shown along with the accompanying statistics, and the model for looking at the quality is shown in bold it indicated in Table 6.

6.2.4 Goodness of Fit Tests:

Any established model considers evaluation to be a crucial component in deciding whether the project is worthwhile in terms of producing the desired results. It is generally accepted that statistical correlation tests are used to evaluate empirical models(Chellaian and Engineering 2019; Prabakaran, Kumar, and Tarun 2017). Several error metrics and statistical performance tests were used in this study to evaluate the developed LMR models' performances in Table 6.

6.2.4.1 Root Mean Square of the Errors (RMSE):

The RMSE assists us in finding the average size of the mistake so that we may evaluate the dependability of the available data.

$$\text{RMSE} = \sqrt{\frac{\sum_{i=1}^{n} (P_{\text{obs},i} - P_{\text{pred},i})^2}{n}} \qquad 54)$$

6.2.4.2 The Mean of the Squares of the Errors (MSE):

Take the observed value, take the anticipated value out, and square that differential to get the MSE. That should be done for each observation. Divide the total sum of these squared values by the number of observations. The numerator of the equation is the sum of squared errors (SSE), which itself is minimized using linear regression.

$$MSE = \frac{\sum (y_i - \hat{y}_i)^2}{n} \qquad 55)$$

Where y_i is the ith observed value, $\hat{y}_i$ is the corresponding predicted value, and n = the number of observations. The variance computations are identical to those for the average squared error. Take the given data, take the anticipated value out, and square that ratio to get the MSE. That should be done for each observation. Afterward, add together all of the squared values and reduce the number of observations.

6.2.4.3 Mean Absolute Percentage Error

The average or mean of forecasts' absolute percentage mistakes is known as the mean absolute percentage error or MAPE. Actual or seen value less

predicted value is the definition of error. To calculate MAPE, percentage errors are added without regard to sign. Because it shows the mistake in terms of percentages, this measurement is simple to comprehend. Additionally, the issue of positively and negatively errors canceling out one another is avoided when absolute error bars are employed. As a result, MAPE is a measure that is frequently employed in forecasting and has managerial appeal. The forecast is better the shorter the MAPE

A 10% MAPE, irrespective of whether the variation was positive or negative, indicates that there was an average 10% difference between the anticipated value and the actual value. But there is no accepted industry norm for what constitutes a good MAP.

$$M = \frac{1}{n}\sum_{t=1}^{n}\left|\frac{A_t - F_t}{A_t}\right|$$
  56)

N, Number of times the summation iteration happens, M means absolute percentage error, A_t actual value, and F_t, the forecast value.

Table 6: Goodness of Fit Statistics (Annual Scale From 1951-2019):

Annual	R^2	Adjusted R^2	MSE	RMSE	MAPE
Bagepalli	0.048	0.033	29894.642	172.901	29.995
Bangarapete	0.228	0.216	48089.365	219.293	29.039
Chikkaballapura	**0.003**	**-0.012**	48703.870	220.690	36.878
Gauribidanur	0.021	0.006	42016.768	204.980	24.891
Gudibande	**0.008**	**-0.007**	44879.934	211.849	46.302
Kolar	0.019	0.004	41136.558	202.821	26.176
Malur	0.101	0.088	46099.963	214.709	24.261
Mulubhagilu	0.030	0.030	43190.037	207.822	22.195
Sidhlaghatta	**0.004**	**-0.011**	43353.712	208.216	27.871
Srinivasapura	0.183	0.170	37871.360	194.606	23.548
Srinivasapura-1	0.137	0.124	39368.122	198.414	22.938
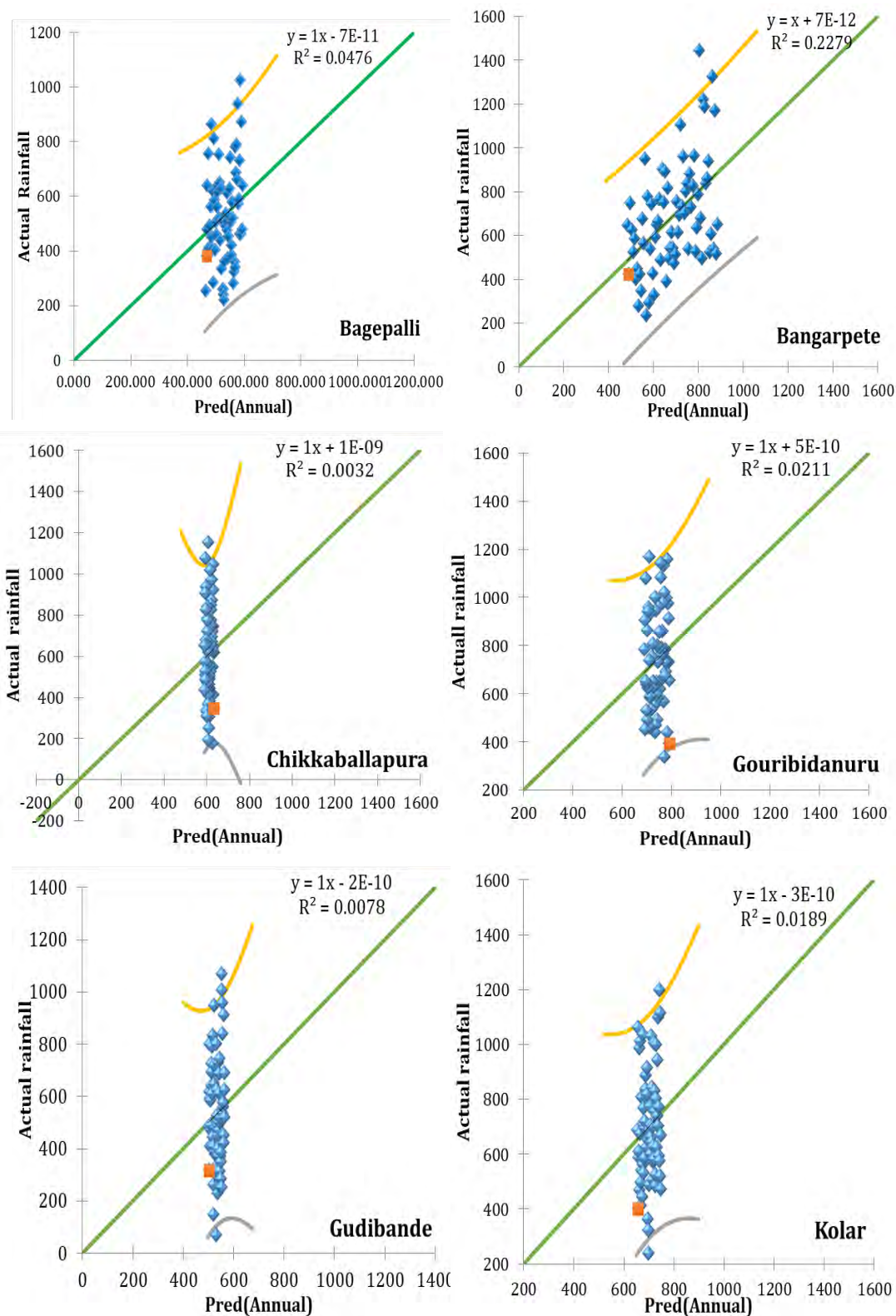
Figure 13. MLR Models Outputs in Regards to Troughs and Peaks for the Selected Stations

175
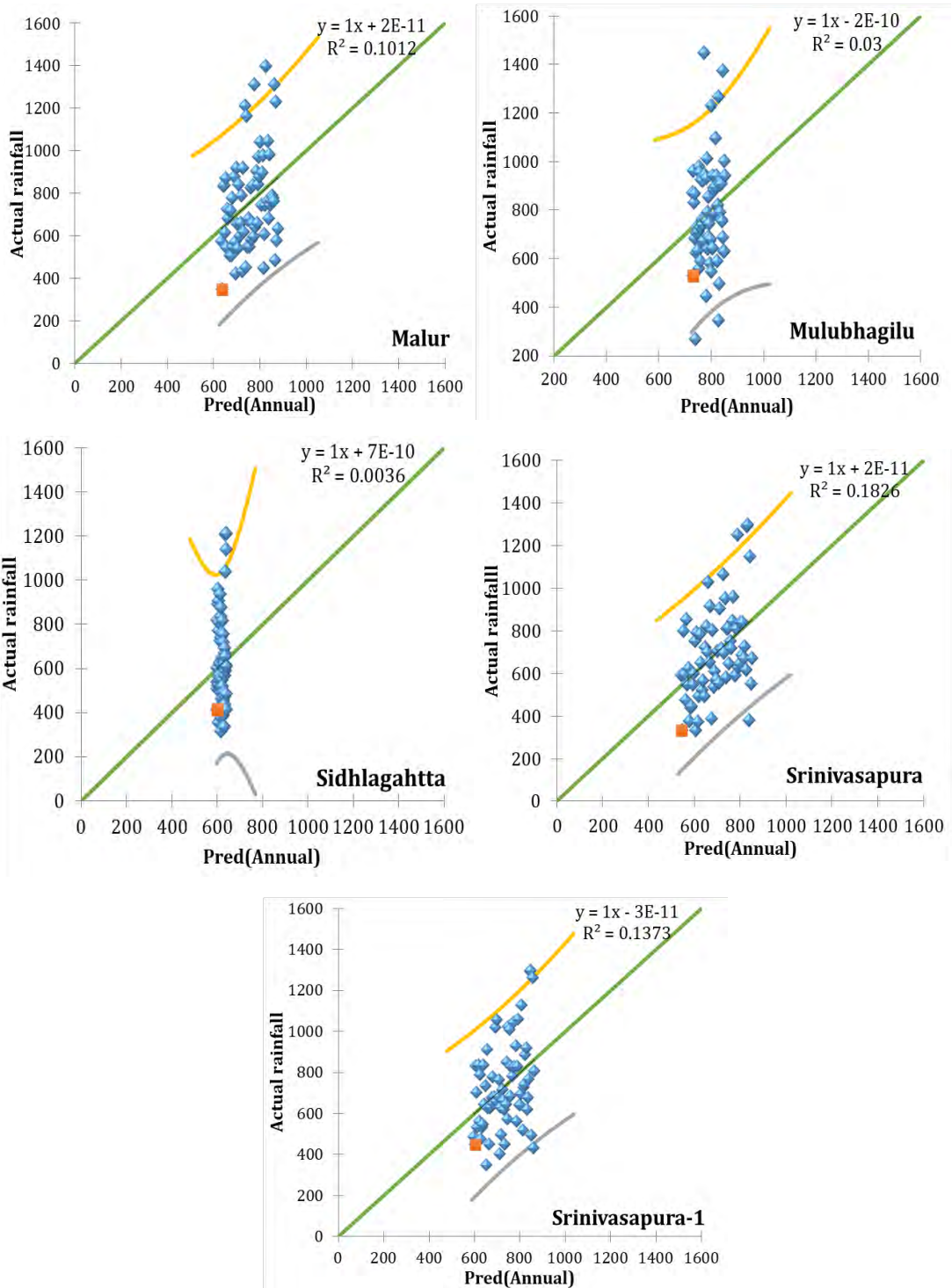
Figure 13. Continued

6.3 Conclusion

The majority of current systems are developed using statistical techniques; the multi-linear regression module described above increased the system's accuracy compared to earlier prediction techniques. The issue with the current modules is that they are unable to take into account how each number of each parameter would affect the relationship. In other words, rather than producing a specific relation, a more generic equation is generated because the impact of every number is not taken into account in the forecasting of rainfall in the semi-arid regions the trend is dependent on the average value of historical data and it predicts the future forecasting with the help of linear trend For the three stations, the correlation coefficients between historical values of the climate indices and annual rainfalls were calculated. As was previously noted, both the LMR model and climate indices with a significant association with yearly rainfall were taken into consideration.

To investigate the potential for predicting annual rainfall, the LMR was analyzed. Afterward, various statistical assessment metrics, including RMSE, MSE, and MAPE, were utilized to assess the efficacy of these two methods. In general, the analysis's RMSEs show that the LMR model is more accurate than the ANN models at forecasting WA's long-term seasonal rainfall. During the prediction interval for the research area, the RMSE of the built LMR models is fairly low.

References

1. Ahmed, Hiyam, and Sondos Mohamed. 2021. "Rainfall Prediction Using Multiple Linear Regressions Model." In , 1–5.
2. Chellaian, Geetha, and R Engineering. 2019. "Rainfall Prediction Using Linear Regression Model." *International Journal of Scientific Research and Management* 7: 613–2321.
3. Ehsan, Muhammad Azhar et al. 2021. "Seasonal Predictability of Ethiopian Kiremt Rainfall and Forecast Skill of ECMWF's SEAS5 Model." *Climate Dynamics* 57.
4. Evapotranspiration, Potential, Remote Sensing, and Data Application. "Agricultural Drought Monitoring by MODIS Potential Evapotranspiration Remote Sensing Data Application."
5. GGleixner, Stephanie et al. 2017. "Seasonal Predictability of Kiremt Rainfall in CGCMs." *Environmental Research Letters* 12.
6. Gobierno de Colombia. 2017. "Smart Cities - SMART CITIES." *Research Gate*: 1–51. https://bibliotecadigital.fgv.br/dspace/handle/10438/18386%0Ahttp://www.smartcities.es/smart-cities/.
7. Gowtham, Sethupathi M, Yenugudhati Sai Ganesh, and Mohammad Mansoor Ali. 2021. "Efficient Rainfall Prediction and Analysis Using Machine Learning Techniques." *Turkish Journal of Computer and Mathematics Education 3467 Research Article* 12(6): 3467–74.
8. Karama, Alphonse. 2021. "East African Seasonal Rainfall Prediction Using Multiple Linear Regression and Regression with ARIMA Errors Models."
9. iyew, Chalachew Muluken, and Haileyesus Amsaya Melese. 2021. "Machine Learning Techniques to Predict Daily Rainfall Amount." *Journal of Big Data* 8(1). https://doi.org/10.1186/s40537-021-00545-4.
10. MMckee, Thomas B, Nolan J Doesken, and John Kleist. 1993. Eighth Conference on Applied Climatology *THE RELATIONSHIP OF DROUGHT FREQUENCY AND DURATION TO TIME SCALES*.
11. Prabakaran, S, P Kumar, and P Tarun. 2017. "Rainfall Prediction Using Modified Linear Regression." *ARPN Journal of Engineering and Applied Sciences* 12: 3715–18.
12. Rafaela, Tarciana et al. 2022. "Climate Indices-Based Analysis of Rainfall Spatiotemporal Variability in Pernambuco State, Brazil." : 1–26.
13. Yashasathreya, Vaishalibv, Sagark, Srinidhihr. 2021. "IRJET- Flood Prediction and Rainfall Analysis Using Machine Learning." *Irjet* 8(7): 2445–49.
14. Yue, Sheng, and Michio Hashino. 2003. "Long Term Trends of Annual and Monthly Precipitation in Japan." *Journal of the American Water Resources Association* 39(3): 587–96.

CHAPTER -7
CONCLUSIONS AND RECOMMENDATIONS

Chapter -6
Conclusions

7. Conclusions and Recommendations

When taking into account the orographic element, the examination of rainfall patterns and drought conditions in the districts of Kolar and Chikkaballapura shows that there is heterogeneity in both time and space. Although rain gauges accurately record rainfall, because they only cover a small portion of the earth's surface, they are insufficient to quantify rainfall variability. The rain gauges are too close together for an accurate representation of the variation in rainfall over time and space. Several uses, such as Agriculture, Hydrological studies, Water resource planning, and Climate and weather forecasts, depending on the measurement technique of precipitation.

Several uses, such as Agriculture, Hydrological studies, Water resource planning, and Climate and Weather forecasts, depending on the measurement technique of precipitation. Today, remote sensing provided a different method for measuring rainfall on both a spatial and temporal scale. There are now several free data products accessible with various prices, accuracy, and spatial resolution features. The rainfall observed by satellites is not directly measured; rather, it is merely estimated with various flaws and uncertainties. Understanding these items' error and accuracy characteristics is crucial if you want to use them for practical purposes.

The temporal and regional variability of precipitation in the semi-arid parts of Karnataka were captured in the proposed investigation using IMD precipitation data. High-resolution spatial and temporal resolution data from space and time are available from the IMD. Additionally, the study compared the variation pattern of precipitation and established the accuracy of IMD estimates using ground data from 11 rain gauge sites. The District's high rainfall variability has a significant impact on the local vegetation's greenness and the runoff output from the reservoirs. A hydrological model was put up to estimate the agricultural drought changes to explore the various precipitation and vegetation indices time series.

The provided details about the study field and the most significant basic statistics. The study area has a diversity of soil types, geomorphic elements, lithological properties, drainage systems; slopes, agricultural use, and land cover types and is situated in the southernmost part of the Indian state of Karnataka. The study of precipitation, temperature, moisture and other weather parameters has a significant impact on the hydrological cycle, resulting in both too much and not enough rainfall. Due to the region's varying climate, the semi-arid zone always implies lower rainfall amounts. The average annual rainfall at Gauribidanur station during the Southwest monsoon was 840.1 mm, whereas the average annual precipitation at Bagepalli station was 546.3 mm. Precipitation during the Pre-monsoon season is quite low everywhere, notably in Bagepalli and Gudibande (79.7-80mm). During the northeast monsoon, Gudibande (165.1mm) had the greatest yearly rainfall in the Srinivasapura taluk (238.2mm/year). In this region, commercial crops like mulberry, grapes, ragi, pulses, and others predominate. Agriculture was the main economic activity in the region, especially during the monsoon season.

Drought is a pernicious meteorological and hydrological natural phenomenon that has numerous negative effects on the environment, agriculture, and socioeconomic status. Drought can last for a season or longer when the amount of precipitation is insufficient to meet human activity demands. The standard precipitation index (SPI), which is frequently used to assess rainfall variability, is being investigated in the current article as a potential tool for identifying drought occurrences. As a result, this study uses SPI to examine drought in the Karnataka state districts of Kolar and Chikkaballapura throughout the pre-monsoon, southwest monsoon, northeast monsoon, and annual periods.

The spatiotemporal characteristics of different time drought indices, including SPI, SPEI, and RAI, are analyzed in the dry semi-arid area of Kolar and Chikkaballapura in Karnataka. The study included 68 years, from 1951 to 2019, and examined the frequency and length of droughts on a seasonal and annual basis at several locations within the study area. The analysis' findings corroborate the actual circumstance, demonstrating that the SPI and SPEI are

appropriate for studying drought situations. In addition to serving as a tool for comprehending the temporal and spatial variance of drought, SPI, SPEI, and RAI also serve as a foundation for engineering projects including drought forecast, prevention, monitoring, and mitigation.

All grid stations showed that SPEI was more evaluation-sensitive than SPI and accurately captured wet and dry conditions in more complex areas. A stronger SPI and SPEI drought trend was observed in the districts' steep north-eastern (N-E) portions. We found that Chikkaballapura faced more severe drought conditions than the Kolar district based on the frequency and duration of droughts. While the N-E region's drought frequency increased progressively from 1.56 to 2.5, the S-W region's drought frequency fluctuated between 0.98 and 1.52 on average. The Gudibande station has been mostly hit by the More Extreme Drought Period for around 17, 18, and 10 months in SPI, with a frequency value of about 3.1%. (3, 6, and 12-month scales, respectively).

Drought-like conditions were observed in the years 1983, 1985, 2002, 2003, and 2004. 2007 and 2017. Due to the dependence of economic activity, water use, and agricultural activity on rainfall, this assessment of dry occurrences is essential in arid areas. It will be easier to develop the short-, medium-, and long-term plans necessary to avoid similar calamities in the future if the region's droughts are characterized and assessed at various periods.

According to the Bagepali stations, 2015 was the wettest year throughout the study period, with an annual rainfall of around 1026.4 mm and EDTI values of approximately 4.5 SMDI 2.1. Additionally, 2018 was the driest year when compared to the other stations, with an average rainfall of 456 mm. The year 2015 has the highest rainfall recorded at the station mulubhagilu; the ETDI is approximately 4.88 and the SMDI is about 2.67, indicating that this year has been particularly wet overall. At the year 2018, there were extreme drought episodes in Sidhghatta, which received 414 mm of rain (EDTI-1.41, SMDI-0.71), and Srinivasapura, which received 432.1 mm (EDTI-1.92, SMDI-1.22). The ETDI, SMDI, and SPI's correlation matrix (R) value to annual rainfall

This study's main objective is to compare the drought conditions that are now present in both areas. In this context, crop management, irrigation

management, the building of irrigation infrastructure, and the design of irrigation facilities all depend on the spatiotemporal classification of drought using diverse approaches. Governments, farmers, and researchers in that area can utilize this information to plan their crops, organize their schedules, and manage their irrigation systems. Additionally, thoughtful planning might boost food production while preserving the environment. Encouraging rural populations to engage in agriculture This study uses long-term rainfall data to characterize the drought using the SPI, SPEI, and RAI methodologies.

The current study examines precipitation trends for the districts of Kolar and Chikkaballapura over the last seven decades under the influence of climate change. Applying the scientific methods, the pattern of precipitation patterns is shown along with a territorial description, statistics, and interpretive figures. Our understanding of precipitation trends in such districts appears to have improved as a result of the evaluation. In 69 years of the research period, this work uses 11 meteorological grid stations to discover whether there is a discernible monthly and annual trend. According to the fitted line LOWESS model for yearly rainfall trends, the grid stations with the highest coefficient (R^2) values were those in Srinivaspura (j) ($R^2 = 0.9505$) as well as the grid stations with the lowest coefficient ($R^2 = 0.3867$).

Although each decade's yearly rainfall time sequence is different as seen by the LOWESS curve, the overall trend was practically constant for several decades. Every station's M-Kendall and Sen Slope estimator trend shows both a descending and ascending trend. The output's coefficient values show a strong correlation between the expected and actual data. At 5% statistical significance levels or 95% confidence levels, the rainfall trend was examined. The seven meteorological grid stations exhibit significantly positive increases in June, and significant negative patterns were observed in October at Shidlagatta. The maximum grid stations at rainfall data were statistically significant (P 0.05).

Drought or floods that alter agricultural cropping patterns are caused by spatial-temporal variability and diverse trends in precipitation. The next study must identify the origin of these changes to link observed patterns with climatic variability. Overall, the research's conclusions will be helpful for the

configuration and consequences of drought management and water resource control measures in the studied area.

The Vegetation Health Index, which is made up of the TCI and VCI agricultural drought indicators, can be used to improve and monitor GIS and remote sensing-based agricultural drought. This study used TCI, NDVI, VCI, and VHI at various grid stations in both districts during the Pre, Southwest, and Northeast monsoon seasons to demonstrate the duration, intensity, and spatial extent of agricultural drought zones. The Vegetation Health Index model shows that the research area experienced an exceptionally dry (ED) phase between 2019 and 2015, with an average VHI value range of less than 10.

Our research's findings offer an assessment of regional vegetation activity growth and drought time and area estimation, which will help manage vegetation growth productivity and assist decision-makers and farmers in their agricultural assessments. The yearly drought model output, in particular, displayed the drought severity status at various spatial resolutions, which is taken into account by drought management decision-makers and former at regional levels. These maps also aid in estimating land conditions if all spatial maps can be appraised by the neighborhood communities. Drought intensity was evaluated in terms of percent area coverage, including intense stress, moderate stress, and severe stress, near normal, poor vegetation, good vegetation, fair healthy vegetation, very good healthy vegetation, and exceptional healthy vegetation. One of the areas of science and technology is weather forecasting, which makes weather predictions based on input attributes. Utilizing statistical methods LMR the majority of the current systems are unable to provide reliable predictions since they are unable to detect unexpected changes in the weather conditions. The suggested method makes use of the multi-linear regression notion, which can deliver superior outcomes to current practices. The general statistical analysis paradigm points to LMR models' superior efficacy over ANN models for predicting rainfall utilizing more climate data. As a result, the new LMR model will yield better results than the current method by using lagged global climate indices to help with proper preparation for the hazards connected with future droughts in the study location.

PUBLICATIONS

List of Publications

1. **Harishnaika, N,** S A Ahmed, Sanjay Kumar, and M Arpitha. 2022. "Computation of the Spatio-Temporal Extent of Rainfall and Long-Term Meteorological Drought Assessment Using Standardized Precipitation Index over Kolar and Chikkaballapura Districts, Karnataka during 1951-2019." Remote Sensing Applications: Society and Environment 27(January):100768. https://doi.org/10.1016/j.rsase.2022.100768. (Journal- **Elsevier**)

2. **Harishnaika, N,** S A Ahmed, Sanjay Kumar, and M Arpitha. 2022. "Spatio-temporal rainfall trend assessment over a semi-arid region of Karnataka state, using non-parametric techniques" Arabian Journal of Geosciences (2022) 15:1392 https://doi.org/10.1007/s12517-022-10665-7 . (Journal-**Springer**)

3. Sanjay Kumar, S A Ahmed, **Harishnaika, N,** and M Arpitha. 2022" Spatial and Temporal Pattern Assessment of Meteorological Drought in Tumakuru District of Karnataka during 1951-2019 using Standardized Precipitation Index" Jour. Geol. Soc. India (2022) 98:822-830 https://doi.org/10.1007/s12594-022-2073-3 . (Journal-**Springer**).

4. **Harishnaika, N,** S A Ahmed, and M Arpitha. 2022 "Spatial and temporal assessment of drought conditions in Arid Steppe Hot (BSh) regions by SPI and SPEI index over Kolar and Chikkaballapura Districts, India during 1979-2019". Communicated-under review (Journal- **Springer**)

5. **Harishnaika, N,** S A Ahmed, and M Arpitha. 2022 "Assessment of drought conditions by combined drought index (CDI) using remote sensing and GIS data products in Kolar and Chikkaballapura districts, Karnataka State". Communicated-under review, (Journal- **Springer**)

6. **Harishnaika, N,** S A Ahmed, and M Arpitha. 2022 "Performance and Comparison of the Drought Indices in assessment Historical Drought for the Kolar and Chikkaballapura districts, Karnataka State." Communicated - under review, (Journal- **Elsevier**).

7. **Harishnaika N,** Shilpa N, S A Ahmed, Govindaraju and Arpitha M. 2022"Assessment of Rainfall changes and trend detection in Karnataka State, using Statistical Approach and Machine learning techniques" Communicated - under review, (Journal- **Springer**).

International and National Conferences

1. **Harishnaika N,** S. A. Ahmed, Arpitha M (2022) "Assessment of Spatial and Temporal Rainfall trend using Mann-Kendall Technique in Kolar and Chikkaballapura Districts, India," Three days international Conference on **"Earth and Environment in Anthropogenic" (ICEEA-2021)**29th and 31th October, 2021 **-Central University of Karnataka, and University of Madras**

2. **Harishnaika N,** S. A. Ahmed, Arpitha M (2022)- "Identification of Temporal and Spatial pattern of drought associated with SPEI and SPI indices, in Kolar and Chikkaballapura districts, Karnataka state". Two days national conference on "Recent trend in Earth Science and Geoinformatics application in engineering practices" **(RTESGAEP-2022) in** March 9Th and 10Th 2022 **University of Mysore, KSTA, and KSECGTA**

3. **Harishnaika N,** S. A. Ahmed "Future forecasting and long term predication climatic conditions in Semi-arid regions state". Two days national Seminar on **"Earth Resource Conservation and Management (ERCM-2019)** in July 1st and 2nd 2022 **Kuvempu University**

Participation and certificates during Research period:

1. I have been awarded a Certificate on completed the course on "Remote sensing, Geographical Information System and Global Navigation System" from the **Indian Institute of Remote sensing (IIRS)** from November to December 2019.
2. I completed the e-Training on "Application of Remote Sensing" exclusively for SC and ST conducted by PGRS Division, **GSITI,** and Hyderabad from 16.06.2020 to 23.06.2020.
3. Earth climate and ocean Research Foundation For attending a webinar on "Making of continental crust Resolving the paradox"
4. Online Round Table Conference on Geographical Perspectives of Water Resources: Issues and Challenges 16 July 2020 Jointly organized by the **Russian Geographical Society (RGS)** and the **National Association of Geographers, India (NAGI)**
5. E-Training on "Refresher Course on Ground Geophysics in Mineral Exploration" (31.08.2020 to 10.09.2020) and making the session very interactive. conducted by PGRS Division, **GSITI,**
6. Completed the e-Training on "Fundamentals of Aero geophysical Survey" Special Programme for Faculty, Research Scholar, PG & Post PG Students of Academic Institutions conducted by **Geophysics Division of GSI Training Institute**, Hyderabad from 04.08.2020 to 06.08.2020.
7. Participation in the online training program on cyclones and storm surges on 28th July 2020 organized by the **National Institute of Disaster Management**, in collaboration with the **India Meteorological Department, India.**